

University of Alberta

Protein Tyrosine Nitration in Mast Cells

by

Yokananth Sekar

A thesis submitted to the Faculty of Graduate Studies and Research
in partial fulfillment of the requirements for the degree of

Doctor of Philosophy
in
Experimental Medicine

Department of Medicine

©Yokananth Sekar
Spring 2011
Edmonton, Alberta

Permission is hereby granted to the University of Alberta Libraries to reproduce single copies of this thesis and to lend or sell such copies for private, scholarly or scientific research purposes only. Where the thesis is converted to, or otherwise made available in digital form, the University of Alberta will advise potential users of the thesis of these terms.

The author reserves all other publication and other rights in association with the copyright in the thesis and, except as herein before provided, neither the thesis nor any substantial portion thereof may be printed or otherwise reproduced in any material form whatsoever without the author's prior written permission.

Examining Committee

Dr. A. Dean Befus, Department of Medicine

Dr. Richard Schulz, Departments of Pediatrics and Pharmacology

Dr. Sandra T. Davidge, Departments of Obstetrics & Gynecology and Physiology

Dr. Lisa Cameron, Department of Medicine

Dr. David M. Olson, Department of Physiology

Dr. Paul Kubes, Departments of Physiology & Pharmacology and Medicine,
University of Calgary

Dedication

I would like to dedicate this thesis to my wife Kirthiga and my kids Rishit, Rohit and Netra.

Abstract

Nitric oxide (NO) is a short-lived free radical that plays a critical role in the regulation of cellular signalling. Mast cell (MC) derived NO and exogenous NO regulate MC activities including the inhibition of MC degranulation. At a molecular level the intermediate metabolites of NO modify protein structure and function through several mechanisms including protein tyrosine nitration. To begin to elucidate the molecular mechanisms underlying the effects of NO in MC, we investigated protein tyrosine nitration in human mast cell lines HMC-1 and LAD2 treated with the NO donor S-nitrosoglutathione (SNOG). Using two dimensional gel western blot analysis with an anti-nitrotyrosine antibody together with mass spectroscopy we identified aldolase A, an enzyme of the glycolytic pathway, as a target for tyrosine nitration in MC.

S-nitrosoglutathione treatment also reduced the V_{max} of aldolase in HMC-1 and LAD2. Nuclear magnetic resonance (NMR) analysis showed that despite these changes in activity of a critical enzyme in glycolysis, there was no significant change in total cellular ATP content, although the AMP/ATP ratio was altered. Elevated levels of lactate and pyruvate suggested that SNOG treatment enhanced glycolysis. Reduced aldolase activity was associated with increased intracellular levels of its substrate, fructose-1,6-bisphosphate (FBP). Interestingly, FBP inhibited IgE-mediated MC degranulation and intracellular Ca^{2+} levels in LAD2 cells.

In addition to aldolase, 15-hydroxy prostaglandin dehydrogenase (PGDH), a critical enzyme in the metabolism of PGE₂, was identified as a prominent target for tyrosine nitration in LAD2 cells. Thus for the first time we report evidence of protein tyrosine nitration in human MC lines and identify aldolase A as a prominent target in HMC-1 and LAD2; and PGDH in LAD2 cells. The post translational nitration of aldolase A and PGDH may be important pathways that regulate MC phenotype and function.

Preface

This thesis has been written in the traditional format of University of Alberta and references were quoted following the style of *The Journal of Immunology*. The manuscript published in *The Journal of Immunology* (*Copyright 2010. The American Association of immunologists, Inc.*) from data in this thesis is attached in Appendix 2.

Acknowledgement

It is my pleasure to acknowledge my supervisor Dr. A. Dean Befus for his continuous support through out the research. He is an excellent mentor who creates the ambient atmosphere for the trainee to develop into an independent researcher. In addition to science, I learned a lot about mentorship, leadership and time management skills from him which are going to help me forever.

Sincere thanks to my supervisory committee members, Dr. Richard Schulz, Dr. Sandra T. Davidge and Dr. Lisa Cameron whose advice and critical appraisals helped to refine research methodologies and thesis preparation. The help rendered by Dr. Carolyn M. Slupsky for NMR work and Paul Semchuk, Randy Whittal and Jing Zheng for mass spectrometry analysis helped me to develop a multi-disciplinary approach to address key issues in my research project. I also thank Dr. Sankaranarayan Ramasamy for his help in structural biology work.

Special thanks to Chris, Tae Chul, Katherine, Candy, Marcelo, Derrick, Wole and Ramses for making my stay as memorable in the lab. The technical advice from these people in understanding the basic science research is much appreciated.

I also thank my family members who stood behind me in all my endeavours. Last, but not least, sincere compliments to the moral support from my wife Kirthiga whose understanding, patience, love and care provided me the right mindset to focus on my research.

Table of Contents

CHAPTER ONE: INTRODUCTION.....	2
1.1 Mast cells	2
1.1.1 Mast cell origin, localization and phenotype.....	2
1.1.2 Heterogeneity	3
1.1.3 Mast cell activation.....	5
1.1.3.1 FcεRI mediated activation of mast cells	6
1.1.4 Mast cell mediator release	8
1.1.4.1 Preformed-granule associated mediators	8
1.1.4.2 Lipid-derived mediators.....	10
1.1.4.3 Cytokines/chemokines	11
1.1.5 Mast cell in homeostasis.....	11
1.1.6 Mast cells in disease	13
1.1.7 Mast cell lines.....	15
1.2 Nitric oxide	17
1.2.1 Nitric oxide synthesis	17
1.2.2 Actions of nitric oxide	18
1.2.2.1 Activation of soluble guanylyl cyclase.....	19
1.2.2.2 cGMP-independent pathways.....	19
1.3 Nitrosylation	21
1.4 Protein tyrosine nitration	22
1.4.1 Mechanisms of nitration.....	22

1.4.2 Factors determining the selectivity of nitration.....	25
1.4.3 Outcome of protein tyrosine nitration	27
1.4.4 Functional consequences of protein tyrosine nitration.....	28
1.4.5 Denitration.....	31
1.4.6 Proteomic analysis of nitration.....	32
1.5 Mast cells and nitric oxide	33
1.5.1 Nitric oxide synthase expression and nitric oxide production in mast cell	33
1.5.2 Nitric oxide and mast cells	34
1.5.2.1 Mast cell degranulation.....	34
1.5.2.2 Mast cell cytokine and chemokine production	35
1.5.2.3 Mast cell lipid mediator production.....	35
1.5.2.4 Other effects of nitric oxide on mast cells	36
1.5.3 Superoxide production by mast cells.....	36
1.5.4 Mast cells and nitration	38
1.6 Conceptual model, hypothesis and aims.....	39
CHAPTER TWO: MATERIALS AND METHODS	43
2.1 Mast cell culture.....	43
2.1.1 HMC-1.....	43
2.1.2 LAD2.....	43
2.1.3 Cord blood-derived mast cells.....	44
2.2 Treatment of mast cells with nitric oxide donor	44
2.3 One dimensional gel electrophoresis	45

2.4 Two dimensional gel electrophoresis (2-DE)	46
2.5 Western blot	47
2.6 Dithionite reduction	49
2.7 Aldolase enrichment	49
2.8 Mass spectrometry	50
2.9 RT-PCR	52
2.10 Aldolase enzyme assay	55
2.11 Fructose-1,6-bisphosphate measurement	56
2.12 Mast cell degranulation assay	57
2.13 Nuclear magnetic resonance analysis of HMC-1 metabolites	58
2.14 ATP assay	59
2.15 Calcium assay	59
2.16 Statistical analysis	60
CHAPTER THREE: RESULTS	62
3.1 Evidence for constitutive nitration in human mast cells	62
3.2 Two dimensional gel electrophoresis and western blot	62
3.2.1 Optimization of isoelectric focusing conditions	62
3.2.2 Optimization of second dimension electrophoresis	62
3.2.3 Manual scoring of the nitrated proteins in the western blot	64
3.2.4 Constitutive nitration versus nitric oxide donor-induced nitration	68
3.2.5 Isolation of S-nitrosoglutathione-induced nitrated spot	68
3.3 Mass Spectrometry	68

3.3.1 Mass spectrometric identification of S-nitrosoglutathione-induced nitrated proteins	68
3.3.2 Confirmation of the identity of the protein using western blot	70
3.3.3 Multiple pI forms of aldolase in HMC-1	70
3.3.4 Identification of isoforms of aldolase using mass spectrometry	74
3.3.5 Confirmation of aldolase C using zebrin II antibody	74
3.4 Identification of mRNA expression of aldolase isoforms in mast cells	77
3.5 Affinity purification of mast cell aldolase	77
3.5.1 Potential aldolase-binding proteins in the affinity purified fractions..	77
3.5.2 Mass spectrometric analysis of aldolase fractions for identification of nitration sites.....	80
3.5.3 Identification criteria for nitrated tyrosines	82
3.5.4 An altered inclusion list for nitrated aldolase peptides	82
3.5.5 Identification of nitration sites in aldolase A	85
3.5.6 Evidence for aldolase nitration in the enriched fractions	88
3.6 Location of nitrated tyrosines on the human aldolase A structure	88
3.7 S-nitrosoglutathione-induced changes in the enzymatic activity of aldolase	92
3.8 S-nitrosoglutathione-induced elevation of fructose-1,6-bisphosphate in mast cells.....	94
3.9 S-nitrosoglutathione-induced changes in glycolytic metabolites	94
3.9.1 Effects of S-nitrosoglutathione on HMC-1 AMP, ADP and ATP	94

3.9.2 Effects of S-nitrosoglutathione on nicotinamide adenine dinucleotide levels	97
3.9.3 Effects of S-nitrosoglutathione on amino acids levels	97
3.9.4 Effects of S-nitrosoglutathione on glutathione levels	101
3.9.5 Effects of S-nitrosoglutathione on the metabolites in the media.....	101
3.10 Effects of S-nitrosoglutathione on the ATP levels of LAD2.....	101
3.11 Effects of exogenous fructose-1,6-bisphosphate on LAD2 degranulation.....	105
3.11.1 Dose dependent entry of exogenous fructose 1,6 bisphosphate into LAD2	105
3.11.2 Fructose-1,6-bisphosphate inhibits LAD2 degranulation.....	105
3.12 Effects of fructose-1,6-bisphosphate on the intracellular Ca ²⁺ levels in LAD2	105
3.13 SNOG-induced nitration targets in LAD2	108
3.13.1 Isolation of S-nitrosoglutathione-induced nitrated spot in LAD2 ...	108
3.13.2 Mass spectrometric identification of SNOG-induced nitrated target in LAD2	112
3.13.3 Confirmation of 15-hydroxy prostaglandin dehydrogenase by western blot.....	112
3.13.4 Mass spectrometric identification of nitration sites in 15-hydroxy prostaglandin dehydrogenase.....	112
CHAPTER FOUR: DISCUSSION.....	117
4.1 Summary of data.....	117

4.2 Significance of aldolase nitration in mast cells	118
4.2.1 Constitutive nitration in mast cells	118
4.2.2 S-nitrosoglutathione-induced nitration of aldolase	120
4.2.3 Multiple pI forms and isoforms of aldolase in mast cells	121
4.2.4 Potential mechanisms of aldolase nitration in mast cells	122
4.2.5 Mass spectrometric evidence for nitration of aldolase	123
4.2.6 Nitric oxide-mediated changes in mast cell aldolase activity	125
4.2.7 Significance of S-nitrosoglutathione-induced elevation of intracellular fructose-1,6-bisphosphate in mast cells.....	126
4.2.8 Significance of nuclear magnetic resonance spectroscopy data in our study.....	127
4.2.9 Role of fructose-1,6-bisphosphate in mast cell function	131
4.2.10 Future directions.....	134
4.3 Significance of nitration of 15-hydroxy prostaglandin dehydrogenase in mast cells.....	135
4.3.1 Role of 15-hydroxy prostaglandin dehydrogenase in physiology and inflammation	139
4.3.2 Role of 15-hydroxy prostaglandin dehydrogenase in cancer	140
4.3.3 Nitration of enzymes involved in the arachidonic acid metabolic pathway	141
4.3.4 Role of prostaglandin E ₂ in mast cell function.....	143
4.3.5 Role of 15- hydroxy eicosatetraenoic acids in mast cells.....	146

4.3.6 Possible links between nitric oxide, prostaglandin E2, cyclooxygenase and lipoxygenase pathways	148
4.4 Future directions	149
4.5 Limitations	150
4.6 Conclusions.....	153
References	155
Appendix 1.....	207
Appendix 2	224

List of Tables

Table 2.1 RT-PCR primers for identification of aldolase isoforms in human mast cells.....	54
Table 3.1 Manual scoring and comparison of nitrotyrosine western blot between sham and S-nitrosoglutathione-treated HMC-1.....	67
Table 3.2 Summary of data from mass spectrometric analysis of constitutive and S-nitrosoglutathione-induced nitrated spots in HMC-1.	75
Table 3.3 Location of tyrosines in aldolase A and reported nitration sites.	81
Table 3.4 Peptide sequences of aldolase A identified from aldolase affinity-purified fractions of S-nitrosoglutathione-treated HMC-1.	83
Table 3.5 Peptide sequences of aldolase C identified from aldolase affinity-purified fractions of S-nitrosoglutathione-treated HMC-1.	84
Table 4.1 Potential aldolase binding proteins reported in the literature	137
Table 4.2 Summary of prostaglandin E ₂ receptor expression and effects of prostaglandin E ₂ on mast cells.	144
Appendix 1, Table 1 List of antibodies used in the study	210
Appendix 1, Table 2 Inclusion list of nitrated peptides of aldolase A	211
Appendix 1, Table 3 Inclusion list of nitrated peptides of aldolase C	215
Appendix 1, Table 4 Inclusion list of nitrated peptides of 15-hydroxy prostaglandin dehydrogenase	219

List of Figures or Illustrations

Figure 1.1 Confocal microscopy analysis of mouse bone marrow derived mast cell stained with berberine sulphate.....	4
Figure 1.2 Model of signalling pathways upon activation of FcεRI of mast cell.....	7
Figure 1.3 Mast cell mediator release.....	9
1.1.4.3 Cytokines/chemokines.....	11
Figure 1.4 Effects of nitric oxide through cGMP-dependent and cGMP-independent pathways.....	20
Figure 1.5 Pathways of nitration.....	23
Figure 1.6 Consequences of protein tyrosine nitration.....	29
Figure 1.7 Conceptual model.....	40
Figure 2.1 Affinity purification of mast cell aldolase.....	51
Figure 3.1 Constitutive protein tyrosine nitration in human mast cell.....	63
Figure 3.2 Two dimensional electrophoretic separation of HMC-1 proteins.....	65
Figure 3.3 Manual scoring of nitrated proteins of HMC-1 in two dimensional gel electrophoresis western blots.....	66

Figure 3.4 S-nitrosoglutathione-induced selective nitration of HMC-1 proteins.....	69
Figure 3.5 Amino acid sequence of human aldolase A.	71
Figure 3.6 Confirmation of S-nitrosoglutathione-induced selective nitration of HMC-1 proteins as aldolase using western blot.	72
Figure 3.7 Confirmation of S-nitrosoglutathione-induced selective nitration of aldolase in LAD2 cells.....	73
Figure 3.8 Confirmation of aldolase C in mast cells.	76
Figure 3.9 Identification of mRNA level expression of aldolase isoforms in mast cells.....	78
Figure 3.10 Affinity purification of aldolase from HMC-1.....	79
Figure 3.11 Tandem mass spectrometry (MS/MS) spectra identifying Tyr ² as nitrated Tyr (nY).	86
Figure 3.12 Tandem mass spectrometry MS/MS spectra identifying Tyr ⁵⁸ as nitrated Tyr (nY).	87
Figure 3.13 Confirmation of constitutive nitration in aldolase enriched fractions of mast cells..	89
Figure 3.14 Diagram showing the location of Tyr ² and Tyr ⁵⁸ in the tertiary structure of aldolase A.	90

Figure 3.15 Location of Tyr ⁵⁸ and interacting amino acid residues in human aldolase A structure.....	91
Figure 3.16 Saturation curve for mast cell aldolase.....	93
Figure 3.17 S-nitrosoglutathione-induced changes in the enzymatic activity of mast cell aldolase.....	95
Figure 3.18 S-nitrosoglutathione-induced elevation of fructose-1,6- bisphosphate (FBP) in mast cells.....	96
Figure 3.19 Effects of S-nitrosoglutathione on HMC-1 AMP, ADP and ATP levels.....	98
Figure 3.20 Effects of S-nitrosoglutathione on HMC-1 nicotinamide adenine dinucleotide (NAD ⁺) levels.....	99
Figure 3.21 Effects of S-nitrosoglutathione on amino acid levels of HMC-1....	100
Figure 3.22 Effects of S-nitrosoglutathione on glutathione levels of HMC-1....	102
Figure 3.23 Effects of S-nitrosoglutathione on HMC-1 metabolites in media...	103
Figure 3.24 Effects of S-nitrosoglutathione on ATP levels in HMC-1 and LAD2.....	104
Figure 3.25 LAD2 cell permeability to exogenously applied fructose-1,6- bisphosphate.....	106

Figure 3.26 Effects of exogenous fructose-1,6-bisphosphate on degranulation of LAD2 cells.....	107
Figure 3.27 Effects of S-nitrosoglutathione, fructose-1,6-bisphosphate on IgE/anti-IgE induced free intracellular Ca ²⁺ levels of LAD2.	109
Figure 3.28 Effects of S-nitrosoglutathione on tyrosine nitration in LAD2.	110
Figure 3.29 Isolation of S-nitrosoglutathione-induced nitrated spot in LAD2...	111
Figure 3.30 Amino acid sequence of 15-hydroxy prostaglandin dehydrogenase	113
Figure 3.31 Confirmation of S-nitrosoglutathione-induced nitrated spot in LAD2 as 15-hydroxy prostaglandin dehydrogenase	114
Figure 4.1 Conceptual model on effects of nitric oxide on mast cell metabolites.....	130
Figure 4.2 Biological effects of fructose-1,6-bisphosphate.....	133
Figure 4.3 Conceptual model of aldolase nitration and elevated fructose-1,6-bisphosphate in mast cells.....	136
Figure 4.4 An overview of arachidonic acid metabolic pathway.	138
Figure 4.5 Enzymes of arachidonic acid metabolic pathway that have been reported to be nitrated.	142
Figure 4.6 An overview of lipoxygenase pathway..	147

Figure 4.7 Conceptual model on effects of 15-hydroxy prostaglandin dehydrogenase nitration in mast cell function.	151
Appendix 1, Figure 1 Dose response of S-nitrosoglutathione treatment on HMC-1 nitration pattern.....	208
Appendix 1, Figure 2 Time course of S-nitrosoglutathione treatment on HMC-1 nitration pattern	209

List of Symbols, Nomenclature and Abbreviations

Symbol	Definition
15-LO	15-lipoxygenase
2-DE	Two dimensional gel electrophoresis
cGMP	3',5'cyclic guanosine monophosphate
COX	Cyclooxygenase
eNOS	Endothelial nitric oxide synthase (NOS3)
FBP	Fructose-1,6-bisphosphate
iNOS	Inducible nitric oxide synthase (NOS2)
IP ₃	Inositol 1,4,5 trisphosphate
IPG	Immobilized pH gradient
IEF	Isoelectric focusing
K _m	Michaelis Menten constant
MC	Mast cell
MS	Mass spectrometry
MS/MS	Tandem mass spectrometry
NAD ⁺	Nicotinamide adenine dinucleotide
NMR	Nuclear magnetic resonance
nNOS	Neuronal nitric oxide synthase (NOS1)
NO	Nitric oxide
ONOO ⁻	Peroxynitrite
PGDH	15-hydroxy prostaglandin dehydrogenase
pI	Isoelectric point

PKC	Protein kinase C
PLC	Phospholipase C
SDS-PAGE	Sodium dodecyl sulphate polyacrylamide gel electrophoresis
sGC	Soluble guanylyl cyclase
SNOG	S-nitrosoglutathione
$\cdot\text{O}_2^-$	Superoxide
TBS-T	Tris buffered saline with tween
TLR	Toll like receptor
Tyr	Tyrosine
V _{max}	Maximum velocity

Chapter – 1 Introduction

Chapter One: Introduction

1.1 Mast cells

1.1.1 Mast cell origin, localization and phenotype

Mast cells (MC) are bone-marrow derived leukocytes that develop into mature forms in the peripheral tissues. MC normally reside in proximity to mucosal surfaces that interface with the external environment and are the common portal for pathogen entry. MC are present in all vertebrate classes and the evolution of MC has been traced back 450-500 million years (1). MC were discovered in the late 19th century by Paul Ehrlich as “Mastzellen” meaning “well-fed cells” (2, 3). The German word ‘Mast’ indicates ‘fattening’ or ‘suckling’ function. He described that the granules of MC contained an undefined substance that reacted metachromatically with aniline dyes. This substance was later identified as heparin and other proteoglycans.

MC arise from pluripotent CD34⁺ bone marrow precursors and enter the circulation in an immature form. In humans, circulating MC precursors have the following surface expression phenotype: CD34⁺, c-kit (CD117)⁺, LY⁻, CD17⁻ and CD14⁻ (4). The homing of MC precursors to different anatomical locations and their differentiation into mature phenotypes are controlled by distinct environmental factors. For example, localization of MC to the small intestine depends on adhesive interactions controlled by β 7 integrin, α 4 β 7 integrin, vascular cell adhesion molecule 1 and mucosal addressin cell adhesion molecule 1 (5). Many growth factors including interleukin-3 (IL-3), IL-4, IL-9, IL-10 and fibroblast-derived stem cell factor have been shown to be important for the

maturation of MC (6, 7). The lifespan of MC varies between months to years and they can proliferate in response to appropriate stimuli (8).

The size of MC varies between 10 to 20 μm and they may be round, oval or spindle-shaped, with finger-like cytoplasmic projections on their surface (9). MCs are metabolically active and possess all the organelles required for their metabolism such as mitochondria, endoplasmic reticulum and a large nucleus (10). The cytoplasm is packed with numerous granules that are characteristic of MC (Figure 1.1).

1.1.2 Heterogeneity

Microenvironmental influences generate functionally heterogeneous and phenotypically malleable MC populations at different anatomical locations (11). The two major well-defined subtypes of mouse MCs are mucosal type MCs that express mouse MC protease-1 and 2, and connective tissue MCs expressing mouse MC protease-4, 5, 6 and carboxypeptidase A (12, 13). These proteases are unique to MC and are often used as phenotypic markers to distinguish MC from other cells. These MCs can be further differentiated using their granule contents, varying responses to pharmacological stimuli and their ability to proliferate upon parasitic challenge (14). Tryptases and chymases are proteases that bind to heparin in mouse connective tissue MCs, whereas only chymases are bound to chondroitin sulphate in mucosal MCs (14).

The heterogeneity among the different MC populations has been studied extensively using different techniques (15, 16). Human MCs are classified based upon their serine protease content into tryptase-only MC (MC_T), chymase-only

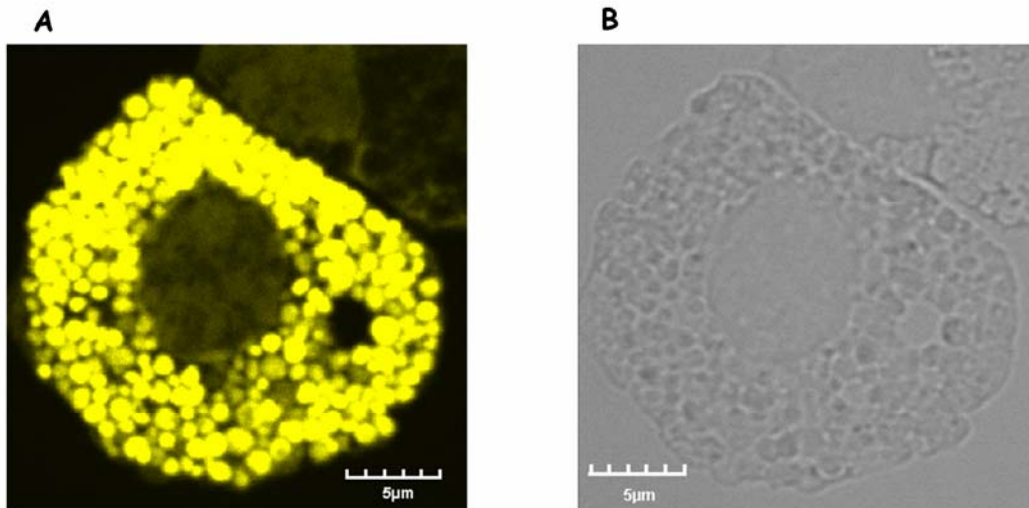


Figure 1.1 Confocal microscopy analysis of mouse bone marrow derived mast cell stained with berberine sulphate. A) Note the characteristic round granules stained greenish yellow by berberine sulphate in the cytoplasm of mast cell. B) Differential interference contrast image of the same cell. Tae Chul Moon prepared this image using berberine sulphate staining (17).

MC (MC_C) and both tryptase and chymase-positive MC (MC_{TC}) (18). However, most human tissues have been reported to have a mixed population of MC types (13). The protease content of MC not only varies between different MC types but also within a particular MC type depending upon the stimuli. For example, treatment of human MC with IL-4 promotes tryptase positive MC to differentiate into a tryptase, chymase double positive cell population (19).

Thus the heterogeneity of MC is a dynamic event that varies with the microenvironmental conditions. For example, culture of bone marrow cells in presence of IL-4 and stem cell factor results in development of MC with characteristics of connective tissue MC (20). IL-4 in presence of stem cell factor enhanced the expression of FcεRI and c-kit receptors, presence of heparin positive granules and histamine synthesis. Precise understanding of this heterogeneity is necessary to understand the role of MC in homeostasis and in targeting MC as a critical mediator of inflammatory diseases.

1.1.3 Mast cell activation

MC activation can be classified as either IgE-dependent or IgE-independent. IgE-dependent activation occurs through FcεRI, the high affinity receptor for IgE that is expressed on the MC surface (21). This is mentioned as classical activation throughout the thesis. There are other pathways through which MC can be activated including toll like receptors (TLRs) (22), adenosine receptors (23) and many others (24). However, the classical activation through FcεRI receptors will be discussed in this section because of its relevance to this thesis.

1.1.3.1 FcεRI mediated activation of mast cells

Antigen cross-linking of antigen-specific antibodies attached to FcεRI receptors on MC results in the classical activation of MC (Figure 1.2). FcεRI-mediated activation of MC results in activation of many intracellular signalling events (21, 25). The distal receptor signalling events diverge to regulate the release of different mediators in MC. FcεRI, a tetrameric receptor consists of a α chain subunit, a β chain and disulphide-linked γ chain homodimer units. The α chain binds with IgE, whereas the β and γ chain subunits initiate the signalling events. The β and γ chain subunits contain specific sequence motifs called ‘immunoreceptor tyrosine-based activation motifs’ through which the receptor subunits interact with many intracellular signalling molecules.

FcεRI cross-linking results in rapid tyrosine phosphorylation of the src related kinase, Lyn, and spleen tyrosine kinase followed by phosphorylation of the transmembrane adaptor molecule LAT (linker for activation of T cells). LAT phosphorylation leads to recruitment of the following molecules: GRB2 (growth factor receptor bound protein), GADS (GRB2 related adaptor protein), SHC (SH2 domain containing transforming protein C), SLP76 (SH2 domain containing leukocyte protein of 65 kDa), SOS (son of sevenless homologue), and VAV along with phospholipase C γ (PLC γ) (Figure 1.2). This macromolecular signalling complex facilitates diversification of the downstream signalling pathways and release of different mediators.

Upon activation, PLC γ catalyses the conversion of membrane bound phosphatidylinositol-4,5-bisphosphate into inositol-1,4,5-trisphosphate (IP₃) and

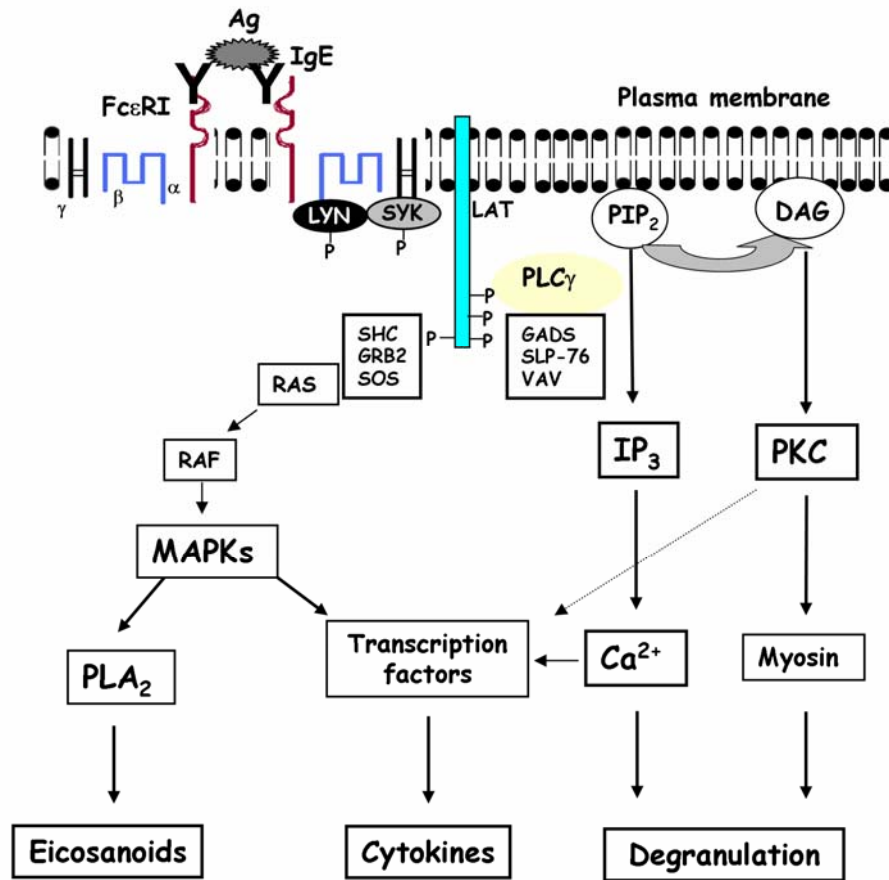


Figure 1.2 Model of signalling pathways upon activation of FcεRI of mast cell. Antigen (Ag) cross-linking of IgE attached to the α-chain of high affinity FcεRI results in phosphorylation of Src related kinase LYN, spleen tyrosine kinase (SYK) and linker for activation of T cells (LAT), which in turn activate phospholipase C gamma (PLCγ). PLCγ activation converts phosphatidylinositol-4,5-bisphosphate (PIP₂) to inositol-1,4,5-trisphosphate (IP₃) and diacylglycerol (DAG). Both IP₃-mediated intracellular Ca²⁺ release and DAG-mediated protein kinase C (PKC) activation facilitates MC degranulation. Activation of RAS/RAF signalling pathway and mitogen activated protein kinase (MAPK) pathway results in eicosanoid and cytokine generation.

diacylglycerol (25). IP₃ combines with IP₃ receptors on the endoplasmic reticulum and triggers intracellular calcium release. Diacylglycerol activates protein kinase C leading to cytoskeletal changes and degranulation (26). PLC γ -dependent increase of intracellular calcium levels and activation of protein kinase C together orchestrate the degranulation of MC.

Phosphorylation of LAT initiates the RAF/RAS pathway through recruitment of GRB2 and leads to lipid mediator production (27). Activation of RAS-RAF-MAPK (mitogen activated protein kinase) pathway leads to eicosanoid generation, including leukotriene C₄ (LTC₄) and prostaglandin D₂ (PGD₂). The activation of PKC facilitates phosphorylation of many transcription factors and leads to the synthesis of cytokines in MC.

1.1.4 Mast cell mediator release

MC activation through differential stimuli results in the release of a wide range of potent mediators. These MC-derived mediators released upon its classical activation have immediate effects on mucous secretion, vascular flow and permeability and smooth muscle tone (14). Mast cells have the potential to respond to invading pathogens within seconds to minutes by releasing the preformed mediators (28). A summary of the mediators released by MC is depicted in the Figure 1.3. The mediators released by MC can be classified as follows: i) preformed-granule associated, ii) lipid-derived, and iii) cytokines, chemokines and growth factors.

1.1.4.1 Preformed-granule associated mediators

MCs have numerous distinct membrane bound granules with a proteoglycan core. Heparin and chondroitin sulfate are the major proteoglycans in

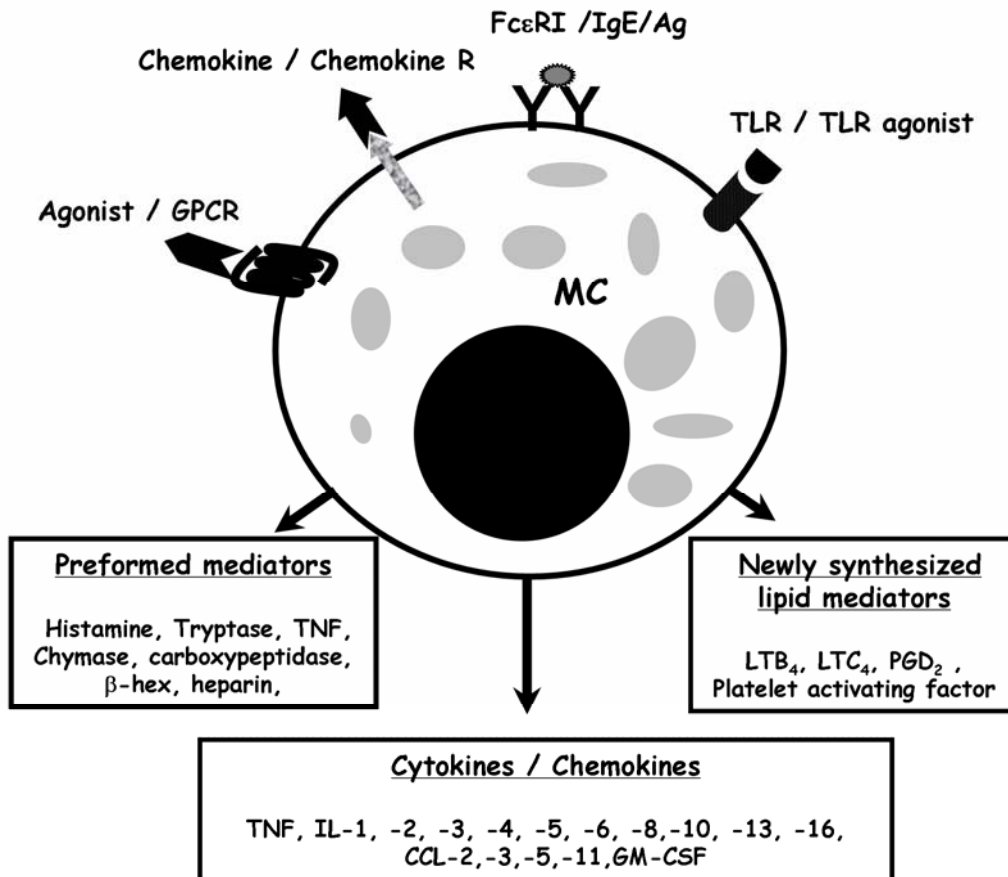


Figure 1.3 Mast cell mediator release. Mast cell can respond to different stimuli by secreting preformed mediators (14) (29), cytokines and chemokines (30) (31) or synthesize lipid and other mediators de novo (32).

MC (14). These proteoglycans have a strong negative charge that is associated with granule mediators (33). The well-known preformed mediator histamine is tightly associated with proteoglycans inside the granule. MC activation followed by granule release results in a pH change that releases histamine from the granule by a cationic exchange process (34).

In human MC, tryptase and chymase are the major proteases that are associated with the granules. MC proteases play a major role in MC-mediated inflammation (35). MC granules also have hydrolases like β -hexosaminidase, the activity of which is predominantly elevated in inflammatory conditions such as asthma (29). β -hexosaminidase release is an indicator of MC degranulation and is often used in *in vitro* assays to measure MC activation including in our current study.

1.1.4.2 Lipid-derived mediators

MC synthesizes many lipid mediators such as prostaglandins and leukotrienes upon stimulation. Arachidonic acid metabolism is well developed in MC and the enzyme phospholipase A₂ (PLA₂) generates arachidonic acid from the plasma and nuclear membranes (36). The cyclooxygenase (COX) enzymes convert arachidonic acid into prostaglandins and thromboxanes, whereas lipoxygenase (LO) enzymes generate leukotrienes (32). In addition to bronchoconstriction and vasoactive properties of prostaglandins and leukotrienes, these mediators play pivotal roles on leukocyte activation, antigen presentation and matrix deposition (37). MC exhibit heterogeneity in the release of arachidonic acid metabolites. Rat peritoneal MC produce PGD₂ but little leukotriene (38),

whereas mucosal type MC produce leukotriene B₄ (LTB₄) and leukotriene C₄ along with PGD₂ (39). Similarly heterogeneity in eicosanoid production exists among the human MC populations. For example human lung MC synthesizes nine times more leukotrienes when compared to human skin MC (40, 41). Multiple mechanisms including microenvironmental factors regulate this heterogeneity in lipid mediator secretion by MC.

1.1.4.3 Cytokines/chemokines

Cytokines and chemokines are secreted proteins involved in cell growth, differentiation and activation (42). MC can synthesize and secrete a wide array of cytokines (30) and chemokines (31). Upon MC stimulation these proteins are synthesized and released at later time points. TNF can be preformed and stored in MC for subsequent secretion (43). In inflammatory conditions, cytokines and chemokines mediate their effects through both autocrine and paracrine loops on MC or other immune cells (44). The cytokines (30) and chemokines (31) synthesized by various MC are summarised in the Figure 1.3.

MC also secrete anti-microbial peptides such as cathelicidin that influence the immune defence of multiple epithelial surfaces (45). In addition, MC also synthesise free radicals such as nitric oxide (NO) and superoxide ($\cdot\text{O}_2^-$) which will be discussed in the section 1.5 (page 31).

1.1.5 Mast cell in homeostasis

The ubiquitous distribution of MC, differential release of mediators, along with their association with blood vessels, lymphatics, epithelial surfaces and smooth muscle underscore their critical role in physiological conditions (46). MC have long been considered as a major culprit in immediate hypersensitivity and

inflammatory responses through their release of mediators. However, growing evidence suggests that they may also modulate inflammatory responses and in some cases can downregulate allergic inflammation (47). For example, mouse MC protease 4, the major chymase in murine airways has been shown to control smooth muscle cell hyperplasia and/or hypertrophy of primary airways, thereby protecting against development of allergic inflammation (48).

MC also play a major role in wound healing and tissue remodelling (49). MC secrete mediators such as histamine that increase vascular permeability and initiate collagen deposition and facilitate wound healing (50). Moreover, MC recruit other inflammatory cells to the site of injury and facilitate degradation and/or production of extracellular matrix proteins (14). They also play a pivotal role in angiogenesis by releasing angiogenic mediators such as TNF, CXCL-8, basic fibroblast growth factor and vascular endothelial growth factor (51).

MC represent 2-3 % of lamina propria cells in the gastrointestinal mucosa and regulate many physiological functions such as gastrointestinal motility, secretion of acid, electrolytes and mucous by epithelial cells (52). In lung, MC are distributed in the intraepithelial locations, bronchioles, around blood vessels and mucous secreting glands and play a critical role in immune surveillance (53). MC can be the source and target for many neuropeptides (54). These neuropeptides have both direct and indirect effects on MC such as: enhancing and suppressing effects on MC degranulation, modulation of MC mediator content and release. MC release osteopontin that plays a regulatory role in bone resorption and calcification (55).

1.1.6 Mast cells in disease

MC play a major role in type-1 hypersensitive responses that result in allergic inflammation (56). Asthma is a chronic disease that is characterised by bronchial hyper-responsiveness, inflammation and airway obstruction and MC play a major role in the pathogenesis of asthma (57). The effects of MC mediators can occur in the early and late phases of airways constriction in asthma. During the early phase reaction MC release histamine, tryptase, LTC₄, PGD₂, IL-13, VEGF and TNF that leads to increased epithelial permeability, mucous production, smooth muscle contraction, vasodilatation and neurogenic signals (11). The late phase response is facilitated by continuous release of MC mediators along with the activation of newly arrived leukocytes and tissue-resident cells.

The role of MC in both innate and acquired immunity is gaining greater recognition (58, 59). Toll like receptors (TLRs) are the major class of pattern recognition receptors expressed in *Drosophila* and mammalian cells (60). TLR recognize the pathogen-associated molecular patterns and trigger the signalling mechanisms that activate innate and adaptive immune responses. Human MC express all TLRs except TLR10 (58, 61) and they respond differentially depending upon the TLR that is being stimulated (22). TLR4 activation through its ligand bacterial lipopolysaccharide on murine MC releases proinflammatory cytokines TNF and IL-6 (62, 63). The importance of TLR4 was demonstrated *in vivo* using a 'MC knock-in' model where reconstitution of MC deficient mice with bone marrow derived MC from TLR4-mutated mice results in higher mortality than mice reconstituted with bone marrow derived MC from wild type mice (63).

Stimulation with peptidoglycan, the TLR2 ligand results in degranulation of human MC (22) and release of TNF, IL-5, IL-13, LTC₄, IL-1 β and granulocyte macrophage colony stimulating factor (64). The synthetic dsRNA polyinosinic-polycytidylic acid, the TLR3 ligand has been shown to release IFN α and IFN β from human MC (61). Moreover, agonists of TLR 3, 7, and 9 have been shown to release TNF, IL-6, CCL5, CCL3 from murine fetal skin derived cultured MC (65).

MC play a critical role in many disease conditions and the roles of MC in these disease conditions have been established using MC-deficient mice and their reconstitution with bone marrow derived MC in these animal models. For example, W/W^v mice carrying spontaneous loss-of-function mutation at both alleles of the dominant white spotting (W) locus (c-kit) exhibit a reduction in c-kit tyrosine kinase mediated signalling resulting in disrupted MC development and survival (66). W-sash (W^{sh}) is an inversion mutation in the transcriptional regulatory elements upstream of the c-kit transcription start site on mouse chromosome 5, that affect the c-kit expression (67). This mast cell deficient c-kit mutant mice (Kit^{W-sh/W-sh}) had a profound deficiency in MC with normal levels of other differentiated hematopoietic and lymphoid cells in tissues (68). Moreover, these mice are fertile and demonstrate milder abnormalities than W/W^v mice in terms of anemia and neutropenia.

For example, the importance of MC in asthma (69), arthritis (70), experimental allergic encephalitis (71), experimental bullous pemphigoid (72),

aortic aneurysms (73), cancer progression (74) and defence against parasitic and bacterial infections (58, 75, 76) has been demonstrated using these animal models.

1.1.7 Mast cell lines

MCs are tissue resident cells and their isolation through enzymatic dispersion of tissues creates difficulty over the potential effects of the isolation procedures on their functions. Even though peritoneal MC from rodents have been used in elucidating many MC functions, the heterogeneity among MC populations hinders the extrapolation of the findings with peritoneal MC to MC at different anatomical locations (11). Significant progress has been made in culturing MC from progenitors in rodent and human bone marrow, peripheral blood (77) and umbilical cord blood. In addition to being expensive and time consuming cultures, only low numbers of MCs are generated through these cultures. Moreover, the outcome of research studies with these cultured MCs cannot be generalized to the functions of MCs *in vivo* without care.

In spite of the availability of MC-deficient mice (W/W^v and W^{sh}/W^{sh}) to understand the role of MC *in vivo* in rodent models, extrapolation of results from rodents to human MCs is problematic (78). Thus, it is a common practice that initial research be conducted in human mast cell lines followed by validation of findings in primary human MCs. An overview of the two human MC lines we used in our studies is described below.

HMC-1 is an immature human MC line derived from the peripheral blood of a patient with MC leukemia by Joseph H. Butterfield at the Mayo Clinic, USA (79). It has been widely used as a source of immature human MCs. HMC-1 cells are sparsely granulated and contain low levels of histamine. They lack some

myeloid markers and IgE receptors. MC expresses the proto oncogene c-kit (CD117) that encodes a transmembrane tyrosine kinase receptor. Binding of the c-kit ligand, stem cell factor, to c-kit activates the receptor tyrosine kinase leading to autophosphorylation of tyrosine residues and association with its substrate phosphatidylinositol-3-kinase. This event is important in the differentiation and proliferation of many leukemic cell lines. In HMC-1 there is mutation of CD117 that leads to its constitutive phosphorylation in the absence of its ligand stem cell factor. Thus, HMC-1 cells proliferate rapidly and differentiate poorly, thereby expressing the immature MC phenotype.

A more mature MC line LAD2 was derived from bone marrow aspirates of a patient with MC sarcoma/leukemia at the Laboratory of Allergic Diseases, National Institutes of Health, USA (80). LAD2 are granulated and dependent on human stem cell factor for their growth and survival. Using electron microscopy LAD2 cells were 8-15 μm in diameter with rough surfaces and cytoplasmic projections. They express IgE receptors and can be activated by IgE cross-linking. LAD2 cells release about 40 % of their stores of β -hexosaminidase upon IgE/anti-IgE stimulation. LAD2 cells do not exhibit a c-kit activating mutation on codon 816 and hence require stem cell factor for their proliferation. LAD2 cells double in 2-3 weeks and despite the slower growth rate of LAD2 in comparison with HMC-1, they are widely used in studying the characteristics of human MC *in vitro*. Flow cytometry of LAD2 cells revealed that more than 98% are tryptase positive and 37% are both tryptase and chymase positive (80). However, a recent study using real-time PCR, western blot and tryptase, chymase activity assays

demonstrated that both HMC-1 and LAD2 MC lines express lower amount of tryptase and chymase and reduced protease activity in comparison to skin derived MC (81). Thus both MC lines have limited potential to serve as replacement for mature MC *in vivo*.

1.2 Nitric oxide

NO is a gas and a free radical. Robert Furchgott described an endothelium-derived relaxing factor that causes relaxation of vascular smooth muscle cells (82). Endothelium-derived relaxing factor was later confirmed as NO by demonstrating their indistinguishable properties such as biological activity, stability and susceptibility to an inhibitor and potentiator (83, 84). Robert F. Furchgott, Louis J. Ignarro and Ferid Murad shared the Nobel Prize for Medicine in 1998 for their discovery on NO as a signalling molecule in the cardiovascular system (85). Since the discovery of this molecule, significant progress has been made in NO research and NO is widely accepted as a critical intracellular and intercellular signalling molecule.

1.2.1 Nitric oxide synthesis

NO is biosynthesised as a by-product in the conversion of L-arginine to L-citrulline by nitric oxide synthase (NOS). A non-enzymatic production of NO from the reduction of nitrite in the acidic environment of gastric mucosa has also been reported (86). Nitrite solutions generate NO, the rate of which depends on both the nitrite and hydrogen ion concentration upon acidification (87). Growing evidence suggest the existence of NOS-independent pathway in mammals to synthesize NO (88). This pathway is considered as an alternative source of NO

generation under hypoxic conditions, the relevance of which needs to be studied in order to understand the precise molecular mechanisms of this pathway (88).

There are three isoforms of NOS, NOS1 (neuronal, nNOS), NOS2 (inducible, iNOS), and NOS3 (endothelial, eNOS). The three NOS are encoded by distinct genes located on different chromosomes. NO has high biological reactivity and diffusability and hence multiple tiers of regulation ranging from transcriptional to post-translational control exist in the regulation of NO synthesis. For example NOS2 is primarily regulated by transcriptional control, whereas NOS1 and NOS3 are regulated by post-translational mechanisms (89-91).

1.2.2 Actions of nitric oxide

NO synthesised by different NOS has different regulatory functions ranging from cell energetics to survival (91, 92). The expression of NOS1 was first characterized in neurons and the NO generated by this isozyme has a role as a neurotransmitter. However, the expression of NOS1 have been indentified in non-neuronal tissues including airways (93) and adrenal glands (94). NOS2 expression was first identified in activated macrophages and epithelial cells and has a protective role in host defence against microbes, parasites and tumors. Moreover, NO derived from this isozyme is also involved in pathophysiology of asthma (95), arthritis (96), neurogenerative diseases (97) and transplant rejection (98). NOS3 expression was reported initially in endothelium and regulates blood flow and blood pressure through vasodilatation. However, its expression is reported in multiple tissues like kidney (99), human testis (100), cardiac myocytes (101) and bronchial epithelium (102).

1.2.2.1 Activation of soluble guanylyl cyclase

NO is a free radical with an unpaired electron in its outer orbital and under physiological conditions has a short half life of 3 to 5 seconds. NO is a highly diffusible molecule with a diffusibility range of 15 to 300 μm for a time of 4 to 15 seconds under physiological conditions (103). NO and NO-derived reactive nitrogen species react with multiple targets inside the cell including lipids, DNA, thiols, amino acids and metals (104). Binding of NO with the heme group of soluble guanylyl cyclase (sGC) activates sGC and elevates intracellular 3',5'-cyclic guanosine monophosphate (cGMP) Figure 1.4 (105). NO binds to the sixth coordination position of heme iron of sGC and breaks the histidine to iron bond leading to formation of a five coordinated heme-nitrosyl complex (106). The opening of histidine-iron bond results in conformational change resulting in activation of sGC. cGMP is an important second messenger molecule that mediates multiple intracellular events including activation of ion channels, protein kinases and phosphodiesterases (107).

1.2.2.2 cGMP-independent pathways

In addition to its action through cGMP, NO also exerts its cellular action in a cGMP-independent manner (108) (Figure 1.4). NO combines with oxygen (O_2) to generate nitrogen dioxide (NO_2) which in turn combines with NO to yield higher order nitrogen oxides such as dinitrogen trioxide (N_2O_3). NO also combines with superoxide (O_2^-) to generate peroxynitrite (ONOO^-). Both N_2O_3 and ONOO^- are more powerful oxidants than NO and they react with an array of substrates such as thiols, esters, carbohydrates, lipids and DNA (109, 110). The

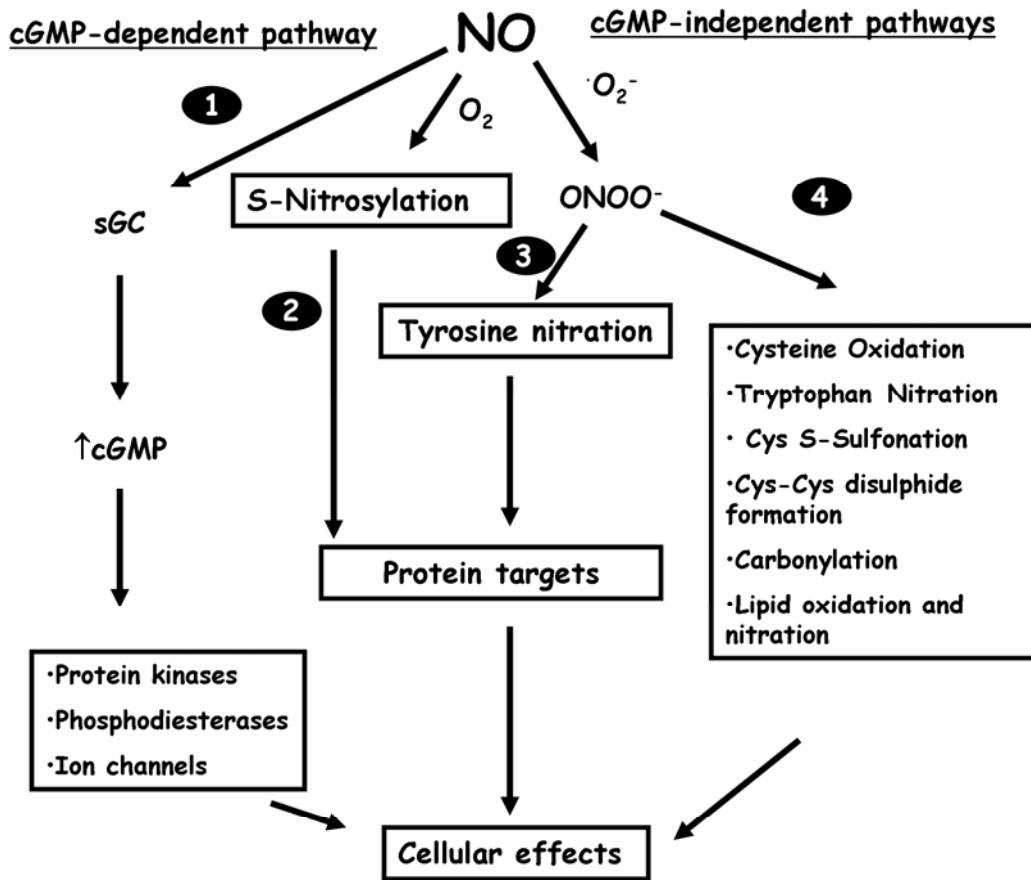


Figure 1.4 Effects of nitric oxide through cGMP-dependent and cGMP-independent pathways. 1) Nitric oxide (NO) activates sGC by binding with its heme group and elevates intracellular cGMP, which in turn activates protein kinases, phosphodiesterases and ion channels resulting in the cellular effects; 2) Nitric oxide nitrosylates some of the proteins and mediates its effects in this manner; 3) nitric oxide combines with superoxide that generates $ONOO^-$ which facilitates tyrosine nitration and 4) other post-translational modifications which mediate its effects on the cell.

post-translational modifications of proteins, S-nitrosylation of cysteine and nitration of tyrosine, are considered to be critical modifications in the effects of NO-derived reactive nitrogen species (111). The consequences and significance of these two modifications will be discussed in this section.

1.3 Nitrosylation

Nitrosylation is a covalent modification of a protein cysteine thiol by a NO group to generate S-nitrosothiol (S-NO) (Figure 1.4). Nitrosylation is reversible in nature and plays a significant role in NO-mediated signalling (112). The literature on protein nitrosylation is increasing and its consequences have been elucidated both in normal physiology and in many pathological conditions (113). Existence of denitrosylation mechanisms through specific denitrosylases such as S-nitrosoglutathione reductase and thioredoxin systems have been reported (114).

Nitrosylation-mediated conformational changes of target proteins results in the disruption of many signalling complexes. For example, nitrosylation of COX-2, the critical enzyme in the prostaglandin pathway increased its activity (115). By contrast, nitrosylation of mitochondrial cytochrome oxidase-c results in the inhibition of its activity in lung endothelial cells (116). Thus nitrosylation of proteins plays a pivotal role in redox-based signalling mechanisms of NO and implications of this regulation are gaining recognition in physiological and pathological conditions (117). With the advent of modern proteomic techniques many proteins were discovered as targets for this important post-translational modification induced by NO (118). Because of the relevance of protein tyrosine nitration to this thesis it is discussed in detail in the following section.

1.4 Protein tyrosine nitration

Protein tyrosine nitration is a post-translational modification in which there is addition of a nitro group (NO₂) at the 3-position on the phenolic ring of selected tyrosine residues in a protein (Figure 1.5) (119). Protein tyrosine nitration is a marker of reactive nitrogen species and serves as a foot-print of nitro-oxidative damage *in vivo* in animal models and human diseases (120). Protein tyrosine nitration has been used as a biomarker and predictor of progression in many diseases. For example, coronary artery disease has been associated with increased nitrotyrosine levels in patients, the levels of which were reduced upon statin therapy (121). This post-translational modification has also been detected under physiological conditions in multiple systems. Nitrotyrosine exists either as a protein-bound form or a free form *in vivo* and has been reported in association with many disease conditions, animal models of inflammation and in cell lines (122). Growing evidence supports that protein tyrosine nitration modifies cellular signalling pathways and that excessive or inappropriate nitration may be a pathogenic component in disease (123). The importance of this post-translational modification is gaining recognition with the discovery that many signalling proteins are targets for nitration (124).

1.4.1 Mechanisms of nitration

Tyrosine can be nitrated through multiple chemical mechanisms that have been extensively reviewed (125-127). The chemistry and possible pathways of protein tyrosine nitration are summarized in Figure 1.5. Protein tyrosine nitration can be accomplished in a two-step process. The initial step involves oxidation of

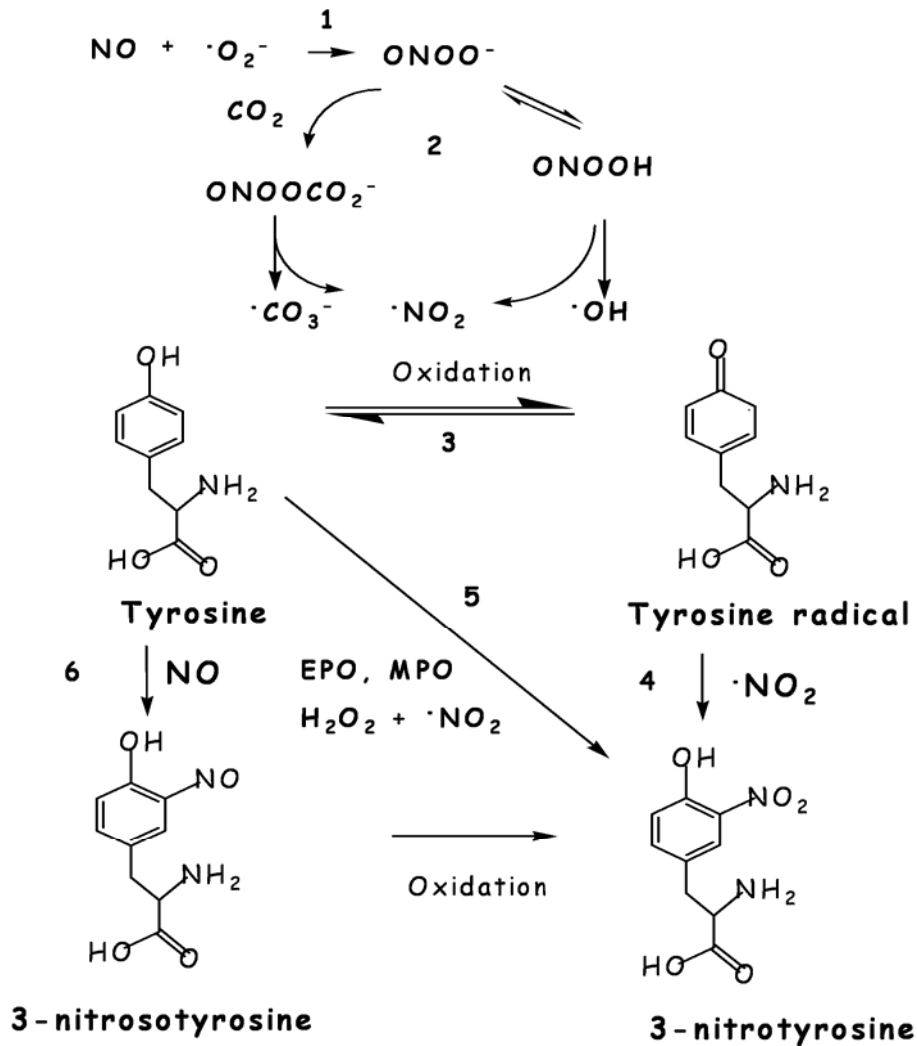


Figure 1.5 Pathways of nitration. 1) Nitric oxide (NO) combines with superoxide ($\cdot\text{O}_2^-$) to generate peroxynitrite (ONOO^-) ; 2) ONOO^- dissociate into either $\cdot\text{NO}_2$ and $\cdot\text{OH}$ or in presence of CO_2 generate nitrosoperoxy carbonate (ONOOCO_2^-) which can then dissociate into $\cdot\text{CO}_3^-$ and $\cdot\text{NO}_2$; 3) The oxidants into $\cdot\text{CO}_3^-$ and $\cdot\text{NO}_2$ and $\cdot\text{OH}$ oxidize tyrosine to tyrosyl radical ; 4) The tyrosyl radical combines with $\cdot\text{NO}_2$ to generate 3-nitrotyrosine ; 5) Eosinophil peroxidase (EPO) and myeloperoxidase (MPO) in the presence of H_2O_2 and $\cdot\text{NO}_2$ convert tyrosine into 3-nitrotyrosine; 6) The tyrosine combines with NO to form 3-nitrosotyrosine which upon two electron oxidation converts into 3-nitrotyrosine.

the phenolic ring of tyrosine (Tyr) to the one-electron oxidation product, Tyr radical (Tyr \cdot) by several one-electron oxidants such as $\cdot\text{CO}_3^-$, $\cdot\text{OH}$ and $\cdot\text{NO}_2$ (125). The next step is the addition of $\cdot\text{NO}_2$ to the Tyr \cdot in a radical-radical termination reaction.

Peroxynitrite is a powerful oxidant and nitrating agent that plays a major role in protein tyrosine nitration of proteins *in vivo* and *in vitro* (128). Peroxynitrite is formed by the rapid reaction between NO and $\cdot\text{O}_2^-$. Peroxynitrite is stable under alkaline conditions, whereas its protonated form peroxynitrous acid (ONOOH) decomposes rapidly by homolysis of its O-O bond to form $\cdot\text{NO}_2$ and $\cdot\text{OH}$ radicals (129). Under physiological conditions ONOO $^-$ combines with CO_2 to form nitrosoperoxycarbonate (ONOO CO_2^-) which homolysis into $\cdot\text{NO}_2$ and $\cdot\text{CO}_3^-$ that are the major one-electron oxidants of the aromatic ring of Tyr.

In addition to protein tyrosine nitration, ONOO $^-$ is a well known oxidant that mediates other modifications such as lipid oxidation and nitration (130), tryptophan nitration (131), carbonyl formation (132), cysteine sulfonation (133) and DNA damage (reviewed in detail (134)). Moreover, ONOO $^-$ has been shown to oxidize the cysteine residues of matrix metalloproteinase-2 and modulate the activity of this protein (135). Interestingly, in the presence of glutathione (GSH), an intracellular antioxidant, ONOO $^-$ mediates S-glutathiolation of cysteine residues of matrix metalloproteinase-2 (135). Thus *in vivo*, the outcome of ONOO $^-$ reactivity depends upon the microenvironmental conditions.

Alternatively, 3-nitrotyrosine can be formed by the reaction of Tyr \cdot with

NO to yield 3-nitrosotyrosine that can be oxidized to 3-nitrotyrosine by a two-electron oxidation process (pathway 6, Figure 1.5). Moreover, hemoperoxidases such as myeloperoxidase and eosinophil peroxidase in the presence of H₂O₂ and NO₂ facilitate 3-nitrotyrosine formation (136, 137).

The hydrophilic and hydrophobic environments of the target molecule greatly influences the mechanism and yield of 3-nitrotyrosine formation (125). Even though protein tyrosine nitration is a relatively common post-translational modification under physiological conditions and has been observed in a large number of proteins, the amount of 3-nitrotyrosine in comparison to tyrosine is very low. For example in inflammatory conditions the extent of protein tyrosine nitration reaches up to five 3-nitrotyrosine residues per 10000 tyrosines (138).

1.4.2 Factors determining the selectivity of nitration

In a biological system protein tyrosine nitration can be accomplished through multiple pathways (125). Several factors determine the mechanism of protein tyrosine nitration including the reactive nitrogen species available at a given time, the half-life kinetics of these radicals and compartmentalization of chemical reactions, availability of antioxidants and free radical scavengers and presence of inflammatory cells (138-140). In spite of multiple pathways in 3-nitrotyrosine formation, protein tyrosine nitration is a selective process where only few proteins are nitrated and only one or few tyrosines residues are modified within each protein (141). The potential mechanisms underlying this selectivity are summarized below.

Protein abundance and number of tyrosine residues: Most proteins contain tyrosine residues, however, neither the abundance of the protein nor the

number of tyrosines in a particular protein determines whether it is a target for protein tyrosine nitration (139, 141, 142). For example human serum albumin contains 18 tyrosine residues and is the most abundant plasma protein on a molar basis. However, human serum albumin is less extensively nitrated than other plasma proteins (139). Moreover, out of the 18 tyrosine residues only two tyrosines are susceptible to nitration when human serum albumin is treated with ONOO^- (143).

Nitrating agents: The outcome of nitration depends on the nitrating agent and the availability of a particular nitrating agent in the microenvironment. Different nitrating systems mediate nitration of different targets and/or nitration of different tyrosine residues in a particular protein. For example, ONOO^- facilitates nitration of a critical tyrosine residue Tyr³⁴ of a mitochondrial enzyme, manganese superoxide dismutase (MnSOD) and inhibits its activity (144). Interestingly, a cytochrome C/ H_2O_2 / NO_2 mediated nitration of MnSOD did not inhibit its activity suggesting that a different tyrosine residue was nitrated in this condition (145).

Microenvironment: Most of the nitrating agents have a short half life and hence proteins are nitrated depending upon the availability of these nitrating species in a particular microenvironment. Protein tyrosine nitration are predominant in sub cellular compartments that are known to generate nitrating species such as mitochondria (146, 147), peroxisomes of hepatocytes, peroxidase-containing secretory granules in eosinophils and neutrophils and the cytosolic side of the membrane of endoplasmic reticulum (148).

Primary sequence of the protein: There is no specific consensus sequence that promotes protein tyrosine nitration. However, the secondary structure of the protein and the local environment of the tyrosine residue influence the site of protein tyrosine nitration (141, 142). Nitrotyrosine is predominantly found in loop structures with turn-inducing amino acids such as proline or glycine. The presence of a nearby negative charge either at -1 position before the tyrosine or several acidic residues within five residues on either side of the tyrosine favors protein tyrosine nitration of that particular residue. The presence of sulphur containing residues such as cysteine or methionine near the tyrosine decreases the probability of protein tyrosine nitration, as these amino acids act as alternate targets for the nitrating agents and are often considered as intramolecular scavengers (141, 142). The presence of hydrophobic amino acids near the target tyrosine increases the susceptibility towards protein tyrosine nitration (141). However, many of these conditions are not applicable to metalloproteins that have a metal centre or a heme group (126).

1.4.3 Outcome of protein tyrosine nitration

Physiochemical properties: The acid dissociation constant (pK_a) values of amino acid side chains play a pivotal role in defining pH-dependent characteristics of a protein. The pK_a of the phenolic hydroxyl group of tyrosine is decreased from 10.1 to 7.2 upon nitration. At physiological pH the hydroxyl group of tyrosine is neutral, whereas it is 50% charged in 3-nitrotyrosine. In case of acidic pH, the hydroxyl group becomes uncharged and the 3-nitrotyrosine becomes more hydrophobic. Conversely in basic pH the higher tendency of 3-nitrotyrosine to carry a negative charge makes it more hydrophilic than tyrosine.

These effects influence the reactivity of tyrosine in multiple ways including prevention of phosphorylation.

Spectrophotometric properties: The absorption coefficient of nitrotyrosine is pH dependent. At acidic pH the absorption maximum is between 357 to 360 nm (149), whereas under basic conditions nitrotyrosine absorb at 427-430 nm (150). These properties are generally used to detect free nitrotyrosine using spectrophotometric analysis.

Structural properties: The addition of a nitro group increases the bulkiness of the tyrosine ring, thereby adding steric restriction on the tyrosine residue. The surface area of the phenolic ring in tyrosine is $\sim 30\text{\AA}^2$, whereas it is increased to $\sim 50\text{\AA}^2$ upon addition of a nitro group (151).

1.4.4 Functional consequences of protein tyrosine nitration

The functional outcome of protein tyrosine nitration depends on the protein, the extent of nitration and is briefly summarized in Figure 1.6.

Protein function: A wide range of proteins were reported as the targets for protein tyrosine nitration. The outcome of protein tyrosine nitration on protein function may: i) not change function, ii) decrease function or iii) increase function of the protein. The functional changes associated -with protein tyrosine nitration have been reviewed extensively (126, 152). Most of the studies were performed *in vitro* to understand the consequences of nitration of the particular protein. The effects of nitration on the function of the protein depend upon multiple factors including the specific tyrosines that are nitrated and the location of the tyrosine in the protein.

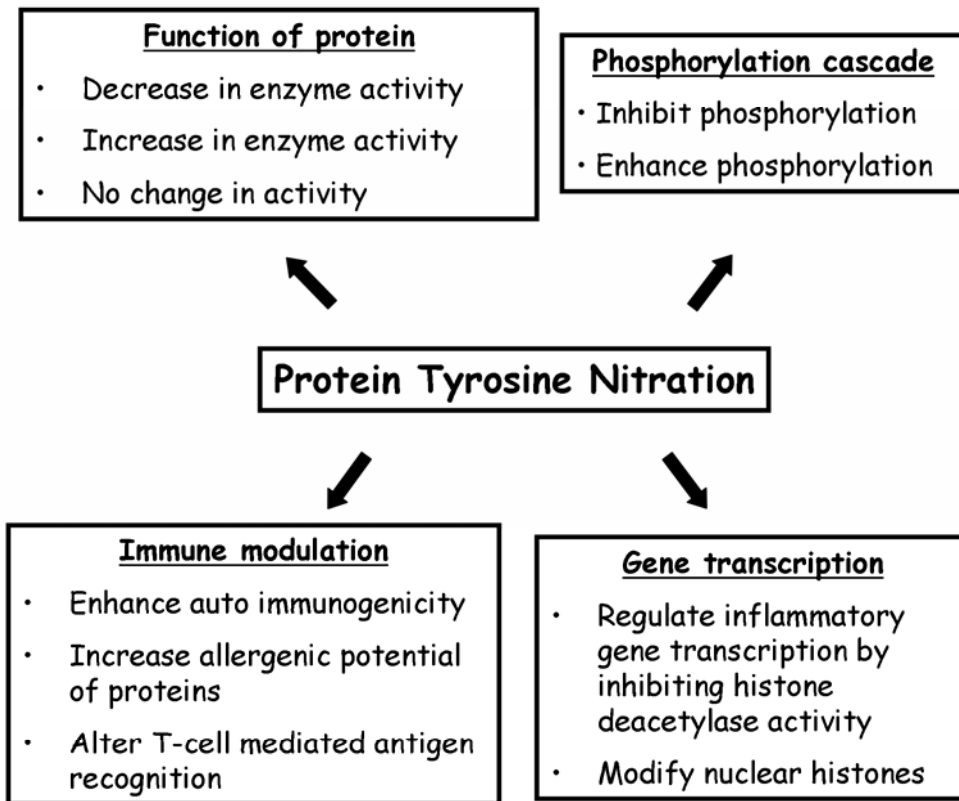


Figure 1.6 Consequences of protein tyrosine nitration. The outcome of protein tyrosine nitration depends on the target protein. The multiple effects are summarized viz. functional changes, phosphorylation events, immune modulation and gene transcription (126, 152).

Phosphorylation: Protein tyrosine nitration plays a major role in inflammation and increasing evidence demonstrates that protein tyrosine nitration serves as an indicator of an ongoing inflammatory process. Phosphorylation by tyrosine kinases are greatly inhibited by protein tyrosine nitration of the substrate peptides (153, 154). However, few reports claim enhancement of phosphorylation of c-Src tyrosine kinase after ONOO⁻ treatment (155). An imbalance of phosphorylation or dephosphorylation events can produce an overall modulatory effect. Since phosphorylation events are critical in the regulation of cellular signal transduction, interference by protein tyrosine nitration of tyrosine phosphorylation has been considered as a major hindrance in cellular signalling (153).

Proteasomal degradation: Protein tyrosine nitration increases the degradation of a protein by the proteasome (reviewed in detail (126)). Many factors including the presence of a nitro group, change in the pI of the protein, displacement of other amino acids and exposure of hydrophobic patches in the protein determine the outcome of proteasome recognition of nitrated proteins (126). For example nitration of tyrosine hydroxylase has been shown to decrease the steady state level enzyme by enhanced proteasomal degradation of nitrated tyrosine hydroxylase (156).

Immune modulation: Protein tyrosine nitration has been shown to trigger autoimmune responses by generating novel epitopes on self-proteins which otherwise were not recognized by the immune system (157). Thus accumulation of nitrated proteins can induce autoimmune responses and sustain a chronic inflammatory response (158). Moreover, nitration of a protein enhances its

allergenic potential by modifying the epitope (159). Protein tyrosine nitration plays a critical role in T cell-mediated antigen recognition. Immunogenic neoepitope formation because of protein tyrosine nitration of a tyrosine in the T cell receptor contact position has been reported (160). Protein tyrosine nitration of T cell receptor leads to CD8⁺ T cell tolerance and facilitates immune evasion by tumour cells (161).

Gene transcription: Under inflammatory conditions histone acetylation leads to transcription of genes that are critical in driving inflammatory responses. Histone deacetylases reverse the acetylation of core histones and thus play a critical role in regulating gene expression. Histone deacetylase-2 has been shown to be inactivated because of protein tyrosine nitration in lung epithelial cells (162). Moreover, histone deacetylase-2 from the lung of chronic obstructive pulmonary disease patients was also shown to be nitrated in this study. Corticosteroid induces histone deacetylase-2 and in case of steroid resistant chronic obstructive pulmonary disease patients, nitration of histone deacetylase-2 has been attributed to their impairment and the patients were unresponsive to corticosteroid-based anti-inflammatory drugs (163).

1.4.5 Denitration

Protein tyrosine nitration was considered a stable modification until evidence for the existence of denitrases was reported (164, 165). At a given time only a subset of nitrated proteins exist in a biological system. This depends upon the balance between nitration and denitration mechanisms along with protein turnover (166). In spite of evidence for denitrases, none of them have been

characterized and more research needs to be done to understand denitrases and their effects.

1.4.6 Proteomic analysis of nitration

There are multiple methods available to detect and quantify 3-nitrotyrosine as a free amino acid (167). However, these analyses of free nitrotyrosine in complex biological samples neither provide information on the identity nor the concentration of individual nitrated proteins. Proteomic studies have been employed to enumerate the “nitroproteome” of many complex biological samples. The concomitant application of two dimensional electrophoresis (2-DE), western blot using anti-nitrotyrosine antibodies and mass spectrometry has been successfully employed to define the nitroproteome of many cellular and tissue types (168, 169). There are many commercially available anti-nitrotyrosine antibodies that have been compared and characterized for their specificity to recognize nitrotyrosine (170, 171). The possibility of non-specific binding of anti-nitrotyrosine antibodies can be tested by reducing the nitrotyrosine to amino tyrosine using sodium dithionite (172).

Analysis of the nitroproteome facilitates identification of proteins that are selectively nitrated *in vitro* and *in vivo* under inflammatory conditions. Advances in proteomics and the possibility of refined analysis of the nitrated peptides of the target protein using mass spectrometric methods enable the identification of many targets in different cells, tissues and organs. There are many shortfalls in using a 2-DE immunoblot approach such as limited loading of the gels only resulting in identification of nitrated proteins that are abundant in the cell. The limitations of this approach are described in the discussion section

(section 4.5, Page 153). Moreover, the recovery of nitrated peptides from the gels is low and often the exact tyrosines that are nitrated cannot be identified using mass spectrometry. In spite of these difficulties, the 2-DE proteomic method remains the standard procedure to generate preliminary data on the nitroproteome of a biological system.

1.5 Mast cells and nitric oxide

1.5.1 Nitric oxide synthase expression and nitric oxide production in mast cell

Expression of all the three NOS isozymes were confirmed in MC using different techniques (reviewed in detail) (173). Many researchers including our research group have provided convincing evidence that MC generates NO (174-176). However controversy exists about NO production by MC (177). Since the earlier studies employed impure MC populations, NO derived from the contaminating cells has been shown to be responsible for some of the effects of NO on MC (178). However, using diaminofluorescein assay in human MC lines HMC-1 and LAD2 it has been demonstrated that MC generate NO (179). The difference among the strains of mice used in different studies and sensitivity of the biological assays used for measuring NO production in MC should be taken into consideration while studying NO production by MC (180). Given marked MC heterogeneity, it is tempting to speculate that similar heterogeneity exists in NOS expression in MC subpopulations. Moreover, microenvironmental factors and epigenetic regulation might regulate NOS expression in MC (181).

1.5.2 Nitric oxide and mast cells

NO has been implicated in the regulation of many MC functions and the following section summarizes the important research on NO in the regulation of MC function.

1.5.2.1 Mast cell degranulation

Endogenous and exogenous NO inhibits MC degranulation. The ability of NO to regulate mediator secretion from MC is considered to be physiologically relevant. NO inhibits the effects of MC-mediated histamine release such as vasodilatation, vasopermeation and leukocyte-endothelial attachment (182). Moreover, NOS inhibitors enhanced the degranulation of MC and increased intestinal permeability (183).

NO have been shown to inhibit histamine release from guinea pig and rat cardiac MC (178, 184), rat peritoneal MC (300 μ M of sodium nitroprusside) (185) and mouse bone marrow-derived MC (100 μ M of sodium nitroprusside) (186). Interferon gamma (IFN- γ) induced NO generation has been shown to inhibit IgE-mediated mediator secretion in peritoneal MC (187). Pretreatment of rat peritoneal MC with the NO donor S-nitrosoglutathione (SNOG) 1000 μ M for 24 h inhibits IgE/anti-IgE induced serotonin release from MC (188). Recently, the inhibitory effects of exogenous NO (10^{-4} mol.L⁻¹ of MAHMA NONOate [NOC-9] and diethylamine NONOate) on histamine release from human cultured MC were reported (189). The authors demonstrated NO should be generated at the time of activation of MC to exhibit its inhibitory action on MC degranulation.

In addition to its effects on degranulation, many other functions of MC were shown to be affected by NO. For example, IFN- γ -mediated NO production in rat basophilic leukemia (RBL-2H3) MC line inhibits its adhesion to fibronectin (190). Pretreatment with the NOS inhibitor L-NAME reduced the effects of IFN- γ , providing evidence for NO in the inhibition of MC adhesion. Moreover, pretreatment for 24 h with 500 μ M of NO donors (sodium nitroprusside and SNOG) also inhibited MC adhesion in this study. It also has been demonstrated that pretreatment for 3 h with either 250 μ M of S-nitroso-N-acetyl penicillamine or 100 μ M of SNOG inhibited adhesion of HMC-1 to fibronectin (191).

1.5.2.2 Mast cell cytokine and chemokine production

Pretreatment of RBL-2H3 and mouse bone marrow-derived MC with 500 μ M SNOG for 4 h inhibited the IgE/Ag-induced mRNA expression of many cytokines (182, 192). IFN- γ -mediated NO production has been shown to inhibit the expression and production of CCL1 and CXCL-8 in HMC-1 cells (180). A 100 μ M of SNOG pretreatment for 30 min mimicked the effects of IFN- γ in this study. A recent report demonstrated that exogenous NO (100 μ M of diethylamine NONOate) inhibited TNF and CXCL-8 production in human cultured MC in a cGMP-dependent manner (193). Since MC synthesize and release a wide range of cytokines and chemokines, NO may affect these mediators through selective pathways.

1.5.2.3 Mast cell lipid mediator production

Cysteinyl leukotrienes are peptide-conjugated lipids produced by many inflammatory cells including MC. They are well known for their potent

inflammatory effects. A 500 μM SNOG pretreatment for 30 min inhibits, whereas NOS inhibitor pretreatment potentiates cysteinyl leukotriene production from HMC-1 and LAD2 (179). Recently our lab reported that exogenous SNOG (100 μM , 5 h) treatment augmented COX-2 expression and enhanced production of COX-2-dependent PGD₂ in mouse bone marrow derived MC (194). Interestingly, a recent study demonstrated that exogenous NO (100 μM of diethylamine NONOate) decreased COX-1-dependent PGD₂ production and cysteinyl leukotriene production in human cultured MC (193). The study did not attempt to study the effects of NO on COX-2-dependent PGD₂ production as we reported. However, reproducible evidences of NO effects (193, 194) on COX-1-dependent PGD₂ production in human and mouse MC with different NO donors reinforce the inhibitory effects of NO on COX-1-dependent PGD₂ generation. Further research is required to elucidate the precise role of NO in prostaglandin pathways in MC.

1.5.2.4 Other effects of nitric oxide on mast cells

Exogenous SNOG (500 μM , 12 h) has been demonstrated to increase CD8 expression on rat peritoneal MC (195). Moreover, NO (sodium nitroprusside 5 μM) treatment potentiates TNF mediated cytotoxicity in rat peritoneal MC (196). The reported effects of NO in other cell types need to be studied in MC. Such research will enhance our knowledge on the effects of NO in MC biology and its relevance in health and disease.

1.5.3 Superoxide production by mast cells

Superoxide production in MC has been reported by many studies. Rat basophilic leukaemia (RBL-2H3) cells generate $\cdot\text{O}_2^-$ upon Fc ϵ RI stimulation

(197). Cypridina luciferin analog-dependent chemiluminescence which is specific for $\cdot\text{O}_2^-$ was used to demonstrate $\cdot\text{O}_2^-$ production by RBL-2H3 cells in this study. They also claim evidence for expression of p47^{phox} and p67^{phox}, the two major components of NADPH oxidase in RBL-2H3 cells (data not shown). The flavozyme inhibitor diphenyleneiodonium reduced $\cdot\text{O}_2^-$ production by RBL-2H3 cells and release of histamine and LTC₄. Protein expression of p40^{phox}, p47^{phox} and p67^{phox} was reported in RBL-2H3 cells (198). They also demonstrated that hydrogen ion-mediated inhibition of NADPH oxidase activity reduced $\cdot\text{O}_2^-$ production in RBL-2H3 cells. Both NADPH oxidase and mitochondria were shown to be the source of $\cdot\text{O}_2^-$ production in RBL-2H3 and mouse bone marrow derived MC (199). Silver induced $\cdot\text{O}_2^-$ production and the scavenging effect of superoxide dismutase was demonstrated in RBL-2H3 cells (200). Gliotoxin, a fungal metabolite has been shown to enhance $\cdot\text{O}_2^-$ production in RBL-2H3 cells (201).

Expression of mRNA of p47^{phox} and inhibition of $\cdot\text{O}_2^-$ by superoxide dismutase-like enzyme in the granules of rat peritoneal MC have been reported (202). Exogenous arachidonic acid induced $\cdot\text{O}_2^-$ production through enzymes that are located on the membrane and in the cytoplasm of rat peritoneal MC (203). *In situ* detection of $\cdot\text{O}_2^-$ production in the granules of MC has been demonstrated in rat esophagus, trachea, skin and intact mesentery (204). Presence of superoxide dismutase in the granules of rat peritoneal MC and $\cdot\text{O}_2^-$ release upon stimulation with compound 48/80 were reported (205). Moreover, this study also demonstrated that antigen-sensitized human lung fragments can generate $\cdot\text{O}_2^-$

upon stimulation with anti-IgE thereby providing indirect evidence for $\cdot\text{O}_2^-$ production by human lung MC.

Using flow cytometry and an intracellular $\cdot\text{O}_2^-$ specific probe dihydroethidium, it has been demonstrated that FcεRI aggregation on human MC and mouse bone marrow derived MC generates $\cdot\text{O}_2^-$ (206). This study also provided evidence for a NADPH oxidase-independent pathway such as 5-lipoxygenase-mediated $\cdot\text{O}_2^-$ production in MC. The reports on $\cdot\text{O}_2^-$ production by human MC lines such as HMC-1, LAD2 and human peripheral blood or cord blood derived MC is limited. However, recent studies in HMC-1 and cord blood derived MC demonstrate that NADPH oxidase-1 (NOX-1)-mediated reactive oxygen species production exists in human MC (207).

1.5.4 Mast cells and nitration

Endogenous and exogenous NO have been widely reported to inhibit many MC functions (reviewed in detail (173)). NO activates soluble guanylyl cyclase (sGC) and increases levels of intracellular 3',5'-cyclic guanosine monophosphate (cGMP), which in turn regulates numerous physiological events in the cell (105). However, many studies identified that non-cGMP mediated pathways are also important in the effects of NO on MC function (179, 191).

A previous study on guinea pig lung MC demonstrated that peroxynitrite can be produced upon antigen/antibody-mediated activation of these cells (208). Using confocal microscopy with anti-nitrotyrosine the authors demonstrated an increase in nitrotyrosine reactivity upon stimulation. Peroxynitrite scavengers were used in their study to demonstrate that ONOO^- production inhibits the

release of inflammatory mediators and intracellular calcium levels. Even though the study provides preliminary evidence for the presence of nitrated proteins in MC, attempts were not made to identify the targets of protein tyrosine nitration. Moreover, so far there is no evidence for the existence of protein tyrosine nitration in human MC.

Interestingly, a recent study using immunohistochemistry and confocal microscopy on lung sections of cystic fibrosis patients claims that there were no nitrotyrosine positive proteins in MC (209). Unfortunately isotype controls were not reported in this study and there was no information about optimization of sensitivity of the immunohistochemistry to detect nitrotyrosine reactivity in MC or the numbers of MC assessed in the tissues. Moreover, no attempts have been made to study protein tyrosine nitration and its relevance in MC biology.

1.6 Conceptual model, hypothesis and aims

Thus, although there is a large literature on MC and NO, there is no work that precisely identifies proteins targeted by tyrosine nitration in MC. We hypothesize that multiple targets for nitration exist in MC, and that NO, through ONOO^- , mediates its effect on MC by selective nitration of proteins (Figure 1.7). Identification of these targets will help to understand the molecular effects of NO on MC and other cell types.

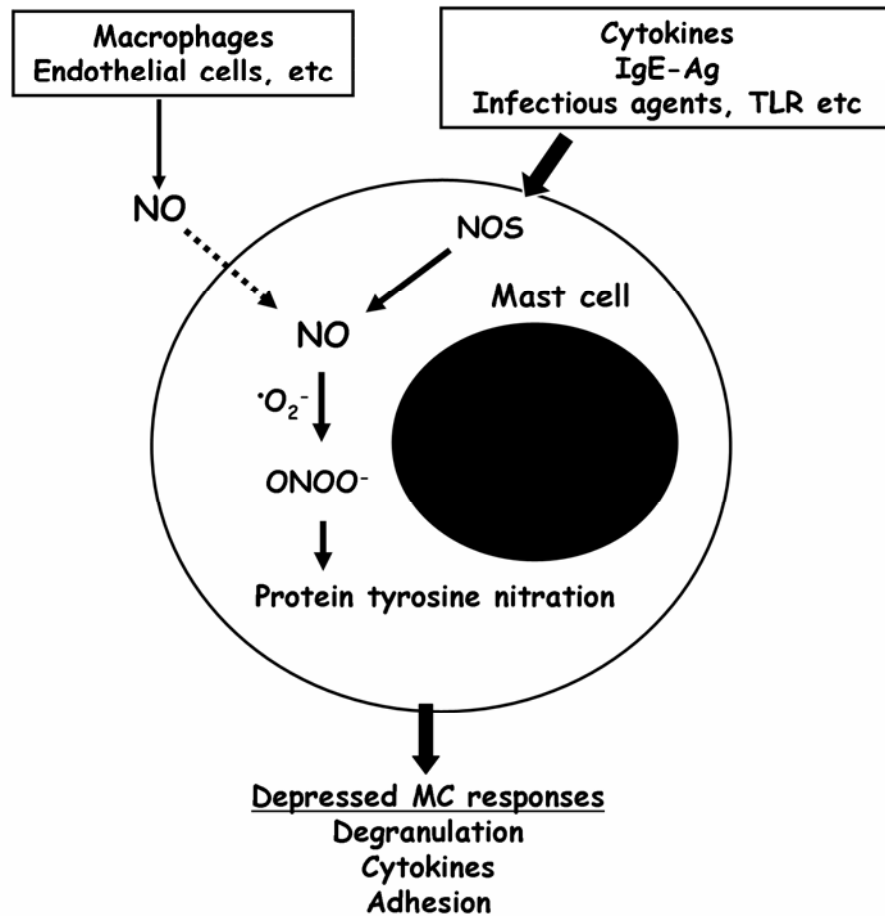


Figure 1.7 Conceptual model. Nitric oxide (NO) can be derived from exogenous sources such as macrophages or endothelial cells and/or from endogenous nitric oxide production through nitric oxide synthase (NOS) pathways induced by mast cell stimulation. Nitric oxide combines with intracellular superoxide radical ($\cdot O_2^-$) and generates peroxynitrite ($ONOO^-$), which in turn nitrates mast cell proteins. Nitration of critical mast cell proteins results in the alteration of mast cell responses including degranulation, adhesion and cytokine production.

This project involves an initial hypothesis-generating proteomic approach to identify targets for protein tyrosine nitration in MC, followed by a hypothesis-driven approach on the identified targets. The objectives of the study are addressed using the following aims:

Aim 1: To identify targets for protein tyrosine nitration in HMC-1 using exogenous NO donor.

Aim 2: To elucidate the effects of protein tyrosine nitration of the identified targets in MC function.

Aim 3: To validate the nitration target in LAD2 and to identify additional targets of protein tyrosine nitration.

Chapter -2 Materials and Methods

Chapter Two: Materials and Methods

2.1 Mast cell culture

2.1.1 HMC-1

HMC-1 cells were cultured in Iscove's medium (Invitrogen, Burlington, Ontario, Canada) with 5% heat inactivated fetal bovine serum (Invitrogen), 2 mM L-glutamine (Invitrogen) and 40 U/ml penicillin/streptomycin (Invitrogen). The cells were harvested in 48 h at about 75% confluency and were used if the passage number was <20. The seeding concentration between each passage was 1×10^5 cells/ml. The cells were maintained at 37°C in a humidified incubator at 5% CO₂. All the cell lines were screened for mycoplasma using Mycoalert® mycoplasma detection kit (Lonza, Rockland, ME) at monthly intervals. See section 1.1.7 (page 15) for a detailed description of the HMC-1 cell line.

2.1.2 LAD2

LAD2 cells, the growth factor-dependent human MC line (generously provided by A. S. Kirshenbaum and D. D. Metcalfe, Laboratory of Allergic Diseases, National Institutes of Health, USA) (80) was cultured in StemPro-34 medium (Invitrogen) supplemented with 100 ng/ml recombinant human stem cell factor (Peprotech, Rocky Hill, NY). LAD2 were cultured by hemidepletion (half of the old media replaced every week with new media containing stem cell factor) of medium every 7 d and maintained at a cell concentration $<5 \times 10^5$ /ml. LAD2 cells are used as an alternative to primary human MCs, as they express IgE receptors and can be activated by IgE cross-linking (80). Moreover, they release their granule contents upon stimulation by IgE cross-linking. The cells were

maintained at 37°C in a humidified incubator at 5% CO₂. See section 1.1.7 (page 16) for a detailed description of the LAD2 cell line.

2.1.3 Cord blood-derived mast cells

Human cord blood-derived mast cells were cultured as described previously (210, 211). Briefly, placentas were obtained within 45 min of delivery in adherence with ethics approval from the University of Alberta and Capital Health Region and informed patient consent at the Royal Alexandra Hospital, Edmonton, Alberta. EDTA-treated umbilical cord blood was diluted with the same volume of 10 mM phosphate buffer (pH 7.4) containing 150 mM NaCl and layered over histopaque-1077 (Sigma, Oakville, Ontario, Canada) at room temperature within 4 h of collection. The cord blood-derived MC progenitor fraction was obtained by centrifugation at 1000 g for 20 min at room temperature. The cells were washed twice with PBS and grown in tissue culture flasks for 8 wk in AIM-V medium (Invitrogen) with 100 ng/ml rhSCF. Non-adherent cells were transferred to fresh culture flasks and grown for ≥ 8 wk. CD117 and IgE receptor expression were confirmed by flow cytometry. All cells were maintained at 37°C in a humidified incubator at 5% CO₂.

2.2 Treatment of mast cells with nitric oxide donor

We chose a NO donor S-nitrosoglutathione (SNOG) (Calbiochem, San Diego, CA), whose dissociation rate is approximately 5% per hour in water at room temperature and the half-life is about 80 h at 37°C (212). SNOG is a well-known NO donor that favors a cGMP-independent mechanism of action of NO in different systems (213). Five hundred μ M SNOG has been widely used in

different studies on MC and inhibits MC function (179, 191, 192, 214). Moreover, SNOG has been used at up to 2 mM for 4 h to induce nitration in MCF-7 cells (215). Hence our use of 500 μ M SNOG over 4 h was designed to be consistent with physiological release of NO under some *in vivo* conditions. It has been demonstrated that photolysis of SNOG at physiological pH generates ONOO⁻ that potentially nitrates tyrosine into 3-nitrotyrosine (216). However, we did not confirm this in the current study. For the sham control, cells were treated with equivalent volumes of the vehicle (distilled H₂O) in the culture media (volume/volume ratio of 1/40 of vehicle/media). The viability of the cells was documented before and after treatment with SNOG using trypan blue dye exclusion and viability in all experiments was >95%.

2.3 One dimensional gel electrophoresis

Sodium dodecyl sulphate polyacrylamide gel electrophoresis (SDS-PAGE) was performed using standard procedures. A 10% resolving gel was prepared using the following recipe: (30% acrylamide - 3.33 ml ; 1.5 M Tris HCl pH 8.3 – 2.5 ml; double distilled water 3.933 ml; glycerol – 100 μ l; 10% SDS- 100 μ l; tetramethyl ethylene diamine (TEMED)- 5 μ l; 10% ammonium per sulphate - 50 μ l. A 5 % resolving gel was prepared: 30% acrylamide – 1.0 ml ; 0.5 M Tris HCl pH 6.8 -1.5 ml; double distilled water - 2.34 ml; glycerol – 90 μ l; 10% SDS- 60 μ l; TEMED- 12 μ l; 10% APS - 60 μ l. Running buffer (25 mM Tris; 0.1% SDS; 192 mM glycine) was prepared and used in the electrophoresis procedure. A standard voltage of 130 V was applied and the gel was run in the cold room until the loading dye reached the bottom of the gel. For mass

spectrometry analysis the gels are fixed using 50% ethanol and 2% phosphoric acid solution for 30 min and washed with distilled water for 20 min, followed by staining with coomassie G-250 stain (0.12% coomassie G-250; 10% ammonium sulphate; 10% phosphoric acid and 20% methanol (217). Alternatively, silver staining using a PlusOne silver staining kit (GE Healthcare, Piscataway, NJ) was performed for better visualization of low abundance proteins. The images were captured using the AlphaimagerTM 2200 (AlphaInnotech, San Leandro, CA).

2.4 Two dimensional gel electrophoresis (2-DE)

MC were removed from the flasks after gentle pipetting to remove all the adherent cells and centrifuged at 300 g for 5 min, 4°C and washed three times with ice cold PBS. The washed cell pellets were stored at -80°C until further use. The cell pellet was lysed by vortexing at high speed for 2 min in 2-DE cell lysis buffer [9 M urea, 4% 3-[(3-cholamidopropyl)dimethylammonio]-1-propanesulfonate (CHAPS), 50 mM dithiothreitol (DTT), 0.5% IPG 3-10 ampholytes (Bio-Rad, Mississauga, Ontario, Canada), 10 µl Protease Arrest (cocktail of protease inhibitors containing reversible and irreversible inhibitors of serine, cysteine, calpain and metalloproteases) from Genotech (St. Louis, MO)] and incubated on ice for 60 min for protein denaturation and solubilization. Cell lysates were collected and stored at -80°C in 100 µl aliquots after centrifuging the homogenate at 17530 g for 20 min at 4°C. Protein concentration was determined using the Bradford reducing agent and detergent compatible protocol (Bio-Rad). The 2D cleanup kit (Bio-Rad) was used according to the manufacturer's instruction. The protein pellet were reconstituted in 2-DE rehydration buffer (8 M

urea, 1.5% CHAPS, 0.2% DTT, 0.2% IPG 3-10 ampholytes) with a final concentration of 75 µg of protein in 125 µl of rehydration buffer and loaded onto 7 cm pI 3-10 linear IPG strips (Bio-Rad). The following isoelectric focusing (IEF) conditions were applied: for 7 cm pI 3-10 linear immobilized pH gradient (IPG) strips (50 V 10 min, 250 V 30 min, 750 V 60 min, 8000 V 13000 volt-hours); for 7 cm pI 4-7 linear IPG strips (4000 V 10,000 volt-hours). After IEF the strips were equilibrated for 10 min with equilibration buffer A [1% DTT, 6 M urea, 30% glycerol, 2% SDS, 50 mM Tris-HCl (pH 8.8), 0.0002% bromophenol blue] followed by 10 min with equilibration buffer B [2.5% iodoacetamide, 6 M urea, 30% glycerol, 2% SDS, 50 mM Tris-HCl (pH 8.8), 0.0002% bromophenol blue]. Strips were loaded in Ready Gel Tris-HCl 10 % gel (IPG) (Bio-Rad) and sealed with PROTEAN Plus overlay agarose (Bio-Rad). The proteins were separated at 130V. Gels were stained with PlusOne silver staining kit (GE Healthcare) and images were captured using AlphaimagerTM 2200 (AlphaInnotech).

2.5 Western blot

Proteins were transferred to polyvinylidene fluoride membranes Immobilon-P pore size 0.45 µm (Millipore, Billerica, MA), using the Transblot SD Semidry transfer system (Bio-Rad) at 15V for 90 min. Bjerrum and Schafer-Nielsen transfer buffer with SDS (48 mM Tris; 0.375 % SDS; 39 mM Glycine; 20% methanol) was used for the SEidry transfer. Membranes were blocked for 60 min at room temperature with 5% non-fat milk (Bio-Rad) in Tris buffered saline (pH 7.4) containing 0.05% tween-20 for anti-nitrotyrosine antibody, and with 5% BSA (Sigma) for anti-aldolase antibody, respectively. Rabbit polyclonal anti-

nitrotyrosine antibody was purchased from Upstate (Millipore, Etobicoke, Ontario, Canada); goat polyclonal anti-rabbit muscle aldolase antibody from Chemicon (Billerica, MA); anti-15 hydroxy prostaglandin dehydrogenase polyclonal antibody from Cayman Chemical (Ann Arbor, MI) and secondary antibodies were from Jackson ImmunoResearch Laboratories Inc. (West grove, PA). Rabbit IgG (Jackson ImmunoResearch Laboratories Inc.) and goat IgG (Chemicon) were used as isotype controls. Nitrotyrosine positive controls (a combination of three proteins: nitrated bovine superoxide dismutase ~16 kDa, nitrated bovine serum albumin ~66 kDa, nitrated rabbit muscle myosin ~212 kDa) were purchased from Millipore. Membranes were incubated overnight with primary antibodies (1:1000 dilution) and with horseradish peroxidase conjugated secondary antibodies (1:10000 dilution) and were visualized using Enhanced Chemiluminescence (Amersham Biosciences, Piscataway, NJ). Images were captured with high performance chemiluminescence Hyperfilm (GE Healthcare). Membranes were stripped using stripping buffer (62 mM Tris base; 69 mM SDS; pH adjusted to 6.7). Three hundred fifty μ l of β -mercaptoethanol was added to the 50 ml of stripping buffer in a 50 ml falcon tube and the membranes were incubated at 50°C for 30 min to achieve maximum stripping. The membranes were washed with Tris buffered saline with 0.1% tween (TBS-T) for 30 min and then blocked with 5% BSA and reprobbed with a different antibody. All the antibodies used in this study are summarized in Appendix 1, Table-1.

We standardised a protocol that greatly reduced the background in western blot studies using anti-nitrotyrosine antibody. We included a 10 min washing step

with 3 M urea in TBS-T, immediately after primary and secondary antibody steps which drastically reduced the background in western blot. Moreover, commercially available blocking agents contain significant levels of nitrotyrosine which leads to non-specific binding of anti-nitrotyrosine antibody and high background staining. Even though we did not check this in our study, powdered milk and bovine serum albumin have been shown to be endogenously nitrated and replacement of the blocking agent with a different lot can reduce the background (<http://www.millipore.com/userguides/tech1/mcproto423>).

2.6 Dithionite reduction

The specificity of anti-nitrotyrosine antibody was demonstrated by treating the PVDF membranes after the protein transfer with 100 mM sodium dithionite (Sigma) in 50 mM sodium borate buffer (pH 9.0) for 2 h at room temperature. Dithionite treatment reduces the nitro group into an amino group, thereby preventing the antibody binding with the nitrated epitope. After dithionite treatment membranes were washed three times with distilled water (5 min each wash) followed by blocking with Odyssey blocking buffer (Li-Cor Biosciences, Lincoln, NE). Secondary antibodies were goat anti-rabbit 800 (Li-Cor; 1:10,000) and goat anti-mouse 680 (Li-Cor; 1:10,000). Blots were visualized with an Odyssey imager (Li-Cor) by scanning simultaneously at 700 and 800 nm. Odyssey software was used for molecular weight determination and quantitation of bands in western blots.

2.7 Aldolase enrichment

An immunoaffinity column was constructed by coupling CNBr-activated sepharose 4B with polyclonal goat anti-aldolase antibody using standard protocols

(218). Briefly, about 5 mg of goat polyclonal antibody against rabbit muscle aldolase was coupled with 2 g of CNBr-activated sepharose 4B (Sigma Aldrich). Similarly, 5 mg of goat IgG was coupled with 2 g of CNBr-activated sepharose 4B and packed in a plastic column and used for preclearing the crude cell lysate (Figure 2.1). HMC-1 and LAD2 cell lysates were precleared in the IgG column and the flow through was applied to the anti-aldolase column and left at room temperature for 60 min to achieve maximum binding with the antibody. After binding, the column was washed with 50 ml of wash buffer. The bound proteins were eluted using low pH elution (glycine 2.5 pH). About 2 ml of the elution fractions were collected and neutralised with 18 μ l of 2 M Tris buffer (pH 11.2). The protocol is outlined in Figure 2.1. The eluted fractions (2 ml) were concentrated to 200 μ l by centrifuging at 5000 g for 30 min using 10 kDa cut-off centrifugal filters (Millipore). The concentrated fractions were separated in a 10% SDS-PAGE gel and transferred to PVDF membrane for western blot analysis. A preparative 10% gel was run with the eluted fractions and silver staining was used to visualise the protein in the gel. The band at ~40 kDa was cut into small pieces in sterile conditions, stored in 1.5 ml eppendorf tubes with sterile water and submitted for mass spectrometry analysis.

2.8 Mass spectrometry

Mass spectrometry (MS) in-gel tryptic digestion, peptide extraction and MS analysis were performed using standard protocols at the Mass Spectrometry Facility, Department of Chemistry, University of Alberta. Briefly, proteins in the

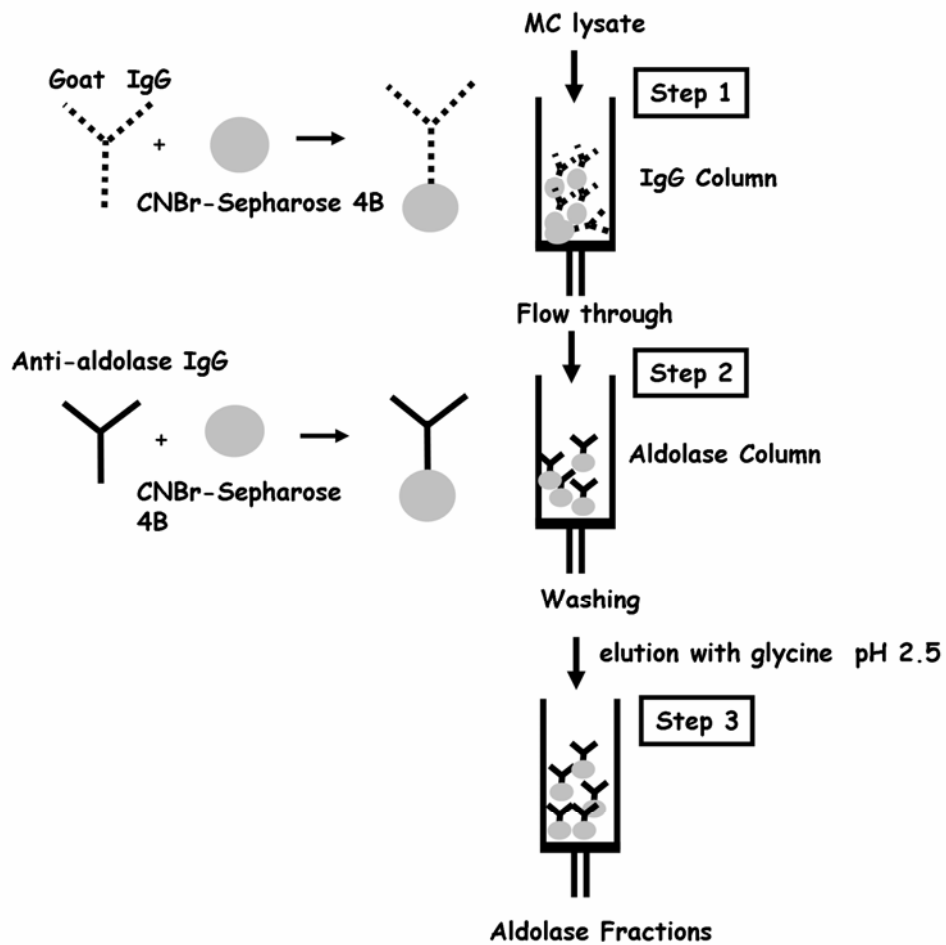


Figure 2.1 Affinity purification of mast cell aldolase. Step 1) Mast cell lysate was precleared using IgG column; step 2) The precleared lysate was passed through the aldolase column; step 3) After washing, proteins bound with aldolase antibodies were eluted using glycine pH 2.5 and the enriched fractions were collected.

gel were reduced with 5 mM DTT and carbamidomethylated with 10 mM iodoacetamide followed by tryptic digestion overnight with 0.06 µg/µl modified bovine trypsin (Fisher Scientific, Mississauga, Ontario, Canada) at 30°C. Five µl of the resultant peptide digests was loaded onto a nanoAcquity ultra performance liquid chromatography system with peptide trap (180 µm x 20 mm, Symmetry® C18 nanoAcquity™ column, Waters Corporation, Milford, MA) and a nano analytical column (75 µm × 100 mm, Atlantis™ dC18 nanoAcquity™ column, Waters Corporation). Desalting on the peptide trap was achieved by flushing the trap with 1% acetonitrile, 0.1% formic acid at a flow rate of 10 µl/min for 3 min. Peptides were separated with a gradient of 2-95% solvent B (acetonitrile, 0.1% formic acid) over 35 min at a flow rate of 300 nl/min. The column was connected to a quadruple time of flight (Q-ToF) premier mass spectrometer (Waters Corporation) for electrospray ionization tandem mass spectrometry (ESI-MS/MS) analysis. Obtained tandem mass spectrometry (MS/MS) data were analyzed using proteomic software PEAKS (Bioinformatics Solutions Inc., Waterloo, Ontario, Canada). Database searches were done with the following settings: carbamidomethylation as fixed modification and oxidation as the variable modification. Peptide identifications were further confirmed by examination of the scores and manual inspection of the original MS/MS spectra. Good spectra with significant numbers of matched high intensity peaks were considered important for the identification of protein.

2.9 RT-PCR

Total RNA was extracted from the MC with RNeasy® Plus mini kit (QIAGEN, Mississauga, Ontario, Canada) according to the manufacturer's

instructions, quantified by measuring optical density at 260 nm, and assessed by applying RNA to 1.2 % formaldehyde-agarose gels. cDNA was synthesized using SuperScript™ First-Strand Synthesis System for RT-PCR (Invitrogen). Five µg of total RNA from each sample was used as template for the reverse transcription reaction. The RNA/primer mixture (5 µg total RNA, 0.5 µg oligo(dT)₁₂₋₁₈ primers and 0.5 mM dNTP mixture in RNase free water) was incubated for 5 min at 65°C, then on ice for 1 min. The reaction mixture [40 units (U) RNase inhibitor in 20 mM Tris-HCl (pH 8.4), 50 mM KCl, 5 mM MgCl₂, 10 mM DTT] was added and incubated at 42°C for 2 min. Then 50 U of SuperScript™ II reverse transcriptase were added and the reaction was continued for 50 min at 42°C, 15 min at 70°C and chilled to 4°C on ice. Before proceeding to PCR, 2 U of RNase H were added and incubated for 20 min at 37°C. Twenty µl of cDNA were diluted to 100 µl for use in PCR amplification. Ten µl of cDNA was used for PCR with recombinant Taq DNA Polymerase (Invitrogen). Human kidney cDNA was a kind gift from Philip F. Halloran, Division of Nephrology, University of Alberta. PCR was carried out with iCycler (Bio-Rad). Isoform-specific primers were designed based on the published human aldolase sequences (Table 2.1). The conditions for PCR amplification were: denaturing at 95°C for 30 s, annealing at 55°C for 30 s and extension at 72°C for 1 min, 25 cycles. The PCR products were analyzed by 1 % agarose gel electrophoresis with ethidium bromide staining and confirmed by automated sequencing using a CEQ2000XL DNA sequenator (Beckman Coulter, Mississauga, Ontario, Canada) at the Biochemistry Department, University of

Table 2.1 RT-PCR primers for identification of aldolase isoforms in human mast cells

gene	Chromosome location	Accession number	Total number of base pairs	Sense primer (location in the coding sequence within parenthesis)	Anti-sense primer (location in the coding sequence within parenthesis)	Amplicon size
Aldolase A	16q22-q24	NM_000034	2353	tgtgggcatcaaggtagaca (1319 to 1339)	caggaaggtgatcccagtg (1802-1821)	603
Aldolase B	9q21.3-q22.2	NM_000035	1669	gatcgtggtgggaatcaagt (431-450)	cgctcataaaagcctcctg (1098 to 1117)	687
Aldolase C	17cen-q12	NM_005165	1665	agcgtacaccctctgcactt (612-631)	agcgtacaccctctgcactt (1039-1058)	447

Alberta. The protocols were standardised by Tae Chul Moon, Research Associate in our lab.

2.10 Aldolase enzyme assay

HMC-1 and LAD2 cells (2×10^6 cells) were treated with 50 μ l of water (sham) or 500 μ M SNOG in 2 ml media (containing 5 % FBS in HMC-1 media, no FBS in LAD2 media) for 4 h at 37 °C and 5 % CO₂, and the cell pellets that were resuspended in 1 ml of Tris buffer (pH 7.4) containing protease inhibitors were rapidly frozen in liquid nitrogen. The frozen cell lysate was subjected to ultrasound treatment for 5 min at 22°C in an ultrasonic bath (FS 30H, Fisher Scientific, Ottawa, Ontario, Canada). Three cycles of freeze-thawing were performed followed by centrifugation at 17,530 g for 15 min at 4°C. The supernatant of cell lysate was kept on ice until measurement of activity. The hydrazine assay (219, 220) was used to measure total aldolase activity in 100 μ l of cell lysate using fructose-1,6-bisphosphate (FBP) as the substrate and hydrazine sulfate as the detection reagent for 3-phosphoglyceraldehyde produced by the reaction. One enzyme unit was described as a change in absorbance of 1.00 per min at 25°C, pH 7.5, and 240 nm wavelength. To calculate the maximum velocity V_{\max} and the Michaelis-Menten constant K_m , the enzymatic activity was measured using a range of substrate FBP concentrations (3.125 μ M to 800 μ M). K_m and V_{\max} values from aldolase activity in terms of change in OD values ($\Delta A_{240}/2 \times 10^5$ cells/min) were calculated using the Michaelis-Menten equation in a non-linear fitting (solver function in Microsoft Excel, Microsoft, Redmond, WA).

2.11 Fructose-1,6-bisphosphate measurement

HMC-1 and LAD2 (1×10^7 cells) were sham treated or treated with 500 μM SNOG for 4 h at 37 °C and 5 % CO_2 . The cells were washed with PBS and the cell pellet was deproteinized using 100 μl of 5% trichloroacetic acid for 15 min on ice and then neutralized with 12 μl of 2 M Tris (pH 11.2). The cell extracts were centrifuged at 17530 g for 20 min and the supernatants containing the metabolite fractions were analyzed for their FBP content. The standard protocol for measuring FBP (219, 221) was used with minor modifications. Briefly, the sample was incubated for 5 min at 22°C with aldolase (rabbit muscle aldolase, Sigma), the enzyme that cleaves FBP into dihydroxyacetone phosphate and D-glyceraldehyde 3-phosphate. Dihydroxyacetone phosphate and glyceraldehyde 3-phosphate are interconverted by the enzyme triose-phosphate isomerase. Glycerol-3-phosphate dehydrogenase catalyzes the reduction of dihydroxyacetone phosphate by NADH. The kinetic measurement of depletion of NADH at 340 nm was measured for 5 min at 22°C in a costar-48 well plate containing 170 μl of 400 mM triethanolamine buffer (pH 7.6), 100 μl of FBP standards, 10 μl of 4.2 mM β -NADH, 10 μl of glycerol-3-phosphate dehydrogenase and triose-phosphate isomerase to give the initial reading. Then 10 μl of rabbit muscle aldolase (0.25 units/ml) was added to the reaction mixture followed by measurement at 340 nm every minute for 5 min at 22°C. Rabbit muscle aldolase and FBP (Sigma) were used to obtain a standard curve and the OD values were calibrated with this curve to quantitate FBP levels in HMC-1 and LAD2 cell lysates.

2.12 Mast cell degranulation assay

LAD2 (1×10^6 cells) were seeded in a six-well plate and sensitized with 1 $\mu\text{g/ml}$ human IgE (Chemicon) overnight at 37°C . Cells were treated for 4 h with 500 μM SNOG, 5 mM FBP, 5 mM fructose-1-phosphate or 5 mM fructose-6-phosphate. Cells were washed and resuspended in HEPES-buffered Tyrode's solution at a concentration of 200,000 cells/200 μl (pH 7.2) followed by stimulation with 10 $\mu\text{g/ml}$ mouse anti-human IgE antibody (Dako, Mississauga, Ontario, Canada) for 30 min at 37°C . The cells were centrifuged and the supernatant was aliquoted and 25 μl was loaded in 96-well black plates (Corning) in triplicates. Two hundred μl of HEPES-buffered Tyrode's solution was added to the cell pellets and crude cell lysate was prepared by freeze-thawing three times using liquid nitrogen and sonication as mentioned earlier (section 2.10, page 56). Twenty five μl of the corresponding cell lysates were loaded in the 96-well plates. Twenty five μl of HEPES-buffered Tyrode's solution was added into all the wells and 50 μl of substrate solution (1 mM 4-methylumbelliferyl N-acetyl- β -D-glucosaminide in 0.2 M sodium citrate buffer pH 4.5), was added to each well and incubated at 37°C for 60 min. The fluorescence was measured using a FL_X800 microplate fluorescence reader (Biotek Instruments, Winooski, VT) at excitation 360 nm and emission at 460 nm. The percentage of β -hexosaminidase release into the supernatant was calculated as described previously (222):

$$\% \beta\text{-hexosaminidase release} = \frac{\text{amount of } \beta\text{-hexosaminidase released in supernatant}}{\text{(\beta-hexosaminidase in supernatant + } \beta\text{-hexosaminidase in cell pellet)}} \times 100$$

2.13 Nuclear magnetic resonance analysis of HMC-1 metabolites

HMC-1 (1×10^8 cells) were treated in their growth media with sham or 500 μM SNOG for 4 h at 37°C. Cells were centrifuged at 300 g for 5 min at 4°C. One ml of supernatant was collected from each and stored at -80°C until NMR analysis. Cell pellets were washed with ice cold PBS and metabolites from the cell pellets were extracted using a modified methanol/chloroform extraction procedure as described in Bligh and Dyer (223). Briefly, cells were treated with 500 μl of methanol : chloroform mixture (2:1) in ice, followed by rapid freezing in liquid nitrogen. Three cycles of freeze-thawing were performed, followed by the addition of 100 μl of ice cold methanol and 100 μl of water. The cell lysates were centrifuged at 100 g for 15 min and 400 μl of the top layer containing metabolite fractions were aliquoted, frozen, lyophilized and stored at -80°C until NMR analysis. Cell culture supernatants were filtered through 3000 Dalton cut-off filters. Cell lysate samples were prepared for NMR analysis by the addition of 185 μl distilled H_2O and 65 μl of internal standard containing 5 mM 2,2-dimethyl-2-silapentane-5-sulfonate and 0.2% NaN_3 in 100% D_2O (deuterium oxide). Filtered cell supernatants were prepared by the addition of 65 μl of internal standard to 585 μl of supernatant. Sample pH was adjusted to 6.8. One-dimensional NMR spectra of the extracted metabolite fractions were acquired using the first increment of the standard NOESY pulse sequence on either a four-channel Varian (Varian Inc., Palo Alto, CA) Inova-800 MHz (cell lysate samples) or 600 MHz (cell supernatants) NMR spectrometer. All spectra were recorded at 25°C with a 12 ppm sweep width, 1 s recycle delay, 100 ms mixing time (τ_{mix}), an

acquisition time of 4 s, 4 dummy scans, and 32 transients as previously described (224). ^1H decoupling of the water resonance was applied for 0.9 s of the recycle delay and -during the 100 ms mixing time. All spectra were zero-filled to 128k data points and multiplied by an exponential weighting function corresponding to a line-broadening of 0.5 Hz (224). All the NMR analyses were conducted at the National High Field Nuclear Magnetic Resonance Centre (NANUC), University of Alberta and Dr. Carolyn M. Slupsky analyzed the results.

2.14 ATP assay

HMC-1 and LAD2 (1×10^6 cells) were treated as before with sham or 500 μM SNOG for 4 h in 6 well culture plate at 37°C (Becton Dickinson, Mississauga, Ontario, Canada). Five thousand cells in 5 μl media were loaded in 96 well flat bottom black plates (Costar) in triplicates. ATPlite 1step Luminescence ATP detection assay kit was used to quantitate ATP in the viable cells by luminescence measured using an I450 Micro Beta Scintillation and Luminescence detector (both from PerkinElmer, Woodbridge, Ontario, Canada).

2.15 Calcium assay

The free intracellular calcium levels of LAD2 cells were measured using Flou-4NW calcium assay kit (Invitrogen, Burlington, Ontario, Canada). One million LAD2 cells were sensitized with 1 $\mu\text{g}/\text{ml}$ of human IgE in media (Chemicon) overnight at 37°C in a six well plate. The sensitized LAD2 were pretreated for 4 h with either 500 μM of SNOG or FBP at increasing concentrations (100, 1000 and 5000 μM). Fructose-1-phosphate and fructose-6-phosphate were used as controls to FBP in these experiments. The cells were

washed three times @ 200 g for 3 min with Hanks' balanced salt solution (Gibco). The cells were reconstituted to a final concentration of 125,000 cells/ 50 µl of the assay buffer. Fifty µl of the sham treated and SNOG or FBP treated cells and 50 µl of dye loading solution (from the assay kit) were loaded in 96-well black plates and kept 30 min at 37°C. The plate was incubated in room temperature for 30 min and the baseline fluorescence was measured using kinetic measurement for 100 sec at 9 sec intervals using FL_X800 microplate fluorescence reader (Biotek Instruments) at excitation 485 nm and emission at 516 nm. The LAD2 cells in the 96-well plate were activated with 10 µg/ml of anti-IgE (Dako) and the kinetic measurement was performed for 10 min at room temperature. The protocols were standardised by Tae Chul Moon, Research Associate in our lab.

2.16 Statistical analysis

Data were analyzed with unpaired student's t-test or one-way analysis of variance (ANOVA) followed by the Tukey-Kramer multiple comparisons. *P* values < 0.05 were considered significant. Graphpad prism version 5.0 (La Jolla, CA) was used in graphical representation of data.

Chapter - 3 Results

Chapter Three: Results

3.1 Evidence for constitutive nitration in human mast cells

To investigate whether there was constitutive nitration among MC proteins, we performed western blot with lysates from normally cultured, unstimulated HMC-1 and LAD2 cells using anti-nitrotyrosine antibody. The anti-nitrotyrosine antibody detected many nitrated proteins (Figure 3.1, lanes 1,2), whereas chemically altering the nitrotyrosine by dithionite treatment (Lanes 4-6, Figure 3.1) diminished the immunoreactivity, thereby confirming the existence of constitutive protein tyrosine nitration in MC.

3.2 Two dimensional gel electrophoresis and western blot

3.2.1 Optimization of isoelectric focusing conditions

The use of 2-DE is a powerful approach to separate proteins based on isoelectric point in the first dimension and then by molecular weight in the second dimension in SDS-PAGE gels. Isoelectric focusing is a critical step where the proteins are separated at higher voltage. We systematically analyzed several reported protocols and for human MC, we standardised four step focusing conditions for pI 3 to 10 IPG strips of 7 cm length (50 V 10 min, 250 V 30 min, 750 V 60 min, 8000 V 13000 volt-hours). Similarly for 7 cm pI 4-7 linear IPG strips we used a single step focusing condition (4000 V 10,000 volt-hours). The amount of protein loaded in each strip was optimized to 75 µg/strip in 125 µl rehydration buffer.

3.2.2 Optimization of second dimension electrophoresis

SDS-PAGE electrophoresis was used to separate proteins in the second

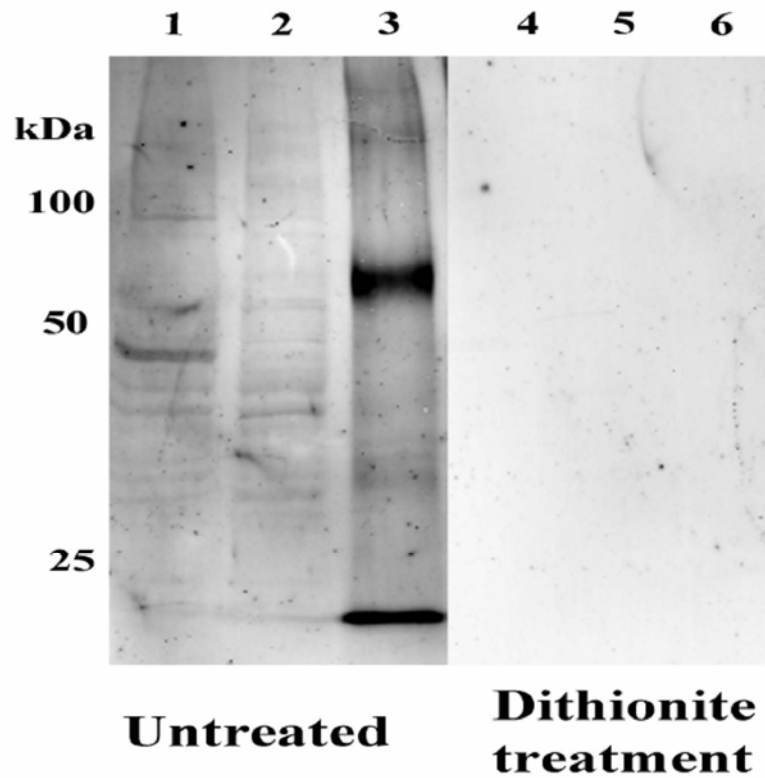


Figure 3.1 Constitutive protein tyrosine nitration in human mast cells. Western blot using anti-nitrotyrosine antibody of HMC-1 proteins (lanes 1,4), LAD2 proteins (lanes 2,5) (100 $\mu\text{g}/\text{lane}$) and nitro tyrosine immunoblotting control (combination of three proteins: nitrated bovine superoxide dismutase ~ 16 kDa, nitrated bovine serum albumin ~ 66 kDa, nitrated rabbit muscle myosin ~ 212 kDa) (lanes 3,6) (10 $\mu\text{g}/\text{lane}$). Dithionite treatment (lanes 4-6) reduces the nitrotyrosine immunoreactivity, establishing that there is constitutive nitration of MC proteins; representative blot from three independent experiments.

dimension. Different percentages of acrylamide including 10%, 12% and 5-15% gradient gels were used in our experiments. When we cast the gels in the lab manually there were variations in resolution and differences in size of the gels between experiments. Hence, commercially available 10% polyacrylamide precast gels (Bio-Rad) were used for the second dimensional separation. The uniform usage of precast gels helped to get better alignment of spots between western blot and corresponding silver-stained gels. To estimate the molecular weight of the separated proteins, molecular weight markers were applied along the IPG strips during the second dimensional separation. The gels were silver-stained, and a representative gel is shown in Figure 3.2.

3.2.3 *Manual scoring of the nitrated proteins in the western blot*

As seen in one dimensional gel western blot studies, 2-DE western blot studies revealed that there are many proteins that are constitutively nitrated in HMC-1. We attempted to analyze the western blots with 2-DE software to identify the proteins that are selectively nitrated upon NO treatment. However, because of large background reactivity in the nitrotyrosine-western blot during initial studies, there was difficulty in using the software to analyse western blots. Accordingly, a manual scoring method was applied where the spots in sham-treated and SNOG-treated gels were numbered as shown in Figure 3.3. The spots that were reproducible among six different experiments (15 spots) were numbered and compared as shown above. The results of the manual comparison between sham and treatment groups are represented in Table 3.1.

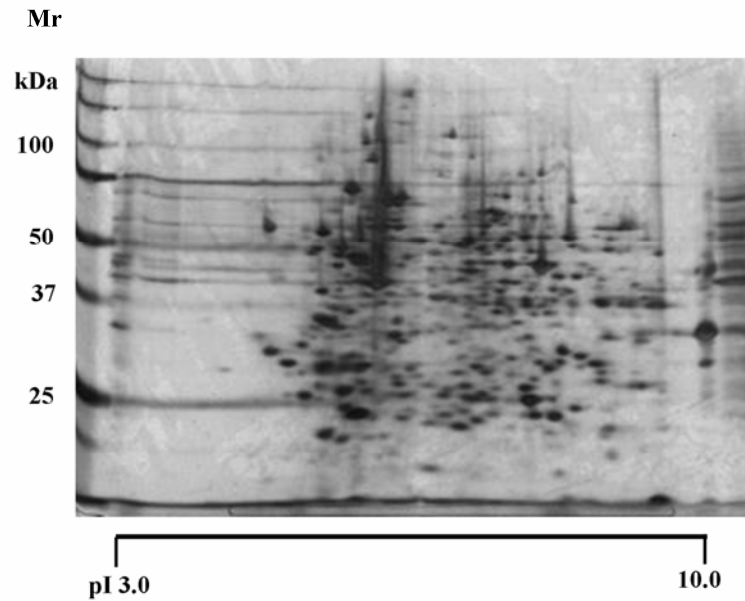


Figure 3.2 Two dimensional electrophoretic separation of HMC-1 proteins.

Five million HMC-1 cells were lysed and centrifuged at 17530 g for 20 min and 75 μ g of protein from the supernatant were separated using two dimensional gel electrophoresis in a 10% polyacrylamide gel. The gels were silver stained and proteins were visualized as distinct spots at different isoelectric points (pI) and molecular weights. Results are representative of seven independent experiments.

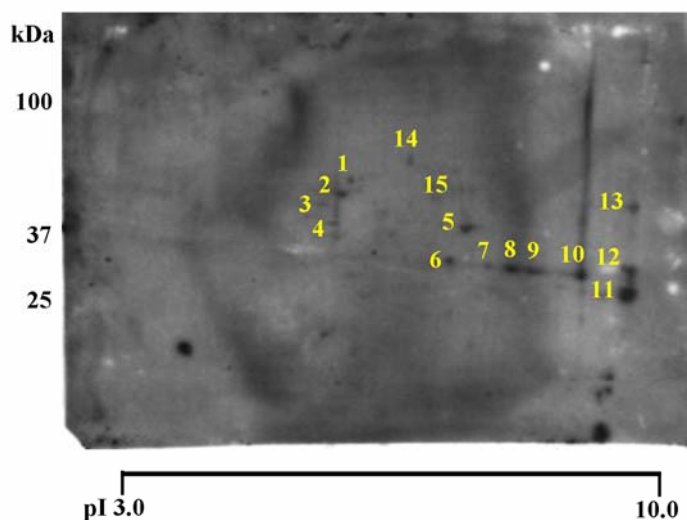


Figure 3.3 Manual scoring of nitrated proteins of HMC-1 in two dimensional gel electrophoresis western blots. Five million HMC-1 cells were treated with 500 μ M S-nitrosoglutathione for 4 h and the proteins were separated by two dimensional gel electrophoresis and western blot was performed with anti-nitrotyrosine antibody. The spots that were reproduced in six different experiments were manually scored from 1 to 15. The difference in the pattern of these spots in sham and of S-nitrosoglutathione-treated gels were compared and tabulated (see table 3.1 for a summary). Note the high background in the western blot during our initial studies. Results are representative of six independent experiments.

Table 3.1 Manual scoring and comparison of nitrotyrosine western blot between sham and S-nitrosoglutathione-treated HMC-1. Nitrated proteins were numbered from 1 to 15 and compared between sham and S-nitrosoglutathione (SNOG)-treatment (refer to Figure 3.3). Data from six independent experiments (marked from i to vi). Spots 7 and 8 (highlighted) in the SNOG-treated gels were submitted to mass spectrometric identification.

No. of Exp.		Presence of nitro tyrosine (NT) positive spots in 2-DE western blot														
		1	2	3	4	5	6	7	8	9	10	11	12	13	14	15
Sham	i	+	+	+	+	+	+				+	+	+	+	+	+
	ii	+	+	+	+	+	+			+	+	+	+	+	+	+
	iii	+	+	+	+	+	+				+	+	+	+	+	+
	iv	+	+	+	+	+	+				+	+	+	+	+	+
	v	+	+	+	+	+	+				+	+	+	+	+	+
	vi	+	+	+	+	+	+			+	+	+	+	+	+	+
SNOG	i	+	+	+	+	+	+	+	+	+	+	+	+	+		
	ii	+	+	+		+	+	+	+	+	+	+	+	+	+	+
	iii	+	+	+	+	+	+	+	+	+	+	+	+	+	+	+
	iv	+	+	+		+		+	+	+	+	+	+	+	+	+
	v	+	+	+	+	+	+	+	+	+	+	+	+	+	+	+
	vi	+	+	+		+	+	+	+	+	+	+	+	+	+	+

3.2.4 Constitutive nitration versus nitric oxide donor-induced nitration

In addition to constitutive protein tyrosine nitration in MC, we tested whether specific proteins would undergo nitration upon cell treatment with a NO donor. We treated HMC-1 cells with different concentrations and at different time periods (50, 250 and 500 μ M for 4 h and 500 μ M for 0.5, 2 and 4 h; see Appendix 1, Figure 1 and 2) with SNOG, a slow releasing NO donor. 2-DE western blots with anti-nitrotyrosine antibody were used to detect changes in the pattern of nitrated proteins in SNOG-treated HMC-1 cells. Treatment with 500 μ M SNOG for 4 h induced a significant change in the nitration pattern (compare top and middle panels in Figure 3.4). Isotype controls using rabbit IgG did not identify any immunoreactivity (bottom panel). The treatment condition of 500 μ M of SNOG for 4 h was used in further studies.

3.2.5 Isolation of S-nitrosoglutathione-induced nitrated spot

SNOG-induced nitration was reproducibly evident on a protein at about ~40 kDa and pI 8.3 (see arrowhead, on middle panel Figure 3.4). The SNOG-induced nitrated spots near pI 8.3, ~40 kDa (numbered 7 and 8 in Figure 3.3; Table 3.1) were matched with the corresponding spots in a silver-stained gel run in parallel. The spots were removed from the gel using a surgical blade under sterile conditions and submitted for MS identification of the protein.

3.3 Mass Spectrometry

3.3.1 Mass spectrometric identification of S-nitrosoglutathione-induced nitrated proteins

We identified the SNOG-induced nitrated spots 7 and 8 from the silver gel using MS. Spot 7 did not have sufficient protein and was identified as cytokeratin,

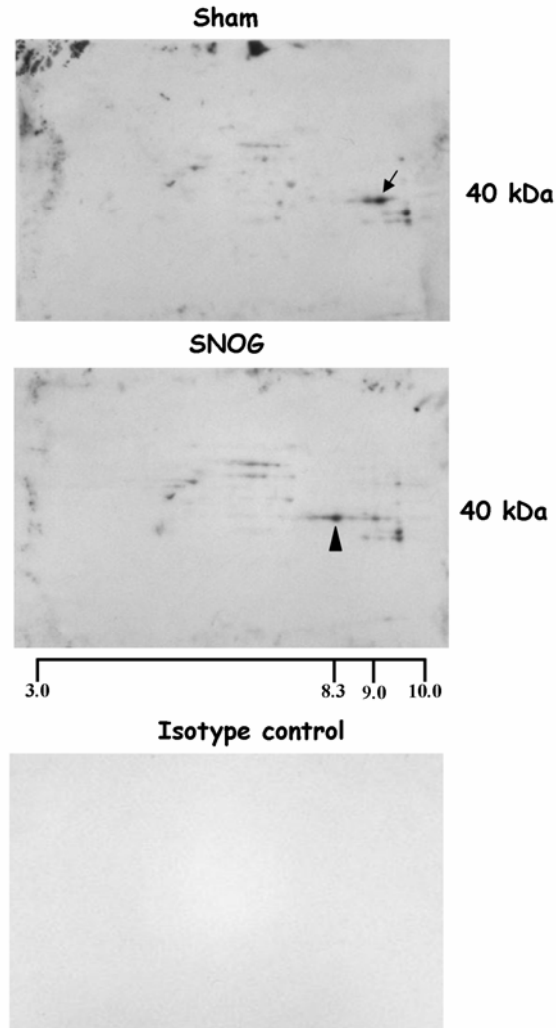


Figure 3.4 S-nitrosoglutathione-induced selective nitration of HMC-1 proteins. Five million HMC-1 cells were treated with (middle panel) or without 500 μ M S-nitrosoglutathione (SNOG) (top panel) for 4 h, and proteins were then extracted for 2-DE. Western blots of 2-DE gels using anti-nitrotyrosine antibody show prominent SNOG-induced nitration at pI 8.3 and \sim 40 kDa (see arrowhead in middle panel). Results are representative of seven independent experiments. Arrow indicates a constitutively nitrated spot at pI 9.0, \sim 40 kDa. Note the isotype control rabbit IgG did not identify any spots (bottom panel).

a common contaminant during sample preparation for mass spectrometry analysis. However, MS analysis of the SNOG-induced nitrated spot 8 (~40 kDa, pI 8.3) revealed peptides that matched human aldolase A. The sequence of aldolase A and the identified peptides are highlighted with bold red font in Figure 3.5.

3.3.2 Confirmation of the identity of the protein using western blot

To ensure that the spot submitted to MS analysis and the protein selectively nitrated upon SNOG treatment were the same, we reprobbed the membranes with anti-aldolase antibody (recognises all isoforms of aldolase A, B and C) and confirmed that the spot at pI 8.3, ~40 kDa was aldolase (see arrow head in lower panel Figure 3.6).

3.3.3 Multiple pI forms of aldolase in HMC-1

We identified multiple immunoreactive spots for aldolase at ~40 kDa but at different pI ranging from 7.0 to 9.0, both in sham and SNOG treated HMC-1 cells (Figure 3.6). Aldolase at pI 9.0 matched the nitrated spot at pI 9.0 (compare and see arrows in top panels Figure 3.4 and 3.6), thereby indicating constitutive nitration of aldolase. SNOG-induced nitration was observed for aldolase A at pI 8.3 (see arrow heads in lower panels Figure 3.4 and 3.6). Similar results were obtained when LAD2 cells were treated with SNOG. The region around 40 kDa in the 2-DE gel was highlighted to demonstrate that SNOG induces selective nitration of aldolase at pI 8.3 in LAD2 cells as well as in HMC-1 (Figure 3.7). Moreover, in addition to aldolase other spots were nitrated following SNOG treatment in LAD2 (see section 3.13, Figure 3.28).

Protein: Aldolase A (*Homo sapiens*)

Amino acids: 364

Mass: 39,706 Da

Calculated pI value: 8.3

Peptides matched: 7

Sequence Coverage: 23%

Accession number: gi/28614

Protein sequence:

1 MPYQYPALTP EOKKELSDIA HRIVAPGKGI LADESTGSI AKRLOSIGTE NTEENRRFYR
61 QLLLTADDRV NPGIGGVILF HETLYQKADD GRFPQVIKS KGGVVGIVD KGVVPLAGTN
121 GETTTQGLDG LSERCAQYKK DGADFAKWRC VLKIGEHTPS ALAIMENANV LARYASICQQ
181 NGIVPIVEPE ILPDGAHDLK RCQYVTEKVL AAVYKALSDH HIYLEGTLN PNMVTPGHAC
241 TQKFSHEEIA MATVTALRRT VPPAVTGITF LSGGQSEES SINLNAINKC PLLKPWALTF
301SYGRALOASA LKAWGGKKEN LKAAQEEYVK RALANSLACQ GKYTPSGQAG AAASESLFVS
361 NHAY

Figure 3.5 Amino acid sequence of human aldolase A. Matched peptides that were identified in the S-nitrosoglutathione-induced nitrated spot were underscored in bold red colour.

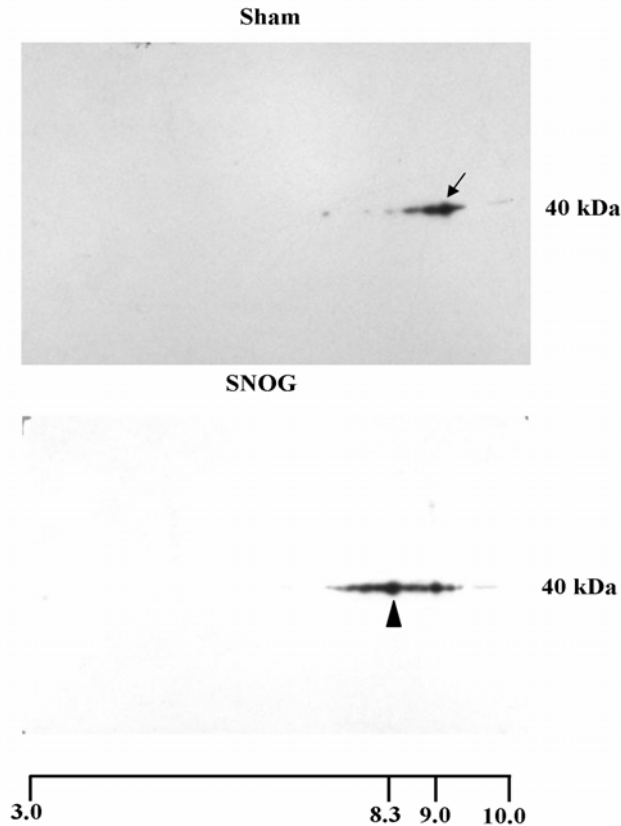


Figure 3.6 Confirmation of S-nitrosoglutathione-induced selective nitration of HMC-1 proteins as aldolase using western blot. The two dimensional gel electrophoresis membranes used in Figure 3.4 were reprobbed using anti-aldolase antibody. Multiple immunoreactive aldolase spots were detected at ~40 kDa with different isoelectric points (pI) (7.0 to 9.3) (arrow in top panel) and S-nitrosoglutathione-induced nitration of aldolase at pI 8.3 (arrowhead in lower panel). Aldolase at pI 9.0 was nitrated constitutively (compare arrows in Figure 3.4 and 3.6 top panels). Seventy five μg of protein was loaded in both gels; representative of seven independent experiments.

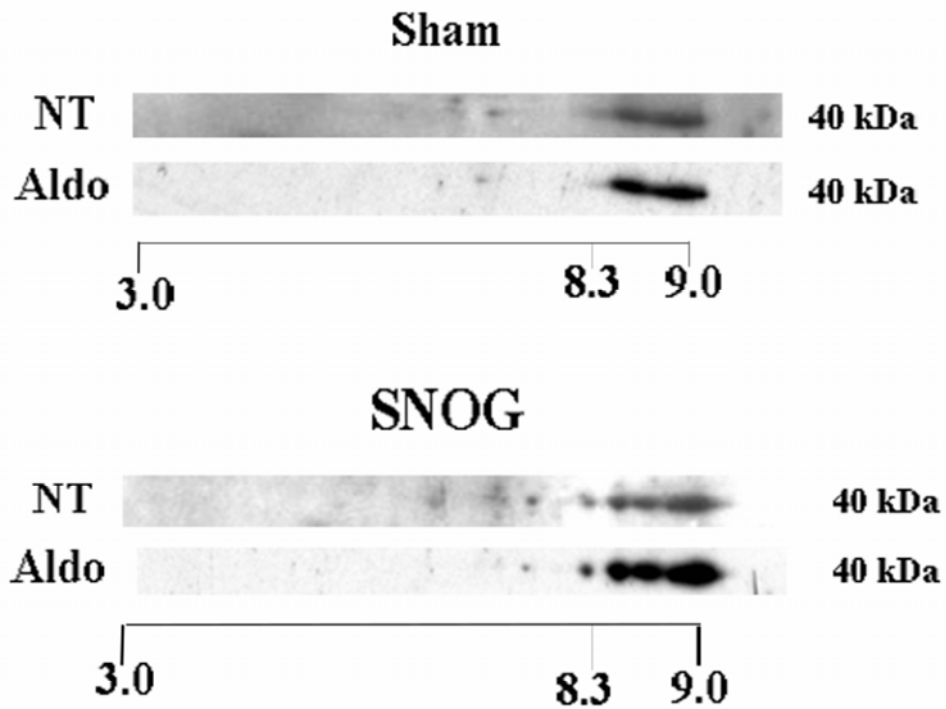


Figure 3.7 Confirmation of S-nitrosoglutathione-induced selective nitration of aldolase in LAD2 cells. Five million LAD2 cells were sham treated (top panel) or treated with 500 μ M S-nitrosoglutathione (SNOG) (bottom panel) for 4 h, and proteins were then extracted for two dimensional electrophoresis. Western blots of two dimensional electrophoresis gels using anti-nitrotyrosine (NT) and anti-aldolase (Aldo). Multiple immunoreactive aldolase spots were detected in LAD2 at \sim 40 kDa with different pI (7.0 to 9.3) and SNOG-induced nitration of aldolase was seen at pI 8.3. Seventy five μ g of protein was loaded in both gels; representative of four independent experiments. The region around 40 kDa is highlighted in this picture. Refer to Figure 3.28 for a picture of a complete gel.

3.3.4 Identification of isoforms of aldolase using mass spectrometry

To understand the multiple pI forms of aldolase and also the difference between the constitutively nitrated spot at pI 9.0 and SNOG-induced nitrated spot at pI 8.3, we sequenced different pI spots from the silver stained 2-DE gels. The spot at pI 9.0 ~ 40 kDa in the sham treated gel was isolated and sent for MS analysis. Similarly, the SNOG-induced nitrated spot at pI 8.3 from the SNOG-treated gels was submitted for MS analysis. The MS analysis is summarized in Table 3.2.

Interestingly, the constitutively nitrated spot at pI 9.0 revealed peptides of both aldolase A and aldolase C, whereas the SNOG-induced nitrated spot revealed peptides for aldolase A only. We performed extensive analysis in both the spots and did not find any peptides for aldolase B, the third isoform of mammalian aldolase.

3.3.5 Confirmation of aldolase C using zebrin II antibody

It is interesting that HMC-1 expresses two different isoforms of aldolase, A and C. Unfortunately, there are no commercially available antibodies against aldolase C. Hence we received a monoclonal antibody against zebrin II as a gift from Richard Hawkes, Department of Cell Biology and Anatomy, University of Calgary. Zebrin II has sequence homology with aldolase C and is often used to identify aldolase C in the cerebellum. Western blot with zebrin II antibody identified an immunoreactive band ~ 40 kDa in HMC-1 and LAD2 and also in mouse bone marrow derived MC (Figure 3.8).

Table 3.2 Summary of data from mass spectrometric analysis of constitutive and S-nitrosoglutathione-induced nitrated spots in HMC-1. Data from a single experiment

Spot location	Protein	G.I. accession No	Calculated pI*	Mr	Sequence coverage%	Peptide matches
Constitutively nitrated spot at ~ pI 9.0, 40 kDa	Aldolase A	28614	8.34 *	39706	22	7
	Aldolase A	229503	9.26	39693	11	4
	Aldolase C	229506	9.06	39449	15	5
SNOG-induced nitrated spot at ~ pI 8.3, 40 kDa	Aldolase A	28614	8.34 *	39706	9	2

* Calculated pI is determined by peptide sequence comparison and matching in mascot analysis and did not reflect the actual pI of the protein.

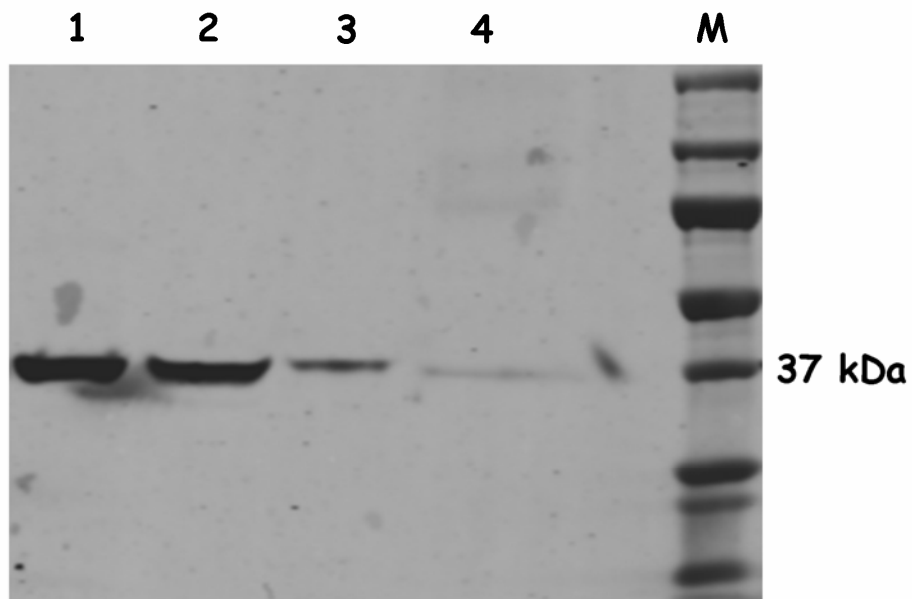


Figure 3.8 Confirmation of aldolase C in mast cells. Western blot with anti-zebrin II antibody revealed a predominant band at 37 kDa identifying aldolase C in different mast cells. Crude cell lysates were loaded into each well. Lane 1) mouse brain (positive control for aldolase C); 2) HMC-1; 3) LAD2; 4) mouse bone marrow derived MC; M) molecular weight markers. Fifty μ g of total protein was loaded in each lane; representative of three independent experiments.

3.4 Identification of mRNA expression of aldolase isoforms in mast cells

As there were multiple pI forms of aldolase in MC, we defined the expression of mRNA for different isoforms of aldolase in MC. The isoforms of aldolase are encoded by three different genes (225). We used RT-PCR with isoform-specific primers for aldolase A, B and C with cDNA of HMC-1, LAD2 and cord blood derived MC. As a positive control for all three isoforms of aldolase, cDNA from non-tumour areas of kidney from a patient who underwent nephrectomy was used. We identified mRNA for two isoforms, aldolase A and C in HMC-1, LAD2 and cord blood derived MC, whereas mRNA for all the three isoforms was found in human kidney (Figure 3.9). The products were sequenced and confirmed to be correct.

3.5 Affinity purification of mast cell aldolase

3.5.1 Potential aldolase-binding proteins in the affinity purified fractions

The HMC-1 cell lysate was pre-cleared using an IgG column. The initial 5 ml flow through from the IgG column was allowed to bind with the anti-aldolase column for 60 min. Proteins that were bound to the anti-aldolase column were eluted and concentrated. The affinity purified fractions were separated using SDS-PAGE in a 10 % polyacrylamide gel and the proteins were visualised using silver staining. The crude cell lysate was loaded in the lane I (Figure 3.10A) and the flow through fractions (1 to 4) after binding were loaded in the lanes II to V. A predominant band at ~40 kDa was consistently separated in the affinity purified fractions (lane VI, Figure 3.10A). This band was confirmed as aldolase by western blotting. Along with the aldolase at ~40 kDa, many bands of higher and lower molecular weight that were also noticed in fraction VI. When we separated

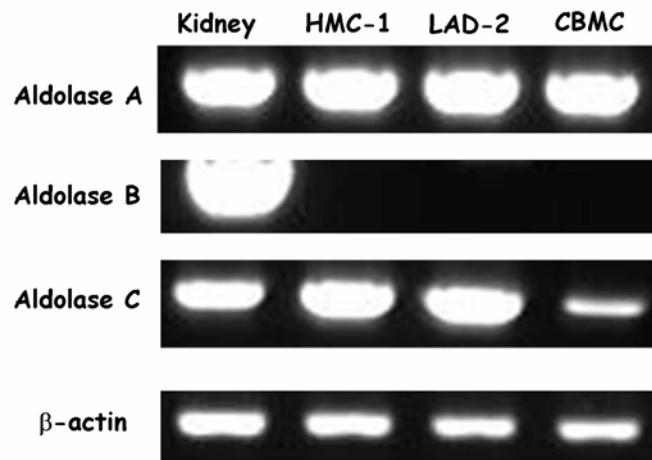


Figure 3.9 Identification of mRNA level expression of aldolase isoforms in mast cells. RT-PCR using cDNA of human kidney, HMC-1, LAD2 and cord blood derived MC (CBMC) using aldolase isoform (aldolase A, B or C) specific and β -actin primers. All PCR products were confirmed by sequencing; representative from five independent experiments.

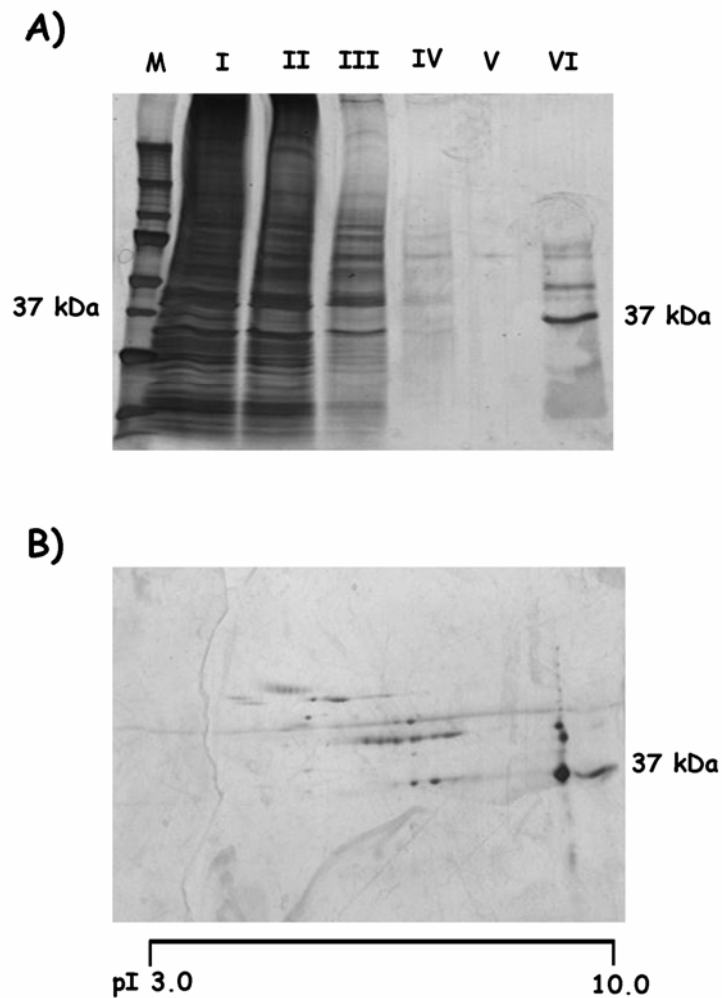


Figure 3.10 Affinity purification of aldolase from HMC-1. A) SDS-PAGE separation of HMC-1 fractions from the aldolase column M) molecular weight marker; I) crude cell lysate; II) flow through fraction 1; III) flow through fraction 2; IV) flow through fraction 3; V) flow through fraction 4; VI) Elution fraction 1. Aldolase was eluted predominantly around 37 kDa in the elution fraction. The identity was confirmed by western blot with anti-aldolase antibody. B) silver stained two dimensional electrophoresis gel of elution fraction 1 (lane VI in A). Note the predominant aldolase spots at 37 kDa, pI 7.0 to 9.0. Also note presence of potential aldolase-binding proteins of different pI and molecular weight in the two dimensional electrophoresis gel; results are from one experiment.

the aldolase-enriched fraction VI by 2-DE we also detected several proteins with distinct molecular weight and different pI in the gel (Figure 3.10B). These proteins might be non-specifically binding with the anti-aldolase antibody or they could be proteins that are associated with aldolase *in vivo* (see section 4.2.10).

3.5.2 Mass spectrometric analysis of aldolase fractions for identification of nitration sites

Mass spectrometric identification of nitrotyrosine sites is a powerful technique to extend the understanding of the presence of nitrotyrosine in a protein. From our 2-DE western blot approach we had evidence of constitutive nitration of aldolase in HMC-1 and LAD2 cell lines and also that there was selective nitration upon SNOG treatment. To differentiate these two nitration events and to identify which tyrosines are nitrated in MC we enriched the aldolase from the SNOG-treated MC and performed mass spectrometric analysis on this isolated protein.

There are 13 tyrosine residues in human aldolase A, but their nitration has not been previously studied. However, there are many studies that reported specific nitration of tyrosines in different locations of aldolase from other species (220, 226, 227). The location of tyrosines and reported nitration sites are summarized in Table 3.3. We pooled the affinity purified fractions of aldolase from HMC-1 and ran 10% SDS-PAGE gels. The gels were either stained with coomassie blue or silver. The band at ~40 kDa was isolated and submitted for MS analysis.

Table 3.3 Location of tyrosines in aldolase A and reported nitration sites.

The number in the table represents the position of the tyrosine residues in aldolase A from different species. The residues that are reported as nitrated are highlighted with ‘*’. Note that references are cited along with the species in the table.

	Species			
	Rabbit (220)	Rat (226, 227)	Mouse	Human
Tyrosine location in aldolase A	-	-	-	2
	-	4	4	4
	58	58	-	58
	84	84	84	74
	137	137	137	137
	173	173	173	173
	203	203*	203	203
	213	213	213	213
	222*	222	222	222
	243*	-	-	-
	301	301	301	301
	327	327*	327	327
	342*	342	342	342
	363*	363	363	363
Total number of tyrosines	12	12	11	13

3.5.3 Identification criteria for nitrated tyrosines

The affinity-purified fractions of aldolase from HMC-1 were analyzed using MS. The mass of unmodified tyrosine is 163 Da. If there is nitration of tyrosine the mass will be increased by 45 Da, i.e. the mass of nitrated tyrosine will be 208 Da. The peptides that contain nitrated tyrosines will exhibit higher mono isotopic mass that can be identified by tandem mass spectrometry (MS/MS) analysis.

As we used iodoacetamide in MS sample preparation protocols, all the cysteine residues would be modified into carbamidomethylated cysteine. Hence carbamidomethylation of cysteine was selected as a fixed modification in search parameters. Each potential site can be tested with and without the modifications by including variable modifications in mascot analysis. Since oxidation of methionine is a common post-translational modification that arises during trypsin digestion and high voltage MS procedures, we included oxidation of methionine as one of the variable modifications. Moreover, because we were interested in nitrated tyrosine, we also included nitration of tyrosine as another variable modification in searching the mascot database. We found peptides for both aldolase A (Table 3.4) and aldolase C (Table 3.5). Unfortunately we could not identify the nitrated tyrosines in any of the analyses using this approach.

3.5.4 An altered inclusion list for nitrated aldolase peptides

Since our first approach to identify nitrated tyrosines was not fruitful, we adopted a second approach of inclusion list preparation for nitrated peptides of aldolase A and then performed MS/MS analysis on that particular mass only.

Table 3.4 Peptide sequences of aldolase A identified from aldolase affinity-purified fractions of SNOG-treated HMC-1.

¹The number of unique peptides for which ion fragmentation was obtained is listed. ²The % of sequence coverage is listed.

Protein Name	Accession No. (NCBI)	# Peptides ¹	% Coverage ₂	Score %	Mr	Peptides
aldolase A	Gi28614	22	74	99	39289	PYQYPALTPEQK KELSDIAHR GILAADESTGIAK RLQSIGTENTEENR QLLLTADDR IGGVILFHETLYQK ADDGRPFQVIK GVVPLAGTNGETTTQGLDGLSER IGEHTPSALAIMENAN YASICQQNGIVPIVEPEILPDGDHDLK AIMENANVLAR PIVEPEILPDGDHDLKR ALSDHHIYLEGTLLKPNMVTPGH VLAAVYK FSHEEIAMATVTALR TVPPAVTGITF LSGGQSEEEASINLNAINK CPLLKPWAL CPLLKPWALTF ALQASALK ALANSLALQGK YTPSGQAGAAASESLFVSNHAY

Table 3.5 Peptide sequences of aldolase C identified from aldolase affinity-purified fractions of SNOG-treated HMC-1.

¹ The number of unique peptides for which ion fragmentation was obtained is listed. ²The % of sequence coverage is listed.

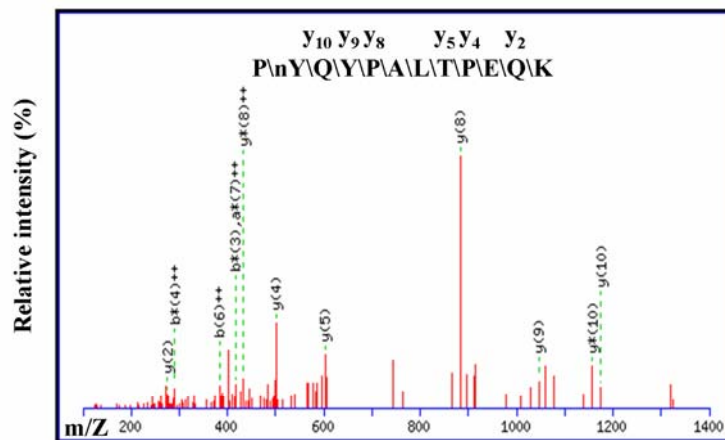
Protein Name	Accession No. (NCBI)	# Peptides ¹	% Coverage ²	Score %	Mr	Peptides
aldolase C	Gi4885063	12	46	99	39456	GILAADES VGSMK LSQIGVENTEENR TPSALAIENANVLAR PIVEPEILPDGDHDLKR YASICQQNGIVPIVEPEILPDGDHDLKR RYASICQQNGIVPIVEPEILPDGDHDLK YTPEEIAMATVTALR ALQASALNAWR AEVNGLAAQ GK YEGSGEDGGIAAAQSLYIANHAY ALSDHHVYLEGTLLKPN GVVPLAGTDGETTTQGLDGLSER

This is one of the standard protocols for identifying nitrated peptides of aldolase in a complex mixture of peptides (220). MassLynxTM software (Waters Corp, Milford, MA) from the Institute for Biomolecular Design, University of Alberta was used in preparing the inclusion list for analysis. The protein sequences of aldolase A and C were used to generate theoretical peptides after simulating tryptic digestion using MassLynxTM software. We replaced the tyrosines with nitro-tyrosines and the software generated theoretical peptides with nitrated tyrosines. The mono isotopic masses of these nitrated peptides along with the doubly and triply charged ions were compiled and then MS/MS analysis was performed on the affinity purified aldolase fractions using this list of peptides.

The ‘include function’ of the instrument operating software was used to program MS/MS analysis of precursor ions of all possible nitrotyrosine-containing tryptic peptides based on human aldolase A and C sequence. The inclusion list prepared for nitrated peptides of both aldolase A (Appendix 1, Table 2) and aldolase C (Appendix 1, Table 3) including the doubly and triply charged ions is summarized.

3.5.5 Identification of nitration sites in aldolase A

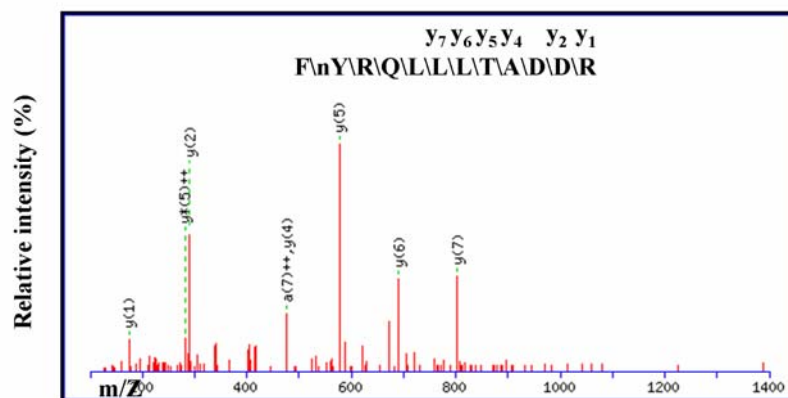
Tandem mass spectrometry analysis of the peptide searches using the inclusion list for nitrated peptides of aldolase A and C from the SNOG-treated HMC-1 aldolase fractions did not identify any nitrated aldolase C peptides. However, aldolase A was identified as nitrated at two different tyrosine residues Tyr² (Figure 3.11) and Tyr⁵⁸ (Figure 3.12) by the inclusion list approach only. Since there was lack of complete peptide coverage in this spectrum we tried to



Monoisotopic mass of neutral peptide Mr (calc): 1478.7041

Sequence	Mono isotopic mass
P	
Y	1382.659
Q	1174.61
Y	1046.552
P	883.4883
A	786.4356
L	715.3985
T	602.3144
P	501.2667
E	404.214
Q	275.1714
K	147.1128

Figure 3.11 Tandem mass spectrometry (MS/MS) spectra identifying Tyr² as nitrated Tyr (nY). The ‘y’ ions that are identified in the spectrum are highlighted in red. Note the difference between the mono isotopic mass of the peptide (YPALTPPEQK) and (PALTPPEQK), (1046-883 = 163, the mass of Tyr), whereas the difference between the peptide (YQYPALTPPEQK) and (QYPALTPPEQK) (1382-1174 = 208, the mass of nitrated Tyr), thus confirming Tyr² as the nitrated Tyr in human aldolase A.



Monoisotopic mass of neutral peptide Mr (calc): 1554.78

Sequence	Mono isotopic mass
F	
Y	1408.72
R	1200.67
Q	1044.57
L	916.51
L	803.43
L	690.34
T	577.26
A	476.21
D	405.17
D	290.15
R	175.12

Figure 3.12 Tandem mass spectrometry MS/MS spectra identifying Tyr⁵⁸ as nitrated Tyr (nY). The 'y' ions that are identified in the spectrum are highlighted in red. Note the difference between the mono isotopic mass of the peptide (YRQLLLTADDR) and (RQLLLTADDR), (1408-1200= 208, the mass of nitrated Tyr), thus confirming Tyr⁵⁸ as the nitrated Tyr in human aldolase A.

repeat the experiments two more times, once at the Institute for Biomolecular Design and once at the mass spectrometric facility in the Department of Chemistry, University of Alberta. In these additional experiments, we were not successful in reproducing the results and confirming sites Tyr² and Tyr⁵⁸ as targets for SNOG-induced nitration in HMC-1; indeed no nitrated tyrosines were identified (see discussion).

3.5.6 Evidence for aldolase nitration in the enriched fractions

In the absence of reproducible sequences for nitrated aldolase using mass spectrometry, we have applied the traditional dithionite reduction method to verify constitutive nitration of aldolase in MC. We performed western blot with anti-nitrotyrosine antibody on the affinity-purified aldolase fractions from SNOG-treated HMC-1 or LAD2 cell lysates. Dithionite treatment significantly reduced the nitrotyrosine reactivity of aldolase fractions by ~80%, thereby confirming constitutive nitration of aldolase in these two MC lines (Figure 3.13). Similar results were observed when we pre-incubated anti-nitrotyrosine antibody with free 3-nitrotyrosine (data not shown).

3.6 Location of nitrated tyrosines on the human aldolase A structure

To investigate the potential consequences of aldolase nitration on Tyr² and Tyr⁵⁸ we have depicted the location of Tyr² and Tyr⁵⁸ on the human aldolase A structure (Figure 3.14). Tyr² was located in the N-terminal of the protein and the residue appears not to interact with other residues in the internal structure of the protein. Tyr⁵⁸ is located in the interior structure of the protein. The precise location of Tyr⁵⁸ and its interacting amino acids is depicted in Figure 3.15.

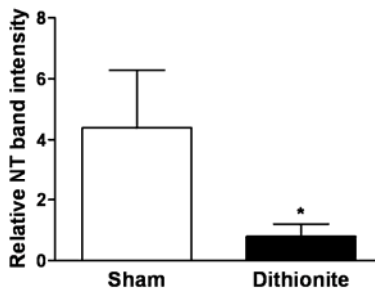
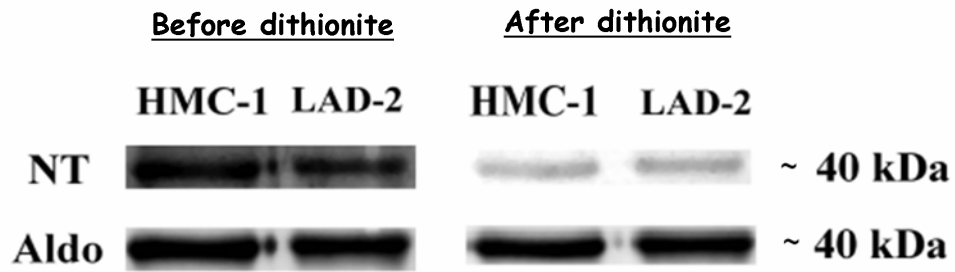


Figure 3.13 Confirmation of constitutive nitration in aldolase enriched fractions of mast cells. Western blots of affinity purified aldolase of HMC-1 and LAD2 before and after dithionite treatment (anti-nitrotyrosine antibody [NT] and anti-aldolase antibody [Aldo]). The magnitude of dithionite reduction (~ 80%) of nitrotyrosine reactivity of HMC-1 is represented as a bar graph (Mean ± SE, densitometry from three independent experiments, * p value < 0.05).

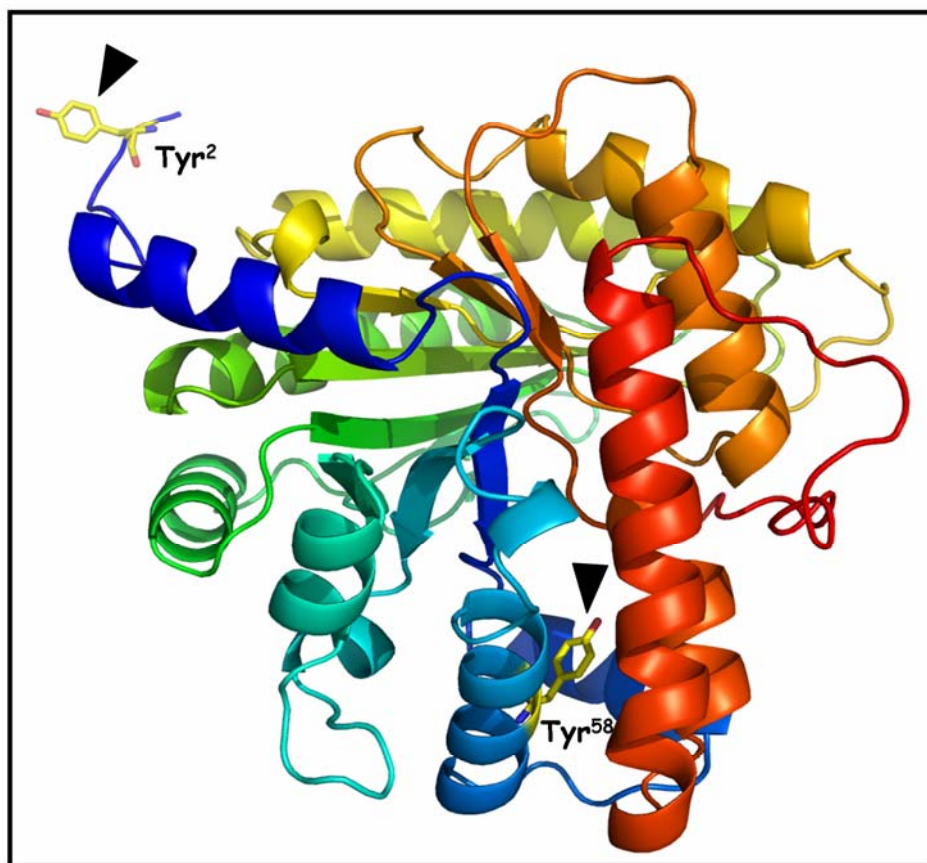


Figure 3.14 Diagram showing the location of Tyr² and Tyr⁵⁸ in the tertiary structure of aldolase A. (Protein data bank ID: 4ALD). Tyr² is located on the N-terminal of the enzyme, whereas Tyr⁵⁸ is embedded in the interior structure of aldolase A. Arrowheads indicate the location of these two Tyr in the aldolase structure. Dr. Sankaranarayanan Ramasamy, Postdoctoral Fellow of Dr. Michael James, Department of Biochemistry, University of Alberta constructed this image using PyMOL software (DeLano Scientific, CA).

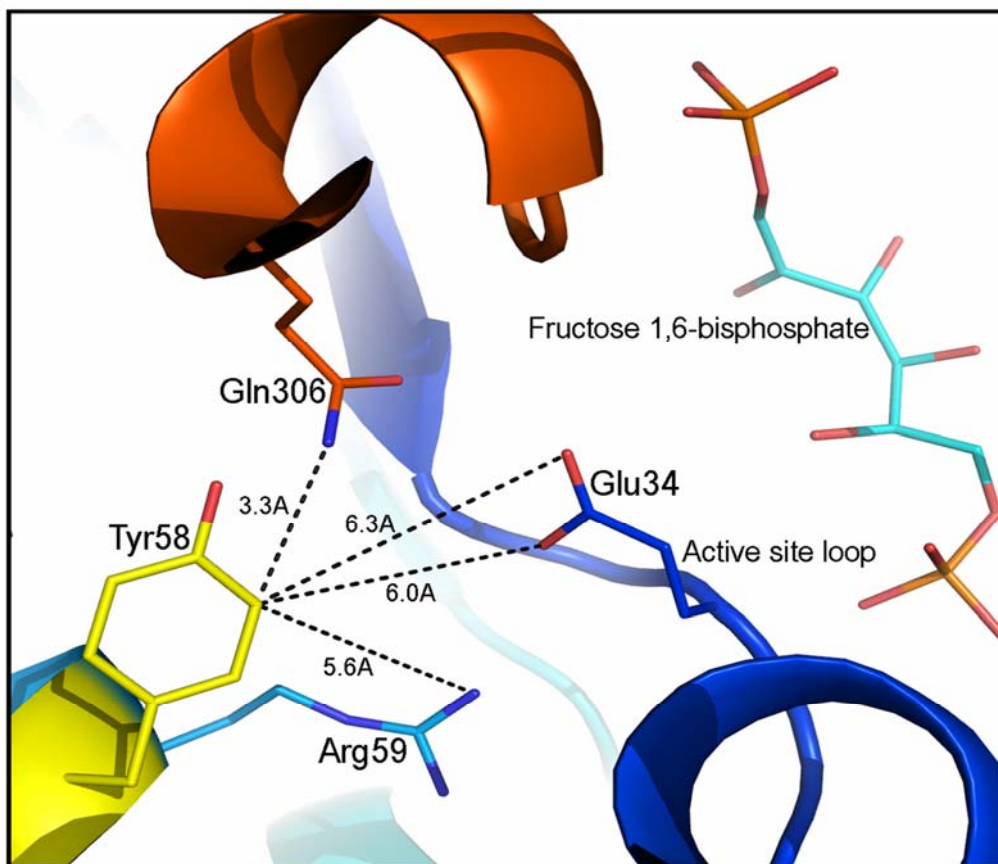


Figure 3.15 Location of Tyr⁵⁸ and interacting amino acid residues in human aldolase A structure. Diagram showing possible interactions of side chain carbon atom of Tyr⁵⁸ with the residues Gln³⁰⁶, Glu³⁴ and Arg⁵⁹ in the human aldolase A structure (Protein data bank ID: 4ALD). The substrate fructose-1,6-bisphosphate is shown as a stick model in the active site. Possible hydrogen bonds upon nitration of Tyr⁵⁸ are represented as dotted lines. Glu³⁴ is located in the active site loop of aldolase A. Dr. Sankaranarayanan Ramasamy, Postdoctoral Fellow of Dr. Michael James, Department of Biochemistry, University of Alberta constructed this image using PyMOL software (DeLano Scientific, CA).

Tyrosine residues are susceptible to nitration where there are negatively charged residues such as Asp, Glu and/or positively charged residues such as Arg, Lys in their vicinity. We analyzed those residues that are located within 3 to 7 Å of Tyr⁵⁸, a procedure reported earlier (161). The side chain carbon atom CE2 of Tyr⁵⁸ is at a atomic distance of 3.3Å from the side chain atoms of Gln³⁰⁶; 5.6 Å from Arg⁵⁹; 6.0 Å from oxygen atom 1 (OE1) and 6.3 Å from oxygen atom 2 (OE2) of Glu³⁴ (Figure 3.15). Addition of a nitro group upon nitration of Tyr⁵⁸ will reduce the inter-atomic distances between these residues, thereby favouring potential hydrogen bonds between Tyr⁵⁸ and Gln³⁰⁶, Arg⁵⁹, Glu³⁴.

Interestingly, Glu³⁴ is located in the active site loop of human aldolase A (228). Both the proximal residue Asp³³ and distal residue Ser³⁵ bind with the substrate fructose-1,6-bisphosphate and are involved in the catalytic mechanism of aldolase A. Thus hydrogen bond formation upon Tyr⁵⁸ nitration might influence the structure of the active site loop of aldolase A, the consequences of which could be better understood by applying molecular modelling studies.

3.7 S-nitrosoglutathione-induced changes in the enzymatic activity of aldolase

The activity of the enzyme is directly measured as the change in optical density (OD) values of hydrazone at 240 nm in our assay. The aldolase activity in terms of change in OD values ($\Delta A_{240}/2 \times 10^5$ cells/min) between sham- and SNOG-treated HMC-1 and LAD2 cells is shown in Figure 3.16. The changes in OD values at different concentrations of FBP demonstrate the reduced activity of aldolase in SNOG-treated HMC-1 and LAD2 cells. To determine whether or not

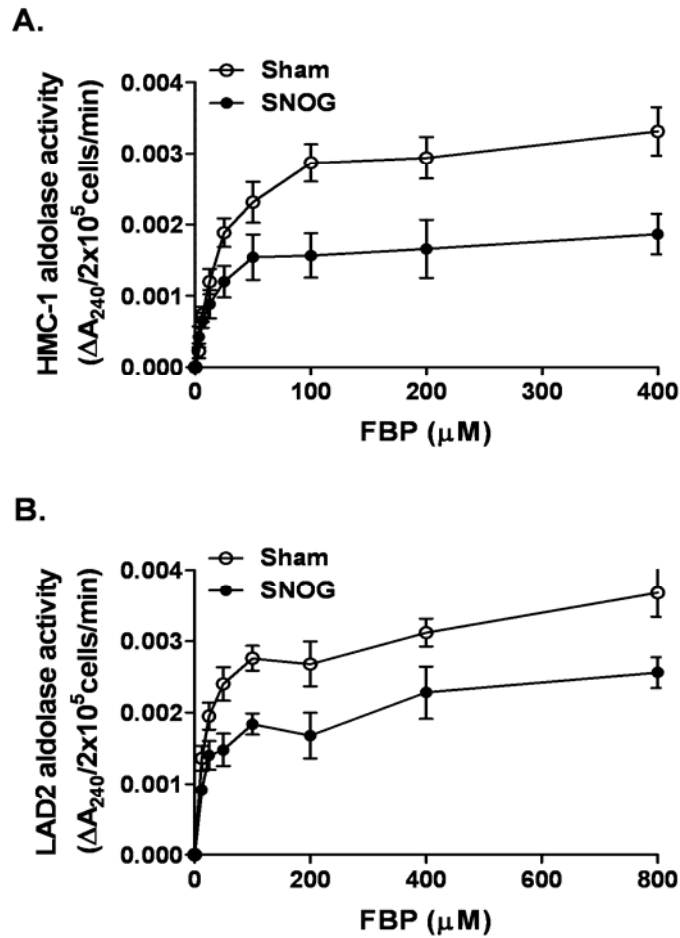


Figure 3.16 Saturation curve for mast cell aldolase. HMC-1 (A) and LAD2 (B) (2×10^6 cells) were treated with 50 μ L of water or 500 μ M SNOG for 4 h at 37°C and the total aldolase activity in the cell lysates was measured as change of optical density values ($\Delta A_{240}/2 \times 10^5$ cells/min). Optical density values at 0 μ M fructose-1,6-bisphosphate (FBP) were subtracted from values at each FBP concentration. Results are expressed as mean \pm SE from seven (HMC-1) and five independent experiments (LAD2).

nitration of aldolase affects the activity of the enzyme, we measured the K_m and V_{max} of aldolase from HMC-1 and LAD2 cell homogenates before and after treatment with SNOG. SNOG reduced the K_m and the V_{max} of aldolase in HMC-1 (Figure 3.17A and B) and reduced V_{max} of aldolase in LAD2 cells (Figure 3.17D).

3.8 S-nitrosoglutathione-induced elevation of fructose-1,6-bisphosphate in mast cells

Since inhibition of the activity of an enzyme could result in accumulation of the substrate, we measured levels of FBP, the substrate for aldolase, before and after treatment with SNOG. The number of cells used for measuring FBP was standardised to 10^7 cells for each measurement. Similarly the extraction volume was standardised to 100 μ l for 10^7 cells. SNOG treatment significantly increased the intracellular FBP levels by 613% in HMC-1 and by 61% in LAD2 (Figure 3.18).

3.9 S-nitrosoglutathione-induced changes in glycolytic metabolites

As aldolase is a crucial enzyme in the glycolytic pathway, we studied if inhibition of aldolase activity might alter ATP levels in MC. We used H^1 NMR to begin to define components of the metabolome (set of <1500 Da metabolites) (224, 229) of HMC-1 treated with SNOG. Both the cell extract and the media were used to measure the metabolites.

3.9.1 Effects of S-nitrosoglutathione on HMC-1 AMP, ADP and ATP

Surprisingly, in contrast to the expectation from the inhibition of aldolase activity, levels of AMP, ADP and AMP in cell extracts were similar in SNOG and

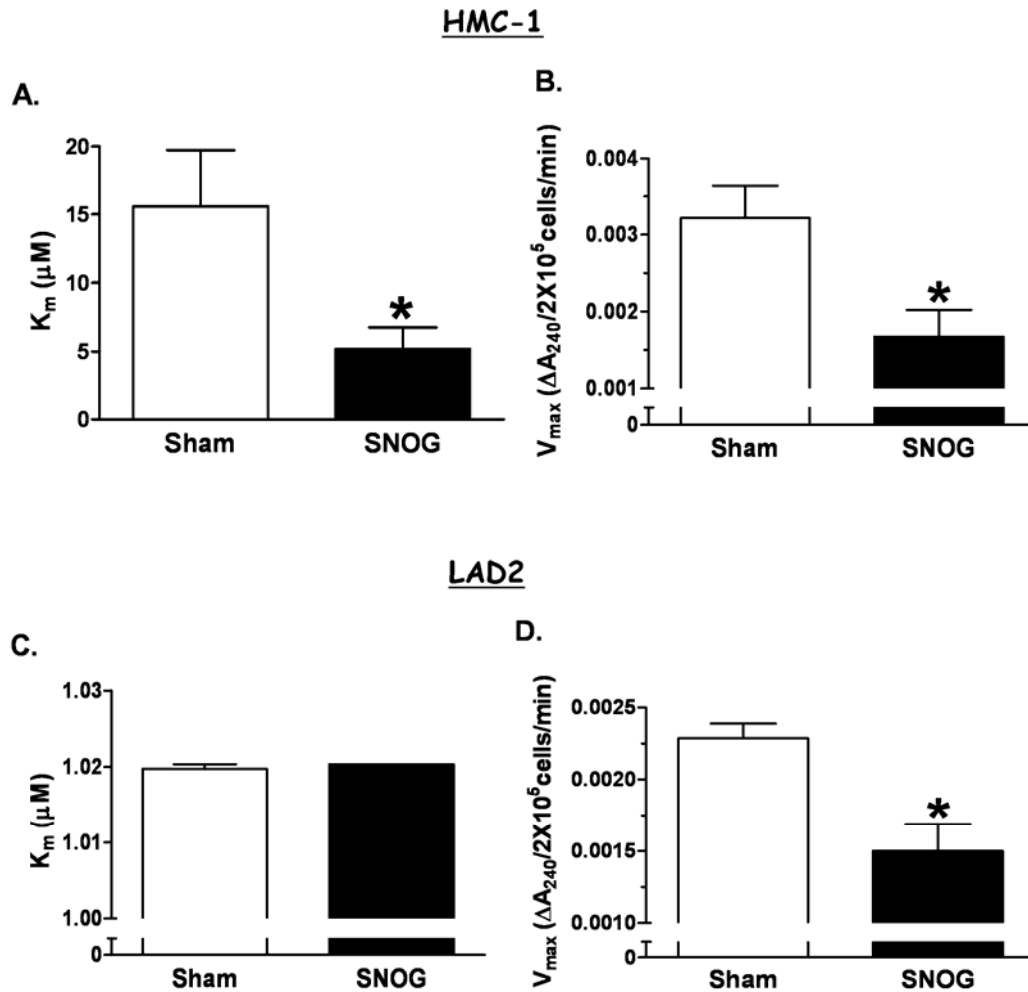
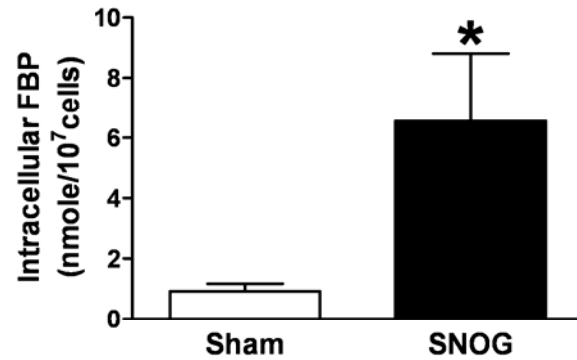


Figure 3.17 S-nitrosoglutathione-induced changes in the enzymatic activity of mast cell aldolase. HMC-1 and LAD2 (2×10^6 cells) were treated with 50 μl of water or 500 μM S-nitrosoglutathione (SNOG) for 4 h at 37°C and the total aldolase activity in the cell lysates was measured. To calculate the maximum velocity (V_{max}) and the Michaelis-Menten constant (K_m), 3.125 μM to 800 μM (serial two fold dilutions) of substrate were used. SNOG treatment reduced the K_m and the V_{max} of aldolase in HMC-1 (A and B) but only V_{max} in LAD2 (C and D). Results are from seven (HMC-1) and five independent experiments (LAD2) (mean \pm SE, * $p < 0.05$)

A. HMC-1



B. LAD2

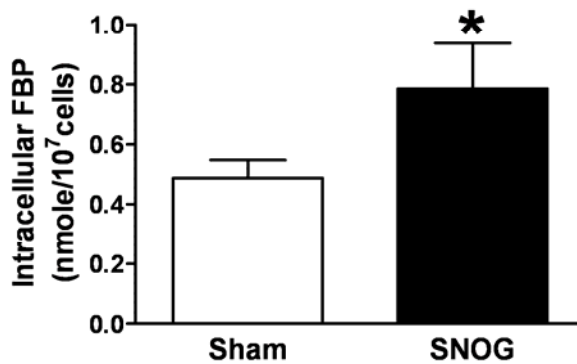


Figure 3.18 S-nitrosoglutathione-induced elevation of fructose-1,6-bisphosphate (FBP) in mast cells. HMC-1 (A) or LAD2 (B) (1×10^7 cells) were sham treated with 250 μ l water or treated with 500 μ M SNOG in 10 ml media for 4 h at 37°C and the total the cell pellet was deproteinized using 5% trichloroacetic acid followed by neutralization with 2M Tris. The intracellular FBP concentration was estimated using the aldolase enzymatic activity assay. Results are from five (A) or eight (B) independent experiments (mean \pm SE, * $p < 0.05$).

sham treated MC (Figure 3.19A). There was no statistically significant change in the AMP, ADP and the sum of total cellular AMP, ADP and ATP levels (Figure 3.19A). Interestingly, the AMP/ATP ratio was increased following SNOG treatment (Figure 3.19B).

3.9.2 Effects of S-nitrosoglutathione on nicotinamide adenine dinucleotide levels

Nicotinamide adenine dinucleotide (NAD⁺) acts as a coenzyme in many redox reactions and also served as a substrate for many enzymes. Hence we measured NAD⁺ levels both in its oxidised form and reduced form (NADH) in cell extracts. There were no significant changes in the levels of NAD⁺ and NADH between the sham and SNOG treated HMC-1 (Figure 3.20).

3.9.3 Effects of S-nitrosoglutathione on amino acids levels

Glucogenic amino acids can be metabolized into pyruvate and other tricarboxylic acid metabolites. To understand the metabolic changes upon SNOG treatment we analyzed levels of amino acids in HMC-1 cell extracts. Amino acid levels that were significantly changed are summarised in (Figure 3.21). SNOG reduced the levels of glutamine, glutamate, alanine, asparagine, glycine and threonine in HMC-1.

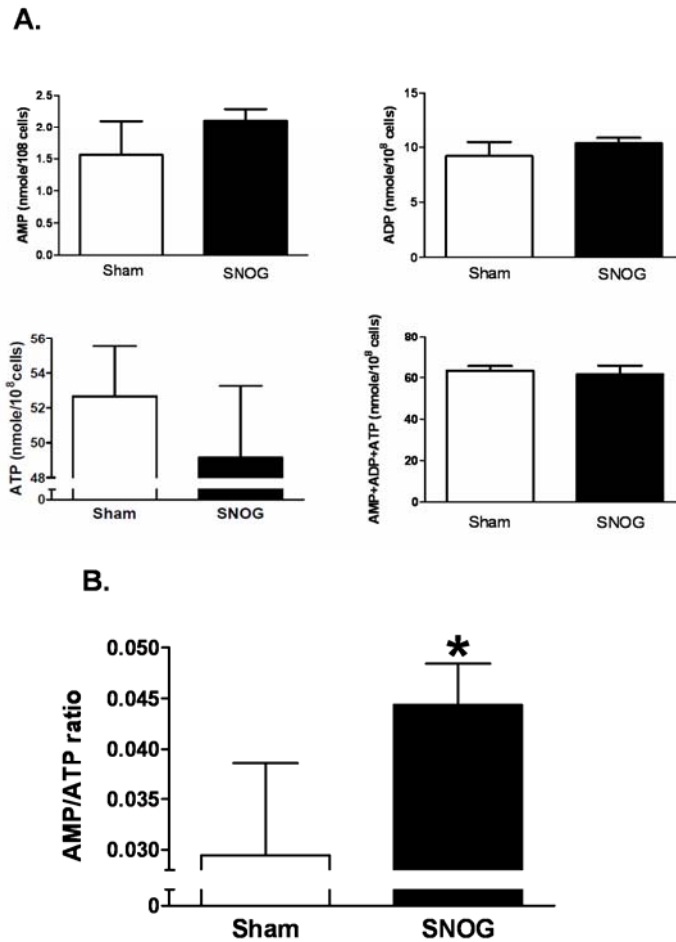


Figure 3.19 Effects of S-nitrosoglutathione on HMC-1 AMP, ADP and ATP levels. HMC-1 (10^8 cells) were treated with either sham or SNOG $500 \mu\text{M}$ for 4 h at 37°C and the metabolites from cell extract levels were analyzed using NMR. A) No significant changes in the levels of AMP, ADP, ATP levels and the total AMP+ADP+ATP levels. B) elevated AMP/ATP ratio upon SNOG treatment. Data shown as mean \pm SE for three independent experiments performed in triplicates.

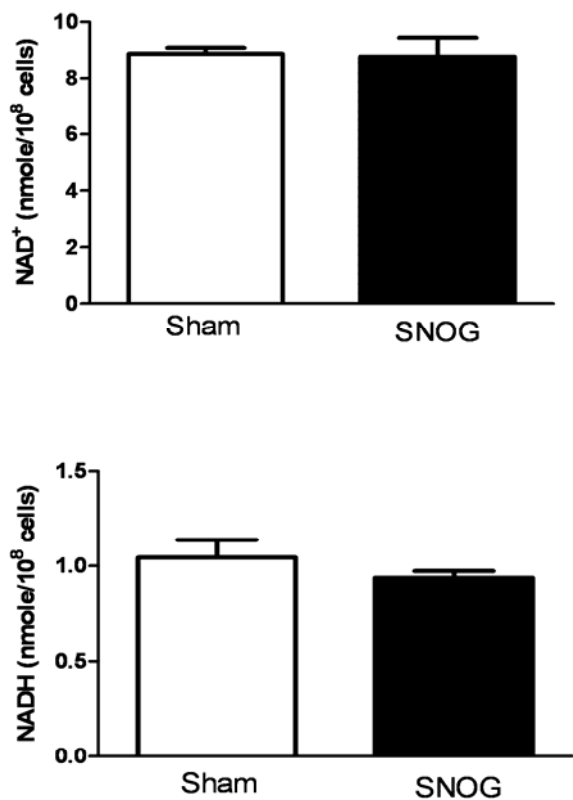


Figure 3.20 Effects of S-nitrosoglutathione on HMC-1 nicotinamide adenine dinucleotide (NAD⁺) levels. HMC-1 (10⁸ cells) were treated with either sham or SNOG 500 μ M for 4 h at 37°C and the metabolites from cell extract levels were analyzed using NMR. There were no significant changes in the levels of NAD⁺ and its reduced form NADH in HMC-1 upon SNOG treatment. Data shown as mean \pm SE for three independent experiments performed in triplicates.

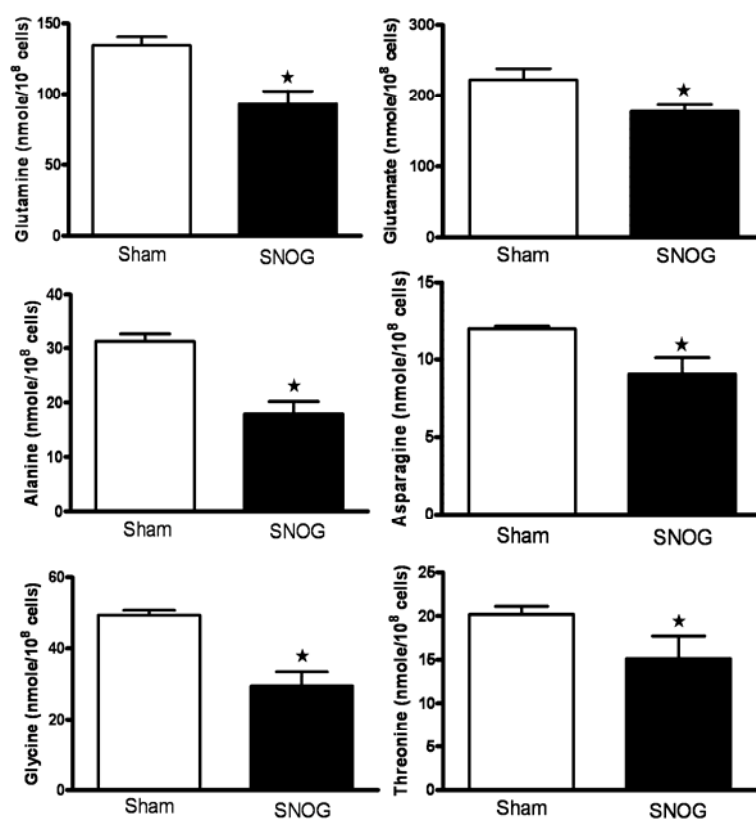


Figure 3.21 Effects of S-nitrosoglutathione on amino acid levels of HMC-1.

HMC-1 (10^8 cells) were treated with either sham or SNOG $500 \mu\text{M}$ for 4 h at 37°C and the metabolite levels from the cell extract were analyzed using nuclear magnetic resonance spectroscopy. SNOG treatment significantly reduced glutamine, glutamate, alanine, asparagine and threonine levels in HMC-1. Data shown as mean \pm SE for three independent experiments performed in triplicates.

3.9.4 Effects of S-nitrosoglutathione on glutathione levels

The levels of glutathione (GSH), the intracellular antioxidant were also measured in HMC-1 cell extracts. We observed that there was a statistically significant rise in the GSH levels after SNOG treatment in HMC-1 (Figure 3.22).

3.9.5 Effects of S-nitrosoglutathione on the metabolites in the media

We measured the metabolite differences in the media using NMR. Interestingly, pyruvate and lactate, measures of cellular glycolytic activity, were significantly elevated in culture media of SNOG-treated MC (Figure 3.23 A and B). We also noticed reduced levels of 2-oxoisocaproate and 3-methyl-2-oxovalerate (Figure 3.23 C and D). Moreover, the amino acid glycine was enhanced and cystine was reduced in the media of SNOG-treated HMC-1 (Figure 3.23 E and F).

3.10 Effects of S-nitrosoglutathione on the ATP levels of LAD2

The difficulty in culturing large numbers of LAD2 cells ($>10^8$ for a single NMR analysis) was a major hindrance to test the effects of SNOG on metabolites in LAD2 cells. In an effort to assess the glycolytic metabolism in LAD2 following SNOG treatment, we tested ATP levels in live cells. Similar results with both HMC-1 and LAD2 were obtained when we measured ATP using an ATPlite™1step ATP kit. As with the HMC-1 studies of metabolism, the ATP levels in LAD2 cells were not significantly altered by SNOG treatment (Figure 3.24).

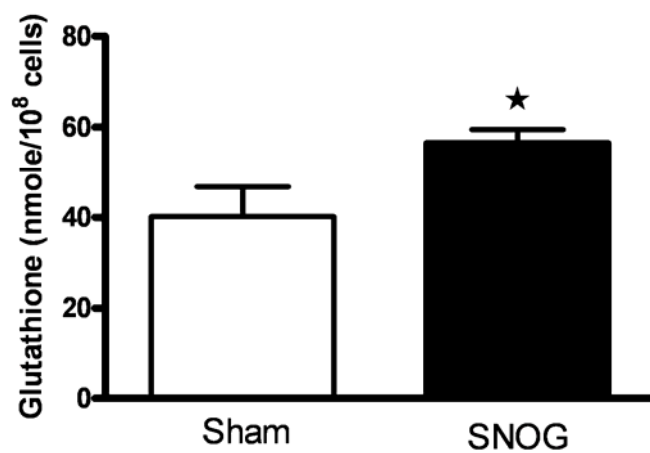


Figure 3.22 Effects of S-nitrosoglutathione on glutathione levels of HMC-1. HMC-1 (10^8 cells) were treated with either sham or SNOG 500 μ M for 4 h at 37°C and the metabolite levels from the cell extract were analyzed using nuclear magnetic resonance spectroscopy. SNOG treatment significantly elevated glutathione levels in HMC-1. Data shown as mean \pm SE for three independent experiments performed in triplicates.

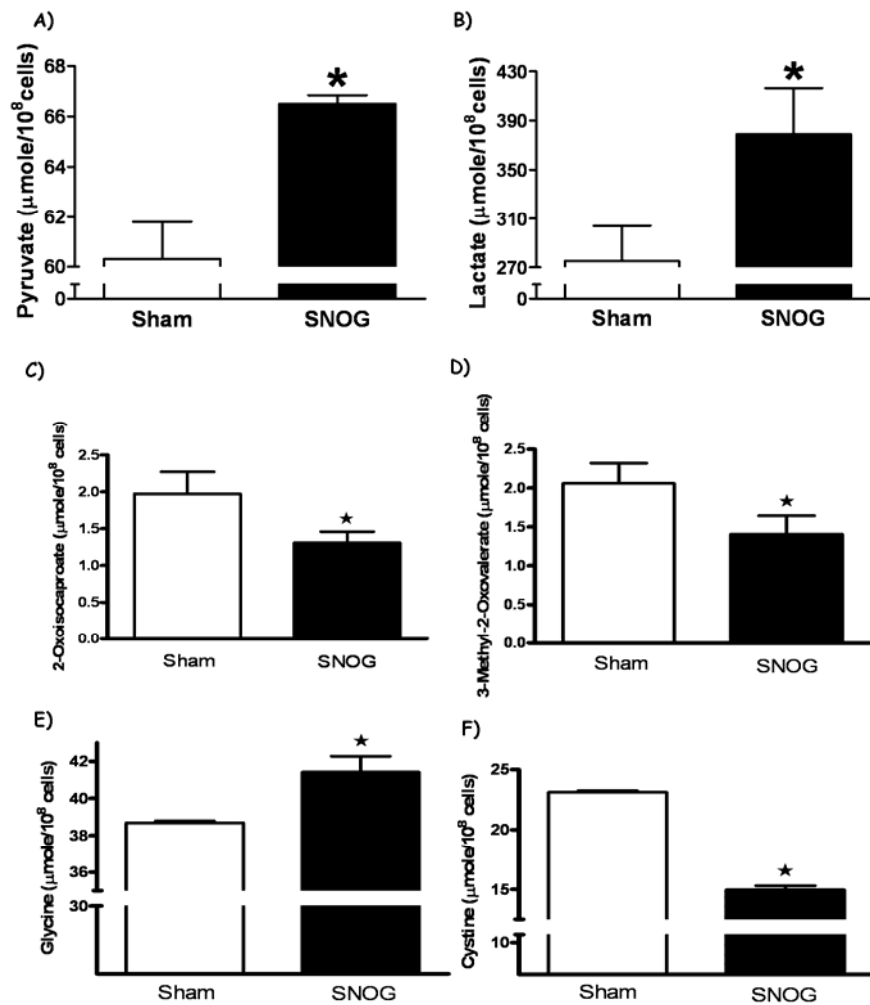


Figure 3.23 Effects of S-nitrosoglutathione on HMC-1 metabolites in media. HMC-1 (10^8 cells) were treated with either sham or SNOG 500 μ M for 4 h at 37°C and the metabolite levels on the media were analyzed using nuclear magnetic resonance technique. SNOG enhanced levels of A) pyruvate and B) lactate; SNOG treatment reduced C) 2-oxoisocaproate, and D) 3-methyl-2-oxovalerate; elevated E) glycine and reduced F) cystine. Data shown as mean \pm SE for three independent experiments performed in triplicates.

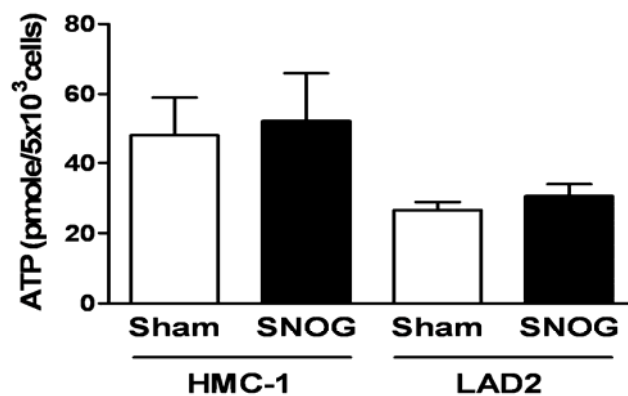


Figure 3.24 Effects of S-nitrosoglutathione on ATP levels in HMC-1 and LAD2. HMC-1 or LAD2 were treated with or without 500 μ M SNOG for 4 h and the total ATP levels in 5×10^3 cells were measured using ATPlite™ 1step ATP kit according to the manufacturer's instructions. ATP levels in 5×10^3 cells were calculated from the ATP standard curve. Results are expressed as mean \pm SE from three independent experiments.

3.11 Effects of exogenous fructose-1,6-bisphosphate on LAD2 degranulation

3.11.1 Dose dependent entry of exogenous fructose 1,6 bisphosphate into LAD2

Because exogenously applied FBP has been shown to enter intracellular compartments poorly (230), we used 5 mM exogenous FBP in our model as others have used previously (231). Indeed when we tested intracellular levels of FBP following treatment with exogenous FBP (100 nmoles to 100 μ moles), only a few nmoles of FBP were available in the intracellular compartment of LAD2 cells (Figure 3.25). At extracellular FBP of 10000 nmole/ 10^7 cells/10 ml of media, the intracellular FBP levels reached a similar level found in SNOG-treated LAD2.

3.11.2 Fructose-1,6-bisphosphate inhibits LAD2 degranulation

To simulate the effects of increased intracellular FBP in MC, and to study effects of FBP on MC function, we employed an *in vitro* IgE-dependent degranulation assay of MC. IgE/anti-IgE stimulation induced β -hexosaminidase release from LAD2 of $21.8 \pm 2.1\%$, whereas pretreatment with SNOG or FBP significantly inhibited the degranulation of LAD2 by 59% or 48% respectively (Figure 3.26). F1P and F6P that were used as controls for FBP did not inhibit MC degranulation.

3.12 Effects of fructose-1,6-bisphosphate on the intracellular Ca^{2+} levels in LAD2

We hypothesized that the intracellular Ca^{2+} levels might be altered in the FBP-mediated inhibition of LAD2 degranulation. To test our hypothesis we used a Ca^{2+} assay kit which measures the intracellular Ca^{2+} in a calcium free buffer system. FBP dose dependently reduced the IgE/anti-IgE induced intracellular Ca^{2+}

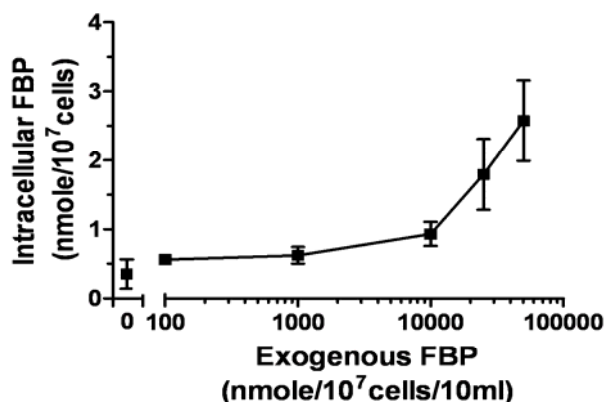


Figure 3.25 LAD2 cell permeability to exogenously applied fructose-1,6-bisphosphate. LAD2 (1×10^7 cells) were treated with increasing concentrations (100, 1000, 10000, 100000 nmole fructose-1,6-bisphosphate (FBP) in 10 ml) for 4 h at 37°C. The cell pellets were deproteinized using 5% trichloroacetic acid followed by neutralization by 2M Tris. The FBP concentration was estimated in the supernatant (metabolite fractions) using the aldolase enzymatic activity method. Results are expressed as mean \pm SE from four to six independent experiments.

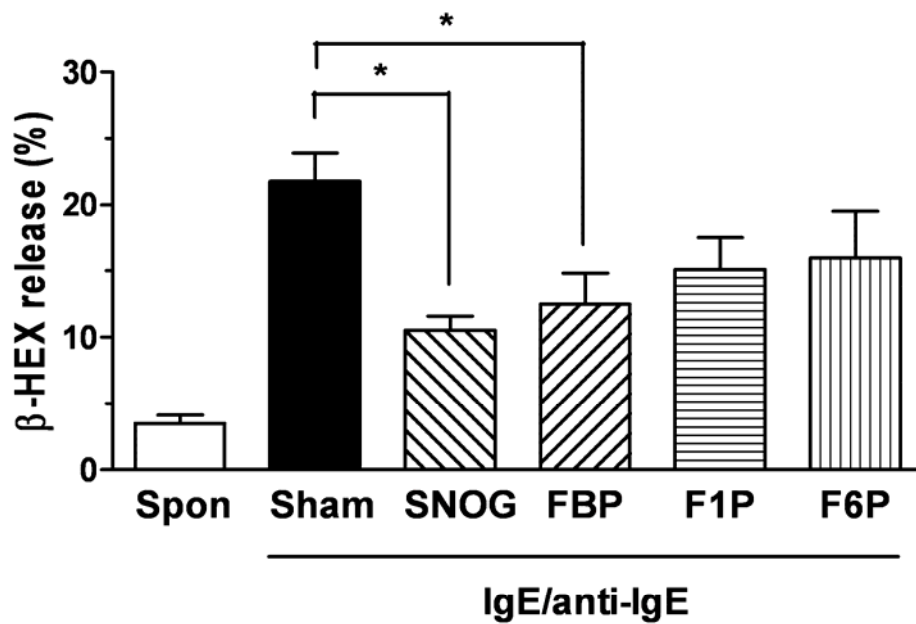


Figure 3.26 Effects of exogenous fructose-1,6-bisphosphate on degranulation of LAD2 cells. LAD2 cells were sensitized with 1 $\mu\text{g/ml}$ human IgE overnight at 37°C and then pretreated with 500 μM SNOG, 5 mM fructose-1,6-bisphosphate (FBP), 5 mM of fructose-1-phosphate (F1P), and 5 mM fructose-6-bisphosphate (F6P) for 4 h at 37°C, respectively. The cells were washed and resuspended in HEPES-buffered Tyrode's solution and stimulated with 10 $\mu\text{g/ml}$ mouse anti-human IgE antibody for 30 min. The cells were centrifuged and the % release of β -hexosaminidase into the supernatant was calculated. Spontaneous release was indicated as 'spon'. Results are expressed as mean \pm SE from six independent experiments performed in triplicates. Data were analyzed using one-way analysis of variance (ANOVA) followed by the Tukey-Kramer multiple comparisons (* $p < 0.05$).

release in LAD2. A 5 mM dose of exogenous FBP that inhibited LAD2 degranulation also reduced the free intracellular Ca^{2+} levels (Figure 3.27). Interestingly, SNOG did not affect the intracellular Ca^{2+} levels in LAD2.

3.13 SNOG-induced nitration targets in LAD2

In our hypothesis-generating proteomic approach in HMC-1 we identified aldolase as a predominant target. Interestingly, in LAD2 MC, in addition to aldolase nitration following SNOG treatment, other spots on 2-DE gel analyses demonstrated tyrosine nitration (arrow, Figure 3.28). A 500 μM SNOG treatment for 4 h predominantly nitrated a protein around ~ 25 kDa and pI ~ 5.5 to 6.0 (arrow, Figure 3.28).

3.13.1 Isolation of S-nitrosoglutathione-induced nitrated spot in LAD2

We performed a fractionation study to isolate the SNOG-induced nitrated spot at ~ 25 kDa and pI 5.5 to 6.0 in LAD2. The LAD2 cell lysates were centrifuged in 50 kDa cut-off filters and the flow-throughs were centrifuged in 10 kDa cut-off filters and the supernatant above the filter was used for 2-DE separation. We used narrow range IPG strips pI 4.0 to 7.0 for enhanced resolution. Western blot with anti-nitrotyrosine antibody revealed a dominant spot at ~ 25 kDa and pI 5.5 to 6.0 nitrated in LAD2 (Figure 3.29). We matched this spot with coomassie G-250 stained gel run in parallel with this experiment and located the protein in the gel.

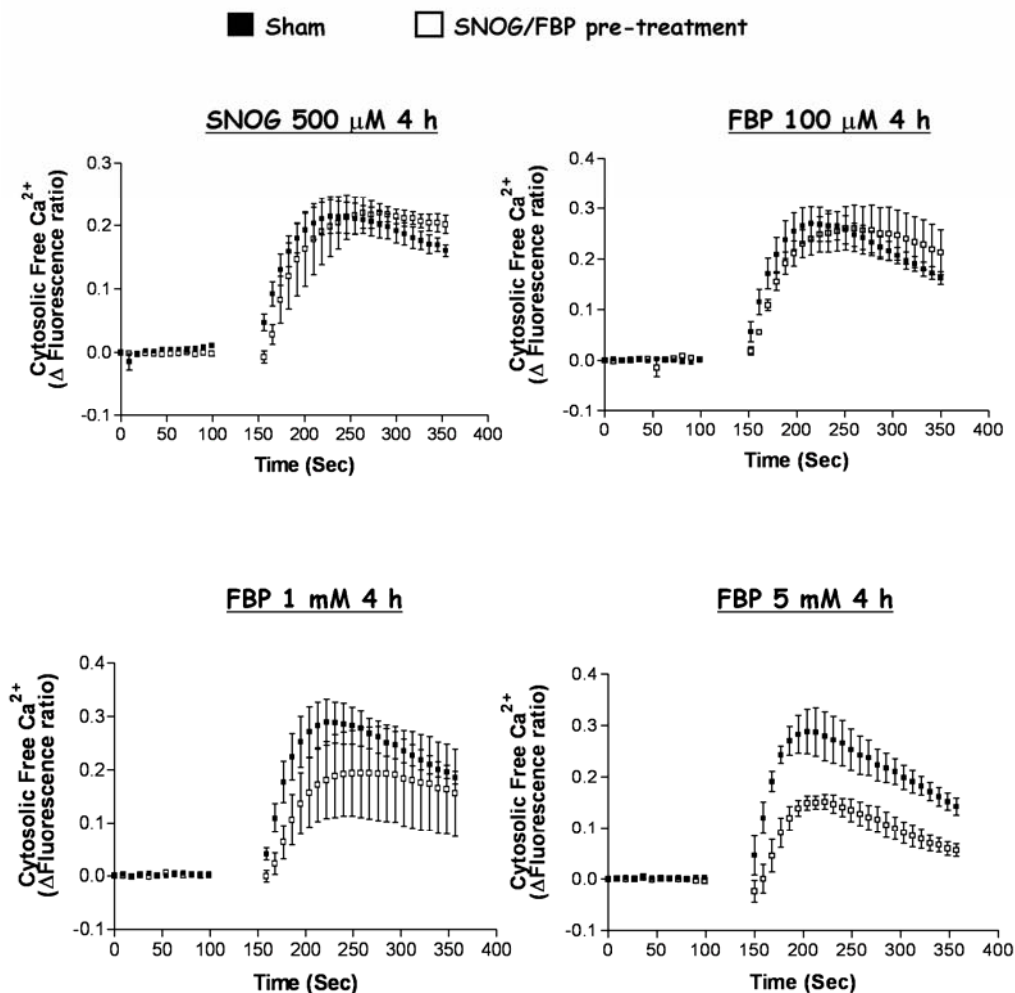


Figure 3.27 Effects of S-nitrosoglutathione, fructose-1,6-bisphosphate (FBP) on IgE/anti-IgE induced free intracellular Ca^{2+} levels of LAD2. LAD2 cells were sensitized with $1 \mu\text{g/ml}$ of human IgE overnight and pretreated for 4 h at 37°C with either $500 \mu\text{M}$ of SNOG or $0.1, 1, 5 \text{ mM}$ of FBP. The cells were stimulated with $10 \mu\text{g/ml}$ of anti-IgE and the intracellular Ca^{2+} were measured using Flou 4 NW Ca^{2+} assay kit. SNOG did not alter, whereas FBP dose dependently inhibited IgE/anti-IgE induced free intracellular Ca^{2+} levels in LAD2. Data shown as mean \pm SE for three independent experiments.

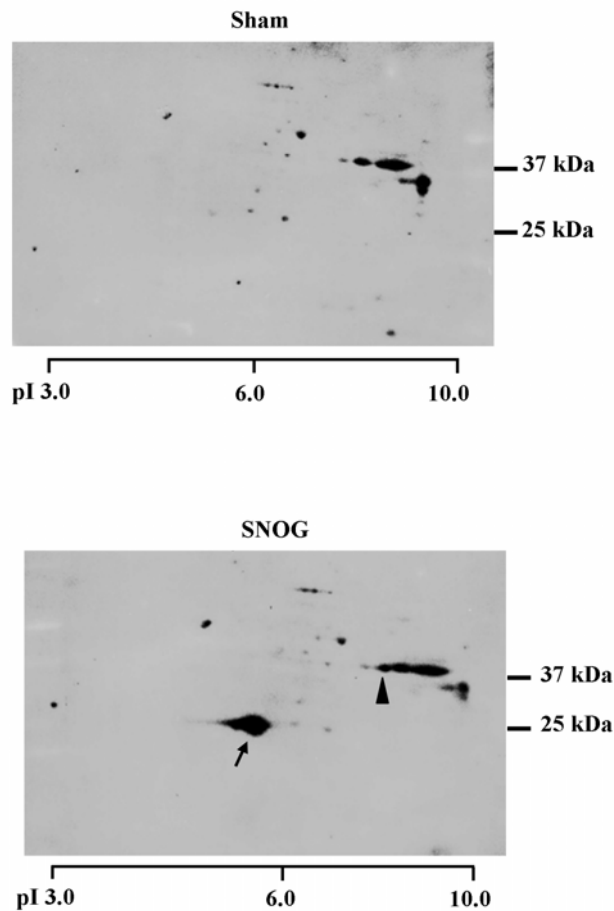


Figure 3.28 Effects of S-nitrosoglutathione on tyrosine nitration in LAD2.

Five million LAD2 cells were treated for 4 h at 37°C with either vehicle or 500 μ M of SNOG and the cells were lysed and separated using two dimensional electrophoresis. The membranes were probed with anti-nitrotyrosine antibody (1:1000) overnight followed by secondary antibody (1:10,000) for 60 min. The signal after addition of enhanced chemiluminescence agent was captured in hyperfilm (Amersham) for 15 min. SNOG-induced selective nitration at ~25 kDa pI 5.6 (arrow) as well as aldolase (arrow head); representative blot of six independent experiments.

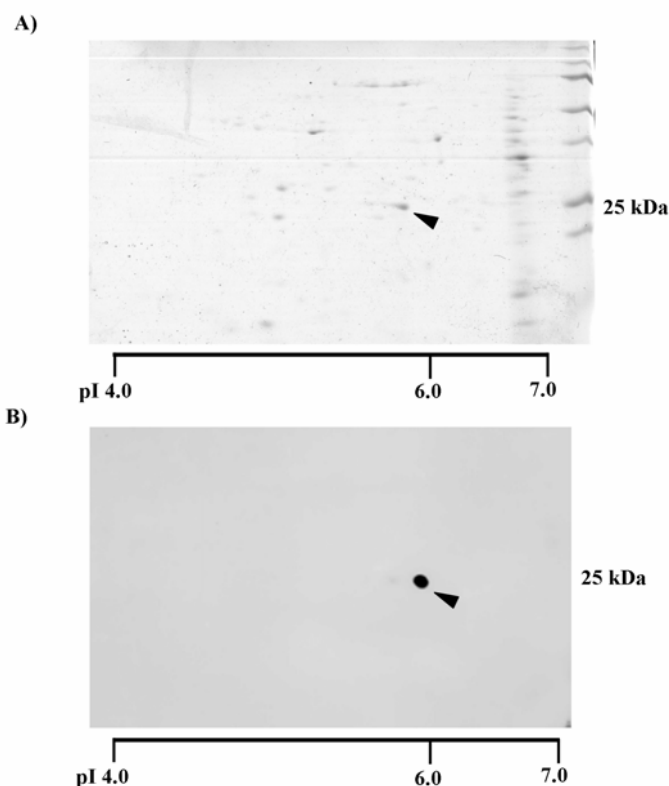


Figure 3.29 Isolation of S-nitrosoglutathione-induced nitrated spot in LAD2.

LAD2 (15×10^6 cells) were treated for 4 h with 500 μ M of SNOG, the cells were lysed, the 50 to 10 kDa fractions were separated using centrifugal cut-off filters and the proteins were focused in a pI 4 to 7 strip in the first dimension and separated using 12% SDS-PAGE gel in the second dimension; A) the gels were stained overnight with coomassie G-250 or B) western blot with anti-nitrotyrosine antibody. The SNOG-induced nitrated spot at \sim 25 kDa pI 5.6 (indicated by arrow head) was isolated from the gel and submitted for mass spectrometric identification; representative blot of three independent experiments.

The spot was isolated under sterile conditions and submitted for mass spectrometric identification.

3.13.2 Mass spectrometric identification of SNOG-induced nitrated target in LAD2

Mass spectrometric analysis revealed peptides that match 15-hydroxy prostaglandin dehydrogenase (PGDH). PGDH is a critical enzyme in metabolism of prostaglandins into inactive 15-keto derivatives. The protein sequence of PGDH and the corresponding peptides that were identified in our mass spectrometric analysis are illustrated in Figure 3.30.

3.13.3 Confirmation of 15-hydroxy prostaglandin dehydrogenase by western blot

To confirm that the spot we submitted to MS analysis is PGDH, we used an anti-PGDH antibody and reprobbed the membranes that were used for nitrotyrosine western blot. The nitrated spots were matched exactly with the PGDH spots in the SNOG-treated LAD2 (Figure 3.31). Moreover, there were multiple pI forms of PGDH in sham treated LAD2 and they were not apparently nitrated constitutively. It is interesting that SNOG-induced selective nitration of PGDH in LAD2 cells, but that this was not detected in HMC-1.

3.13.4 Mass spectrometric identification of nitration sites in 15-hydroxy prostaglandin dehydrogenase

There are eight tyrosine residues in the 266 amino acids of PGDH. We created an inclusion list as mentioned earlier, depicting tryptic digestion of

Protein: 15-hydroxy prostaglandin dehydrogenase (*Homo sapiens*)

Amino acids: 266

Mass: 28,977 Da

Calculated pI value: 5.56

Sequence Coverage: 68%

Protein sequence:

1 MHVNGKVALV TGAAOGIGRA FAEALLLKGA KVALVDWNLE AGVOCKAALD
51 EQFEPOKTLF IQCDVADQQO LRD^TFRKVVD HFGRLDILVN NAGVNNEKN^W
101 E^KTLQINLVS VISGTYLGLD YMSKQNGGEG GIINMSSLA GLMPVAQOPY
151 YCASKHGIVG FTRSAALAN LMNSGVRLNA ICPGFVNTAI LESIEKEENM
201 GQYIEYKD^HI K^DMIKYYGIL DPPLIANGLI TLI^EDDALNG AIMKITT^SK^G
251 IHFODYDTTP FOAKT^Q

Figure 3.30 Amino acid sequence of 15-hydroxy prostaglandin dehydrogenase. Matched peptides were underscored and shown in bold red colour.

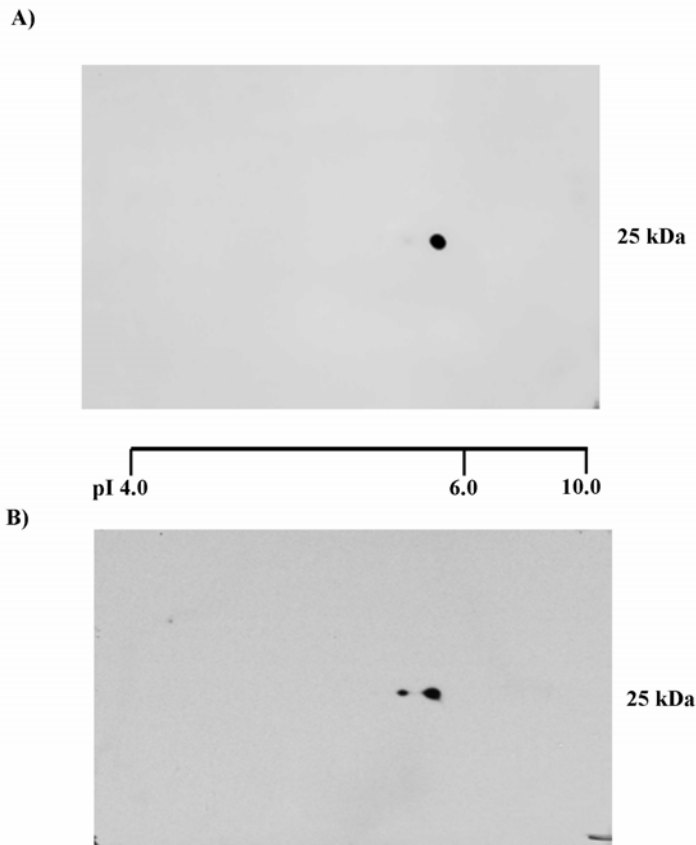


Figure 3.31 Confirmation of S-nitrosoglutathione-induced nitrated spot in LAD2 as 15-hydroxy prostaglandin dehydrogenase. LAD2 cells (15×10^6 cells) were treated for 4 h at 37°C with 500 μ M of SNOG, the cells were lysed, the 50 to 10 kDa fractions were separated using centrifugal cut-off filters and the proteins were resolved in a pI 4 to 7 strip in the first dimension and separated using 12% SDS-PAGE gel in the second dimension. A) western blot with anti-nitrotyrosine antibody B) western blot with anti-15-hydroxy prostaglandin dehydrogenase antibody. Note the multiple pI forms of 15-hydroxy prostaglandin dehydrogenase seen on western blot (B). The pI form on the right side was nitrated, whereas the pI form on the left side was not.

the amino acid sequence of PGDH. We replaced the tyrosines into nitro-tyrosines and the software generates theoretical peptides with nitrated tyrosines. The mono isotopic masses of these nitrated peptides and the double charged ions and triple charged ions were compiled and then MS/MS analysis was performed on the sample we submitted for MS identification. The inclusion list for the nitrated peptides of PGDH is summarized (Appendix 1, Table 4). We did not identify any nitrated peptides in the analysis (see discussion).

Chapter - 4 Discussion

Chapter Four: Discussion

4.1 Summary of data

Nitric oxide is a short-lived free radical gas that plays a critical role in the regulation of cellular signalling. Mast cell derived NO and exogenous NO regulate MC activities including the inhibition of MC degranulation. At a molecular level NO-derived reactive nitrogen species modify protein structure and function through several mechanisms including protein tyrosine nitration. To begin to elucidate the molecular mechanisms underlying the effects of NO in MC, we investigated protein tyrosine nitration in human mast cell lines HMC-1 and LAD2 treated with the NO donor SNOG. Using two dimensional gel electrophoresis and western blot analysis with an anti-nitrotyrosine antibody together with mass spectroscopy, we identified aldolase A, an enzyme of the glycolytic pathway, as a target for tyrosine nitration in MC.

S-nitrosoglutathione treatment conditions that nitrated MC aldolase also reduced the V_{max} of aldolase in HMC-1 and LAD2. Nuclear magnetic resonance analysis showed that despite these changes in activity of a critical enzyme in glycolysis, there was no significant change in total cellular ATP content, although the AMP/ATP ratio was altered. Elevated levels of lactate and pyruvate suggested that SNOG treatment enhanced glycolysis. Reduced aldolase activity was associated with increased intracellular levels of its substrate, fructose-1,6-bisphosphate (FBP). Interestingly, FBP inhibited IgE-mediated MC degranulation and intracellular Ca^{2+} in LAD2 cells. Moreover, 15-hydroxy prostaglandin

dehydrogenase, a critical enzyme in the metabolism of PGE₂ was identified as a prominent target of tyrosine nitration in LAD2 cells.

Thus for the first time we report evidence of protein tyrosine nitration in human MC lines and identify aldolase A as a prominent target in HMC-1 and LAD2; and PGDH in LAD2 cells. The post translational nitration of aldolase A and PGDH may be important pathways that regulate MC phenotype and function.

4.2 Significance of aldolase nitration in mast cells

Endogenous and exogenous NO have been widely reported to modulate several MC functions (173). One common pathway involved is that NO activates sGC and increases intracellular cGMP, which in turn regulates numerous physiological events in the cell (105). However, many studies indicated that non-cGMP mediated pathways are also important in the effects of NO on MC function (179, 182, 188, 191). Earlier work from our lab suggested that S-nitrosylation of calpain decreased its activity and was responsible for the NO-mediated inhibition of MC adhesion (191). In the present study, we provide the first evidence that protein tyrosine nitration plays a role in NO-mediated inhibitory effects on MC function.

4.2.1 Constitutive nitration in mast cells

Using western blot with an anti-nitrotyrosine antibody, we identified constitutive protein tyrosine nitration in MC, thereby providing evidence that this post-translational modification of proteins occurs in a variety of MC (Figure 3.1). Our observation is supported by evidence that constitutive nitration occurs in

other leukocytes such as macrophage cell lines (232), eosinophils (209, 233) and neutrophils (234).

It is interesting that a recent study claims that there are no nitrotyrosine positive proteins in MC on lung sections of cystic fibrosis patients (209). Unfortunately isotype controls were not reported in this study and there was no information about optimization of the sensitivity of the immunohistochemistry to detect nitrotyrosine reactivity in MC, or the numbers of MC assessed in the tissues.

Western blot technique has many advantages over other immunodetection techniques. For example, the high local concentration of the antigen on the membrane can enhance the binding of antibodies through both Fab (antigen binding fragments) thereby increasing the avidity of the interaction. Moreover, the antigen density also facilitates the retention of low affinity antibodies on the membrane by increasing the frequency with which antibodies leaving the membrane rebind to adjacent sites (235). Moreover, western blot employs a denaturing separation using SDS-PAGE, where the antigen will be denatured and hidden epitopes will be exposed thereby increasing binding with the corresponding antibodies. Thus western blot is a proven standard technique in analyzing a mixture of complex proteins for protein tyrosine nitration. Enrichment of MC from human tissues and establishing the presence of nitrated proteins using mass spectrometry will unequivocally provide evidence for protein tyrosine nitration of MC *in vivo* under physiological conditions.

Western blot has many disadvantages such as: i) difficulties in recognising low abundance proteins in crude cell lysates, ii) non-specific binding of antibody with cross reacting epitopes on the antigen and often multiple bands visualised in the blot, iii) high sensitivity antibodies often enhance the background and extensive optimization is necessary to get good quality blot, iv) all the variables including antigen, primary antibody, secondary antibody and time of exposure need to be optimised to use western blot as a semi-quantitative technique, v) optimization of transfer time is critical as high molecular weight proteins need longer duration and low molecular weight proteins require less time, vi) variations in signal-to-noise ratio among different experiments and vii) the antibody may not recognize the antigen if denaturation steps in western blot interfere with antigenic epitopes.

4.2.2 S-nitrosoglutathione-induced nitration of aldolase

In addition to the constitutive nitration of multiple MC proteins, we identified SNOG-induced changes in protein nitration (Figure 3.4). It is interesting that aldolase at pI 9.0 was nitrated constitutively, whereas SNOG-induced nitration of aldolase A was associated with an 8.3 pI form (Figure 3.4, 3.6).

It is intriguing that aldolase A has been identified as a target of tyrosine nitration in several other cells and tissues including diaphragm (236), human skin fibroblasts (220), quadriceps muscle of patients with severe COPD (237) and in lung tissue in a model of asthma (168). However, this is the first report in human MC. Unpublished results in the laboratory of Kulwant Singh Aulak, Cleveland

Clinic Lerner Research Institute, USA (220) suggest that aldolase nitration occurs in human tissues from lung, retina and skin (personal email communication dated 9th June 2009). The discovery of aldolase as one target for nitration in MC might be due to the abundance of this protein, extent of nitration of tyrosines in aldolase and sensitivity of the methods used. Interestingly, other proteins were also nitrated upon SNOG treatment in LAD2 (Figure 3.28).

4.2.3 Multiple pI forms and isoforms of aldolase in mast cells

Presence of multiple pI forms (~7.0 to 9.3) of aldolase in MC is consistent with earlier findings in rat diaphragm and mouse sperm cells (236, 238). Aldolase can also be phosphorylated (239), and regulated by different post-translational modifications. Interestingly, aldolase A can be found in the cytoplasm (240), mitochondria (241) and in the heterochromatin region of the nucleus (242) and *in vivo* nitration can be seen in many intracellular compartments (148) including in association with nuclear histones (243).

There are three genes of mammalian aldolase, A, B and C (225). Aldolase A and C are preferentially involved in the glycolytic cycle and predominantly expressed in muscle and brain, respectively, whereas aldolase B is expressed in liver and preferentially involved in gluconeogenesis pathway (225). However, the expression of these isoforms is not restricted to specific tissues, (e.g. all three isoforms are expressed in kidney) (244, 245). Tyrosine nitration of aldolase A, B and C has been reported in a wide range of tissues and under different inflammatory conditions (168, 236, 246-248).

MC express both mRNA and protein of two isoforms, aldolase A and C (Figure 3.8, 3.9). Aldolase A is the predominant isoform expressed in lymphocytes (249). Aldolase C expression was reported in platelets, but was not detectable in erythrocytes and lymphocytes (250). It is interesting that MC express aldolase C, the isoform predominantly expressed in neuronal tissues. The potential significance of aldolase C expression in MC is multiple. For example, if there is inactivation of one isoform of the enzyme, the other isoform, in this case aldolase C could potentially act as a backup enzyme in the glycolytic cycle. Interestingly, aldolase C was reported to be involved in a stress-response pathway for lung epithelial cell function during hypoxia (251). Moreover, subsets of cerebellar Purkinje cells expressing aldolase C were resistant to excitotoxic insult (252) and aldolase C siRNA transfection results in death of these subsets of Purkinje cells. Since MC play a major role in transforming growth factor beta 1-mediated excitotoxicity (253), expression of aldolase C may be of functional significance in MC homeostasis.

4.2.4 Potential mechanisms of aldolase nitration in mast cells

Tyrosine nitration of a protein can be mediated by multiple mechanisms including a peroxynitrite-mediated pathway (Figure 1.5) (119). In our model, we predict that exogenous NO combines with MC-derived superoxide to generate ONOO^- , which could in turn nitrate aldolase. The half-life of ONOO^- in alkaline solutions at room temperature is 5 h, whereas the ONOO^- decomposes rapidly in acidic conditions and its half-life is only a few seconds under physiological pH 7.4 (254). Thus ONOO^- reactivity may act in a local microenvironment on a

limited spectrum of proteins. In our experiments we decided to use a slow releasing NO donor, SNOG (decomposition rate is approximately 5% per hour in water at room temperature and the half-life is about 80 h at 37°C) that would likely combine with physiologically relevant, MC-derived $\cdot\text{O}_2^-$, thereby facilitating generation of ONOO^- in our experimental conditions. As human MC can generate reactive oxygen species through NADPH oxidase-1 pathway (207), we predict $\cdot\text{O}_2^-$ generation in our experimental conditions. (See section 1.5.3 page 37 for details of $\cdot\text{O}_2^-$ generation in MC). However, we did not use any scavengers of ONOO^- or $\cdot\text{O}_2^-$ in our study to confirm the involvement of ONOO^- in our observations.

Besides ONOO^- there are other mechanisms of nitration by NO such as 3-nitrosotyrosine formation followed by oxidation to 3-nitrotyrosine (pathway 6, Figure 1.5). Moreover, *in vitro* SNOG treatment has been shown to nitrate hexokinase, a mitochondrial enzyme (255). The precise mechanisms underlying the nitration of aldolase in MC are beyond the scope of the current study. However, future studies aimed at understanding these mechanisms are necessary to elucidate the molecular pathways of NO in MC biology. Another consideration is that NO might facilitate selective nitration of aldolase A in different intracellular compartments of HMC-1 and modulate compartment-specific functions of aldolase.

4.2.5 Mass spectrometric evidence for nitration of aldolase

An earlier *in vitro* study using rabbit muscle aldolase treated with ONOO^- demonstrated four different tyrosine residues (Tyr^{222} , Tyr^{243} , Tyr^{342} , Tyr^{363}) that

were targets for tyrosine nitration (220). In our study we have preliminary evidence for nitration at Tyr² and Tyr⁵⁸ (Fig. 3.12, 3.13). This is the first report on nitration sites in human aldolase A and of the unique tyrosine residues (Tyr² and Tyr⁵⁸) found nitrated. Structural localization of Tyr⁵⁸ on aldolase A revealed that potential hydrogen bond formation upon Tyr⁵⁸ nitration might influence the structure of the active site loop of aldolase A (see section 3.6, page 88 for more details). Unfortunately, we could not detect any tyrosine nitration sites in our follow up studies and suspect that our methods were not sensitive enough for the study conducted.

The sensitivity of western blot with anti-nitrotyrosine antibody identified nitrated proteins, but the mass spectrometric identification of the precise nitration sites on protein samples digested from 2-DE gels was challenging. The literature on this approach and associated problems is limited. For example, Koeck *et. al.* (248) showed evidence for aldolase nitration by 2-DE western blot method in human skin fibroblasts, but they could not identify nitration sites using mass spectrometry (personal email communication dated 9th June 2009). Hence they treated enriched rabbit muscle aldolase with ONOO⁻ *in vitro* and performed MS studies to demonstrate the nitrated tyrosine residues of aldolase A.

Moreover, mass spectrometric identification of nitrated tyrosine residues requires large amounts of purified protein. For example, the above mentioned *in vitro* study used 300 µg of rabbit muscle aldolase to demonstrate nitration sites (248). In another study, about 500 µg of fibrinogen was used to enrich the nitrated fractions and MS identification of nitration sites (256). Since identification of the

precise tyrosine nitration sites on aldolase was not the major priority in our project, we did not perform these experiments.

In addition to nitration of tyrosine, we performed MS/MS analysis on the SNOG-treated aldolase enriched fractions of HMC-1 for post-translational modifications such as S-nitrosylation, S-glutathiolation, phosphorylation, and cysteine oxidation. We did not identify any of these post-translational modifications in our analysis.

4.2.6 Nitric oxide-mediated changes in mast cell aldolase activity

In spite of a lack of reproducible data on the precise nitrated tyrosine residues in MC aldolase A, SNOG treatment reproducibly reduced total activity of MC aldolase (Figure 3.17), as previously shown using rabbit muscle aldolase (220). Since it is difficult to separate the two isoforms of aldolase A and C from the whole cell lysate, we studied total aldolase activity, as reported earlier in different tissues and under different conditions (242, 257). The tyrosine at the carboxyl terminal end of aldolase A, i.e. Tyr³⁶³ is critical for enzymatic activity, and nitration of this residue significantly reduced the V_{max} of the enzyme activity of rabbit muscle aldolase (220). We have preliminary evidence in our MS data for nitration of Tyr⁵⁸ in HMC-1 aldolase A, which might also interfere with the active site loop of aldolase A, thereby reducing its activity.

Interestingly, our observation that NO induced a reduction in both K_m and V_{max} of HMC-1 aldolase is consistent with earlier studies where substitution of Tyr³⁶³ with serine in human aldolase A also reduced enzyme K_m and V_{max} (258). SNOG reduced K_m of HMC-1 aldolase, whereas there was no change in K_m of LAD2 (Figure 3.18). Moreover, there is a tenfold difference between the K_m

values of HMC-1 and LAD2 (Figure 3.18). Thus, there may be cell-type specific differences in the effects of nitration, i.e. LAD2 is a more mature MC line, whereas HMC-1 is an immature cell line. Moreover, the expression and intracellular distribution of aldolase isoforms A and C between these two cell lines may be different and the tyrosine nitration sites may differ as well.

4.2.7 Significance of S-nitrosoglutathione-induced elevation of intracellular fructose-1,6-bisphosphate in mast cells

Given the reduction in enzymatic activity of aldolase, we postulated that this would increase levels of its substrate, FBP. Indeed we found that the intracellular FBP in HMC-1 cell extracts significantly increased following SNOG treatment (Figure 3.19). Similarly, statistically significant elevation of FBP levels following SNOG treatment was documented in LAD2 (Figure 3.19). It is interesting to note that the SNOG-induced FBP levels between HMC-1 and LAD2 also differ, as the K_m values of these two MC lines (see above). Thus the difference in magnitude of K_m values, unaltered K_m values of LAD2 compared to reduction in K_m of HMC-1 after SNOG treatment, along with variable intracellular FBP levels strongly suggests that the outcome of nitration might be different between HMC-1 and LAD2. Further detailed study is necessary to understand the relevance of our observations.

Interestingly a mutation of aldolase A (Glu206Lys) was reported in a patient suffering from an inherited metabolic myopathy and haemolysis and was associated with increased FBP levels (182.9 % of control) in the patient's red blood cells (259). Moreover, NO-induced inhibition of glyceraldehyde-3-

phosphate dehydrogenase, the enzyme downstream of aldolase in the glycolytic cycle, and a corresponding increase in FBP levels in rat intestinal tissues were reported (260). Thus increased FBP levels upon inactivation of aldolase A may have physiological relevance.

4.2.8 Significance of nuclear magnetic resonance spectroscopy data in our study

To assess the effects of aldolase nitration on the metabolic pathways of MC we analyzed metabolites using nuclear magnetic resonance spectroscopy. ATP levels in cell extracts were similar in sham and SNOG treated HMC-1 (Figure 3.19A). It is interesting that cellular ATP levels remained similar despite reduction in the activity of aldolase, thereby suggesting restoration of ATP levels through homeostatic mechanisms. AMP-activated protein kinase (AMPK) was reported to act as a fuel gauge in mammalian cells. It can enhance cellular ATP levels by switching off energy-using pathways and switching on energy-generating pathways (261, 262). AMPK activation occurs when there is an increase in AMP and decrease in ATP levels (increased AMP/ATP ratio) (261). We predicted that this regulatory pathway also exists in MC and therefore measured the AMP/ATP ratio before and after SNOG treatment. Indeed, AMP/ATP ratio was increased following SNOG-treatment in HMC-1 (Figure 3.19B) thereby providing evidence for homeostatic regulation of ATP levels in our model. In addition to HMC-1, the ATP levels in LAD2 were also unaltered after SNOG treatment (Figure 3.24). The lower ATP levels detected using NMR (Figure 3.19) compared with live cell based ATP assay (Figure 3.24) may be due

to the loss of ATP during the preparation of sample for NMR. For NMR sample preparation, cell pellets were extracted with methanol: chloroform mixture (2:1) followed by rapid freeze-thawing and centrifugation at 100g for 15 min. The supernatant fraction was aliquoted, frozen, lyophilized and stored at -80°C until NMR analysis.

Measurement of pyruvate, the end product of glycolysis and lactate, the end product of anaerobic glycolysis in the media of cultured cells provides clear understanding on the metabolic status of the cells (263). Interestingly, both pyruvate and lactate were significantly elevated in culture media of NO-treated MC (Figure 3.23) indicating enhanced glycolysis, as previously shown in astrocytes treated with NO (264). NO down-regulates mitochondrial energy production by inhibiting cytochrome C oxidase, but the cells maintain energy production by up regulating glycolysis through AMP protein kinase in astrocytes (265). It seems paradoxical that, although aldolase enzymatic activity is depressed (Figure 3.17), glycolysis appears to be enhanced. In support of our observations, studies of skeletal muscle have shown that elevated FBP is associated with increased glycolysis (265) and FBP activation of 6-phosphofructo-1-kinase a key rate-limiting enzyme in glycolysis (265). It is interesting that some cells can respond to NO by activating glycolysis (astrocytes), whereas others do not (neurons) (265). Our results suggest that in spite of SNOG-induced decrease in aldolase activity, energy production was restored in HMC-1 through homeostatic mechanisms.

Glutathione, a tripeptide containing glycine, cysteine and glutamic acid is well known for its intracellular antioxidant properties (266). Glutathione and glutathione-dependent enzymes play a pivotal role in the defence against oxidative stress (267). It is interesting that in HMC-1 intracellular glutathione was increased upon SNOG treatment (Figure 3.23). We do not know whether the increased glutathione level is due to the cellular response to oxidative stress or glutathione is released from SNOG, the NO donor itself. Future studies involving the NO and glutathione pathway are necessary to understand the role of NO and anti-oxidative responses in MC biology.

Even though we have documented significant changes in different metabolites in our NMR analysis, precise interpretation of our data is difficult from our preliminary findings. From our data we have created a conceptual model (Figure 4.1) which may help to understand the effects of NO on MC metabolism.

The levels of glucogenic amino acids such as glutamine, glutamate, alanine, asparagine, glycine, and threonine have been reduced upon SNOG treatment in HMC-1 cells (Figure 3.21). We can predict that these amino acids might be incorporated into the tricarboxylic acid cycle (Figure 4.1). For example, alanine, glycine and threonine could have been converted into pyruvate as the levels of these amino acids were decreased upon SNOG treatment. This observation can be correlated with enhanced pyruvate level after SNOG treatment. Asparagine can be converted into oxaloacetate, and glutamine or glutamate can be converted into α -keto-glutarate. In the absence of elevated levels of oxaloacetate and α -keto-glutarate in

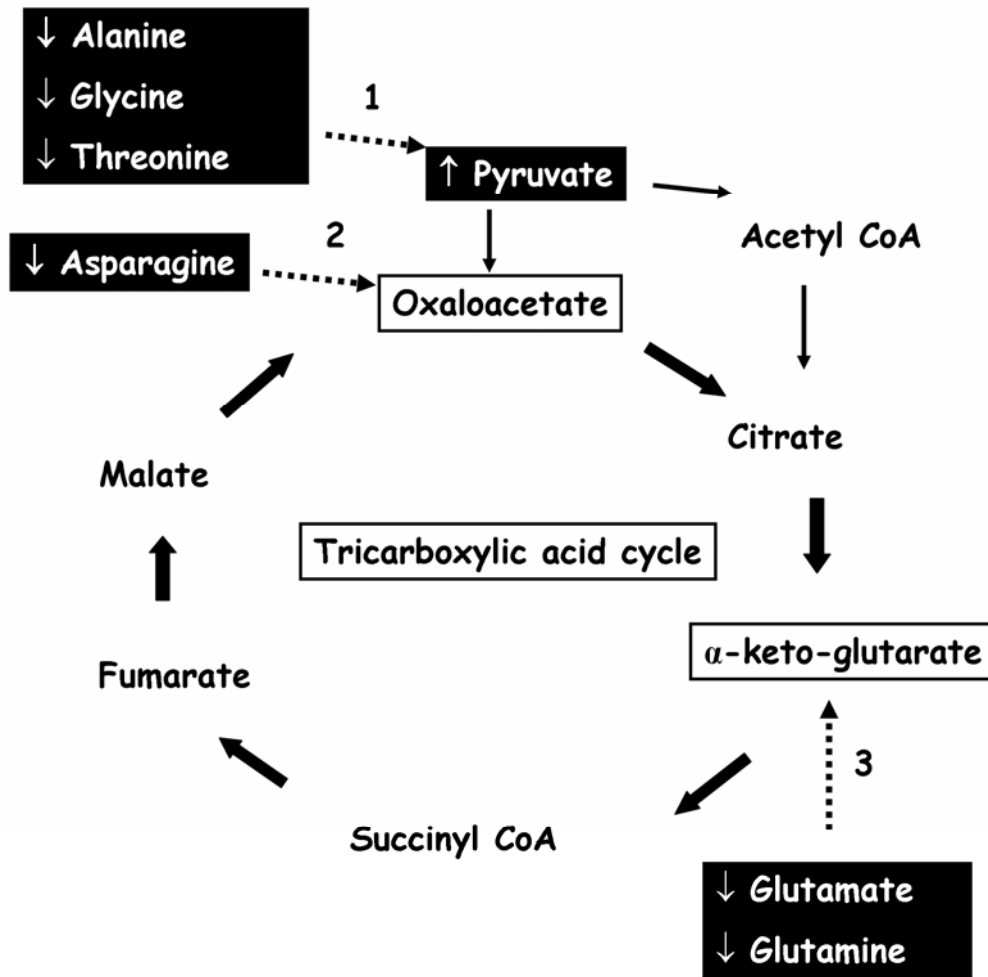


Figure 4.1 Conceptual model on effects of nitric oxide on mast cell metabolites. 1) SNOG-induced decrease in alanine, glycine and threonine in cell extracts can be linked with increased pyruvate (enhanced glycolysis); 2) Decrease in asparagine might be due to conversion into oxaloacetate; 3) Decrease in glutamate and glutamine in cell extracts might be a result of their conversion into α -keto-glutarate.

our NMR data it is hard to predict such an interconversion occurred after NO treatment in MC.

Metabolite profiling using a NMR approach has its limitations. NMR analyses have lower sensitivity when compared with MS based techniques (268). For example, in our experiments we could not identify intracellular FBP in HMC-1 cells using NMR. However all the glycolytic metabolites including FBP were identified using liquid chromatography/MS/MS methods (269). Moreover, NMR is not widely accepted as a quantitative technique for studies of the metabolome. The data represents a snapshot at one time and may not represent the dynamic changes in the cellular metabolites over a period of time.

The effect of NO on the glycolytic metabolism could be better understood using tracer studies such as C¹³-glucose and C¹³-glutamate in our media to dissect the effects of NO on the glycolytic pathway and tricarboxylic acid cycle respectively. Future experiments employing C¹³-glucose in the media and tracing the fate of the C¹³-labeled carbon in HMC-1 treated with or without SNOG will help to understand the consequences of aldolase nitration on the glycolytic metabolites of MC.

4.2.9 Role of fructose-1,6-bisphosphate in mast cell function

FBP has several activities including protection in ischemia/reperfusion injury and hypoxia (260, 270) and suppression of T-cell proliferation (271). FBP has been used as a component of protective solutions in transport of donor organs such as liver prior to transplantation (272). Others have filed a patent on FBP as a therapeutic for asthma (273) and recent *in vivo* work in rats demonstrated that

FBP has an inhibitory role on MC degranulation and histamine release (274). The biological effects of FBP are summarized in the Figure 4.2.

We hypothesized that increased FBP levels, following aldolase A nitration in MC, might inhibit some MC functions. Indeed FBP significantly inhibited β -hexosaminidase release by LAD2 (Figure 3.26), whereas similar concentrations of neither fructose-1-phosphate nor fructose-6-phosphate had significant effects, supporting the specific effects of FBP on MC degranulation. It has been reported that the effects of NO donors on human MC activation depends on their NO release kinetics rather than the amount of NO released (275). Hence our data on the effects of SNOG pretreatment followed by MC activation in a NO free environment, supports NO-mediated post-translational modification, in this case nitration of aldolase. Moreover, the slow NO releasing donor SNOG has been widely reported to mediate its action through non-cGMP pathways in inhibition of platelet aggregation (213) and inhibition of MC adhesion (191).

Exogenous FBP pretreatment also inhibited the IgE/anti-IgE induced intracellular Ca^{2+} levels in LAD2 (Figure 3.27). In spite of our observation that both SNOG and FBP inhibited IgE/anti-IgE induced β -hexosaminidase release from LAD2 (Figure 3.26), SNOG did not inhibit Ca^{2+} levels in LAD2. It is interesting that SNOG treatment did not alter intracellular Ca^{2+} in our assay system where only the intracellular Ca^{2+} was measured in a Ca^{2+} free buffer.

Future studies measuring Ca^{2+} in a buffer containing Ca^{2+} should be conducted to measure the effects of SNOG on Ca^{2+} influx into the MC. It is clear that the HEPES Tyrode's buffer we used in our β -hexosaminidase experiments

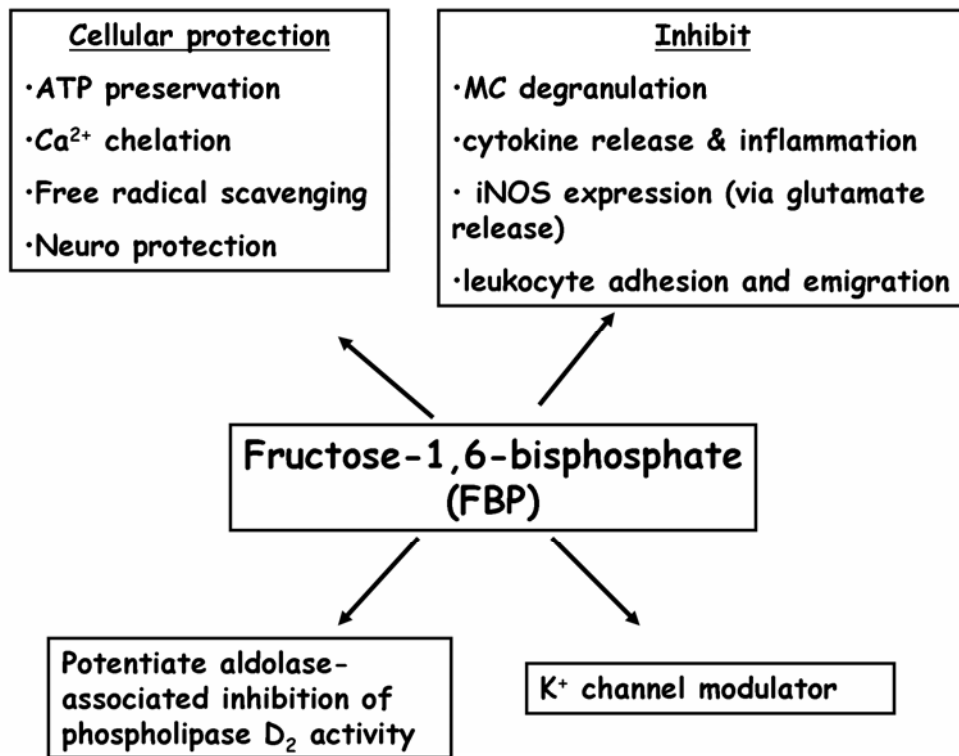


Figure 4.2 Biological effects of fructose-1,6-bisphosphate. FBP plays diverse roles in many biological systems including, neuroprotection (270), inhibitory actions on MC degranulation and histamine release (274) and potentiation of the inhibitory activity of aldolase on phospholipase D₂ (276).

contains Ca^{2+} (1 mM) and the assay conditions contain extracellular Ca^{2+} thereby facilitating Ca^{2+} influx into the cell.

Analysis of the temporal relationship between Ca^{2+} and NO levels revealed that both Ca^{2+} and NO levels were enhanced after antigen stimulation and *in situ* production of NO did not inhibit the Ca^{2+} levels in rat peritoneal MC (277). Interestingly, a recent report claims that NOS-independent NO enhances intracellular Ca^{2+} levels in RBL-2H3 MC (278). Many differences between these studies and ours such as, different types of Ca^{2+} assays, MC from rat versus human, endogenous NO versus exogenous NO could account for the discrepancies. Further detailed studies using multiple NO donors, multiple MC types and different Ca^{2+} assay systems are warranted to understand the effects of NO on Ca^{2+} pathways in MC.

4.2.10 Future directions

Phospholipase C (PLC) cleaves phosphatidylinositol-bisphosphate (PIP_2) to diacylglycerol (DAG) and inositol 1,4,5-trisphosphate (IP_3), a critical intracellular messenger. Phospholipase C gamma ($\text{PLC}\gamma$) mediated signalling plays a pivotal role in MC degranulation (21). Interestingly, some effects of FBP in other cells depend on PLC signalling (270). Moreover, FBP shares a binding site on aldolase A with IP_3 (279) and significantly inhibits IP_3 binding to aldolase A (279, 280). This binding also inhibits aldolase A enzymatic activity and influences release/repartition of aldolase A from binding to cytoskeletal elements (280). The post-translational modification of tyrosine nitration of aldolase A may alter its relative affinity for FBP and/or IP_3 . Thus, it is possible that NO acts

through excess FBP that modifies IP₃ and PLC signalling cascades critical in MC secretion in IgE-dependent responses (Figure 4.3). Interestingly, aldolase can bind to many intracellular proteins such as actin and the ryanodine receptor (Table 4.1) (281, 282). Aldolase nitration might alter some of these interactions and in turn regulate MC function. Further studies with mature MC may enhance our insights into these pathways.

4.3 Significance of nitration of 15-hydroxy prostaglandin dehydrogenase in mast cells

Prostaglandins are lipid-derived inflammatory mediators that are derived from arachidonic acid through cyclooxygenase (COX) pathway (Figure 4.4). COX-1, and COX-2 are the two COX enzymes expressed in different cell types (283). COX catalyses the oxidation and cyclization of arachidonic acid into prostaglandin endoperoxidase (PGH₂). PGH₂ is further converted into thromboxanes, various prostaglandins and prostacyclin by their respective synthases in different cell types (Figure 4.4). Prostaglandins are catabolised into biologically inactive 15-keto prostaglandins by initial oxidation of 15(S) hydroxyl group catalyzed by the NAD⁺-linked enzyme 15-hydroxy prostaglandin dehydrogenase (PGDH) (284). PGDH is an important catabolic enzyme that inactivates prostaglandins and related eicosanoids (285).

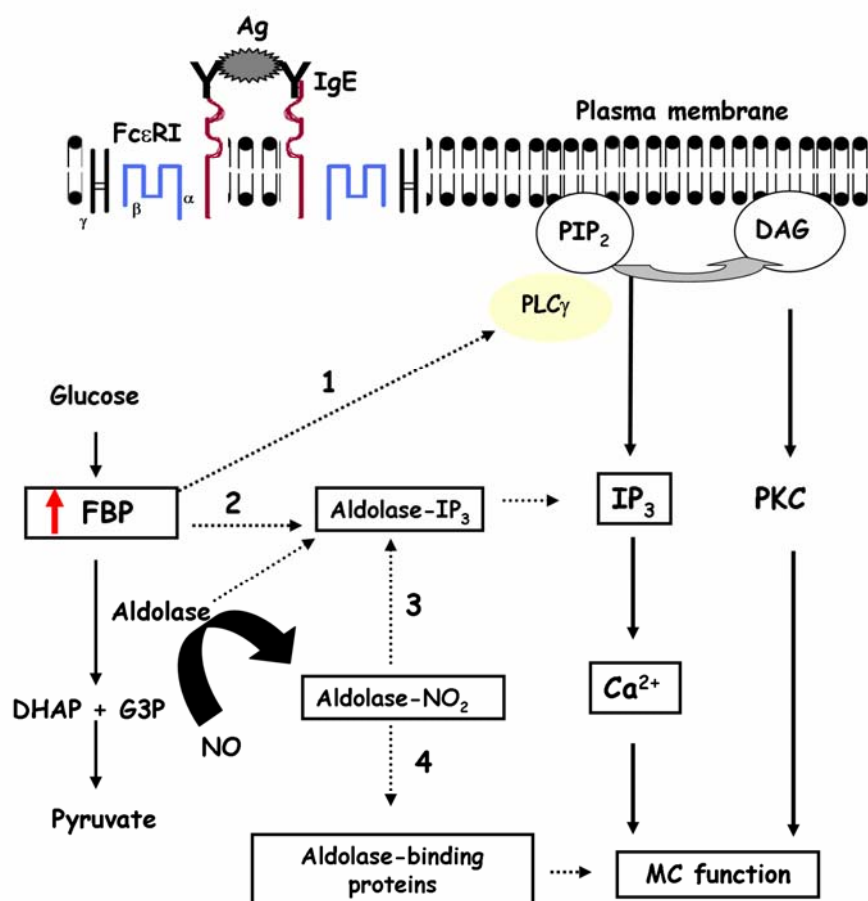


Figure 4.3 Conceptual model of aldolase nitration and elevated fructose-1,6-bisphosphate in mast cells. Exogenous nitric oxide (NO) treatment facilitates aldolase nitration and decreases its activity and a corresponding elevation of its substrate, fructose-1,6-bisphosphate (FBP) in MC. 1) Elevated FBP might influence the phospholipase C gamma (PLC γ) pathway; and 2) affect the aldolase-inositol 1,4,5-trisphosphate (aldolase-IP $_3$) interactions inside the MC; 3) nitration of aldolase might alter its affinity for IP $_3$ thereby regulating intracellular IP $_3$ levels in MC; 4) nitration of aldolase might alter interactions with aldolase-binding proteins which in turn could regulate MC function.

Table 4.1 Potential aldolase binding proteins reported in the literature

Aldolase-binding protein	Species/cells	Activity modulated by aldolase binding	References
glucose transporter GLUT4; F-actin	muscle and adipose cells	promotes exocytosis of GLUT4 to the plasma membrane	(286)
thrombospondin-related anonymous protein	Plasmodium	parasite gliding motion used in host infection	(287)
Mn-superoxide dismutase	Mycobacteria	facilitates bacterial penetration into epithelial cells through binding with host aldolase	(288)
band 3 membrane protein	oxygenated erythrocytes	inhibits glycolytic flux	(289)
pleckstrin homology domain of phospholipase D ₂	rat brain	inhibits phosphatidic acid generation	(276)
vacuolar H ⁺ -ATPase	yeast	coupling of glycolysis directly to the ATP-hydrolyzing proton pump	(290)
Sorting nexin 9 (SNX9)	rabbit	blocks localization of SNX9-dynamin-2 complex to clathrin coated pits	(291)
Wiskott-Aldrich syndrome protein (WASP)	HeLa cells	modulates actin dynamics in cell motility	(292)

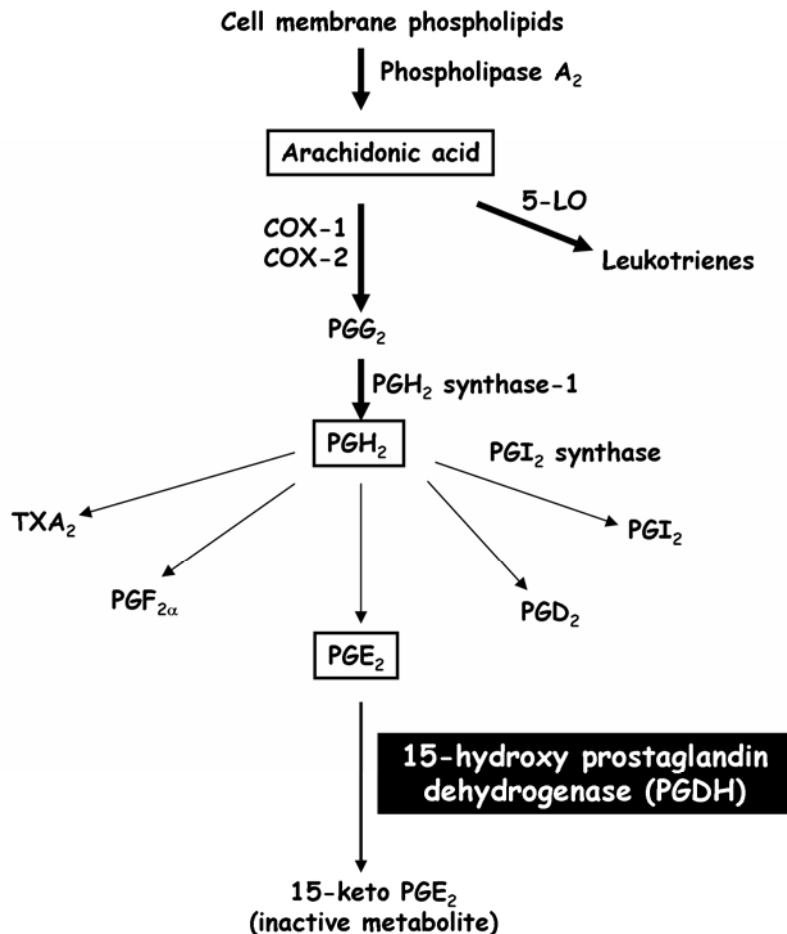


Figure 4.4 An overview of arachidonic acid metabolic pathway.

Cyclooxygenase-1 (COX-1) and COX-2 converts arachidonic acid into prostaglandin G₂ (PGG₂) followed by conversion into prostaglandin H₂ (PGH₂) by PGH₂ synthase-1. All prostaglandins and thromboxane A (TXA₂) are synthesised by their respective synthases. PGDH converts the active prostaglandin E₂ (PGE₂) into inactive 15-keto PGE₂. Note that leukotriene synthesis through 5-lipoxygenase (5-LO) pathway is not expanded in this figure.

PGDH is ubiquitously expressed in mammalian tissues (293) and measurement of its activity was reported as early as 1976 (294). However, in the current study we discovered PGDH expression in MC. PGDH is usually expressed as a dimer with a molecular weight of 29 kDa. It uses a wide range of prostaglandins as its substrates with different *K_m* values (10 μ M for PGE₂; 27 μ M for PGE₁; 32 μ M for PGA₂; 33 μ M for PGA₁ and 59 μ M for PGF_{2 α}) (295). PGB, PGD and TXA₂ are poor substrates (296, 297). In addition to prostaglandins, omega-6 fatty acids such as 15-hydroxyeicosatetraenoic acid (15-HETE), 5,15-diHETE, 8,15-diHETE (298), 12-hydroxy-5,8,10-heptadecatrienoic acid (12-HHT) (299) and lipoxin A₄ (300) were also reported to be substrates for PGDH. The regulatory role of PGDH in inflammatory conditions is gaining recognition because it catabolises both proinflammatory prostaglandins and anti-inflammatory lipoxins (296).

4.3.1 Role of 15-hydroxy prostaglandin dehydrogenase in physiology and inflammation

Most of the prostaglandins including PGE₂ are metabolised in lung (301) and the expression of PGDH has been linked with metabolism of PGE₂ in the lung. Moreover, a significant increase in PGDH levels during late gestation has been demonstrated in fetal lung (302). Coggins *et. al.* using a PGDH knockout mouse, demonstrated that alteration in PGE₂ metabolism by PGDH during the perinatal period is essential for the permanent closure of the ductus arteriosus (303). The indirect effect of PGDH in inflammation is proposed through its regulatory role on PGE₂ levels. For example, lipopolysaccharide treatment leads

to decreased expression of PGDH and corresponding increased PGE₂ levels in mouse lung (304).

PGE₂ has both bronchodilator and anti-inflammatory roles in the lung (305, 306). A recent study claims that PGE₂ levels were elevated in sputum of both moderate and severe asthmatic patients in comparison to control subjects (307). There are no reports on the expression of PGDH in asthmatic lung and this represents a potential area of future research. The enhanced NO levels in asthmatic patients together with elevated PGE₂ levels leads to the speculation about whether NO play regulatory role on PGE₂ levels in asthma by inhibiting PGDH activity. Moreover, given the role of MC in asthma, nitration of PGDH in MC represents a potential area of informative research about molecular changes in the lungs in asthma.

4.3.2 Role of 15-hydroxy prostaglandin dehydrogenase in cancer

PGE₂, major substrate for PGDH, has a critical role in promoting tumour growth. Elevated levels of PGE₂ have been linked with poor prognosis in many human malignancies such as colon, lung, breast, head and neck cancer (reviewed in detail (308)). Lack of expression of PGDH, the enzyme that catabolises PGE₂ has been reported in human colon, lung, gastric and breast cancer (309-312). The lack of PGDH results in elevated levels of endogenous PGE₂ that mediates tumour growth. The *in vivo* relevance of PGDH in tumour progression has been studied using PGDH knockout mice. For example, PGDH has been shown to be the physiological antagonist of the prostaglandin synthesising activity of COX-2 and acts as a tumour suppressor in colonic neoplasia development (313).

4.3.3 Nitration of enzymes involved in the arachidonic acid metabolic pathway

Enzymes of the arachidonic acid metabolic pathway that were reported as nitrated in the literature are summarized in this section. Tetranitromethane treatment of porcine, bovine and equine pancreatic phospholipase A₂ results in nitration of Tyr⁷⁰ which is located in the phospholipid binding site of the enzyme (314, 315). Peroxynitrite treatment has been shown to nitrate COX-1 and decreased its activity (316). NO has been shown to nitrate COX-2 and inhibits PGE₂ biosynthesis in lipopolysaccharide-stimulated macrophages (317). Prostaglandin H₂ synthase-1 (PGHS-1), the enzyme that metabolizes arachidonic acid to PGG₂ and PGH₂ in two sequential reactions has been shown to be nitrated (318, 319). Moreover iNOS-mediated nitration of PGHS-1 and suppression of PGE₂ production were reported in mouse aortic smooth muscle cells (320). Prostacyclin is generated from PGH₂ by the action of the enzyme prostacyclin synthase. In bovine aorta, ONOO⁻-mediated nitration of prostacyclin synthase results in decreased PGI₂ and concomitant increase in the substrate PGH₂ (321). Recently, nitration of prostacyclin synthase has been demonstrated in atherosclerotic carotid arteries in patients with type 2 diabetes (322).

It is interesting that of all prostaglandin synthases only COX-1 and prostacyclin synthase have been reported as nitrated (Figure 4.5). Moreover, there are no reports of nitration of any prostaglandin catabolizing enzymes. Our discovery that SNOG treatment nitrates PGDH, the major prostaglandin catabolizing enzyme in MC, is novel and has multiple implications in MC functions and in the regulation of PGE₂ levels in other cells. Since PGE₂ is the

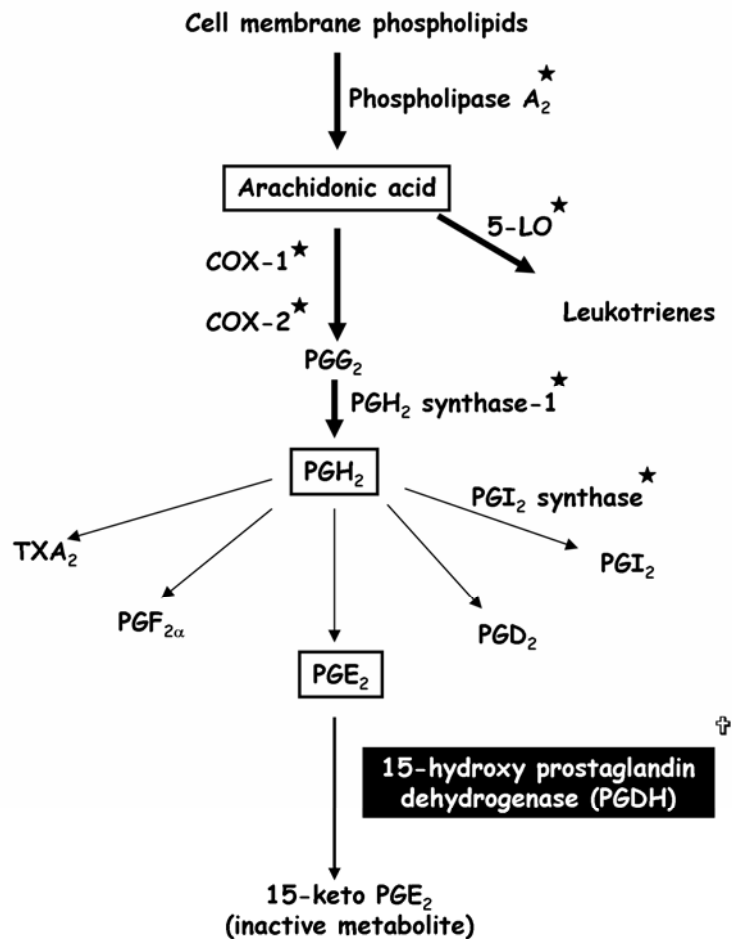


Figure 4.5 Enzymes of arachidonic acid metabolic pathway that have been reported to be nitrated.

★ Nitration of phospholipase A₂ (315), cyclooxygenase-1 (COX-1) (316), COX-2 (317), prostaglandin H₂ (PGH₂) synthase-1 (318), prostaglandin I₂ (PGI₂) synthase (322) has been reported.

† We have the first evidence for S-nitrosoglutathione-mediated nitration of 15-hydroxy prostaglandin dehydrogenase in MC.

major substrate for PGDH activity, we predict that nitration of PGDH might reduce its activity, with a corresponding elevation of PGE₂. Our hypothesis needs to be tested. The biological significance of PGE₂ in MC function is discussed in the following section.

4.3.4 Role of prostaglandin E₂ in mast cell function

PGE₂ is a multifunctional eicosanoid exerting its action through cell surface G-protein coupled receptors called EP receptors. There are four distinct EP receptors EP₁, EP₂, EP₃ and EP₄ that are encoded by different genes. Studies on mice deficient in each of the EP receptor subtypes revealed that the outcome of effects of PGE₂ depends upon the EP receptors expressed under physiological and pathological conditions (323). Heterogeneity exists in the expression of EP receptors in MC and accounts for the differences in the outcome of PGE₂ actions on MC. EP receptor expression and the effects of PGE₂ on different MC are summarized in Table 4.2.

Human cord blood derived MC express EP₂, EP₃ and EP₄ receptors, and EP₃ receptor-dependent signalling potentiates MC mediator release, whereas EP₂ receptor stimulation inhibits MC mediator release (324). One explanation for these observations lies in the mode of action of EP receptors. For example, EP₁ receptors facilitate intracellular calcium release through activation of PLC; EP₂/EP₄ receptors are coupled to stimulation of adenylyl cyclase via G-protein α -subunit stimulation and increases in intracellular cAMP are inhibitory to MC activation. EP₃ receptors are coupled to inhibition of adenylyl cyclase via G-protein α -subunit inhibition and decrease cAMP levels (325).

Table 4.2 Summary of prostaglandin E₂ receptor expression and effects of prostaglandin E₂ on mast cells.

Mast cell	Prostaglandin E₂ receptor (EP receptor)	Effects of PGE₂ on MC
Human cord blood derived MC (324)	EP ₂ , EP ₃ and EP ₄	Potentiate degranulation through EP ₃ Inhibit degranulation through EP ₂
human lung MC (326)	EP ₂ receptors	Inhibit degranulation through EP ₂
Peripheral blood derived MC (327)	EP ₁ and EP ₃	Enhance histamine release
Human cord blood derived MC (328)	EP ₁ ,EP ₂ ,EP ₃ ,EP ₄	Potentiate vascular endothelial growth factor A release through EP ₂
Mouse bone marrow derived MC (329)	EP ₁ , EP ₃ and EP ₄	Enhances CCL2 secretion

The *in vivo* relevance of the differential response of MC to PGE₂ was demonstrated in patients with aspirin tolerant asthma and aspirin exacerbated respiratory disease (330). PGE₂ has no effects on anti-IgE induced cysteinyl leukotriene release from MC from normal and aspirin tolerant asthma patients, whereas it suppressed cysteinyl leukotriene release from MC of aspirin exacerbated respiratory disease patients. Moreover, PGE₂ enhanced PGD₂ release from MC of normal subjects but not of aspirin tolerant asthma and aspirin exacerbated respiratory disease patients.

It is interesting that PGE₂ can activate EP₂ receptors and inhibit degranulation in human lung MC (326), whereas PGE₂ activates EP₁/EP₃ receptors of human peripheral blood derived MC and enhances histamine release (327). These discordant findings can be explained by the existence of functional heterogeneity among MC at different anatomical locations. Human cord blood derived MC express all the subtypes of EP receptors and PGE₂ induces degranulation-independent release of VEGF-A, a pro-angiogenic factor by activation of EP₂ receptor in cord blood derived MC (328). Mouse bone marrow derived MC lack EP₂ receptor expression, and PGE₂ enhances CCL2 secretion by activating EP₁/EP₃ receptors (329).

Pretreatment with PGE₂ has inhibitory effects on histamine release from rat peritoneal MC and TNF release from rat intestinal mucosal MC and peritoneal MC (331). Thus the effect of PGE₂ on MC function is regulated by the expression of different subtypes of EP receptors and their coupling to intracellular signalling pathways. The number of reports on PGE₂ production by MC is limited. Most of

the studies reported that MC produce very little PGE₂ compared to PGD₂ upon IgE/anti-IgE cross-linking (332). However, PGE₂ has been reported to be released along with other prostaglandins upon different stimuli in MC from different species (333). Unpublished results from the laboratory of Joshua A. Boyce, Division of Rheumatology, Immunology and Allergy, Harvard Medical School, USA indicated that human cord blood derived MC respond to stimulation with staphylococcal peptidoglycan, a ligand for TLR-2, and to poly I:C, a ligand for TLR-3, with delayed, sustained secretion of PGE₂ (334). Moreover, exogenous PGE₂ markedly inhibited cysteinyl leukotrienes and PGD₂ generation by cord blood derived MC, and substantially inhibited the production of TNF and IL-5 in response to either FcεRI cross linkage or stimulation with peptidoglycan. Thus MC might release differing amounts of PGE₂ depending upon the stimuli that triggers their activation e.g. innate or acquired immune pathways.

4.3.5 Role of 15- hydroxy eicosatetraenoic acids in mast cells

Lipoxygenases are lipid peroxidising enzymes that are involved in oxygenation of polyunsaturated fatty acids to their respective hydroperoxy derivatives. They are classified based upon their positional specificity of arachidonic acid oxygenation into 5-, 8-, 12-, and 15-lipoxygenase (15-LO) (335). 15-LO converts arachidonic acid into 15-hydroxy eicosatetraenoic acids (Figure 4.6), reported to be one of the substrates for PGDH (298). IL-4 has been shown to induce 15-LO type-1 expression in human cord blood derived MC (336). The metabolites of 15-LO type-1, 15-ketoeicosatetraenoic acid (15-KETE) and 15-hydroxyeicosatetraenoic acid (15-HETE) were reported to be produced in cord

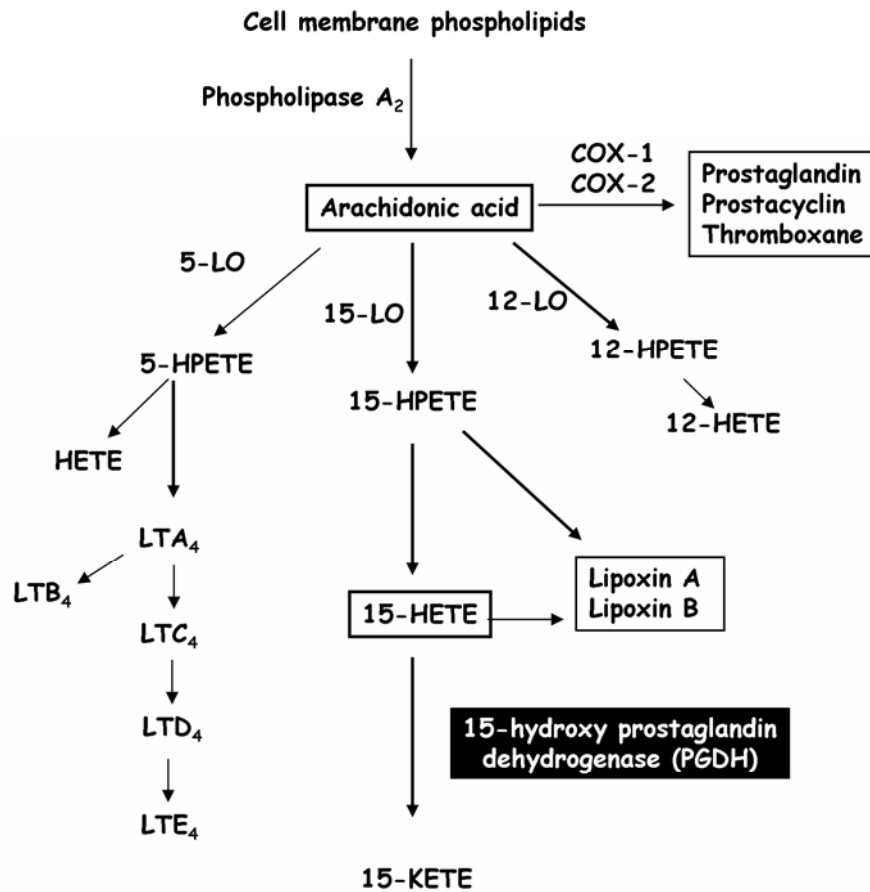


Figure 4.6 An overview of lipoxygenase pathway. Arachidonic acid is metabolized by lipoxygenases (LO) such as 5-LO, 12-LO, 15-LO into their respective hydroxy eicosatetraenoic acids (HETE) through hydroperoxy eicosatetraenoic acids (HPETE). PGDH converts 15-HETE into 15- keto eicosatetraenoic acid (15-KETE).

blood derived MC from arachidonic acid. Moreover, *in vivo* expression of 15-LO type-1 in human lung and skin MCs were reported in this study.

Enhanced levels of 15-HETE have been reported in sputum samples from asthmatic subjects when compared to normal controls (337). Stimulation of HMC-1 with arachidonic acid generate 15-HETE (79). In this study the COX-dependent generation of 15-HETE was reported. It is interesting that arachidonic acid can be metabolized into 15-HETE through multiple pathways: 15-LO, COX-1, COX-2 and cytochrome P-450. So far no reports are available for the expression of PGDH in MC, and its expression in LAD2 suggest that the catabolic pathway of 15-HETE to 15-KETE is active in MC.

4.3.6 Possible links between nitric oxide, prostaglandin E2, cyclooxygenase and lipoxygenase pathways

Nitric oxide produced by NOS can have multiple roles in carcinogenesis. A recent study claims that both NOS inhibitors and COX-2 inhibitors can be used as anti-tumour therapy (338). NO enhances the generation of PGE₂ in osteoblasts (339), astroglial cells (340), and a macrophage cell line (341). Interestingly, NO (sodium nitroprusside 120 μ M) can activate COX in astroglial cells and macrophage cell lines through a cGMP-independent pathway. There are no reports of NO-mediated elevation of PGE₂ in MC. However, our lab reported that NO enhances COX-2 mediated PGD₂ synthesis in mouse BMDC (194). The cGMP-independent effect of NO on PGD₂ production of MC, and enhanced COX-2 mRNA stability were demonstrated in this study.

Our lab also reported that eNOS co-localizes with 5-LO in MC and that exogenous NO inhibits 5-LO mediated cysteinyl leukotriene production by human MC (179). The cGMP independent inhibition of cysteinyl leukotriene production by NO in this study argued that post-translational modifications such as nitration or nitrosylation might be responsible for the observed effect. Our current observation that SNOG treatment nitrates PGDH, supports the postulate that NO also regulates the 15-LO pathway in MC.

Nitrosylation of cytosolic phospholipase $A_2\alpha$ and corresponding increases in its activity and elevation of PGE_2 in epithelial cells was reported (342). There was a synergistic interaction between iNOS, COX-2 and cytosolic phospholipase $A_2\alpha$ in increasing PGE_2 . Since elevation on PGE_2 also occurs if PGDH is inactivated or downregulated, our observation on nitration of PGDH in MC needs further study to understand its effects on levels of PGE_2 or other arachidonic acid metabolites.

4.4 Future directions

Thus, the role of nitration of PGDH in MC is worthy of further study and the following action plan is recommended. The activity of the PGDH in MC needs to be measured under resting conditions and after SNOG treatment to understand the effects of nitration on its activity. It is critical to determine whether native or nitrated PGDH from MC has an altered interaction with PGE_2 or 15-HETE as its substrate, and measurement of K_m and V_{max} values for each substrate are recommended. Depending upon the substrate preferences of PGDH from MC, the corresponding pathway can be dissected in future experiments.

Given that PGE₂ was reported as a major substrate in general, the following model is proposed.

In case of reduced enzyme activity of nitrated PGDH, the accumulation of PGE₂, the major substrate of PGDH, should be studied by measuring PGE₂ in MC. Since MC are not well known for PGE₂ production and secretion (332), the measurement of both intracellular and excreted PGE₂ is warranted to understand the site of action of PGDH on PGE₂ in MC. EP receptors are generally expressed on cell surfaces. However, they are also expressed inside the cell such as with the perinuclear membrane (343, 344). Hence intracellular PGE₂ measurement is necessary along with characterization of expression of EP receptors in MC.

Our conceptual model based on nitration of PGDH in MC is depicted in Figure 4.7. Nitration of PGDH might reduce the activity of the enzyme followed by elevation of its substrate PGE₂. PGE₂ in turn could regulate MC function, depending upon its selective action on the subtype of EP receptors.

4.5 Limitations

Although our study identified two interesting targets of protein tyrosine nitration in MC, there are limitations in our approach that must be considered. Firstly, most of the work was conducted using human MC lines HMC-1 and LAD2. It will be critically important to validate our findings in primary human MC such as those cultured from cord blood or peripheral blood progenitors, or human MC dispersed from tissues. Given that MC are pleotropic and their phenotype is susceptible to the effects of microenvironmental conditions, it is

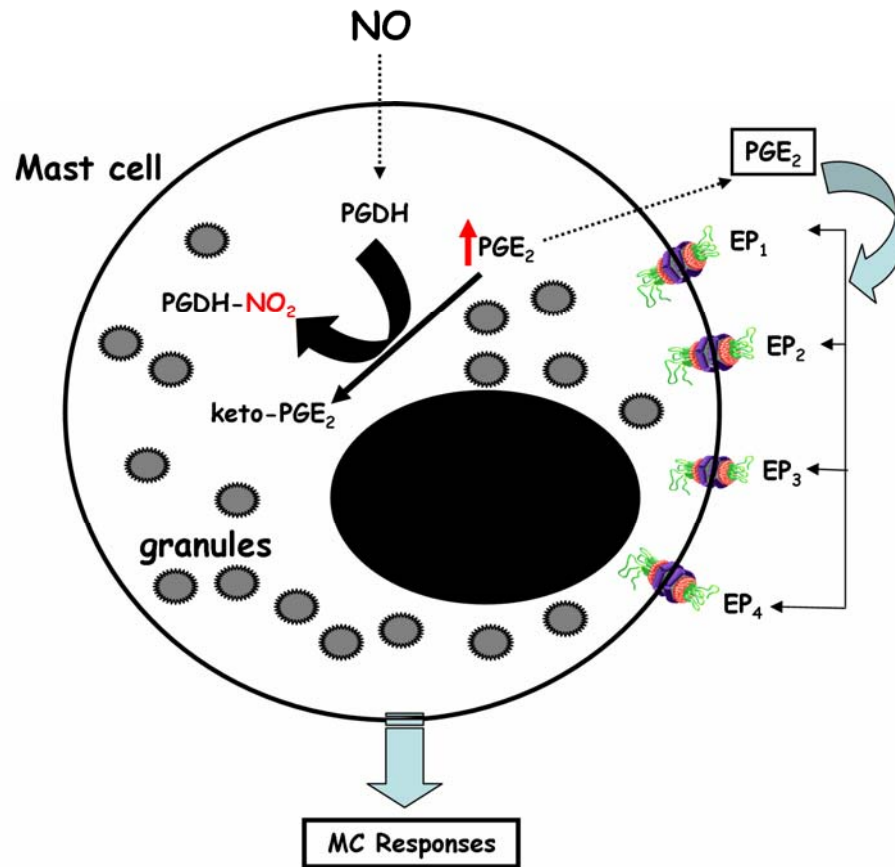


Figure 4.7 Conceptual model on effects of 15-hydroxy prostaglandin dehydrogenase nitration in mast cell function. S-nitrosoglutathione treatment facilitates nitration of 15-hydroxy prostaglandin dehydrogenase (PGDH) in mast cells. PGDH nitration might decrease its activity and elevate its substrate PGE₂. PGE₂ has potential regulatory role on MC mediator release depending upon activation of the subtype of EP receptors.

possible that there are many alternative targets for protein tyrosine nitration in primary MC from different microenvironments.

For example, the nitrated proteins in human lung MC may be different from those in skin MC and even in one site, inflammatory responses could alter the nitration of various proteins. Identification of these nitrated proteins in MC isolated from different human tissues will help us to understand the role of protein tyrosine nitration in regulation of MC phenotype and function *in vivo*. It should also be emphasised that isolation of tissue-derived MC has its limitations. For example, enzymatic digestion and density gradient centrifugation steps often result in cells with low viability and purity. However, advancements in techniques and protocols facilitate isolation of more viable and enriched MC populations. For example, magnetic-activated cell sorting for c-kit positive cells along with 2 weeks culture with stem cell factor results in restoration of normal cell functions that were disrupted during the isolation procedure of human intestinal MC (345).

A second important limitation to our studies is that we used only one NO donor, SNOG, a slow releasing NO donor. After initial studies to optimize the dose and time for experimentation, we used 500 μM of SNOG for 4 h to identify targets for nitration. Thus, other experimental or *in vivo* conditions could produce different results. For example, ONOO⁻ treatment might nitrate different targets in MC.

Thirdly, we do not know the precise chemical pathways involved in the tyrosine nitration in our study. Our hypothesis is that exogenous NO reacts with MC produced endogenous [•]O₂⁻ to generate ONOO⁻ which in turn leads to protein

tyrosine nitration. However, there are other pathways of tyrosine nitration (Figure 1.5). Further studies with multiple NO donors, ONOO⁻ and scavengers of [•]O₂⁻ and ONOO⁻ are necessary to elucidate the mechanisms of nitration in MC and thus understand how it might be regulated.

A fourth limitation is that we did not use a physiological stimulus to investigate if it would induce protein tyrosine nitration of selected targets in MC. Would a natural pathophysiological stimulus such as cross-linking of IgE alter the nitration pattern and provide relevant information to further understand the regulation of MC functions?

Despite its power in protein analyses, our 2-DE western blot approach has disadvantages such as, limited amount of protein that can be loaded into the gel, potential insolubility of some membrane proteins, loss of proteins that have pI < 3 or >10 during isoelectric focusing conditions and the need for specific antibodies. Advanced proteomic techniques employing the whole cell lysate and demonstration of nitration using MS will give a more complete picture of nitroproteome of MC.

Although there are lots of limitations, the pilot data generated from our study serves as a reference point for further investigations of the inexplicable effects of NO on MC.

4.6 Conclusions

Targeting MC and MC-released mediators have long been considered as potential therapeutic approaches in controlling inflammatory diseases where MC plays a central role. NO represents one of the regulators of MC function through

its effects on multiple pathways in MC. In this thesis, we demonstrated existence of protein tyrosine nitration in MC and its potential implications on some MC functions.

Since MC express all the isoforms of NOS and generate NO, future studies involving identification of targets for protein tyrosine nitration in MC that generate endogenous NO will enhance our knowledge on NO-mediated regulation of MC function. Studies on primary human MCs such as cord blood derived MC and peripheral blood derived MC will generate a wealth of information that could explain the multiple functions of NO.

In conclusion, we have provided evidence that protein tyrosine nitration regulates MC function. We identified that critical enzymes aldolase A, of glycolytic pathway and PGDH of arachidonic acid catabolic pathway, are targets for nitration in MC. Because of the importance of aldolase A and PGDH in cellular metabolism and homeostasis, further dissection of the relevance of our observations is necessary to more fully elucidate the role of tyrosine nitration in the regulation of MC function in allergic and other diseases.

References

1. Crivellato, E., and D. Ribatti. 2010. The mast cell: an evolutionary perspective. *Biol Rev Camb Philos Soc* 85:347-360.
2. Ehrlich, P. 1877. Beiträge zur Kenntnis der Anilinfärbungen und ihrer Verwendung in der mikroskopischen Technik. *Arch. Mikr. Anat.* 13:263-277.
3. Beaven, M. A. 2009. Our perception of the mast cell from Paul Ehrlich to now. *Eur J Immunol* 39:11-25.
4. Agis, H., M. Willheim, W. R. Sperr, A. Wilfing, E. Kromer, E. Kabrna, E. Spanblochl, H. Strobl, K. Geissler, A. Spittler, G. Boltz-Nitulescu, O. Majdic, K. Lechner, and P. Valent. 1993. Monocytes do not make mast cells when cultured in the presence of SCF. Characterization of the circulating mast cell progenitor as a c-kit+, CD34+, Ly-, CD14-, CD17-, colony-forming cell. *J Immunol* 151:4221-4227.
5. Gurish, M. F., H. Tao, J. P. Abonia, A. Arya, D. S. Friend, C. M. Parker, and K. F. Austen. 2001. Intestinal mast cell progenitors require CD49beta7 (alpha4beta7 integrin) for tissue-specific homing. *J Exp Med* 194:1243-1252.
6. Lantz, C. S., and T. F. Huff. 1995. Differential responsiveness of purified mouse c-kit+ mast cells and their progenitors to IL-3 and stem cell factor. *J Immunol* 155:4024-4029.

7. Tsuji, K., K. M. Zsebo, and M. Ogawa. 1991. Murine mast cell colony formation supported by IL-3, IL-4, and recombinant rat stem cell factor, ligand for c-kit. *J Cell Physiol* 148:362-369.
8. Abraham, S. N., and R. Malaviya. 1997. Mast cells in infection and immunity. *Infect Immun* 65:3501-3508.
9. Eguchi, M. 1991. Comparative electron microscopy of basophils and mast cells, in vivo and in vitro. *Electron Microsc Rev* 4:293-318.
10. Dvorak, A. M., and S. Kissell. 1991. Granule changes of human skin mast cells characteristic of piecemeal degranulation and associated with recovery during wound healing in situ. *J Leukoc Biol* 49:197-210.
11. Moon, T. C., C. D. St Laurent, K. E. Morris, C. Marcet, T. Yoshimura, Y. Sekar, and A. D. Befus. 2010. Advances in mast cell biology: new understanding of heterogeneity and function. *Mucosal Immunol* 3:111-128.
12. Enerback, L. 1966. Mast cells in rat gastrointestinal mucosa. 2. Dye-binding and metachromatic properties. *Acta Pathol Microbiol Scand* 66:303-312.
13. Welle, M. 1997. Development, significance, and heterogeneity of mast cells with particular regard to the mast cell-specific proteases chymase and tryptase. *J Leukoc Biol* 61:233-245.
14. Metcalfe, D. D., D. Baram, and Y. A. Mekori. 1997. Mast cells. *Physiol Rev* 77:1033-1079.

15. Benyon, R. C., T. Imai, T. Abe, and D. Befus. 1991. Mast cell heterogeneity: protein composition, biosynthesis and mRNA characterization. *Int Arch Allergy Appl Immunol* 94:218-219.
16. Abe, T., M. Swieter, T. Imai, N. D. Hollander, and A. D. Befus. 1990. Mast cell heterogeneity: two-dimensional gel electrophoretic analyses of rat peritoneal and intestinal mucosal mast cells. *Eur J Immunol* 20:1941-1947.
17. Enerback, L. 1974. Berberine sulphate binding to mast cell polyanions: a cytofluorometric method for the quantitation of heparin. *Histochemistry* 42:301-313.
18. Irani, A. M., and L. B. Schwartz. 1994. Human mast cell heterogeneity. *Allergy Proc* 15:303-308.
19. Toru, H., M. Eguchi, R. Matsumoto, M. Yanagida, J. Yata, and T. Nakahata. 1998. Interleukin-4 promotes the development of tryptase and chymase double-positive human mast cells accompanied by cell maturation. *Blood* 91:187-195.
20. Karimi, K., F. A. Redegeld, B. Heijdra, and F. P. Nijkamp. 1999. Stem cell factor and interleukin-4 induce murine bone marrow cells to develop into mast cells with connective tissue type characteristics in vitro. *Exp Hematol* 27:654-662.
21. Gilfillan, A. M., and C. Tkaczyk. 2006. Integrated signalling pathways for mast-cell activation. *Nat Rev Immunol* 6:218-230.

22. Varadaradjalou, S., F. Feger, N. Thieblemont, N. B. Hamouda, J. M. Pleau, M. Dy, and M. Arock. 2003. Toll-like receptor 2 (TLR2) and TLR4 differentially activate human mast cells. *Eur J Immunol* 33:899-906.
23. Yip, K. H., L. L. Wong, and H. Y. Lau. 2009. Adenosine: roles of different receptor subtypes in mediating histamine release from human and rodent mast cells. *Inflamm Res* 58 Suppl 1:17-19.
24. Aridor, M., L. M. Traub, and R. Sagi-Eisenberg. 1990. Exocytosis in mast cells by basic secretagogues: evidence for direct activation of GTP-binding proteins. *J Cell Biol* 111:909-917.
25. Beaven, M. A., and H. Metzger. 1993. Signal transduction by Fc receptors: the Fc epsilon RI case. *Immunol Today* 14:222-226.
26. Vosseller, K., G. Stella, N. S. Yee, and P. Besmer. 1997. c-kit receptor signaling through its phosphatidylinositide-3'-kinase-binding site and protein kinase C: role in mast cell enhancement of degranulation, adhesion, and membrane ruffling. *Mol Biol Cell* 8:909-922.
27. Kopec, A., B. Panaszek, and A. M. Fal. 2006. Intracellular signaling pathways in IgE-dependent mast cell activation. *Arch Immunol Ther Exp (Warsz)* 54:393-401.
28. Abraham, S. N., and A. L. St John. 2010. Mast cell-orchestrated immunity to pathogens. *Nat Rev Immunol* 10:440-452.
29. Tomasiak, M. M., M. Tomasiak, Z. Zietkowski, R. Skiepkowski, and A. Bodzenta-Lukaszyk. 2008. N-acetyl-beta-hexosaminidase activity in asthma. *Int Arch Allergy Immunol* 146:133-137.

30. Kobayashi, H., T. Ishizuka, and Y. Okayama. 2000. Human mast cells and basophils as sources of cytokines. *Clin Exp Allergy* 30:1205-1212.
31. Toda, M., T. Nakamura, M. Ohbayashi, Y. Ikeda, M. Dawson, R. M. Richardson, A. Alban, B. Leed, D. Miyazaki, and S. J. Ono. 2005. Role of CC chemokines and their receptors in multiple aspects of mast cell biology: comparative protein profiling of FcepsilonRI- and/or CCR1-engaged mast cells using protein chip technology. *Novartis Found Symp* 271:131-140; discussion 140-151.
32. Boyce, J. A. 2007. Mast cells and eicosanoid mediators: a system of reciprocal paracrine and autocrine regulation. *Immunol Rev* 217:168-185.
33. Hallgren, J., D. Spillmann, and G. Pejler. 2001. Structural requirements and mechanism for heparin-induced activation of a recombinant mouse mast cell tryptase, mouse mast cell protease-6: formation of active tryptase monomers in the presence of low molecular weight heparin. *J Biol Chem* 276:42774-42781.
34. Alfonso, A., A. G. Cabado, M. R. Vieytes, and L. M. Botana. 2000. Calcium-pH crosstalks in rat mast cells: cytosolic alkalinization, but not intracellular calcium release, is a sufficient signal for degranulation. *Br J Pharmacol* 130:1809-1816.
35. Pejler, G., E. Ronnberg, I. Waern, and S. Wernersson. 2010. Mast cell proteases: multifaceted regulators of inflammatory disease. *Blood* 115:4981-4990.

36. Scott, K. F., K. J. Bryant, and M. J. Bidgood. 1999. Functional coupling and differential regulation of the phospholipase A2-cyclooxygenase pathways in inflammation. *J Leukoc Biol* 66:535-541.
37. Boyce, J. A. 2005. Eicosanoid mediators of mast cells: receptors, regulation of synthesis, and pathobiologic implications. *Chem Immunol Allergy* 87:59-79.
38. Ishimoto, T., S. Akiba, and T. Sato. 1996. Importance of the phospholipase D-initiated sequential pathway for arachidonic acid release and prostaglandin D2 generation by rat peritoneal mast cells. *J Biochem* 120:616-623.
39. Heavey, D. J., P. B. Ernst, R. L. Stevens, A. D. Befus, J. Bienenstock, and K. F. Austen. 1988. Generation of leukotriene C4, leukotriene B4, and prostaglandin D2 by immunologically activated rat intestinal mucosa mast cells. *J Immunol* 140:1953-1957.
40. Robinson, C., C. Benyon, S. T. Holgate, and M. K. Church. 1989. The IgE- and calcium-dependent release of eicosanoids and histamine from human purified cutaneous mast cells. *J Invest Dermatol* 93:397-404.
41. Church, M. K., R. C. Benyon, P. H. Rees, M. A. Lowman, A. M. Campbell, C. Robinson, S. T. Holgate. . 1989. Functional heterogeneity of human mast cells. In *Mast cell and basophil differentiation and function in health and disease*. S. J. Galli, Austen, K. F., ed. Raven Press, New York. 161-170.

42. Commins, S. P., L. Borish, and J. W. Steinke. 2010. Immunologic messenger molecules: cytokines, interferons, and chemokines. *J Allergy Clin Immunol* 125:S53-72.
43. Bissonnette, E. Y., B. Chin, and A. D. Befus. 1995. Interferons differentially regulate histamine and TNF-alpha in rat intestinal mucosal mast cells. *Immunology* 86:12-17.
44. Schuh, J. M., K. Blease, S. L. Kunkel, and C. M. Hogaboam. 2003. Chemokines and cytokines: axis and allies in asthma and allergy. *Cytokine Growth Factor Rev* 14:503-510.
45. Di Nardo, A., K. Yamasaki, R. A. Dorschner, Y. Lai, and R. L. Gallo. 2008. Mast cell cathelicidin antimicrobial peptide prevents invasive group A Streptococcus infection of the skin. *J Immunol* 180:7565-7573.
46. Maurer, M., T. Theoharides, R. D. Granstein, S. C. Bischoff, J. Bienenstock, B. Henz, P. Kovanen, A. M. Piliponsky, N. Kambe, H. Vliagoftis, F. Levi-Schaffer, M. Metz, Y. Miyachi, D. Befus, P. Forsythe, Y. Kitamura, and S. Galli. 2003. What is the physiological function of mast cells? *Exp Dermatol* 12:886-910.
47. Hakim-Rad, K., M. Metz, and M. Maurer. 2009. Mast cells: makers and breakers of allergic inflammation. *Curr Opin Allergy Clin Immunol* 9:427-430.
48. Waern, I., S. Jonasson, J. Hjoberg, A. Bucht, M. Abrink, G. Pejler, and S. Wernersson. 2009. Mouse mast cell protease 4 is the major chymase in

- murine airways and has a protective role in allergic airway inflammation. *J Immunol* 183:6369-6376.
49. Noli, C., and A. Miolo. 2001. The mast cell in wound healing. *Vet Dermatol* 12:303-313.
 50. Abe, M., Y. Yokoyama, H. Amano, Y. Matsushima, C. Kan, and O. Ishikawa. 2002. Effect of activated human mast cells and mast cell-derived mediators on proliferation, type I collagen production and glycosaminoglycans synthesis by human dermal fibroblasts. *Eur J Dermatol* 12:340-346.
 51. Boesiger, J., M. Tsai, M. Maurer, M. Yamaguchi, L. F. Brown, K. P. Claffey, H. F. Dvorak, and S. J. Galli. 1998. Mast cells can secrete vascular permeability factor/ vascular endothelial cell growth factor and exhibit enhanced release after immunoglobulin E-dependent upregulation of fc epsilon receptor I expression. *J Exp Med* 188:1135-1145.
 52. Bischoff, S. C. 2009. Physiological and pathophysiological functions of intestinal mast cells. *Semin Immunopathol* 31:185-205.
 53. Abraham, S. N., K. Thankavel, and R. Malaviya. 1997. Mast cells as modulators of host defense in the lung. *Front Biosci* 2:d78-87.
 54. Tore, F., and N. Tuncel. 2009. Mast cells: target and source of neuropeptides. *Curr Pharm Des* 15:3433-3445.
 55. Nagasaka, A., H. Matsue, H. Matsushima, R. Aoki, Y. Nakamura, N. Kambe, S. Kon, T. Uede, and S. Shimada. 2008. Osteopontin is produced

- by mast cells and affects IgE-mediated degranulation and migration of mast cells. *Eur J Immunol* 38:489-499.
56. Galli, S. J., M. Tsai, and A. M. Piliponsky. 2008. The development of allergic inflammation. *Nature* 454:445-454.
 57. Brightling, C. E., P. Bradding, I. D. Pavord, and A. J. Wardlaw. 2003. New insights into the role of the mast cell in asthma. *Clin Exp Allergy* 33:550-556.
 58. Marshall, J. S. 2004. Mast-cell responses to pathogens. *Nat Rev Immunol* 4:787-799.
 59. Galli, S. J., and M. Tsai. 2010. Mast cells in allergy and infection: Versatile effector and regulatory cells in innate and adaptive immunity. *Eur J Immunol* 40:1843-1851.
 60. Chang, Z. L. 2010. Important aspects of Toll-like receptors, ligands and their signaling pathways. *Inflamm Res* 59:791-808.
 61. Kulka, M., L. Alexopoulou, R. A. Flavell, and D. D. Metcalfe. 2004. Activation of mast cells by double-stranded RNA: evidence for activation through Toll-like receptor 3. *J Allergy Clin Immunol* 114:174-182.
 62. McCurdy, J. D., T. J. Lin, and J. S. Marshall. 2001. Toll-like receptor 4-mediated activation of murine mast cells. *J Leukoc Biol* 70:977-984.
 63. Supajatura, V., H. Ushio, A. Nakao, K. Okumura, C. Ra, and H. Ogawa. 2001. Protective roles of mast cells against enterobacterial infection are mediated by Toll-like receptor 4. *J Immunol* 167:2250-2256.

64. McCurdy, J. D., T. J. Olynych, L. H. Maher, and J. S. Marshall. 2003. Cutting edge: distinct Toll-like receptor 2 activators selectively induce different classes of mediator production from human mast cells. *J Immunol* 170:1625-1629.
65. Matsushima, H., N. Yamada, H. Matsue, and S. Shimada. 2004. TLR3-, TLR7-, and TLR9-mediated production of proinflammatory cytokines and chemokines from murine connective tissue type skin-derived mast cells but not from bone marrow-derived mast cells. *J Immunol* 173:531-541.
66. Kitamura, Y., S. Go, and K. Hatanaka. 1978. Decrease of mast cells in W/W^v mice and their increase by bone marrow transplantation. *Blood* 52:447-452.
67. Lyon, M. F., and P. H. Glenister. 1982. A new allele sash (W^{sh}) at the W-locus and a spontaneous recessive lethal in mice. *Genet Res* 39:315-322.
68. Grimbaldston, M. A., C. C. Chen, A. M. Piliponsky, M. Tsai, S. Y. Tam, and S. J. Galli. 2005. Mast cell-deficient W-sash c-kit mutant Kit W^{sh}/W^{sh} mice as a model for investigating mast cell biology in vivo. *Am J Pathol* 167:835-848.
69. Nakae, S., L. H. Ho, M. Yu, R. Monteforte, M. Iikura, H. Suto, and S. J. Galli. 2007. Mast cell-derived TNF contributes to airway hyperreactivity, inflammation, and TH2 cytokine production in an asthma model in mice. *J Allergy Clin Immunol* 120:48-55.

70. Lee, D. M., D. S. Friend, M. F. Gurish, C. Benoist, D. Mathis, and M. B. Brenner. 2002. Mast cells: a cellular link between autoantibodies and inflammatory arthritis. *Science* 297:1689-1692.
71. Tanzola, M. B., M. Robbie-Ryan, C. A. Gutekunst, and M. A. Brown. 2003. Mast cells exert effects outside the central nervous system to influence experimental allergic encephalomyelitis disease course. *J Immunol* 171:4385-4391.
72. Chen, R., G. Ning, M. L. Zhao, M. G. Fleming, L. A. Diaz, Z. Werb, and Z. Liu. 2001. Mast cells play a key role in neutrophil recruitment in experimental bullous pemphigoid. *J Clin Invest* 108:1151-1158.
73. Sun, J., J. Zhang, J. S. Lindholt, G. K. Sukhova, J. Liu, A. He, M. Abrink, G. Pejler, R. L. Stevens, R. W. Thompson, T. L. Ennis, M. F. Gurish, P. Libby, and G. P. Shi. 2009. Critical role of mast cell chymase in mouse abdominal aortic aneurysm formation. *Circulation* 120:973-982.
74. Coussens, L. M., W. W. Raymond, G. Bergers, M. Laig-Webster, O. Behrendtsen, Z. Werb, G. H. Caughey, and D. Hanahan. 1999. Inflammatory mast cells up-regulate angiogenesis during squamous epithelial carcinogenesis. *Genes Dev* 13:1382-1397.
75. Echtenacher, B., D. N. Mannel, and L. Hultner. 1996. Critical protective role of mast cells in a model of acute septic peritonitis. *Nature* 381:75-77.
76. Malaviya, R., T. Ikeda, E. Ross, and S. N. Abraham. 1996. Mast cell modulation of neutrophil influx and bacterial clearance at sites of infection through TNF-alpha. *Nature* 381:77-80.

77. Saito, H., A. Kato, K. Matsumoto, and Y. Okayama. 2006. Culture of human mast cells from peripheral blood progenitors. *Nat Protoc* 1:2178-2183.
78. Bischoff, S. C. 2007. Role of mast cells in allergic and non-allergic immune responses: comparison of human and murine data. *Nat Rev Immunol* 7:93-104.
79. Macchia, L., M. Hamberg, M. Kumlin, J. H. Butterfield, and J. Z. Haeggstrom. 1995. Arachidonic acid metabolism in the human mast cell line HMC-1: 5-lipoxygenase gene expression and biosynthesis of thromboxane. *Biochim Biophys Acta* 1257:58-74.
80. Kirshenbaum, A. S., C. Akin, Y. Wu, M. Rottem, J. P. Goff, M. A. Beaven, V. K. Rao, and D. D. Metcalfe. 2003. Characterization of novel stem cell factor responsive human mast cell lines LAD 1 and 2 established from a patient with mast cell sarcoma/leukemia; activation following aggregation of FcepsilonRI or FcgammaRI. *Leuk Res* 27:677-682.
81. Guhl, S., M. Babina, A. Neou, T. Zuberbier, and M. Artuc. 2010. Mast cell lines HMC-1 and LAD2 in comparison with mature human skin mast cells--drastically reduced levels of tryptase and chymase in mast cell lines. *Exp Dermatol* 19:845-847.
82. Furchgott, R. F., and J. V. Zawadzki. 1980. The obligatory role of endothelial cells in the relaxation of arterial smooth muscle by acetylcholine. *Nature* 288:373-376.

83. Palmer, R. M., A. G. Ferrige, and S. Moncada. 1987. Nitric oxide release accounts for the biological activity of endothelium-derived relaxing factor. *Nature* 327:524-526.
84. Ignarro, L. J., G. M. Buga, K. S. Wood, R. E. Byrns, and G. Chaudhuri. 1987. Endothelium-derived relaxing factor produced and released from artery and vein is nitric oxide. *Proc Natl Acad Sci U S A* 84:9265-9269.
85. Smith, O. 1998. Nobel Prize for NO research. *Nat Med* 4:1215.
86. Lundberg, J. O., E. Weitzberg, J. M. Lundberg, and K. Alving. 1994. Intra-gastric nitric oxide production in humans: measurements in expelled air. *Gut* 35:1543-1546.
87. Benjamin, N., F. O'Driscoll, H. Dougall, C. Duncan, L. Smith, M. Golden, and H. McKenzie. 1994. Stomach NO synthesis. *Nature* 368:502.
88. Lundberg, J. O., and E. Weitzberg. 2010. NO-synthase independent NO generation in mammals. *Biochem Biophys Res Commun* 396:39-45.
89. Goligorsky, M. S., H. Li, S. Brodsky, and J. Chen. 2002. Relationships between caveolae and eNOS: everything in proximity and the proximity of everything. *Am J Physiol Renal Physiol* 283:F1-10.
90. Fleming, I., and R. Busse. 2003. Molecular mechanisms involved in the regulation of the endothelial nitric oxide synthase. *Am J Physiol Regul Integr Comp Physiol* 284:R1-12.
91. Kone, B. C., T. Kuncewicz, W. Zhang, and Z. Y. Yu. 2003. Protein interactions with nitric oxide synthases: controlling the right time, the

- right place, and the right amount of nitric oxide. *Am J Physiol Renal Physiol* 285:F178-190.
92. Oess, S., A. Icking, D. Fulton, R. Govers, and W. Muller-Esterl. 2006. Subcellular targeting and trafficking of nitric oxide synthases. *Biochem J* 396:401-409.
93. Shan, J., P. Carbonara, N. Karp, M. Tulic, Q. Hamid, and D. H. Eidelman. 2007. Localization and distribution of NOS1 in murine airways. *Nitric Oxide* 17:25-32.
94. Qadri, F., T. Arens, E. C. Schwartz, W. Hauser, and P. Dominiak. 2001. Angiotensin-converting enzyme inhibitors and AT1-receptor antagonist restore nitric oxide synthase (NOS) activity and neuronal NOS expression in the adrenal glands of spontaneously hypertensive rats. *Jpn J Pharmacol* 85:365-369.
95. Barnes, P. J., and F. Y. Liew. 1995. Nitric oxide and asthmatic inflammation. *Immunol Today* 16:128-130.
96. Connor, J. R., P. T. Manning, S. L. Settle, W. M. Moore, G. M. Jerome, R. K. Webber, F. S. Tjoeng, and M. G. Currie. 1995. Suppression of adjuvant-induced arthritis by selective inhibition of inducible nitric oxide synthase. *Eur J Pharmacol* 273:15-24.
97. Arimoto, T., and G. Bing. 2003. Up-regulation of inducible nitric oxide synthase in the substantia nigra by lipopolysaccharide causes microglial activation and neurodegeneration. *Neurobiol Dis* 12:35-45.

98. Wang, G. Y., W. Meng, B. Ji, X. H. Du, and J. Zhao. 2005. Expression of inducible nitric oxide synthase in transplanted rat liver and its inhibitory effect. *Hepatobiliary Pancreat Dis Int* 4:360-363.
99. Tracey, W. R., J. S. Pollock, F. Murad, M. Nakane, and U. Forstermann. 1994. Identification of an endothelial-like type III NO synthase in LLC-PK1 kidney epithelial cells. *Am J Physiol* 266:C22-28.
100. Zini, A., M. K. O'Bryan, M. S. Magid, and P. N. Schlegel. 1996. Immunohistochemical localization of endothelial nitric oxide synthase in human testis, epididymis, and vas deferens suggests a possible role for nitric oxide in spermatogenesis, sperm maturation, and programmed cell death. *Biol Reprod* 55:935-941.
101. Schulz, R., E. Nava, and S. Moncada. 1992. Induction and potential biological relevance of a Ca(2+)-independent nitric oxide synthase in the myocardium. *Br J Pharmacol* 105:575-580.
102. Shaul, P. W., A. J. North, L. C. Wu, L. B. Wells, T. S. Brannon, K. S. Lau, T. Michel, L. R. Margraf, and R. A. Star. 1994. Endothelial nitric oxide synthase is expressed in cultured human bronchiolar epithelium. *J Clin Invest* 94:2231-2236.
103. Lancaster, J. R., Jr. 1997. A tutorial on the diffusibility and reactivity of free nitric oxide. *Nitric Oxide* 1:18-30.
104. Eiserich, J. P., R. P. Patel, and V. B. O'Donnell. 1998. Pathophysiology of nitric oxide and related species: free radical reactions and modification of biomolecules. *Mol Aspects Med* 19:221-357.

105. Krumenacker, J. S., K. A. Hanafy, and F. Murad. 2004. Regulation of nitric oxide and soluble guanylyl cyclase. *Brain Res Bull* 62:505-515.
106. Reynolds, M. F., and J. N. Burstyn. 2000. Mechanism of activation of soluble guanylyl cyclase by NO. In *Nitric oxide biology and pathobiology*. L. J. Ignarro, ed. Academic Press, San Diego. 381-400.
107. Friebe, A., and D. Koesling. 2003. Regulation of nitric oxide-sensitive guanylyl cyclase. *Circ Res* 93:96-105.
108. Wanstall, J. C., K. L. Homer, and S. A. Doggrell. 2005. Evidence for, and importance of, cGMP-independent mechanisms with NO and NO donors on blood vessels and platelets. *Curr Vasc Pharmacol* 3:41-53.
109. Grisham, M. B., D. Jour'd'Heuil, and D. A. Wink. 1999. Nitric oxide. I. Physiological chemistry of nitric oxide and its metabolites: implications in inflammation. *Am J Physiol* 276:G315-321.
110. Maeda, H., and T. Akaike. 1998. Nitric oxide and oxygen radicals in infection, inflammation, and cancer. *Biochemistry (Mosc)* 63:854-865.
111. Gow, A. J., C. R. Farkouh, D. A. Munson, M. A. Posencheg, and H. Ischiropoulos. 2004. Biological significance of nitric oxide-mediated protein modifications. *Am J Physiol Lung Cell Mol Physiol* 287:L262-268.
112. Stamler, J. S., S. Lamas, and F. C. Fang. 2001. Nitrosylation. the prototypic redox-based signaling mechanism. *Cell* 106:675-683.
113. Foster, M. W., D. T. Hess, and J. S. Stamler. 2009. Protein S-nitrosylation in health and disease: a current perspective. *Trends Mol Med* 15:391-404.

114. Benhar, M., M. T. Forrester, and J. S. Stamler. 2009. Protein denitrosylation: enzymatic mechanisms and cellular functions. *Nat Rev Mol Cell Biol* 10:721-732.
115. Kim, S. F., D. A. Huri, and S. H. Snyder. 2005. Inducible nitric oxide synthase binds, S-nitrosylates, and activates cyclooxygenase-2. *Science* 310:1966-1970.
116. Zhang, J., B. Jin, L. Li, E. R. Block, and J. M. Patel. 2005. Nitric oxide-induced persistent inhibition and nitrosylation of active site cysteine residues of mitochondrial cytochrome-c oxidase in lung endothelial cells. *Am J Physiol Cell Physiol* 288:C840-849.
117. Hess, D. T., A. Matsumoto, S. O. Kim, H. E. Marshall, and J. S. Stamler. 2005. Protein S-nitrosylation: purview and parameters. *Nat Rev Mol Cell Biol* 6:150-166.
118. Tello, D., C. Tarin, P. Ahicart, R. Breton-Romero, S. Lamas, and A. Martinez-Ruiz. 2009. A "fluorescence switch" technique increases the sensitivity of proteomic detection and identification of S-nitrosylated proteins. *Proteomics* 9:5359-5370.
119. Abello, N., H. A. Kerstjens, D. S. Postma, and R. Bischoff. 2009. Protein tyrosine nitration: selectivity, physicochemical and biological consequences, denitration, and proteomics methods for the identification of tyrosine-nitrated proteins. *J Proteome Res* 8:3222-3238.
120. Ischiropoulos, H. 2009. Protein tyrosine nitration--an update. *Arch Biochem Biophys* 484:117-121.

121. Shishehbor, M. H., R. J. Aviles, M. L. Brennan, X. Fu, M. Goormastic, G. L. Pearce, N. Gokce, J. F. Keaney, Jr., M. S. Penn, D. L. Sprecher, J. A. Vita, and S. L. Hazen. 2003. Association of nitrotyrosine levels with cardiovascular disease and modulation by statin therapy. *Jama* 289:1675-1680.
122. Greenacre, S. A., and H. Ischiropoulos. 2001. Tyrosine nitration: localisation, quantification, consequences for protein function and signal transduction. *Free Radic Res* 34:541-581.
123. Koeck, T., D. J. Stuehr, and K. S. Aulak. 2005. Mitochondria and regulated tyrosine nitration. *Biochem Soc Trans* 33:1399-1403.
124. Balafanova, Z., R. Bolli, J. Zhang, Y. Zheng, J. M. Pass, A. Bhatnagar, X. L. Tang, O. Wang, E. Cardwell, and P. Ping. 2002. Nitric oxide (NO) induces nitration of protein kinase Cepsilon (PKCepsilon), facilitating PKCepsilon translocation via enhanced PKCepsilon -RACK2 interactions: a novel mechanism of no-triggered activation of PKCepsilon. *J Biol Chem* 277:15021-15027.
125. Bartesaghi, S., G. Ferrer-Sueta, G. Peluffo, V. Valez, H. Zhang, B. Kalyanaraman, and R. Radi. 2007. Protein tyrosine nitration in hydrophilic and hydrophobic environments. *Amino Acids* 32:501-515.
126. Souza, J. M., G. Peluffo, and R. Radi. 2008. Protein tyrosine nitration--functional alteration or just a biomarker? *Free Radic Biol Med* 45:357-366.

127. Schopfer, F. J., P. R. Baker, and B. A. Freeman. 2003. NO-dependent protein nitration: a cell signaling event or an oxidative inflammatory response? *Trends Biochem Sci* 28:646-654.
128. Salvemini, D., T. M. Doyle, and S. Cuzzocrea. 2006. Superoxide, peroxynitrite and oxidative/nitrative stress in inflammation. *Biochem Soc Trans* 34:965-970.
129. Goldstein, S., and G. Merenyi. 2008. The chemistry of peroxynitrite: implications for biological activity. *Methods Enzymol* 436:49-61.
130. Rubbo, H., A. Trostchansky, and V. B. O'Donnell. 2009. Peroxynitrite-mediated lipid oxidation and nitration: mechanisms and consequences. *Arch Biochem Biophys* 484:167-172.
131. Alvarez, B., H. Rubbo, M. Kirk, S. Barnes, B. A. Freeman, and R. Radi. 1996. Peroxynitrite-dependent tryptophan nitration. *Chem Res Toxicol* 9:390-396.
132. Tiago, T., P. S. Palma, C. Gutierrez-Merino, and M. Aureliano. 2010. Peroxynitrite-mediated oxidative modifications of myosin and implications on structure and function. *Free Radic Res* 44:1317-1327.
133. Zhang, L., C. L. Chen, P. T. Kang, V. Garg, K. Hu, K. B. Green-Church, and Y. R. Chen. 2010. Peroxynitrite-mediated oxidative modifications of complex II: relevance in myocardial infarction. *Biochemistry* 49:2529-2539.

134. Szabo, C., H. Ischiropoulos, and R. Radi. 2007. Peroxynitrite: biochemistry, pathophysiology and development of therapeutics. *Nat Rev Drug Discov* 6:662-680.
135. Viappiani, S., A. C. Nicolescu, A. Holt, G. Sawicki, B. D. Crawford, H. Leon, T. van Mulligen, and R. Schulz. 2009. Activation and modulation of 72kDa matrix metalloproteinase-2 by peroxynitrite and glutathione. *Biochem Pharmacol* 77:826-834.
136. van der Vliet, A., J. P. Eiserich, B. Halliwell, and C. E. Cross. 1997. Formation of reactive nitrogen species during peroxidase-catalyzed oxidation of nitrite. A potential additional mechanism of nitric oxide-dependent toxicity. *J Biol Chem* 272:7617-7625.
137. Wu, W., Y. Chen, and S. L. Hazen. 1999. Eosinophil peroxidase nitrates protein tyrosyl residues. Implications for oxidative damage by nitrating intermediates in eosinophilic inflammatory disorders. *J Biol Chem* 274:25933-25944.
138. Radi, R. 2004. Nitric oxide, oxidants, and protein tyrosine nitration. *Proc Natl Acad Sci U S A* 101:4003-4008.
139. Ischiropoulos, H. 1998. Biological tyrosine nitration: a pathophysiological function of nitric oxide and reactive oxygen species. *Arch Biochem Biophys* 356:1-11.
140. Halliwell, B. 1997. What nitrates tyrosine? Is nitrotyrosine specific as a biomarker of peroxynitrite formation in vivo? *FEBS Lett* 411:157-160.

141. Souza, J. M., E. Daikhin, M. Yudkoff, C. S. Raman, and H. Ischiropoulos. 1999. Factors determining the selectivity of protein tyrosine nitration. *Arch Biochem Biophys* 371:169-178.
142. Ischiropoulos, H. 2003. Biological selectivity and functional aspects of protein tyrosine nitration. *Biochem Biophys Res Commun* 305:776-783.
143. Jiao, K., S. Mandapati, P. L. Skipper, S. R. Tannenbaum, and J. S. Wishnok. 2001. Site-selective nitration of tyrosine in human serum albumin by peroxynitrite. *Anal Biochem* 293:43-52.
144. Yamakura, F., H. Taka, T. Fujimura, and K. Murayama. 1998. Inactivation of human manganese-superoxide dismutase by peroxynitrite is caused by exclusive nitration of tyrosine 34 to 3-nitrotyrosine. *J Biol Chem* 273:14085-14089.
145. Castro, L., J. P. Eiserich, S. Sweeney, R. Radi, and B. A. Freeman. 2004. Cytochrome c: a catalyst and target of nitrite-hydrogen peroxide-dependent protein nitration. *Arch Biochem Biophys* 421:99-107.
146. Ghafourifar, P., and C. A. Colton. 2003. Compartmentalized nitrosation and nitration in mitochondria. *Antioxid Redox Signal* 5:349-354.
147. Valdez, L. B., S. Alvarez, S. L. Arnaiz, F. Schopfer, M. C. Carreras, J. J. Poderoso, and A. Boveris. 2000. Reactions of peroxynitrite in the mitochondrial matrix. *Free Radic Biol Med* 29:349-356.
148. Heijnen, H. F., E. van Donselaar, J. W. Slot, D. M. Fries, B. Blachard-Fillion, R. Hodara, R. Lightfoot, M. Polydoro, D. Spielberg, L. Thomson, E. A. Regan, J. Crapo, and H. Ischiropoulos. 2006. Subcellular

localization of tyrosine-nitrated proteins is dictated by reactive oxygen species generating enzymes and by proximity to nitric oxide synthase. *Free Radic Biol Med* 40:1903-1913.

149. Crow, J. P., and H. Ischiropoulos. 1996. Detection and quantitation of nitrotyrosine residues in proteins: in vivo marker of peroxynitrite. *Methods Enzymol* 269:185-194.
150. van der Vliet, A., J. P. Eiserich, H. Kaur, C. E. Cross, and B. Halliwell. 1996. Nitrotyrosine as biomarker for reactive nitrogen species. *Methods Enzymol* 269:175-184.
151. Savvides, S. N., M. Scheiwein, C. C. Bohme, G. E. Arteel, P. A. Karplus, K. Becker, and R. H. Schirmer. 2002. Crystal structure of the antioxidant enzyme glutathione reductase inactivated by peroxynitrite. *J Biol Chem* 277:2779-2784.
152. Pacher, P., J. S. Beckman, and L. Liaudet. 2007. Nitric oxide and peroxynitrite in health and disease. *Physiol Rev* 87:315-424.
153. Gow, A. J., D. Duran, S. Malcolm, and H. Ischiropoulos. 1996. Effects of peroxynitrite-induced protein modifications on tyrosine phosphorylation and degradation. *FEBS Lett* 385:63-66.
154. Kong, S. K., M. B. Yim, E. R. Stadtman, and P. B. Chock. 1996. Peroxynitrite disables the tyrosine phosphorylation regulatory mechanism: Lymphocyte-specific tyrosine kinase fails to phosphorylate nitrated cdc2(6-20)NH₂ peptide. *Proc Natl Acad Sci U S A* 93:3377-3382.

155. MacMillan-Crow, L. A., J. S. Greendorfer, S. M. Vickers, and J. A. Thompson. 2000. Tyrosine nitration of c-SRC tyrosine kinase in human pancreatic ductal adenocarcinoma. *Arch Biochem Biophys* 377:350-356.
156. Souza, J. M., I. Choi, Q. Chen, M. Weisse, E. Daikhin, M. Yudkoff, M. Obin, J. Ara, J. Horwitz, and H. Ischiropoulos. 2000. Proteolytic degradation of tyrosine nitrated proteins. *Arch Biochem Biophys* 380:360-366.
157. Ohmori, H., and N. Kanayama. 2005. Immunogenicity of an inflammation-associated product, tyrosine nitrated self-proteins. *Autoimmun Rev* 4:224-229.
158. Birnboim, H. C., A. M. Lemay, D. K. Lam, R. Goldstein, and J. R. Webb. 2003. Cutting edge: MHC class II-restricted peptides containing the inflammation-associated marker 3-nitrotyrosine evade central tolerance and elicit a robust cell-mediated immune response. *J Immunol* 171:528-532.
159. Gruijthuisen, Y. K., I. Grieshuber, A. Stocklinger, U. Tischler, T. Fehrenbach, M. G. Weller, L. Vogel, S. Vieths, U. Poschl, and A. Duschl. 2006. Nitration enhances the allergenic potential of proteins. *Int Arch Allergy Immunol* 141:265-275.
160. Hardy, L. L., D. A. Wick, and J. R. Webb. 2008. Conversion of tyrosine to the inflammation-associated analog 3'-nitrotyrosine at either TCR- or MHC-contact positions can profoundly affect recognition of the MHC

- class I-restricted epitope of lymphocytic choriomeningitis virus glycoprotein 33 by CD8 T cells. *J Immunol* 180:5956-5962.
161. Nagaraj, S., K. Gupta, V. Pisarev, L. Kinarsky, S. Sherman, L. Kang, D. L. Herber, J. Schneck, and D. I. Gabrilovich. 2007. Altered recognition of antigen is a mechanism of CD8+ T cell tolerance in cancer. *Nat Med* 13:828-835.
162. Osoata, G. O., S. Yamamura, M. Ito, C. Vuppusetty, I. M. Adcock, P. J. Barnes, and K. Ito. 2009. Nitration of distinct tyrosine residues causes inactivation of histone deacetylase 2. *Biochem Biophys Res Commun* 384:366-371.
163. Barnes, P. J., K. Ito, and I. M. Adcock. 2004. Corticosteroid resistance in chronic obstructive pulmonary disease: inactivation of histone deacetylase. *Lancet* 363:731-733.
164. Leger, C. L., E. Torres-Rasgado, G. Fouret, and M. A. Carbonneau. 2008. First evidence for an LDL- and HDL-associated nitratase activity that denitrates albumin-bound nitrotyrosine--physiological consequences. *IUBMB Life* 60:73-78.
165. Kuo, W. N., R. N. Kanadia, V. P. Shanbhag, and R. Toro. 1999. Denitration of peroxynitrite-treated proteins by 'protein nitratases' from rat brain and heart. *Mol Cell Biochem* 201:11-16.
166. Schoneich, C. 2005. Mass spectrometry in aging research. *Mass Spectrom Rev* 24:701-718.

167. Herce-Pagliai, C., S. Kotecha, and D. E. Shuker. 1998. Analytical methods for 3-nitrotyrosine as a marker of exposure to reactive nitrogen species: a review. *Nitric Oxide* 2:324-336.
168. Ghosh, S., A. J. Janocha, M. A. Aronica, S. Swaidani, S. A. Comhair, W. Xu, L. Zheng, S. Kaveti, M. Kinter, S. L. Hazen, and S. C. Erzurum. 2006. Nitrotyrosine proteome survey in asthma identifies oxidative mechanism of catalase inactivation. *J Immunol* 176:5587-5597.
169. Zhan, X., and D. M. Desiderio. 2009. Mass spectrometric identification of in vivo nitrotyrosine sites in the human pituitary tumor proteome. *Methods Mol Biol* 566:137-163.
170. Franze, T., M. G. Weller, R. Niessner, and U. Poschl. 2004. Comparison of nitrotyrosine antibodies and development of immunoassays for the detection of nitrated proteins. *Analyst* 129:589-596.
171. Ye, Y. Z., M. Strong, Z. Q. Huang, and J. S. Beckman. 1996. Antibodies that recognize nitrotyrosine. *Methods Enzymol* 269:201-209.
172. Aulak, K. S., T. Koeck, J. W. Crabb, and D. J. Stuehr. 2004. Proteomic method for identification of tyrosine-nitrated proteins. *Methods Mol Biol* 279:151-165.
173. Sekar, Y., T. C. Moon, S. Munoz, and A. D. Befus. 2005. Role of nitric oxide in mast cells: controversies, current knowledge, and future applications. *Immunol Res* 33:223-239.

174. Gilchrist, M., M. Savoie, O. Nohara, F. L. Wills, J. L. Wallace, and A. D. Befus. 2002. Nitric oxide synthase and nitric oxide production in in vivo-derived mast cells. *J Leukoc Biol* 71:618-624.
175. Yip, K. H., Y. Huang, M. M. Waye, and H. Y. Lau. 2008. Induction of nitric oxide synthases in primary human cultured mast cells by IgE and proinflammatory cytokines. *Int Immunopharmacol* 8:764-768.
176. Bidri, M., S. Ktorza, I. Vouldoukis, L. Le Goff, P. Debre, J. J. Guillosson, and M. Arock. 1997. Nitric oxide pathway is induced by Fc epsilon RI and up-regulated by stem cell factor in mouse mast cells. *Eur J Immunol* 27:2907-2913.
177. Swindle, E. J., D. D. Metcalfe, and J. W. Coleman. 2004. Rodent and human mast cells produce functionally significant intracellular reactive oxygen species but not nitric oxide. *J Biol Chem* 279:48751-48759.
178. Masini, E., D. Salvemini, A. Pistelli, P. F. Mannaioni, and J. R. Vane. 1991. Rat mast cells synthesize a nitric oxide like-factor which modulates the release of histamine. *Agents Actions* 33:61-63.
179. Gilchrist, M., S. D. McCauley, and A. D. Befus. 2004. Expression, localization, and regulation of NOS in human mast cell lines: effects on leukotriene production. *Blood* 104:462-469.
180. Gilchrist, M., and A. D. Befus. 2008. Interferon-gamma regulates chemokine expression and release in the human mast cell line HMC1: role of nitric oxide. *Immunology* 123:209-217.

181. Moon, T. C., Sekar, Y. , and Befus, A. D. 2009. Effects of nitric oxide on mast cells: production, functions and mechanisms of action. In *Allergy Frontiers: From Epigenetics to Future Perspectives*. S. H. R Pawanker, L Rosenwasser, ed. Springer-Verlag Tokyo Inc, Tokyo. 315-327.
182. Coleman, J. W. 2002. Nitric oxide: a regulator of mast cell activation and mast cell-mediated inflammation. *Clin Exp Immunol* 129:4-10.
183. Kanwar, S., J. L. Wallace, D. Befus, and P. Kubes. 1994. Nitric oxide synthesis inhibition increases epithelial permeability via mast cells. *Am J Physiol* 266:G222-229.
184. Parikh, V., and M. Singh. 2001. Possible role of nitric oxide and mast cells in endotoxin-induced cardioprotection. *Pharmacol Res* 43:39-45.
185. Iikura, M., T. Takaishi, K. Hirai, H. Yamada, M. Iida, T. Koshino, and Y. Morita. 1998. Exogenous nitric oxide regulates the degranulation of human basophils and rat peritoneal mast cells. *Int Arch Allergy Immunol* 115:129-136.
186. Bidri, M., P. A. Becherel, L. Le Goff, L. Pieroni, J. J. Guillosson, P. Debre, and M. Arock. 1995. Involvement of cyclic nucleotides in the immunomodulatory effects of nitric oxide on murine mast cells. *Biochem Biophys Res Commun* 210:507-517.
187. Eastmond, N. C., E. M. Banks, and J. W. Coleman. 1997. Nitric oxide inhibits IgE-mediated degranulation of mast cells and is the principal intermediate in IFN-gamma-induced suppression of exocytosis. *J Immunol* 159:1444-1450.

188. Deschoolmeester, M. L., N. C. Eastmond, R. J. Dearman, I. Kimber, D. A. Basketter, and J. W. Coleman. 1999. Reciprocal effects of interleukin-4 and interferon-gamma on immunoglobulin E-mediated mast cell degranulation: a role for nitric oxide but not peroxynitrite or cyclic guanosine monophosphate. *Immunology* 96:138-144.
189. Yip, K. H., F. P. Leung, Y. Huang, and H. Y. Lau. 2009. Inhibition of anti-IgE mediated human mast cell activation by NO donors is dependent on their NO release kinetics. *Br J Pharmacol* 156:1279-1286.
190. Wills, F. L., M. Gilchrist, and A. D. Befus. 1999. Interferon-gamma regulates the interaction of RBL-2H3 cells with fibronectin through production of nitric oxide. *Immunology* 97:481-489.
191. Forsythe, P., and A. D. Befus. 2003. Inhibition of calpain is a component of nitric oxide-induced down-regulation of human mast cell adhesion. *J Immunol* 170:287-293.
192. Davis, B. J., B. F. Flanagan, A. M. Gilfillan, D. D. Metcalfe, and J. W. Coleman. 2004. Nitric oxide inhibits IgE-dependent cytokine production and Fos and Jun activation in mast cells. *J Immunol* 173:6914-6920.
193. Yip, K. H., Y. Huang, F. P. Leung, and H. Y. Lau. 2010. Cyclic guanosine monophosphate dependent pathway contributes to human mast cell inhibitory actions of the nitric oxide donor, diethylamine NONOate. *Eur J Pharmacol* 632:86-92.
194. Moon, T. C., and A. D. Befus. 2008. Exogenous nitric oxide regulates cyclooxygenase-2 expression and prostaglandin D(2) generation through

- p38 MAPK in mouse bone marrow-derived mast cells. *Free Radic Biol Med* 45:780-788.
195. Nohara, O., M. Kulka, R. E. Dery, F. L. Wills, N. S. Hirji, M. Gilchrist, and A. D. Befus. 2001. Regulation of CD8 expression in mast cells by exogenous or endogenous nitric oxide. *J Immunol* 167:5935-5939.
196. Bissonnette, E. Y., C. M. Hogaboam, J. L. Wallace, and A. D. Befus. 1991. Potentiation of tumor necrosis factor-alpha-mediated cytotoxicity of mast cells by their production of nitric oxide. *J Immunol* 147:3060-3065.
197. Yoshimaru, T., Y. Suzuki, T. Matsui, K. Yamashita, T. Ochiai, M. Yamaki, and K. Shimizu. 2002. Blockade of superoxide generation prevents high-affinity immunoglobulin E receptor-mediated release of allergic mediators by rat mast cell line and human basophils. *Clin Exp Allergy* 32:612-618.
198. Itoh, T., Y. Fujita, M. Ito, A. Masuda, K. Ohno, M. Ichihara, T. Kojima, Y. Nozawa, and M. Ito. 2009. Molecular hydrogen suppresses FcepsilonRI-mediated signal transduction and prevents degranulation of mast cells. *Biochem Biophys Res Commun* 389:651-656.
199. Inoue, T., Y. Suzuki, T. Yoshimaru, and C. Ra. 2008. Reactive oxygen species produced up- or downstream of calcium influx regulate proinflammatory mediator release from mast cells: role of NADPH oxidase and mitochondria. *Biochim Biophys Acta* 1783:789-802.
200. Yoshimaru, T., Y. Suzuki, T. Inoue, O. Niide, and C. Ra. 2006. Silver activates mast cells through reactive oxygen species production and a

- thiol-sensitive store-independent Ca^{2+} influx. *Free Radic Biol Med* 40:1949-1959.
201. Niide, O., Y. Suzuki, T. Yoshimaru, T. Inoue, T. Takayama, and C. Ra. 2006. Fungal metabolite gliotoxin blocks mast cell activation by a calcium- and superoxide-dependent mechanism: implications for immunosuppressive activities. *Clin Immunol* 118:108-116.
202. Akagi, M., N. Fukuishi, M. Sakaguchi, N. Matsui, and H. Takahashi. 1998. [Role of superoxide generation and degradation system of mast cells in allergic inflammation]. *Nippon Yakurigaku Zasshi* 112 Suppl 1:73P-77P.
203. Sakaguchi, M., N. Fukuishi, K. Teramoto, M. Miyazaki, N. H. Huh, M. Namba, and M. Akagi. 2003. Involvement of arachidonic acid in nonimmunologic production of superoxide in mast cells. *Int Arch Allergy Immunol* 130:288-299.
204. Frederiks, W. M., K. S. Bosch, and H. A. Vreeling-Sindelarova. 1997. In situ detection of constitutive superoxide anion production in granules of mast cells. *Histochem J* 29:287-291.
205. Henderson, W. R., and M. Kaliner. 1978. Immunologic and nonimmunologic generation of superoxide from mast cells and basophils. *J Clin Invest* 61:187-196.
206. Swindle, E. J., J. W. Coleman, F. R. DeLeo, and D. D. Metcalfe. 2007. FcepsilonRI- and Fcgamma receptor-mediated production of reactive

- oxygen species by mast cells is lipoxygenase- and cyclooxygenase-dependent and NADPH oxidase-independent. *J Immunol* 179:7059-7071.
207. Kim, G. Y., J. W. Lee, H. C. Ryu, J. D. Wei, C. M. Seong, and J. H. Kim. 2010. Proinflammatory cytokine IL-1beta stimulates IL-8 synthesis in mast cells via a leukotriene B4 receptor 2-linked pathway, contributing to angiogenesis. *J Immunol* 184:3946-3954.
208. Kim, J. Y., K. H. Lee, B. K. Lee, and J. Y. Ro. 2005. Peroxynitrite modulates release of inflammatory mediators from guinea pig lung mast cells activated by antigen-antibody reaction. *Int Arch Allergy Immunol* 137:104-114.
209. Ulrich, M., A. Petre, N. Youhnovski, F. Promm, M. Schirle, M. Schumm, R. S. Pero, A. Doyle, J. Checkel, H. Kita, N. Thiyagarajan, K. R. Acharya, P. Schmid-Grendelmeier, H. U. Simon, H. Schwarz, M. Tsutsui, H. Shimokawa, G. Bellon, J. J. Lee, M. Przybylski, and G. Doring. 2008. Post-translational tyrosine nitration of eosinophil granule toxins mediated by eosinophil peroxidase. *J Biol Chem* 283:28629-28640.
210. Moon, T. C., E. Lee, S. H. Baek, M. Murakami, I. Kudo, N. S. Kim, J. M. Lee, H. K. Min, N. Kambe, and H. W. Chang. 2003. Degranulation and cytokine expression in human cord blood-derived mast cells cultured in serum-free medium with recombinant human stem cell factor. *Mol Cells* 16:154-160.
211. Kambe, N., M. Kambe, H. W. Chang, A. Matsui, H. K. Min, M. Hussein, C. A. Oskerizian, J. Kochan, A. A. Irani, and L. B. Schwartz. 2000. An

- improved procedure for the development of human mast cells from dispersed fetal liver cells in serum-free culture medium. *J Immunol Methods* 240:101-110.
212. Askew, S. C., A. R. Butler, F. W. Flitney, G. D. Kemp, and I. L. Megson. 1995. Chemical mechanisms underlying the vasodilator and platelet anti-aggregating properties of S-nitroso-N-acetyl-DL-penicillamine and S-nitrosoglutathione. *Bioorg Med Chem* 3:1-9.
213. Gordge, M. P., J. S. Hothersall, and A. A. Noronha-Dutra. 1998. Evidence for a cyclic GMP-independent mechanism in the anti-platelet action of S-nitrosoglutathione. *Br J Pharmacol* 124:141-148.
214. Koranteng, R. D., R. J. Dearman, I. Kimber, and J. W. Coleman. 2000. Phenotypic variation in mast cell responsiveness to the inhibitory action of nitric oxide. *Inflamm Res* 49:240-246.
215. Chazotte-Aubert, L., P. Hainaut, and H. Ohshima. 2000. Nitric oxide nitrates tyrosine residues of tumor-suppressor p53 protein in MCF-7 cells. *Biochem Biophys Res Commun* 267:609-613.
216. Mutus, B., R. W. Redmond, and S. Akhter. 1999. Evidence for peroxynitrite formation during S-nitrosoglutathione photolysis in air saturated solutions. *FEBS Lett* 449:79-82.
217. Candiano, G., M. Bruschi, L. Musante, L. Santucci, G. M. Ghiggeri, B. Carnemolla, P. Orecchia, L. Zardi, and P. G. Righetti. 2004. Blue silver: a very sensitive colloidal Coomassie G-250 staining for proteome analysis. *Electrophoresis* 25:1327-1333.

218. Springer, T. A. 1995. Immunoaffinity chromatography. In *In 'Current protocols in molecular biology'*. F. M. Ausubel, Brent, R., Kingston, R. E., Moore, D. D., Seidman, J. G., Smith, J. A., Struhl, K., ed. John Wiley & Sons, Inc., Hoboken, NJ. 10.11.11 - 10.11.19.
219. Michal, G. 1984. D-fructose 1,6-bisphosphate, dihydroxyacetone phosphate and D-glyceraldehyde 3-phosphate. In *Methods of Enzymatic analysis*, Third ed. B. H.U., ed. Academic Press, NY 342-350.
220. Koeck, T., B. Levison, S. L. Hazen, J. W. Crabb, D. J. Stuehr, and K. S. Aulak. 2004. Tyrosine nitration impairs mammalian aldolase A activity. *Mol Cell Proteomics* 3:548-557.
221. Xu, K., and J. L. Stringer. 2008. Pharmacokinetics of fructose-1,6-diphosphate after intraperitoneal and oral administration to adult rats. *Pharmacol Res* 57:234-238.
222. Hohman, R. J., and S. C. Dreskin. 2001. Measuring degranulation of mast cells. *Curr Protoc Immunol* Chapter 7:Unit 7 26.
223. Bligh, E. G., and W. J. Dyer. 1959. A rapid method of total lipid extraction and purification. *Can J Biochem Physiol* 37:911-917.
224. Weljie, A. M., J. Newton, P. Mercier, E. Carlson, and C. M. Slupsky. 2006. Targeted profiling: quantitative analysis of 1H NMR metabolomics data. *Anal Chem* 78:4430-4442.
225. Lebherz, H. G., and W. J. Rutter. 1969. Distribution of fructose diphosphate aldolase variants in biological systems. *Biochemistry* 8:109-121.

226. Kanski, J., M. A. Alterman, and C. Schoneich. 2003. Proteomic identification of age-dependent protein nitration in rat skeletal muscle. *Free Radic Biol Med* 35:1229-1239.
227. Kanski, J., S. J. Hong, and C. Schoneich. 2005. Proteomic analysis of protein nitration in aging skeletal muscle and identification of nitrotyrosine-containing sequences in vivo by nanoelectrospray ionization tandem mass spectrometry. *J Biol Chem* 280:24261-24266.
228. Dalby, A., Z. Dauter, and J. A. Littlechild. 1999. Crystal structure of human muscle aldolase complexed with fructose 1,6-bisphosphate: mechanistic implications. *Protein Sci* 8:291-297.
229. Wishart, D. S., D. Tzur, C. Knox, R. Eisner, A. C. Guo, N. Young, D. Cheng, K. Jewell, D. Arndt, S. Sawhney, C. Fung, L. Nikolai, M. Lewis, M. A. Coutouly, I. Forsythe, P. Tang, S. Shrivastava, K. Jeroncic, P. Stothard, G. Amegbey, D. Block, D. D. Hau, J. Wagner, J. Miniaci, M. Clements, M. Gebremedhin, N. Guo, Y. Zhang, G. E. Duggan, G. D. Macinnis, A. M. Weljie, R. Dowlatabadi, F. Bamforth, D. Clive, R. Greiner, L. Li, T. Marrie, B. D. Sykes, H. J. Vogel, and L. Querengesser. 2007. HMDB: the Human Metabolome Database. *Nucleic Acids Res* 35:D521-526.
230. Hardin, C. D., and T. M. Roberts. 1994. Metabolism of exogenously applied fructose 1,6-bisphosphate in hypoxic vascular smooth muscle. *Am J Physiol* 267:H2325-2332.

231. Ehringer, W. D., W. Niu, B. Chiang, O. L. Wang, L. Gordon, and S. Chien. 2000. Membrane permeability of fructose-1,6-diphosphate in lipid vesicles and endothelial cells. *Mol Cell Biochem* 210:35-45.
232. Palazzolo-Ballance, A. M., C. Suquet, and J. K. Hurst. 2007. Pathways for intracellular generation of oxidants and tyrosine nitration by a macrophage cell line. *Biochemistry* 46:7536-7548.
233. Takemoto, K., K. Ogino, D. H. Wang, T. Takigawa, C. M. Kurosawa, Y. Kamyabashi, Y. Hibino, Y. Hitomi, and H. Ichimura. 2007. Biochemical characterization of reactive nitrogen species by eosinophil peroxidase in tyrosine nitration. *Acta Med Okayama* 61:17-30.
234. Klink, M., K. Bednarska, K. Jastrzemska, M. Banasik, and Z. Sulowska. 2007. Signal transduction pathways affected by nitric oxide donors during neutrophil functional response in vitro. *Inflamm Res* 56:282-290.
235. Harlow, E., Lane, David. 1988. *Antibodies: A Laboratory manual*. Cold Spring Harbor Laboratory Press, Cold Spring Harbor, New York.
236. Vassilakopoulos, T., K. Govindaraju, D. Parthenis, D. H. Eidelman, Y. Watanabe, and S. N. Hussain. 2007. Nitric oxide production in the ventilatory muscles in response to acute resistive loading. *Am J Physiol Lung Cell Mol Physiol* 292:L1013-1022.
237. Barreiro, E., R. Rabinovich, J. Marin-Corral, J. A. Barbera, J. Gea, and J. Roca. 2009. Chronic endurance exercise induces quadriceps nitrosative stress in patients with severe COPD. *Thorax* 64:13-19.

238. Dukes, A. A., V. S. Van Laar, M. Cascio, and T. G. Hastings. 2008. Changes in endoplasmic reticulum stress proteins and aldolase A in cells exposed to dopamine. *J Neurochem* 106:333-346.
239. Arcelay, E., A. M. Salicioni, E. Wertheimer, and P. E. Visconti. 2008. Identification of proteins undergoing tyrosine phosphorylation during mouse sperm capacitation. *Int J Dev Biol* 52:463-472.
240. Schindler, R., E. Weichselsdorfer, O. Wagner, and J. Bereiter-Hahn. 2001. Aldolase-localization in cultured cells: cell-type and substrate-specific regulation of cytoskeletal associations. *Biochem Cell Biol* 79:719-728.
241. MacDonnell, P. C., and O. Greengard. 1974. Enzymes in intracellular organelles of adult and developing rat brain. *Arch Biochem Biophys* 163:644-655.
242. Mamczur, P., and A. Dzugaj. 2004. Nuclear localization of aldolase A in pig cardiomyocytes. *Histol Histopathol* 19:753-758.
243. Haqqani, A. S., J. F. Kelly, and H. C. Birnboim. 2002. Selective nitration of histone tyrosine residues in vivo in mutataect tumors. *J Biol Chem* 277:3614-3621.
244. Yanez, A. J., H. C. Ludwig, R. Bertinat, C. Spichiger, R. Gatica, G. Berlien, O. Leon, M. Brito, Concha, II, and J. C. Slebe. 2005. Different involvement for aldolase isoenzymes in kidney glucose metabolism: aldolase B but not aldolase A colocalizes and forms a complex with FBPase. *J Cell Physiol* 202:743-753.

245. Takashi, M., H. Haimoto, T. Koshikawa, and K. Kato. 1990. Expression of aldolase C isozyme in renal cell carcinoma. *Am J Clin Pathol* 93:631-636.
246. Miyagi, M., H. Sakaguchi, R. M. Darrow, L. Yan, K. A. West, K. S. Aulak, D. J. Stuehr, J. G. Hollyfield, D. T. Organisciak, and J. W. Crabb. 2002. Evidence that light modulates protein nitration in rat retina. *Mol Cell Proteomics* 1:293-303.
247. Kanski, J., A. Behring, J. Pelling, and C. Schoneich. 2005. Proteomic identification of 3-nitrotyrosine-containing rat cardiac proteins: effects of biological aging. *Am J Physiol Heart Circ Physiol* 288:H371-381.
248. Aulak, K. S., M. Miyagi, L. Yan, K. A. West, D. Massillon, J. W. Crabb, and D. J. Stuehr. 2001. Proteomic method identifies proteins nitrated in vivo during inflammatory challenge. *Proc Natl Acad Sci U S A* 98:12056-12061.
249. Steinhagen-Thiessen, E., and H. Hilz. 1979. Aldolase activity and cross-reacting material in lymphocytes of aged individuals. *Gerontology* 25:132-135.
250. Day, I. N., and R. J. Thompson. 1984. Levels of immunoreactive aldolase C, creatine kinase-BB, neuronal and non-neuronal enolase, and 14-3-3 protein in circulating human blood cells. *Clin Chim Acta* 136:219-228.
251. Jean, J. C., C. B. Rich, and M. Joyce-Brady. 2006. Hypoxia results in an HIF-1-dependent induction of brain-specific aldolase C in lung epithelial cells. *Am J Physiol Lung Cell Mol Physiol* 291:L950-956.

252. Slemmer, J. E., E. D. Haasdijk, D. C. Engel, N. Plesnila, and J. T. Weber. 2007. Aldolase C-positive cerebellar Purkinje cells are resistant to delayed death after cerebral trauma and AMPA-mediated excitotoxicity. *Eur J Neurosci* 26:649-656.
253. Mesples, B., R. H. Fontaine, V. Lelievre, J. M. Launay, and P. Gressens. 2005. Neuronal TGF-beta1 mediates IL-9/mast cell interaction and exacerbates excitotoxicity in newborn mice. *Neurobiol Dis* 18:193-205.
254. Koppenol, W. H., J. J. Moreno, W. A. Pryor, H. Ischiropoulos, and J. S. Beckman. 1992. Peroxynitrite, a cloaked oxidant formed by nitric oxide and superoxide. *Chem Res Toxicol* 5:834-842.
255. Miller, S., C. Ross-Inta, and C. Giulivi. 2007. Kinetic and proteomic analyses of S-nitrosoglutathione-treated hexokinase A: consequences for cancer energy metabolism. *Amino Acids* 32:593-602.
256. Parastatidis, I., L. Thomson, A. Burke, I. Chernysh, C. Nagaswami, J. Visser, S. Stamer, D. C. Liebler, G. Koliakos, H. F. Heijnen, G. A. Fitzgerald, J. W. Weisel, and H. Ischiropoulos. 2008. Fibrinogen beta-chain tyrosine nitration is a prothrombotic risk factor. *J Biol Chem* 283:33846-33853.
257. Madej, J. A., K. A. Sobiech, and S. Klimentowski. 1989. In vitro studies into some parameters of protein and carbohydrate metabolism in lymphocytes infected with bovine leucosis virus. *Arch Exp Veterinarmed* 43:923-927.

258. Takahashi, I., Y. Takasaki, and K. Hori. 1989. Site-directed mutagenesis of human aldolase isozymes: the role of Cys-72 and Cys-338 residues of aldolase A and of the carboxy-terminal Tyr residues of aldolases A and B. *J Biochem* 105:281-286.
259. Kreuder, J., A. Borkhardt, R. Repp, A. Pekrun, B. Gottsche, U. Gottschalk, H. Reichmann, W. Schachenmayr, K. Schlegel, and F. Lampert. 1996. Brief report: inherited metabolic myopathy and hemolysis due to a mutation in aldolase A. *N Engl J Med* 334:1100-1104.
260. Sola, A., J. Rosello-Catafau, E. Gelpi, and G. Hotter. 2001. Fructose-1,6-biphosphate in rat intestinal preconditioning: involvement of nitric oxide. *Gut* 48:168-175.
261. Hardie, D. G., and D. Carling. 1997. The AMP-activated protein kinase--fuel gauge of the mammalian cell? *Eur J Biochem* 246:259-273.
262. Carling, D. 2004. Ampk. *Curr Biol* 14:R220.
263. Sonnewald, U., T. B. Muller, N. Westergaard, G. Unsgard, S. B. Petersen, and A. Schousboe. 1994. NMR spectroscopic study of cell cultures of astrocytes and neurons exposed to hypoxia: compartmentation of astrocyte metabolism. *Neurochem Int* 24:473-483.
264. Almeida, A., J. Almeida, J. P. Bolanos, and S. Moncada. 2001. Different responses of astrocytes and neurons to nitric oxide: the role of glycolytically generated ATP in astrocyte protection. *Proc Natl Acad Sci U S A* 98:15294-15299.

265. Almeida, A., S. Moncada, and J. P. Bolanos. 2004. Nitric oxide switches on glycolysis through the AMP protein kinase and 6-phosphofructo-2-kinase pathway. *Nat Cell Biol* 6:45-51.
266. Pompella, A., A. Visvikis, A. Paolicchi, V. De Tata, and A. F. Casini. 2003. The changing faces of glutathione, a cellular protagonist. *Biochem Pharmacol* 66:1499-1503.
267. Hayes, J. D., and L. I. McLellan. 1999. Glutathione and glutathione-dependent enzymes represent a co-ordinately regulated defence against oxidative stress. *Free Radic Res* 31:273-300.
268. Fernie, A. R., R. N. Trethewey, A. J. Krotzky, and L. Willmitzer. 2004. Metabolite profiling: from diagnostics to systems biology. *Nat Rev Mol Cell Biol* 5:763-769.
269. Ross, K. L., and J. J. Dalluge. 2009. Liquid chromatography/tandem mass spectrometry of glycolytic intermediates: deconvolution of coeluting structural isomers based on unique product ion ratios. *Anal Chem* 81:4021-4026.
270. Donohoe, P. H., C. S. Fahlman, P. E. Bickler, Z. S. Vexler, and G. A. Gregory. 2001. Neuroprotection and intracellular Ca²⁺ modulation with fructose-1,6-bisphosphate during in vitro hypoxia-ischemia involves phospholipase C-dependent signaling. *Brain Res* 917:158-166.
271. Cohly, H., J. Jenkins, T. Skelton, E. Meydrech, and A. K. Markov. 2004. Fructose-1,6-diphosphate suppresses T-lymphocyte proliferation,

- promotes apoptosis and inhibits interleukins-1, 6, beta-actin mRNAs, and transcription factors expression. *Immunol Invest* 33:407-421.
272. Moresco, R. N., R. C. Santos, J. C. Alves Filho, A. A. Cunha, C. Dos Reis, C. L. Reichel, and J. R. De Oliveira. 2004. Protective effect of fructose-1,6-bisphosphate in the cold storage solution for liver preservation in rat hepatic transplantation. *Transplant Proc* 36:1261-1264.
273. Markov, A. K. 1999. "Treatment of asthma with fructose-1,6-diphosphate". *United States Patent #5858985, Jan 12*.
274. Cuesta, E., J. Boada, R. Calafell, J. C. Perales, T. Roig, and J. Bermudez. 2006. Fructose 1,6-bisphosphate prevented endotoxemia, macrophage activation, and liver injury induced by D-galactosamine in rats. *Crit Care Med* 34:807-814.
275. Yip, K., F. Leung, Y. Huang, and H. Lau. 2009. Inhibition of anti-IgE mediated human mast cell activation by NO donors is dependent on their NO release kinetics. *Br J Pharmacol*.
276. Kim, J. H., S. Lee, J. H. Kim, T. G. Lee, M. Hirata, P. G. Suh, and S. H. Ryu. 2002. Phospholipase D2 directly interacts with aldolase via Its PH domain. *Biochemistry* 41:3414-3421.
277. Gilchrist, M., C. Hesslinger, and A. D. Befus. 2003. Tetrahydrobiopterin, a critical factor in the production and role of nitric oxide in mast cells. *J Biol Chem* 278:50607-50614.
278. Inoue, T., Y. Suzuki, T. Yoshimaru, and C. Ra. 2009. Nitric Oxide positively regulates Ag (I)-induced Ca(2+) influx and mast cell activation:

- role of a Nitric Oxide Synthase-independent pathway. *J Leukoc Biol* 86:1365-1375.
279. Baron, C. B., S. Ozaki, Y. Watanabe, M. Hirata, E. F. LaBelle, and R. F. Coburn. 1995. Inositol 1,4,5-trisphosphate binding to porcine tracheal smooth muscle aldolase. *J Biol Chem* 270:20459-20465.
280. Koppitz, B., F. Vogel, and G. W. Mayr. 1986. Mammalian aldolases are isomer-selective high-affinity inositol polyphosphate binders. *Eur J Biochem* 161:421-433.
281. Waingeh, V. F., C. D. Gustafson, E. I. Kozliak, S. L. Lowe, H. R. Knull, and K. A. Thomasson. 2006. Glycolytic enzyme interactions with yeast and skeletal muscle F-actin. *Biophys J* 90:1371-1384.
282. Seo, I. R., S. H. Moh, E. H. Lee, G. Meissner, and H. Kim do. 2006. Aldolase potentiates DIDS activation of the ryanodine receptor in rabbit skeletal sarcoplasmic reticulum. *Biochem J* 399:325-333.
283. Smith, W. L., D. L. DeWitt, and R. M. Garavito. 2000. Cyclooxygenases: structural, cellular, and molecular biology. *Annu Rev Biochem* 69:145-182.
284. Tai, H. H., C. M. Ensor, M. Tong, H. Zhou, and F. Yan. 2002. Prostaglandin catabolizing enzymes. *Prostaglandins Other Lipid Mediat* 68-69:483-493.
285. Tai, H. H., H. Cho, M. Tong, and Y. Ding. 2006. NAD⁺-linked 15-hydroxyprostaglandin dehydrogenase: structure and biological functions. *Curr Pharm Des* 12:955-962.

286. Kao, A. W., Y. Noda, J. H. Johnson, J. E. Pessin, and A. R. Saltiel. 1999. Aldolase mediates the association of F-actin with the insulin-responsive glucose transporter GLUT4. *J Biol Chem* 274:17742-17747.
287. Bosch, J., C. A. Buscaglia, B. Krumm, B. P. Ingason, R. Lucas, C. Roach, T. Cardozo, V. Nussenzweig, and W. G. Hol. 2007. Aldolase provides an unusual binding site for thrombospondin-related anonymous protein in the invasion machinery of the malaria parasite. *Proc Natl Acad Sci U S A* 104:7015-7020.
288. Reddy, V. M., and F. G. Suleman. 2004. Mycobacterium avium-superoxide dismutase binds to epithelial cell aldolase, glyceraldehyde-3-phosphate dehydrogenase and cyclophilin A. *Microb Pathog* 36:67-74.
289. Perrotta, S., A. Borriello, A. Scaloni, L. De Franceschi, A. M. Brunati, F. Turrini, V. Nigro, E. M. del Giudice, B. Nobili, M. L. Conte, F. Rossi, A. Iolascon, A. Donella-Deana, V. Zappia, V. Poggi, W. Anong, P. Low, N. Mohandas, and F. Della Ragione. 2005. The N-terminal 11 amino acids of human erythrocyte band 3 are critical for aldolase binding and protein phosphorylation: implications for band 3 function. *Blood* 106:4359-4366.
290. Lu, M., L. S. Holliday, L. Zhang, W. A. Dunn, Jr., and S. L. Gluck. 2001. Interaction between aldolase and vacuolar H⁺-ATPase: evidence for direct coupling of glycolysis to the ATP-hydrolyzing proton pump. *J Biol Chem* 276:30407-30413.

291. Rangarajan, E. S., H. Park, E. Fortin, J. Sygusch, and T. Izard. 2010. Mechanism of aldolase control of sorting nexin 9 function in endocytosis. *J Biol Chem* 285:11983-11990.
292. Buscaglia, C. A., D. Penesetti, M. Tao, and V. Nussenzweig. 2006. Characterization of an aldolase-binding site in the Wiskott-Aldrich syndrome protein. *J Biol Chem* 281:1324-1331.
293. Anggard, E., C. Larsson, and B. Samuelsson. 1971. The distribution of 15-hydroxy prostaglandin dehydrogenase and prostaglandin-delta 13-reductase in tissues of the swine. *Acta Physiol Scand* 81:396-404.
294. Tai, H. H. 1976. Enzymatic synthesis of (15s)-[15-3h]prostaglandins and their use in the development of a simple and sensitive assay for 15-hydroxyprostaglandin dehydrogenase. *Biochemistry* 15:4586-4592.
295. Schlegel, W., L. M. Demers, H. E. Hildebrandt-Stark, H. R. Behrman, and R. O. Greep. 1974. Partial purification of human placental 15-hydroxyprostaglandin dehydrogenase: kinetic properties. *Prostaglandins* 5:417-433.
296. Ensor, C. M., and H. H. Tai. 1995. 15-Hydroxyprostaglandin dehydrogenase. *J Lipid Mediat Cell Signal* 12:313-319.
297. Tai, H. H., C. M. Ensor, H. Zhou, and F. Yan. 2002. Structure and function of human NAD(+)-linked 15-hydroxyprostaglandin dehydrogenase. *Adv Exp Med Biol* 507:245-250.
298. Bergholte, J. M., R. J. Soberman, R. Hayes, R. C. Murphy, and R. T. Okita. 1987. Oxidation of 15-hydroxyeicosatetraenoic acid and other

- hydroxy fatty acids by lung prostaglandin dehydrogenase. *Arch Biochem Biophys* 257:444-450.
299. Liu, Y., K. Yoden, R. F. Shen, and H. H. Tai. 1985. 12-L-hydroxy-5,8,10-heptadecatrienoic acid (HHT) is an excellent substrate for NAD⁺-dependent 15-hydroxyprostaglandin dehydrogenase. *Biochem Biophys Res Commun* 129:268-274.
300. Serhan, C. N., S. Fiore, D. A. Brezinski, and S. Lynch. 1993. Lipoxin A4 metabolism by differentiated HL-60 cells and human monocytes: conversion to novel 15-oxo and dihydro products. *Biochemistry* 32:6313-6319.
301. Piper, P. J., J. R. Vane, and J. H. Wyllie. 1970. Inactivation of prostaglandins by the lungs. *Nature* 225:600-604.
302. Sun, F. F., and S. B. Armour. 1974. Prostaglandin 15-hydroxy dehydrogenase and delta13 reductase levels in the lungs of maternal, fetal and neonatal rabbits. *Prostaglandins* 7:327-338.
303. Coggins, K. G., A. Latour, M. S. Nguyen, L. Audoly, T. M. Coffman, and B. H. Koller. 2002. Metabolism of PGE₂ by prostaglandin dehydrogenase is essential for remodeling the ductus arteriosus. *Nat Med* 8:91-92.
304. Hahn, E. L., K. D. Clancy, H. H. Tai, J. D. Ricken, L. K. He, and R. L. Gamelli. 1998. Prostaglandin E₂ alterations during sepsis are partially mediated by endotoxin-induced inhibition of prostaglandin 15-hydroxydehydrogenase. *J Trauma* 44:777-781; discussion 781-772.

305. Pavord, I. D., and A. E. Tattersfield. 1995. Bronchoprotective role for endogenous prostaglandin E2. *Lancet* 345:436-438.
306. Gauvreau, G. M., R. M. Watson, and P. M. O'Byrne. 1999. Protective effects of inhaled PGE2 on allergen-induced airway responses and airway inflammation. *Am J Respir Crit Care Med* 159:31-36.
307. Aggarwal, S., Y. P. Moodley, P. J. Thompson, and N. L. Misso. 2010. Prostaglandin E2 and cysteinyl leukotriene concentrations in sputum: association with asthma severity and eosinophilic inflammation. *Clin Exp Allergy* 40:85-93.
308. Wang, D., and R. N. Dubois. 2010. Eicosanoids and cancer. *Nat Rev Cancer* 10:181-193.
309. Backlund, M. G., J. R. Mann, V. R. Holla, F. G. Buchanan, H. H. Tai, E. S. Musiek, G. L. Milne, S. Katkuri, and R. N. DuBois. 2005. 15-Hydroxyprostaglandin dehydrogenase is down-regulated in colorectal cancer. *J Biol Chem* 280:3217-3223.
310. Wolf, I., J. O'Kelly, T. Rubinek, M. Tong, A. Nguyen, B. T. Lin, H. H. Tai, B. Y. Karlan, and H. P. Koeffler. 2006. 15-hydroxyprostaglandin dehydrogenase is a tumor suppressor of human breast cancer. *Cancer Res* 66:7818-7823.
311. Hughes, D., T. Otani, P. Yang, R. A. Newman, R. K. Yantiss, N. K. Altorki, J. L. Port, M. Yan, S. D. Markowitz, M. Mazumdar, H. H. Tai, K. Subbaramaiah, and A. J. Dannenberg. 2008. NAD⁺-dependent 15-

- hydroxyprostaglandin dehydrogenase regulates levels of bioactive lipids in non-small cell lung cancer. *Cancer Prev Res (Phila Pa)* 1:241-249.
312. Thiel, A., A. Ganesan, J. Mrena, S. Junnila, A. Nykanen, A. Hemmes, H. H. Tai, O. Monni, A. Kokkola, C. Haglund, T. V. Petrova, and A. Ristimaki. 2009. 15-hydroxyprostaglandin dehydrogenase is down-regulated in gastric cancer. *Clin Cancer Res* 15:4572-4580.
313. Myung, S. J., R. M. Rerko, M. Yan, P. Platzer, K. Guda, A. Dotson, E. Lawrence, A. J. Dannenberg, A. K. Lovgren, G. Luo, T. P. Pretlow, R. A. Newman, J. Willis, D. Dawson, and S. D. Markowitz. 2006. 15-Hydroxyprostaglandin dehydrogenase is an in vivo suppressor of colon tumorigenesis. *Proc Natl Acad Sci U S A* 103:12098-12102.
314. Meyer, H., W. C. Puijk, R. Dijkman, M. M. Foda-van der Hoorn, F. Pattus, A. J. Slotboom, and G. H. de Haas. 1979. Comparative studies of tyrosine modification in pancreatic phospholipases. 2. Properties of the nitrotyrosyl, aminotyrosyl, and dansylaminotyrosyl derivatives of pig, horse, and ox phospholipases A2 and their zymogens. *Biochemistry* 18:3589-3597.
315. Meyer, H., H. Verhoef, F. F. Hendriks, A. J. Slotboom, and G. H. de Haas. 1979. Comparative studies of tyrosine modification in pancreatic phospholipases. 1. Reaction of tetranitromethane with pig, horse, and ox phospholipases A2 and their zymogens. *Biochemistry* 18:3582-3588.

316. Boulos, C., H. Jiang, and M. Balazy. 2000. Diffusion of peroxynitrite into the human platelet inhibits cyclooxygenase via nitration of tyrosine residues. *J Pharmacol Exp Ther* 293:222-229.
317. Clancy, R., B. Varenika, W. Huang, L. Ballou, M. Attur, A. R. Amin, and S. B. Abramson. 2000. Nitric oxide synthase/COX cross-talk: nitric oxide activates COX-1 but inhibits COX-2-derived prostaglandin production. *J Immunol* 165:1582-1587.
318. Deeb, R. S., G. Hao, S. S. Gross, M. Laine, J. H. Qiu, B. Resnick, E. J. Barbar, D. P. Hajjar, and R. K. Upmacis. 2006. Heme catalyzes tyrosine 385 nitration and inactivation of prostaglandin H2 synthase-1 by peroxynitrite. *J Lipid Res* 47:898-911.
319. Deeb, R. S., M. J. Resnick, D. Mittar, T. McCaffrey, D. P. Hajjar, and R. K. Upmacis. 2002. Tyrosine nitration in prostaglandin H(2) synthase. *J Lipid Res* 43:1718-1726.
320. Deeb, R. S., H. Shen, C. Gamss, T. GavriloVA, B. D. Summers, R. Kraemer, G. Hao, S. S. Gross, M. Laine, N. Maeda, D. P. Hajjar, and R. K. Upmacis. 2006. Inducible nitric oxide synthase mediates prostaglandin h2 synthase nitration and suppresses eicosanoid production. *Am J Pathol* 168:349-362.
321. Zou, M. H., and V. Ullrich. 1996. Peroxynitrite formed by simultaneous generation of nitric oxide and superoxide selectively inhibits bovine aortic prostacyclin synthase. *FEBS Lett* 382:101-104.

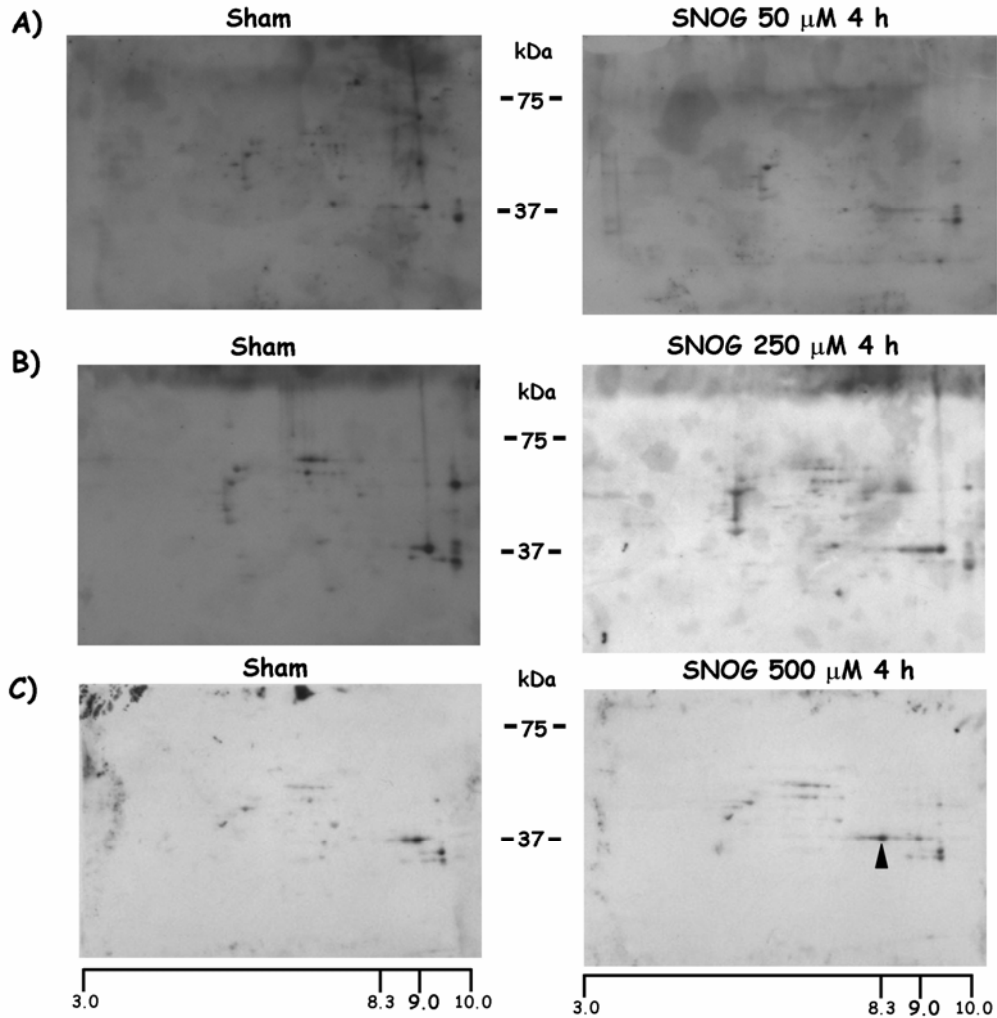
322. He, C., H. C. Choi, and Z. Xie. 2010. Enhanced tyrosine nitration of prostacyclin synthase is associated with increased inflammation in atherosclerotic carotid arteries from type 2 diabetic patients. *Am J Pathol* 176:2542-2549.
323. Sugimoto, Y., and S. Narumiya. 2007. Prostaglandin E receptors. *J Biol Chem* 282:11613-11617.
324. Feng, C., E. M. Beller, S. Bagga, and J. A. Boyce. 2006. Human mast cells express multiple EP receptors for prostaglandin E2 that differentially modulate activation responses. *Blood* 107:3243-3250.
325. Narumiya, S., Y. Sugimoto, and F. Ushikubi. 1999. Prostanoid receptors: structures, properties, and functions. *Physiol Rev* 79:1193-1226.
326. Kay, L. J., W. W. Yeo, and P. T. Peachell. 2006. Prostaglandin E2 activates EP2 receptors to inhibit human lung mast cell degranulation. *Br J Pharmacol* 147:707-713.
327. Wang, X. S., and H. Y. Lau. 2006. Prostaglandin E potentiates the immunologically stimulated histamine release from human peripheral blood-derived mast cells through EP1/EP3 receptors. *Allergy* 61:503-506.
328. Abdel-Majid, R. M., and J. S. Marshall. 2004. Prostaglandin E2 induces degranulation-independent production of vascular endothelial growth factor by human mast cells. *J Immunol* 172:1227-1236.
329. Nakayama, T., N. Mutsuga, L. Yao, and G. Tosato. 2006. Prostaglandin E2 promotes degranulation-independent release of MCP-1 from mast cells. *J Leukoc Biol* 79:95-104.

330. Wang, X. S., A. Y. Wu, P. S. Leung, and H. Y. Lau. 2007. PGE suppresses excessive anti-IgE induced cysteinyl leucotrienes production in mast cells of patients with aspirin exacerbated respiratory disease. *Allergy* 62:620-627.
331. Hogaboam, C. M., E. Y. Bissonnette, B. C. Chin, A. D. Befus, and J. L. Wallace. 1993. Prostaglandins inhibit inflammatory mediator release from rat mast cells. *Gastroenterology* 104:122-129.
332. Lewis, R. A., N. A. Soter, P. T. Diamond, K. F. Austen, J. A. Oates, and L. J. Roberts, 2nd. 1982. Prostaglandin D2 generation after activation of rat and human mast cells with anti-IgE. *J Immunol* 129:1627-1631.
333. Lin, T. Y., and C. A. London. 2010. Characterization and modulation of canine mast cell derived eicosanoids. *Vet Immunol Immunopathol* 135:118-127.
334. Boyce, J. A. 2007. Role of PGE2 in human mast cell biology. In <http://www.labome.org/grant/p01/hl/role/of/role-of-pge2-in-human-mast-cell-biology-7422408.html>.
335. Kuhn, H., M. Walther, and R. J. Kuban. 2002. Mammalian arachidonate 15-lipoxygenases structure, function, and biological implications. *Prostaglandins Other Lipid Mediat* 68-69:263-290.
336. Gulliksson, M., A. Brunnstrom, M. Johannesson, L. Backman, G. Nilsson, I. Harvima, B. Dahlen, M. Kumlin, and H. E. Claesson. 2007. Expression of 15-lipoxygenase type-1 in human mast cells. *Biochim Biophys Acta* 1771:1156-1165.

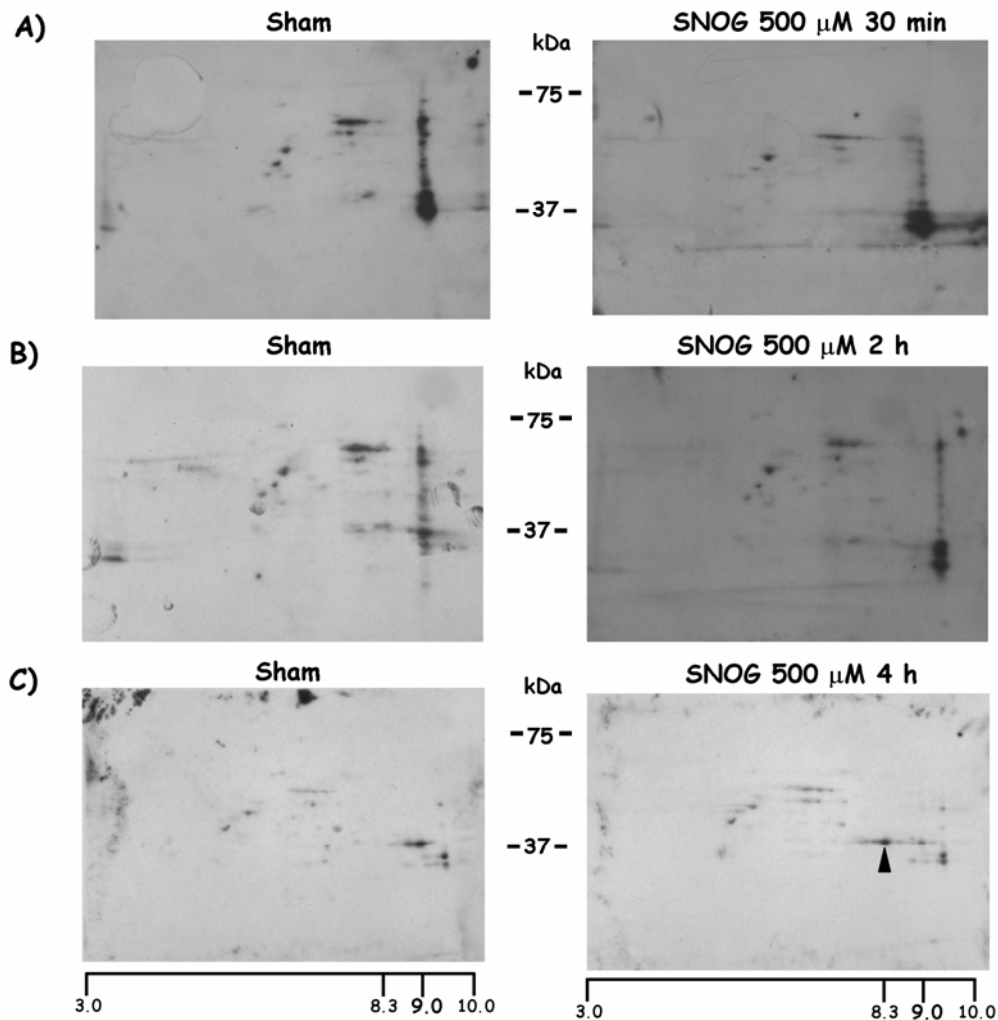
337. Profita, M., A. Sala, L. Riccobono, A. Paterno, A. Mirabella, A. Bonanno, D. Guerrero, E. Pace, G. Bonsignore, J. Bousquet, and A. M. Vignola. 2000. 15-Lipoxygenase expression and 15(S)-hydroxyeicoisatetraenoic acid release and reincorporation in induced sputum of asthmatic subjects. *J Allergy Clin Immunol* 105:711-716.
338. Ohtsu, N., K. Takaoka, E. Segawa, S. Hashitani, K. Noguchi, H. Kishimoto, and M. Urade. 2010. Antitumor effects of inhibitors of nitric oxide synthase or cyclooxygenase-2 on human KB carcinoma cells overexpressing COX-2. *Oncol Rep* 24:31-36.
339. Kanematsu, M., K. Ikeda, and Y. Yamada. 1997. Interaction between nitric oxide synthase and cyclooxygenase pathways in osteoblastic MC3T3-E1 cells. *J Bone Miner Res* 12:1789-1796.
340. Mollace, V., M. Colasanti, C. Muscoli, G. M. Lauro, M. Iannone, D. Rotiroti, and G. Nistico. 1998. The effect of nitric oxide on cytokine-induced release of PGE2 by human cultured astroglial cells. *Br J Pharmacol* 124:742-746.
341. Salvemini, D., T. P. Misko, J. L. Masferrer, K. Seibert, M. G. Currie, and P. Needleman. 1993. Nitric oxide activates cyclooxygenase enzymes. *Proc Natl Acad Sci U S A* 90:7240-7244.
342. Xu, L., C. Han, K. Lim, and T. Wu. 2008. Activation of cytosolic phospholipase A2alpha through nitric oxide-induced S-nitrosylation. Involvement of inducible nitric-oxide synthase and cyclooxygenase-2. *J Biol Chem* 283:3077-3087.

343. Gobeil, F., Jr., I. Dumont, A. M. Marrache, A. Vazquez-Tello, S. G. Bernier, D. Abran, X. Hou, M. H. Beauchamp, C. Quiniou, A. Bouayad, S. Choufani, M. Bhattacharya, S. Molotchnikoff, A. Ribeiro-Da-Silva, D. R. Varma, G. Bkaily, and S. Chemtob. 2002. Regulation of eNOS expression in brain endothelial cells by perinuclear EP(3) receptors. *Circ Res* 90:682-689.
344. Bhattacharya, M., K. Peri, A. Ribeiro-da-Silva, G. Almazan, H. Shichi, X. Hou, D. R. Varma, and S. Chemtob. 1999. Localization of functional prostaglandin E2 receptors EP3 and EP4 in the nuclear envelope. *J Biol Chem* 274:15719-15724.
345. Bischoff, S. C., G. Sellge, S. Schwengberg, A. Lorentz, and M. P. Manns. 1999. Stem cell factor-dependent survival, proliferation and enhanced releasability of purified mature mast cells isolated from human intestinal tissue. *Int Arch Allergy Immunol* 118:104-107.

Appendix – 1



Appendix 1, Figure 1 Dose response of S-nitrosoglutathione treatment on HMC-1 nitration pattern. Five million HMC-1 cells were treated for 4 h at 37°C with A) 50 μ M of S-nitrosoglutathione (SNOG); B) 250 μ M of SNOG and C) 500 μ M of SNOG. Proteins were extracted for two dimensional electrophoresis and western blot was performed using anti-nitrotyrosine antibody. Arrowhead (right panel in C) indicates the protein that was nitrated upon 500 μ M of SNOG 4 h treatment which was not seen in A and B. Also note the reduced background of blots in C after 3 M urea washing. Results are representative of two independent experiments (A, B); seven independent experiments (C).



Appendix 1, Figure 2 Time course of S-nitrosoglutathione treatment on HMC-1 nitration pattern. Five million HMC-1 cells were treated at 37°C with 500 μM of S-nitrosoglutathione (SNOG) for a time period of A) 30 min; B) 2 h and C) 4 h. Proteins were extracted for two dimensional electrophoresis and western blot was performed using anti-nitrotyrosine antibody. Arrowhead (right panel in C) indicates the protein that was nitrated upon 500 μM of SNOG treatment for 4 h which was not seen in A and B. Results are representative of two independent experiments (A, B); seven independent experiments (C).

Appendix 1, Table 1 List of antibodies used in the study

Antigen	Species	Source
Nitrated KLH (keyhole limpet hemocyanin)	rabbit polyclonal	Millipore (Etobicoke, Ontario, Canada)
Rabbit muscle aldolase	goat polyclonal	Chemicon (Billerica, MA)
15-hydroxy prostaglandin dehydrogenase	rabbit polyclonal	Cayman Chemical (Ann Arbor, MI)
Rabbit IgG	goat polyclonal	Jackson Immunoresearch Laboratories Inc. (West Grove, PA)
Goat IgG	donkey polyclonal	Jackson Immunoresearch Laboratories Inc.
Human IgE	mouse	Dako (Mississauga, Ontario, Canada)
Rabbit IgG	goat	LI-COR biosciences (Lincoln, NE)
Mouse IgG	goat	LI-COR biosciences
Zebrin II	mouse monoclonal	Dr. Richard Hawkes, University of Calgary

Appendix 1, Table 2 Inclusion list of nitrated peptides of aldolase A

M+H *	M+2H *	M+3H *	Modifications	Peptide Sequence containing nitro tyrosine
714.287	357.643	238.7625	1Nitro	(R)C(Carbamidomethyl)AQYK(K)
808.456	404.728	270.1521	1Nitro	(K)VLAAYK(A)
842.382	421.691	281.4608	1Nitro	(R)C(Carbamidomethyl)AQYKK(D)
972.409	486.704	324.803	1Nitro	(R)C(Carbamidomethyl)QYVTEK(V)
982.447	491.723	328.1492	1Nitro	(K)AAQEEYVK(R)
1128.51	564.7551	376.8367	1Nitro	(K)RC(Carbamidomethyl)QYVTEK(V)
1138.549	569.7744	380.1829	1Nitro	(K)AAQEEYVKR(A)
1466.712	733.8561	489.5707	1Nitro	(K)ENLKAAQEEYVK(R)
1546.696	773.8478	516.2318	1Nitro	(R)C(Carbamidomethyl)AQYKKDGADFAK(W)
1555.786	778.3932	519.2621	1Nitro	(R)FYRQLLLTADDR(V)
1594.807	797.9036	532.269	1Nitro	(K)KENLKAAQEEYVK(R)
1610.752	805.876	537.584	1Nitro	(-)MPYQYPALTPEQK(K)
1622.813	811.9067	541.6044	1Nitro	(K)ENLKAAQEEYVKR(A)
1626.747	813.8734	542.9156	1Nitro 1Oxidation	(-)MPYQYPALTPEQK(K)
1655.737	828.3685	552.579	2Nitro	(-)MPYQYPALTPEQK(K)
1671.732	836.366	557.9106	2Nitro 1Oxidation	(-)MPYQYPALTPEQK(K)
1711.887	856.4437	571.2958	1Nitro	(R)RFYRQLLLTADDR(V)
1716.863	858.9313	572.9542	1Nitro	(R)C(Carbamidomethyl)QYVTEKVLAAVYK(A)
1738.847	869.9235	580.2823	1Nitro	(-)MPYQYPALTPEQKK(E)
1754.842	877.9209	585.6139	1Nitro 1Oxidation	(-)MPYQYPALTPEQKK(E)
1761.848	881.4238	587.9492	2Nitro	(R)C(Carbamidomethyl)QYVTEKVLAAVYK(A)
1783.832	892.416	595.2773	2Nitro	(-)MPYQYPALTPEQKK(E)
1799.827	900.4135	600.609	2Nitro 1Oxidation	(-)MPYQYPALTPEQKK(E)
1853.937	927.4684	618.6456	1Nitro	(K)C(Carbamidomethyl)PLLKPWALTFSYGR(A)
1872.964	936.9818	624.9879	1Nitro	(K)RC(Carbamidomethyl)QYVTEKVLAAVYK(A)
1917.949	959.4744	639.9829	2Nitro	(K)RC(Carbamidomethyl)QYVTEKVLAAVYK(A)
2030.071	1015.535	677.3569	1Nitro	(R)VNPGIGGVILFHETLYQK(A)
2158.027	1079.514	720.0091	1Nitro	(R)LQSIGTENTEENRRFYR(Q)
2252.109	1126.554	751.3696	1Nitro	(K)AAQEEYVKRALANSLAC(Carbamidomethyl)QGK(Y)
2273.011	1137.005	758.3368	1Nitro	(K)YTPSGQAGAAASESLFVSNHAY(-)
2317.996	1159.498	773.3319	2Nitro	(K)YTPSGQAGAAASESLFVSNHAY(-)
2636.402	1318.701	879.4672	1Nitro	(K)C(Carbamidomethyl)PLLKPWALTFSYGRALQASALK(A)
2660.314	1330.657	887.4379	1Nitro	(-)MPYQYPALTPEQKKELSDIAHR(I)
2676.309	1338.654	892.7695	1Nitro 1Oxidation	(-)MPYQYPALTPEQKKELSDIAHR(I)

2705.299	1353.149	902.4329	2Nitro	(-)MPYQYPALTPEQKKELSDIAHR(I)
2721.294	1361.147	907.7646	2Nitro 1Oxidation	(-)MPYQYPALTPEQKKELSDIAHR(I) (K)GVVPLAGTNGETTTQGLDGLSERC(Carbamidomethyl)AQYK
2967.411	1484.206	989.8038	1Nitro	(K)
3021.499	1511.249	1007.833	1Nitro	(R)YASIC(Carbamidomethyl)QQNGIVPIVEPEILPDGAHDLK(R)
3055.621	1528.311	1019.207	1Nitro	(R)QLLLTADDRVNP GIGGVILFHETLYQK(A)
3135.656	1568.328	1045.885	1Nitro	(K)C(Carbamidomethyl)PLLKPWAL TFSYGRALQASALKAWGG K(K)
3162.51	1581.755	1054.837	1Nitro	(K)ALSDHHIYLEGTLLNPNMVTPGHAC(Carbamidomethyl)TQK
3177.6	1589.3	1059.867	1Nitro	(F) (R)YASIC(Carbamidomethyl)QQNGIVPIVEPEILPDGAHDLKR(C)
3178.504	1589.752	1060.168	1Nitro 1Oxidation	(K)ALSDHHIYLEGTLLNPNMVTPGHAC(Carbamidomethyl)TQK (F)
3309.602	1655.301	1103.867	1Nitro	(K)VDKGVVPLAGTNGETTTQGLDGLSERC(Carbamidomethyl)A QYK(K)
3353.764	1677.382	1118.588	1Nitro	(R)VNP GIGGVILFHETLYQKADDGRPFQVIK(S)
3386.571	1693.785	1129.524	1Nitro	(R)ALANSLAC(Carbamidomethyl)QGKYTPSGQAGAAASESLFV SNHAY(-)
3431.556	1716.278	1144.519	2Nitro	(R)ALANSLAC(Carbamidomethyl)QGKYTPSGQAGAAASESLFV SNHAY(-)
3521.854	1761.427	1174.618	1Nitro	(R)FYRQLLLTADDRVNP GIGGVILFHETLYQK(A)
3542.672	1771.836	1181.557	1Nitro	(K)RALANSLAC(Carbamidomethyl)QGKYTPSGQAGAAASESLF VSNHAY(-)
3566.839	1783.92	1189.613	2Nitro	(R)FYRQLLLTADDRVNP GIGGVILFHETLYQK(A)
3568.891	1784.946	1190.297	1Nitro	(R)VNP GIGGVILFHETLYQKADDGRPFQVIKSK(G)
3587.657	1794.328	1196.552	2Nitro	(K)RALANSLAC(Carbamidomethyl)QGKYTPSGQAGAAASESLF VSNHAY(-)
3906.963	1953.981	1302.988	1Nitro	(K)VLAAVYKALSDHHIYLEGTLLNPNMVTPGHAC(Carbamido methyl)TQK(F)
3922.958	1961.979	1308.319	1Nitro 1Oxidation	(K)VLAAVYKALSDHHIYLEGTLLNPNMVTPGHAC(Carbamido methyl)TQK(F)
3951.948	1976.474	1317.983	2Nitro	(K)VLAAVYKALSDHHIYLEGTLLNPNMVTPGHAC(Carbamido methyl)TQK(F)
3967.943	1984.471	1323.314	2Nitro 1Oxidation	(K)VLAAVYKALSDHHIYLEGTLLNPNMVTPGHAC(Carbamido methyl)TQK(F)
4086.006	2043.503	1362.669	1Nitro	(R)YASIC(Carbamidomethyl)QQNGIVPIVEPEILPDGAHDLKRC(Carbamidomethyl)QYVTEK(V)
4130.991	2065.996	1377.664	2Nitro	(R)YASIC(Carbamidomethyl)QQNGIVPIVEPEILPDGAHDLKRC(Carbamidomethyl)QYVTEK(V)

4379.315	2190.157	1460.438	1Nitro	Carbamidomethyl)QYVTEK(V) (R)QLLLTADDRVNP GIGGVILFHETLYQKADDGRPFQVIK(S)
4815.369	2408.185	1605.79	1Nitro	(R)C(Carbamidomethyl)QYVTEKVLAAVYKALSDHHIYLEG TLL NPNMVTPGHAC(Carbamidomethyl)TQK(F)
4819.339	2410.169	1607.113	1Nitro	(K)ALSDHHIYLEG TLLNPNMVTPGHAC(Carbamidomethyl)TQK FSHEEIAMATVTALR(R)
4831.364	2416.182	1611.121	1Nitro 1Oxidation	(R)C(Carbamidomethyl)QYVTEKVLAAVYKALSDHHIYLEG TLL NPNMVTPGHAC(Carbamidomethyl)TQK(F)
4835.334	2418.167	1612.445	1Nitro 1Oxidation	(K)ALSDHHIYLEG TLLNPNMVTPGHAC(Carbamidomethyl)TQK FSHEEIAMATVTALR(R)
4851.329	2426.164	1617.776	1Nitro 2Oxidation	(K)ALSDHHIYLEG TLLNPNMVTPGHAC(Carbamidomethyl)TQK FSHEEIAMATVTALR(R)
4860.354	2430.677	1620.785	2Nitro	(R)C(Carbamidomethyl)QYVTEKVLAAVYKALSDHHIYLEG TLL NPNMVTPGHAC(Carbamidomethyl)TQK(F)
4876.349	2438.675	1626.116	2Nitro 1Oxidation	(R)C(Carbamidomethyl)QYVTEKVLAAVYKALSDHHIYLEG TLL NPNMVTPGHAC(Carbamidomethyl)TQK(F)
4905.339	2453.17	1635.78	3Nitro	(R)C(Carbamidomethyl)QYVTEKVLAAVYKALSDHHIYLEG TLL NPNMVTPGHAC(Carbamidomethyl)TQK(F)
4908.488	2454.744	1636.829	1Nitro	(R)TVPPAVTGITFLSGGQSEESSINLNAINKC(Carbamidomethyl))PLLKPWALTFSYGR(A)
4921.334	2461.167	1641.111	3Nitro 1Oxidation	(R)C(Carbamidomethyl)QYVTEKVLAAVYKALSDHHIYLEG TLL NPNMVTPGHAC(Carbamidomethyl)TQK(F)
4975.44	2488.22	1659.147	1Nitro	(K)ALSDHHIYLEG TLLNPNMVTPGHAC(Carbamidomethyl)TQK FSHEEIAMATVTALRR(T)
4991.435	2496.217	1664.478	1Nitro 1Oxidation	(K)ALSDHHIYLEG TLLNPNMVTPGHAC(Carbamidomethyl)TQK FSHEEIAMATVTALRR(T)
5007.43	2504.215	1669.81	1Nitro 2Oxidation	(K)ALSDHHIYLEG TLLNPNMVTPGHAC(Carbamidomethyl)TQK FSHEEIAMATVTALRR(T)
5064.589	2532.794	1688.863	1Nitro	(R)RTVPPAVTGITFLSGGQSEESSINLNAINKC(Carbamidomethyl) yl)PLLKPWALTFSYGR(A)
5109.577	2555.289	1703.859	1Nitro	(K)IGEHTPSALAIMENANVLARYASIC(Carbamidomethyl)QQNG IVPIVEPEILPDGAHDLK(R)
5125.572	2563.286	1709.191	1Nitro 1Oxidation	(K)IGEHTPSALAIMENANVLARYASIC(Carbamidomethyl)QQNG IVPIVEPEILPDGAHDLK(R)
5265.678	2633.339	1755.893	1Nitro	(K)IGEHTPSALAIMENANVLARYASIC(Carbamidomethyl)QQNG IVPIVEPEILPDGAHDLKR(C)
5281.673	2641.337	1761.224	1Nitro 1Oxidation	(K)IGEHTPSALAIMENANVLARYASIC(Carbamidomethyl)QQNG IVPIVEPEILPDGAHDLKR(C)

5563.792	2782.396	1855.264	1Nitro	(K)VLAAVYKALSDHHIYLEGTLLNPNMVTPGHAC(Carbamidomethyl)TQKFSHEEIAMATVTALR(R)
5579.787	2790.394	1860.596	1Nitro 1Oxidation	(K)VLAAVYKALSDHHIYLEGTLLNPNMVTPGHAC(Carbamidomethyl)TQKFSHEEIAMATVTALR(R)
5595.782	2798.391	1865.927	1Nitro 2Oxidation	(K)VLAAVYKALSDHHIYLEGTLLNPNMVTPGHAC(Carbamidomethyl)TQKFSHEEIAMATVTALR(R)
5608.777	2804.889	1870.259	2Nitro	(K)VLAAVYKALSDHHIYLEGTLLNPNMVTPGHAC(Carbamidomethyl)TQKFSHEEIAMATVTALR(R)
5609.855	2805.428	1870.618	1Nitro	(R)C(Carbamidomethyl)VLKIGEHTPSALAIMENANVLARYASIC(Carbamidomethyl)QQNGIVPIVEPEILPDGAHDLK(R)
5624.772	2812.886	1875.591	2Nitro 1Oxidation	(K)VLAAVYKALSDHHIYLEGTLLNPNMVTPGHAC(Carbamidomethyl)TQKFSHEEIAMATVTALR(R)
5625.85	2813.425	1875.95	1Nitro 1Oxidation	(R)C(Carbamidomethyl)VLKIGEHTPSALAIMENANVLARYASIC(Carbamidomethyl)QQNGIVPIVEPEILPDGAHDLK(R)
5640.767	2820.884	1880.922	2Nitro 2Oxidation	(K)VLAAVYKALSDHHIYLEGTLLNPNMVTPGHAC(Carbamidomethyl)TQKFSHEEIAMATVTALR(R)
5690.953	2845.976	1897.651	1Nitro	(R)TVPPAVTGITFLSGGQSEEESSINLNAINK(Carbamidomethyl)PLLKPWALTFSYGRALQASALK(A)

* The mass/charge ratio (m/z) of the peptide sequences were calculated based on the formula: $m/z = (M + nH^+)/n$.

Where, M = the molecular mass of the peptide sequence; n = the integer number of charges on the ions; H = the mass of a proton = 1.008 Da.

Appendix 1, Table 3 Inclusion list of nitrated peptides of aldolase C

M+H *	M+2H *	M+3H *	Modifications	Peptide Sequence containing nitro tyrosine
714.2876	357.6438	238.7625	1Nitro	(R)C(Carbamidomethyl)AQYK(K)
808.4563	404.7282	270.1521	1Nitro	(K)VLAAVYK(A)
842.3825	421.6913	281.4608	1Nitro	(R)C(Carbamidomethyl)AQYKK(D)
972.4091	486.7046	324.803	1Nitro	(R)C(Carbamidomethyl)QYVTEK(V)
1128.51	564.7551	376.8367	1Nitro	(K)RC(Carbamidomethyl)QYVTEK(V)
1503.69	752.3449	501.8966	1Nitro	(-)MPHSYPALSAEQK(K)
1519.685	760.3423	507.2282	1Nitro 1Oxidation	(-)MPHSYPALSAEQK(K)
1527.755	764.3775	509.9183	1Nitro	(R)LYRQVLFSADDR(V)
1546.696	773.8478	516.2318	1Nitro	(R)C(Carbamidomethyl)AQYKKDGADFAK(W)
1631.785	816.3923	544.5949	1Nitro	(-)MPHSYPALSAEQKK(E)
1647.78	824.3898	549.9265	1Nitro 1Oxidation	(-)MPHSYPALSAEQKK(E)
1683.856	842.4281	561.952	1Nitro	(R)RLYRQVLFSADDR(V)
1710.837	855.9184	570.9456	1Nitro	(K)YTPEEIAMATVTALR(R)
1716.863	858.9313	572.9542	1Nitro	(R)C(Carbamidomethyl)QYVTEKVLAAVYK(A)
1726.832	863.9158	576.2772	1Nitro 1Oxidation	(K)YTPEEIAMATVTALR(R)
1754.918	877.9592	585.6395	1Nitro	(R)LYRQVLFSADDRVK(K)
1761.848	881.4238	587.9492	2Nitro	(R)C(Carbamidomethyl)QYVTEKVLAAVYK(A)
1856.9	928.95	619.6333	1Nitro	(K)C(Carbamidomethyl)IGGVIFFHETLYQK(D)
1865.912	933.4558	622.6372	1Nitro	(R)C(Carbamidomethyl)PLPRPWALTFSYGR(A)
1866.938	933.9689	622.9793	1Nitro	(K)YTPEEIAMATVTALRR(T)
1872.964	936.9818	624.9879	1Nitro	(K)RC(Carbamidomethyl)QYVTEKVLAAVYK(A)
1882.933	941.9664	628.3109	1Nitro 1Oxidation	(K)YTPEEIAMATVTALRR(T)
1917.949	959.4744	639.9829	2Nitro	(K)RC(Carbamidomethyl)QYVTEKVLAAVYK(A)
1984.995	992.9975	662.3316	1Nitro	(K)KC(Carbamidomethyl)IGGVIFFHETLYQK(D)
2122.064	1061.532	708.0212	1Nitro	(R)LSQIGVENTEENRRLYR(Q)
2212.158	1106.579	738.0528	1Nitro	(R)VKKC(Carbamidomethyl)IGGVIFFHETLYQK(D)
2288.969	1144.985	763.6564	1Nitro	(K)YEGSGEDGGAAAQSLYIANHAY(-)
2333.954	1167.477	778.6514	2Nitro	(K)YEGSGEDGGAAAQSLYIANHAY(-)
2378.939	1189.97	793.6464	3Nitro	(K)YEGSGEDGGAAAQSLYIANHAY(-)
2529.277	1265.138	843.7589	1Nitro	(-)MPHSYPALSAEQKKELSDIALR(I)
2545.272	1273.136	849.0905	1Nitro 1Oxidation	(-)MPHSYPALSAEQKKELSDIALR(I)
2856.377	1428.689	952.7925	1Nitro	(K)C(Carbamidomethyl)IGGVIFFHETLYQKDDNGVPFVR(T)

2968.395	1484.698	990.1318	1Nitro	(K)GVVPLAGTDGETTTQGLDGLSERC(Carbamidomethyl)AQYK(K)
2984.472	1492.736	995.4908	1Nitro	(K)KC(Carbamidomethyl)IGGVIFFHETLYQKDDNGVPFVR(T)
3047.542	1524.271	1016.514	1Nitro	(R)C(Carbamidomethyl)PLPRPWALTFSYGRALQASALNAWR(G)
3065.488	1533.244	1022.496	1Nitro	(R)YASIC(Carbamidomethyl)QQNGIVPIVEPEILPDGDHDLK(R)
3096.49	1548.745	1032.83	1Nitro	(K)GVVPLAGTDGETTTQGLDGLSERC(Carbamidomethyl)AQYK(K)
3143.577	1572.288	1048.526	1Nitro	(K)ALSDHHVYLEGTLLKPNMVTPGHAC(Carbamidomethyl)PIK(Y)
3159.571	1580.286	1053.857	1Nitro 1Oxidation	(K)ALSDHHVYLEGTLLKPNMVTPGHAC(Carbamidomethyl)PIK(Y)
3221.59	1611.295	1074.53	1Nitro	(R)YASIC(Carbamidomethyl)QQNGIVPIVEPEILPDGDHDLK(R)
3310.586	1655.793	1104.195	1Nitro	(K)VDKGVVPLAGTDGETTTQGLDGLSERC(Carbamidomethyl)AQYK(K)
3327.515	1664.257	1109.838	1Nitro	(R)AEVNGLAAQKYEKSGEDGGAAAQSLYIANHAY(-)
3372.5	1686.75	1124.833	2Nitro	(R)AEVNGLAAQKYEKSGEDGGAAAQSLYIANHAY(-)
3388.723	1694.862	1130.241	1Nitro	(R)C(Carbamidomethyl)PLPRPWALTFSYGRALQASALNAWRGQR(D)
3417.485	1709.243	1139.828	3Nitro	(R)AEVNGLAAQKYEKSGEDGGAAAQSLYIANHAY(-)
3441.69	1721.345	1147.897	1Nitro	(K)C(Carbamidomethyl)IGGVIFFHETLYQKDDNGVPFVRTIQDK(G)
3483.616	1742.308	1161.872	1Nitro	(K)RAEVNGLAAQKYEKSGEDGGAAAQSLYIANHAY(-)
3528.601	1764.801	1176.867	2Nitro	(K)RAEVNGLAAQKYEKSGEDGGAAAQSLYIANHAY(-)
3573.586	1787.293	1191.862	3Nitro	(K)RAEVNGLAAQKYEKSGEDGGAAAQSLYIANHAY(-)
3888.03	1944.515	1296.677	1Nitro	(K)VLAAVYKALSDHHVYLEGTLLKPNMVTPGHAC(Carbamidomethyl)PIK(Y)
3904.025	1952.512	1302.008	1Nitro 1Oxidation	(K)VLAAVYKALSDHHVYLEGTLLKPNMVTPGHAC(Carbamidomethyl)PIK(Y)
3933.015	1967.008	1311.672	2Nitro	(K)VLAAVYKALSDHHVYLEGTLLKPNMVTPGHAC(Carbamidomethyl)PIK(Y)
3949.01	1975.005	1317.003	2Nitro 1Oxidation	(K)VLAAVYKALSDHHVYLEGTLLKPNMVTPGHAC(Carbamidomethyl)PIK(Y)
4129.996	2065.498	1377.332	1Nitro	(R)YASIC(Carbamidomethyl)QQNGIVPIVEPEILPDGDHDLKRC(Carbamidomethyl)QYVTEK(V)
4174.981	2087.99	1392.327	2Nitro	(R)YASIC(Carbamidomethyl)QQNGIVPIVEPEILPDGDHDLKRC(Carbamidomethyl)QYVTEK(V)
4699.404	2350.202	1567.135	1Nitro	(R)TPSALAILANANVLARYASIC(Carbamidomethyl)QQNGIVPIVEPEILPDGDHDLK(R)
4790.41	2395.705	1597.47	1Nitro	(K)ALSDHHVYLEGTLLKPNMVTPGHAC(Carbamidomethyl)PIKYTPEEIAMATVTALR(R)
4796.436	2398.718	1599.479	1Nitro	(R)C(Carbamidomethyl)QYVTEK(VLAAVYKALSDHHVYLEGTLLKPNMVTPGHAC(Carbamidomethyl)PIK(Y)
4806.405	2403.703	1602.802	1Nitro 1Oxidation	(K)ALSDHHVYLEGTLLKPNMVTPGHAC(Carbamidomethyl)PIKYTPEEIAMATVTALR(R)

4812.431	2406.716	1604.81	1Nitro 1Oxidation	(R)C(Carbamidomethyl)QYVTEKVLAAVYKALSDHHVYLEGTLLKPNM VTPGHAC(Carbamidomethyl)PIK(Y)
4822.4	2411.7	1608.133	1Nitro 2Oxidation	(K)ALSDHHVYLEGTLLKPNMVTPGHAC(Carbamidomethyl)PIKYTPEEI AMATVTALR(R)
4841.421	2421.211	1614.474	2Nitro	(R)C(Carbamidomethyl)QYVTEKVLAAVYKALSDHHVYLEGTLLKPNM VTPGHAC(Carbamidomethyl)PIK(Y)
4851.39	2426.195	1617.797	2Nitro 1Oxidation	(K)ALSDHHVYLEGTLLKPNMVTPGHAC(Carbamidomethyl)PIKYTPEEI AMATVTALR(R)
4855.505	2428.252	1619.168	1Nitro	(R)TPSALAIENANVLARYASIC(Carbamidomethyl)QQNGIVPIVEPEILP DGDHDLKR(C)
4857.416	2429.208	1619.805	2Nitro 1Oxidation	(R)C(Carbamidomethyl)QYVTEKVLAAVYKALSDHHVYLEGTLLKPNM VTPGHAC(Carbamidomethyl)PIK(Y)
4867.385	2434.193	1623.128	2Nitro 2Oxidation	(K)ALSDHHVYLEGTLLKPNMVTPGHAC(Carbamidomethyl)PIKYTPEEI AMATVTALR(R)
4886.406	2443.703	1629.469	3Nitro	(R)C(Carbamidomethyl)QYVTEKVLAAVYKALSDHHVYLEGTLLKPNM VTPGHAC(Carbamidomethyl)PIK(Y)
4902.401	2451.701	1634.8	3Nitro 1Oxidation	(R)C(Carbamidomethyl)QYVTEKVLAAVYKALSDHHVYLEGTLLKPNM VTPGHAC(Carbamidomethyl)PIK(Y)
4946.511	2473.756	1649.504	1Nitro	(K)ALSDHHVYLEGTLLKPNMVTPGHAC(Carbamidomethyl)PIKYTPEEI AMATVTALRR(T)
4948.448	2474.724	1650.149	1Nitro	(R)TVPPAVPGVTFSLGGQSEEEASFNLNAINRC(Carbamidomethyl)PLP RPWALTFSYGR(A)
4949.474	2475.237	1650.491	1Nitro	(K)YTPEEIAMATVTALRRTVPPAVPGVTFSLGGQSEEEASFNLNAINR(C) C)
4962.506	2481.753	1654.835	1Nitro 1Oxidation	(K)ALSDHHVYLEGTLLKPNMVTPGHAC(Carbamidomethyl)PIKYTPEEI AMATVTALRR(T)
4965.469	2483.234	1655.823	1Nitro 1Oxidation	(K)YTPEEIAMATVTALRRTVPPAVPGVTFSLGGQSEEEASFNLNAINR(C) C)
4978.501	2489.751	1660.167	1Nitro 2Oxidation	(K)ALSDHHVYLEGTLLKPNMVTPGHAC(Carbamidomethyl)PIKYTPEEI AMATVTALRR(T)
5007.491	2504.246	1669.83	2Nitro 1Oxidation	(K)ALSDHHVYLEGTLLKPNMVTPGHAC(Carbamidomethyl)PIKYTPEEI AMATVTALRR(T)
5023.486	2512.243	1675.162	2Nitro 2Oxidation	(K)ALSDHHVYLEGTLLKPNMVTPGHAC(Carbamidomethyl)PIKYTPEEI AMATVTALRR(T)
5104.549	2552.774	1702.183	1Nitro	(R)RTVPPAVPGVTFSLGGQSEEEASFNLNAINRC(Carbamidomethyl)PL RPWALTFSYGR(A)
5184.663	2592.832	1728.888	1Nitro	(K)ISERTPSALAIENANVLARYASIC(Carbamidomethyl)QQNGIVPIVE PEILPDGDHDLK(R)
5534.864	2767.932	1845.621	1Nitro	(K)VLAAVYKALSDHHVYLEGTLLKPNMVTPGHAC(Carbamidomethyl) PIKYTPEEIAMATVTALR(R)

5550.859	2775.929	1850.953	1Nitro 1Oxidation	(K)VLAAVYKALSDHHVYLEGTLLKPNMVTPGHAC(Carbamidomethyl)PIKYTPEEIAMATVTALR(R)
5566.854	2783.927	1856.285	1Nitro 2Oxidation	(K)VLAAVYKALSDHHVYLEGTLLKPNMVTPGHAC(Carbamidomethyl)PIKYTPEEIAMATVTALR(R)
5579.849	2790.424	1860.616	2Nitro	(K)VLAAVYKALSDHHVYLEGTLLKPNMVTPGHAC(Carbamidomethyl)PIKYTPEEIAMATVTALR(R)
5595.844	2798.422	1865.948	2Nitro 1Oxidation	(K)VLAAVYKALSDHHVYLEGTLLKPNMVTPGHAC(Carbamidomethyl)PIKYTPEEIAMATVTALR(R)
5611.839	2806.419	1871.28	2Nitro 2Oxidation	(K)VLAAVYKALSDHHVYLEGTLLKPNMVTPGHAC(Carbamidomethyl)PIKYTPEEIAMATVTALR(R)
5640.829	2820.914	1880.943	3Nitro 1Oxidation	(K)VLAAVYKALSDHHVYLEGTLLKPNMVTPGHAC(Carbamidomethyl)PIKYTPEEIAMATVTALR(R)
5656.824	2828.912	1886.275	3Nitro 2Oxidation	(K)VLAAVYKALSDHHVYLEGTLLKPNMVTPGHAC(Carbamidomethyl)PIKYTPEEIAMATVTALR(R)

* The mass/charge ratio (m/z) of the peptide sequences were calculated based on the formula: $m/z = (M + nH^+)/n$.

Where, M = the molecular mass of the peptide sequence; n = the integer number of charges on the ions; H = the mass of a proton = 1.008 Da.

Appendix 1, Table 4 Inclusion list of nitrated peptides of 15-hydroxy prostaglandin dehydrogenase

M+H *	M+2H *	M+3H *	Modifications	Peptide Sequence containing nitro tyrosine
1449.608	725.304	483.869	1Nit	(K)EENMGQYIEYK(D)
1465.603	733.302	489.201	1Nit 1Met-ox	(K)EENMGQYIEYK(D)
1495.601	748.301	499.200	2Nit	(K)EENMGQYIEYK(D)
1511.596	756.298	504.532	2Nit 1Met-ox	(K)EENMGQYIEYK(D)
1813.827	907.414	605.276	1Nit	(K)GIHFQDYDTPFQAK(T)
1942.873	971.937	648.291	1Nit	(K)EENMGQYIEYKDHIK(D)
1958.868	979.934	653.623	1Nit 1Met-ox	(K)EENMGQYIEYKDHIK(D)
1988.866	994.933	663.622	2Nit	(K)EENMGQYIEYKDHIK(D)
2004.861	1002.930	668.954	2Nit 1Met-ox	(K)EENMGQYIEYKDHIK(D)
2042.933	1021.967	681.644	1Nit	(K)GIHFQDYDTPFQAKTQ(-)
2344.134	1172.567	782.045	1Nit	(K)ITTSKGIHFQDYDTPFQAK(T)
2430.12	1215.560	810.707	1Nit	(K)EENMGQYIEYKDHIKDMIK(Y)
2446.115	1223.557	816.038	1Nit 1Met-ox	(K)EENMGQYIEYKDHIKDMIK(Y)
2461.277	1231.139	821.092	1Nit	(K)TLQINLVSVISGTYLGLDYMSK(Q)
2462.109	1231.555	821.370	1Nit 2Met-ox	(K)EENMGQYIEYKDHIKDMIK(Y)
2476.112	1238.556	826.037	2Nit	(K)EENMGQYIEYKDHIKDMIK(Y)
2477.272	1239.136	826.424	1Nit 1Met-ox	(K)TLQINLVSVISGTYLGLDYMSK(Q)
2492.107	1246.554	831.369	2Nit 1Met-ox	(K)EENMGQYIEYKDHIKDMIK(Y)
2507.27	1254.135	836.423	2Nit	(K)TLQINLVSVISGTYLGLDYMSK(Q)
2508.102	1254.551	836.701	2Nit 2Met-ox	(K)EENMGQYIEYKDHIKDMIK(Y)
2523.265	1262.133	841.755	2Nit 1Met-ox	(K)TLQINLVSVISGTYLGLDYMSK(Q)
2573.24	1287.120	858.413	1Nit	(K)ITTSKGIHFQDYDTPFQAKTQ(-)
3018.537	1509.769	1006.846	1Nit	(K)NWEKTLQINLVSVISGTYLGLDYMSK(Q)
3034.532	1517.766	1012.177	1Nit 1Met-ox	(K)NWEKTLQINLVSVISGTYLGLDYMSK(Q)
3064.53	1532.765	1022.177	2Nit	(K)NWEKTLQINLVSVISGTYLGLDYMSK(Q)
3080.525	1540.763	1027.508	2Nit 1Met-ox	(K)NWEKTLQINLVSVISGTYLGLDYMSK(Q)
3162.652	1581.826	1054.884	1Nit	(K)YYGILDPPLIANGTLIEDDALNGAIMK(I)
3178.647	1589.824	1060.216	1Nit 1Met-ox	(K)YYGILDPPLIANGTLIEDDALNGAIMK(I)
3208.645	1604.823	1070.215	2Nit	(K)YYGILDPPLIANGTLIEDDALNGAIMK(I)
3224.64	1612.820	1075.547	2Nit 1Met-ox	(K)YYGILDPPLIANGTLIEDDALNGAIMK(I)
3236.563	1618.781	1079.521	1Nit	(K)QNGGEGGIIINMSSLAGLMPVAQQPVYCASK(H)
3252.558	1626.779	1084.853	1Nit 1Met-ox	(K)QNGGEGGIIINMSSLAGLMPVAQQPVYCASK(H)
3268.553	1634.776	1090.184	1Nit 2Met-ox	(K)QNGGEGGIIINMSSLAGLMPVAQQPVYCASK(H)
3519.69	1760.345	1173.897	1Nit	(R)LNAICPGFVNTAILESIEKEENMGQYIEYK(D)

3535.685	1768.343	1179.228	1Nit 1Met-ox	(R)LNAICPGFVNTAILESIEKEENMGQYIEYK(D)
3565.683	1783.342	1189.228	2Nit	(R)LNAICPGFVNTAILESIEKEENMGQYIEYK(D)
3581.678	1791.339	1194.559	2Nit 1Met-ox	(R)LNAICPGFVNTAILESIEKEENMGQYIEYK(D)
3649.899	1825.449	1217.300	1Nit	(K)DMIKYYGILDPPLIANGLITLIEDDALNGAIMK(I)
3662.961	1833.447	1222.631	1Met-ox	(K)YYGILDPPLIANGLITLIEDDALNGAIMKITT(SK)(G)
3665.894	1841.444	1227.963	1Nit 1Met-ox	(K)DMIKYYGILDPPLIANGLITLIEDDALNGAIMK(I)
3681.889	1846.979	1231.653	1Nit 2Met-ox	(K)DMIKYYGILDPPLIANGLITLIEDDALNGAIMK(I)
3692.959	1848.446	1232.631	1Nit	(K)YYGILDPPLIANGLITLIEDDALNGAIMKITT(SK)(G)
3695.892	1854.977	1236.985	2Nit	(K)DMIKYYGILDPPLIANGLITLIEDDALNGAIMK(I)
3708.954	1856.443	1237.962	1Nit 1Met-ox	(K)YYGILDPPLIANGLITLIEDDALNGAIMKITT(SK)(G)
3711.887	1864.441	1243.294	2Nit 1Met-ox	(K)DMIKYYGILDPPLIANGLITLIEDDALNGAIMK(I)
3727.881	1869.976	1246.984	2Nit 2Met-ox	(K)DMIKYYGILDPPLIANGLITLIEDDALNGAIMK(I)
3738.952	1877.973	1252.316	2Nit	(K)YYGILDPPLIANGLITLIEDDALNGAIMKITT(SK)(G)
3754.947	2006.978	1338.318	2Nit 1Met-ox	(K)YYGILDPPLIANGLITLIEDDALNGAIMKITT(SK)(G)
4012.955	2014.975	1343.650	1Nit	(R)LNAICPGFVNTAILESIEKEENMGQYIEYKDH(K)(D)
4028.95	2029.974	1353.649	1Nit 1Met-ox	(R)LNAICPGFVNTAILESIEKEENMGQYIEYKDH(K)(D)
4058.948	2037.971	1358.981	2Nit	(R)LNAICPGFVNTAILESIEKEENMGQYIEYKDH(K)(D)
4074.943	2052.517	1368.678	2Nit 1Met-ox	(R)LNAICPGFVNTAILESIEKEENMGQYIEYKDH(K)(D)
4104.034	2060.515	1374.010	1Nit	(K)QNGGEGGIIINMSSLAGLMPVAQQPVY(C)ASKHGIVGFTR(S)
4120.029	2068.512	1379.341	1Nit 1Met-ox	(K)QNGGEGGIIINMSSLAGLMPVAQQPVY(C)ASKHGIVGFTR(S)
4136.024	2072.082	1381.721	1Nit 2Met-ox	(K)QNGGEGGIIINMSSLAGLMPVAQQPVY(C)ASKHGIVGFTR(S)
4143.164	2080.079	1387.053	1Nit	(K)DH(K)DMIKYYGILDPPLIANGLITLIEDDALNGAIMK(I)
4159.159	2088.077	1392.384	1Nit 1Met-ox	(K)DH(K)DMIKYYGILDPPLIANGLITLIEDDALNGAIMK(I)
4175.153	2090.603	1394.068	1Nit 2Met-ox	(K)DH(K)DMIKYYGILDPPLIANGLITLIEDDALNGAIMK(I)
4180.205	2095.078	1397.052	1Nit	(K)DMIKYYGILDPPLIANGLITLIEDDALNGAIMKITT(SK)(G)
4189.157	2098.600	1399.400	2Nit	(K)DH(K)DMIKYYGILDPPLIANGLITLIEDDALNGAIMK(I)
4196.2	2103.076	1402.384	1Nit 1Met-ox	(K)DMIKYYGILDPPLIANGLITLIEDDALNGAIMKITT(SK)(G)
4205.151	2106.597	1404.732	2Nit 1Met-ox	(K)DH(K)DMIKYYGILDPPLIANGLITLIEDDALNGAIMK(I)
4212.195	2111.073	1407.715	1Nit 2Met-ox	(K)DMIKYYGILDPPLIANGLITLIEDDALNGAIMKITT(SK)(G)
4221.146	2113.599	1409.399	2Nit 2Met-ox	(K)DH(K)DMIKYYGILDPPLIANGLITLIEDDALNGAIMK(I)
4226.198	2121.596	1414.731	2Nit	(K)DMIKYYGILDPPLIANGLITLIEDDALNGAIMKITT(SK)(G)
4242.193	2129.594	1420.063	2Nit 1Met-ox	(K)DMIKYYGILDPPLIANGLITLIEDDALNGAIMKITT(SK)(G)
4258.188	2256.661	1504.774	2Nit 2Met-ox	(K)DMIKYYGILDPPLIANGLITLIEDDALNGAIMKITT(SK)(G)
4512.321	2264.658	1510.105	1Nit	(R)LDILVNNAGVNN(E)KNWEK(TL)QINLVSVISGTYLGLDYMSK(Q)
4528.316	2279.657	1520.105	1Nit 1Met-ox	(R)LDILVNNAGVNN(E)KNWEK(TL)QINLVSVISGTYLGLDYMSK(Q)
4558.314	2287.654	1525.436	2Nit	(R)LDILVNNAGVNN(E)KNWEK(TL)QINLVSVISGTYLGLDYMSK(Q)
4574.309	2438.194	1625.796	2Nit 1Met-ox	(R)LDILVNNAGVNN(E)KNWEK(TL)QINLVSVISGTYLGLDYMSK(Q)
4875.388	2446.192	1631.127	1Nit	(R)SAALANLMNSGVR(L)NAICPGFVNTAILESIEKEENMGQYIEYK(D)
4891.383	2454.189	1636.459	1Nit 1Met-ox	(R)SAALANLMNSGVR(L)NAICPGFVNTAILESIEKEENMGQYIEYK(D)
4907.378	2461.191	1641.127	1Nit 2Met-ox	(R)SAALANLMNSGVR(L)NAICPGFVNTAILESIEKEENMGQYIEYK(D)

4921.381	2469.188	1646.458	2Nit	(R)SAALAANLMNSGVRLNAICPGFVNTAILESIEKEENMGQYIEYK(D)
4937.376	725.304	483.869	2Nit 1Met-ox	(R)SAALAANLMNSGVRLNAICPGFVNTAILESIEKEENMGQYIEYK(D)
4953.371	733.302	489.201	2Nit 2Met-ox	(R)SAALAANLMNSGVRLNAICPGFVNTAILESIEKEENMGQYIEYK(D)
5441.775	748.301	499.200	1Nit	(K)YYGILDPPLIANGLITLIEDDALNGAIMKITTSGIHFQDYDTPPFQAK(T)
5457.769	756.298	504.532	1Nit 1Met-ox	(K)YYGILDPPLIANGLITLIEDDALNGAIMKITTSGIHFQDYDTPPFQAK(T)
5459.732	907.414	605.276	1Nit	(K)QNGGEGGIIINMSSLAGLMPVAQQPVY CASHGIVGFTRSAALAANLMN SGVR(L)
5475.727	971.937	648.291	1Nit 1Met-ox	(K)QNGGEGGIIINMSSLAGLMPVAQQPVY CASHGIVGFTRSAALAANLMN SGVR(L)
5487.767	979.934	653.623	2Nit	(K)YYGILDPPLIANGLITLIEDDALNGAIMKITTSGIHFQDYDTPPFQAK(T)
5491.722	994.933	663.622	1Nit 2Met-ox	(K)QNGGEGGIIINMSSLAGLMPVAQQPVY CASHGIVGFTRSAALAANLMN SGVR(L)
5503.762	1002.930	668.954	2Nit 1Met-ox	(K)YYGILDPPLIANGLITLIEDDALNGAIMKITTSGIHFQDYDTPPFQAK(T)
5507.717	1021.967	681.644	1Nit 3Met-ox	(K)QNGGEGGIIINMSSLAGLMPVAQQPVY CASHGIVGFTRSAALAANLMN SGVR(L)
5533.76	1172.567	782.045	3Nit	(K)YYGILDPPLIANGLITLIEDDALNGAIMKITTSGIHFQDYDTPPFQAK(T)
5549.755	1215.560	810.707	3Nit 1Met-ox	(K)YYGILDPPLIANGLITLIEDDALNGAIMKITTSGIHFQDYDTPPFQAK(T)
5632.829	1223.557	816.038	1Nit	(K)TLQINLVSVISGYTLGLDYMSKQNGGEGGIIINMSSLAGLMPVAQQPVY C ASK(H)
5648.824	1231.139	821.092	1Nit 1Met-ox	(K)TLQINLVSVISGYTLGLDYMSKQNGGEGGIIINMSSLAGLMPVAQQPVY C ASK(H)
5664.819	1231.555	821.370	1Nit 2Met-ox	(K)TLQINLVSVISGYTLGLDYMSKQNGGEGGIIINMSSLAGLMPVAQQPVY C ASK(H)
5678.822	1238.556	826.037	2Nit	(K)TLQINLVSVISGYTLGLDYMSKQNGGEGGIIINMSSLAGLMPVAQQPVY C ASK(H)
5680.814	1239.136	826.424	1Nit 3Met-ox	(K)TLQINLVSVISGYTLGLDYMSKQNGGEGGIIINMSSLAGLMPVAQQPVY C ASK(H)
5694.817	1246.554	831.369	2Nit 1Met-ox	(K)TLQINLVSVISGYTLGLDYMSKQNGGEGGIIINMSSLAGLMPVAQQPVY C ASK(H)
5710.812	1254.135	836.423	2Nit 2Met-ox	(K)TLQINLVSVISGYTLGLDYMSKQNGGEGGIIINMSSLAGLMPVAQQPVY C ASK(H)
5724.815	1254.551	836.701	3Nit	(K)TLQINLVSVISGYTLGLDYMSKQNGGEGGIIINMSSLAGLMPVAQQPVY C ASK(H)
5726.807	1262.133	841.755	2Nit 3Met-ox	(K)TLQINLVSVISGYTLGLDYMSKQNGGEGGIIINMSSLAGLMPVAQQPVY C ASK(H)
5740.81	1287.120	858.413	3Nit 1Met-ox	(K)TLQINLVSVISGYTLGLDYMSKQNGGEGGIIINMSSLAGLMPVAQQPVY C ASK(H)
5756.805	1509.769	1006.846	3Nit 2Met-ox	(K)TLQINLVSVISGYTLGLDYMSKQNGGEGGIIINMSSLAGLMPVAQQPVY C ASK(H)
5772.8	1517.766	1012.177	3Nit 3Met-ox	(K)TLQINLVSVISGYTLGLDYMSKQNGGEGGIIINMSSLAGLMPVAQQPVY C ASK(H)

6190.089	1532.765	1022.177	1Nit	ASK(H) (K)NWEKTLQINLVSVISGTYLGLDYMSKQNGGEGGIIINMSSLAGLMPVAQ QPVYCASK(H)
6206.084	1540.763	1027.508	1Nit 1Met-ox	(K)NWEKTLQINLVSVISGTYLGLDYMSKQNGGEGGIIINMSSLAGLMPVAQ QPVYCASK(H)
6222.079	1581.826	1054.884	1Nit 2Met-ox	(K)NWEKTLQINLVSVISGTYLGLDYMSKQNGGEGGIIINMSSLAGLMPVAQ QPVYCASK(H)
6236.082	1589.824	1060.216	2Nit	(K)NWEKTLQINLVSVISGTYLGLDYMSKQNGGEGGIIINMSSLAGLMPVAQ QPVYCASK(H)
6238.074	1604.823	1070.215	1Nit 3Met-ox	(K)NWEKTLQINLVSVISGTYLGLDYMSKQNGGEGGIIINMSSLAGLMPVAQ QPVYCASK(H)
6252.077	1612.820	1075.547	2Nit 1Met-ox	(K)NWEKTLQINLVSVISGTYLGLDYMSKQNGGEGGIIINMSSLAGLMPVAQ QPVYCASK(H)
6268.072	1618.781	1079.521	2Nit 2Met-ox	(K)NWEKTLQINLVSVISGTYLGLDYMSKQNGGEGGIIINMSSLAGLMPVAQ QPVYCASK(H)
6282.075	1626.779	1084.853	3Nit	(K)NWEKTLQINLVSVISGTYLGLDYMSKQNGGEGGIIINMSSLAGLMPVAQ QPVYCASK(H)
6284.066	1634.776	1090.184	2Nit 3Met-ox	(K)NWEKTLQINLVSVISGTYLGLDYMSKQNGGEGGIIINMSSLAGLMPVAQ QPVYCASK(H)
6298.07	1760.345	1173.897	3Nit 1Met-ox	(K)NWEKTLQINLVSVISGTYLGLDYMSKQNGGEGGIIINMSSLAGLMPVAQ QPVYCASK(H)
6314.064	1768.343	1179.228	3Nit 2Met-ox	(K)NWEKTLQINLVSVISGTYLGLDYMSKQNGGEGGIIINMSSLAGLMPVAQ QPVYCASK(H)
6330.059	1783.342	1189.228	3Nit 3Met-ox	(K)NWEKTLQINLVSVISGTYLGLDYMSKQNGGEGGIIINMSSLAGLMPVAQ QPVYCASK(H)
6500.301	1791.339	1194.559	1Nit	(K)TLQINLVSVISGTYLGLDYMSKQNGGEGGIIINMSSLAGLMPVAQQPVYC ASKHGIVGFTR(S)
6516.295	1825.449	1217.300	1Nit 1Met-ox	(K)TLQINLVSVISGTYLGLDYMSKQNGGEGGIIINMSSLAGLMPVAQQPVYC ASKHGIVGFTR(S)
6532.29	1833.447	1222.631	1Nit 2Met-ox	(K)TLQINLVSVISGTYLGLDYMSKQNGGEGGIIINMSSLAGLMPVAQQPVYC ASKHGIVGFTR(S)
6546.293	1841.444	1227.963	2Nit	(K)TLQINLVSVISGTYLGLDYMSKQNGGEGGIIINMSSLAGLMPVAQQPVYC ASKHGIVGFTR(S)
6548.285	1846.979	1231.653	1Nit 3Met-ox	(K)TLQINLVSVISGTYLGLDYMSKQNGGEGGIIINMSSLAGLMPVAQQPVYC ASKHGIVGFTR(S)
6562.288	1848.446	1232.631	2Nit 1Met-ox	(K)TLQINLVSVISGTYLGLDYMSKQNGGEGGIIINMSSLAGLMPVAQQPVYC ASKHGIVGFTR(S)
6578.283	1854.977	1236.985	2Nit 2Met-ox	(K)TLQINLVSVISGTYLGLDYMSKQNGGEGGIIINMSSLAGLMPVAQQPVYC ASKHGIVGFTR(S)
6592.286	1856.443	1237.962	3Nit	(K)TLQINLVSVISGTYLGLDYMSKQNGGEGGIIINMSSLAGLMPVAQQPVYC

6594.278	1864.441	1243.294	2Nit 3Met-ox	ASKHGIVGFTR(S) (K)TLQINLVSVISGTYLGLDYMSKQNGGEGGIIINMSSLAGLMPVAQQPVYC
6608.281	1869.976	1246.984	3Nit 1Met-ox	ASKHGIVGFTR(S) (K)TLQINLVSVISGTYLGLDYMSKQNGGEGGIIINMSSLAGLMPVAQQPVYC
6624.276	1877.973	1252.316	3Nit 2Met-ox	ASKHGIVGFTR(S) (K)TLQINLVSVISGTYLGLDYMSKQNGGEGGIIINMSSLAGLMPVAQQPVYC
6640.271	2006.978	1338.318	3Nit 3Met-ox	ASKHGIVGFTR(S) (K)TLQINLVSVISGTYLGLDYMSKQNGGEGGIIINMSSLAGLMPVAQQPVYC

* The mass/charge ratio (m/z) of the peptide sequences were calculated based on the formula: $m/z = (M + nH^+)/n$.

Where, M = the molecular mass of the peptide sequence; n = the integer number of charges on the ions; H = the mass of a proton = 1.008 Da.

Appendix – 2

THE JOURNAL OF IMMUNOLOGY
ASSOCIATION OF IMMUNOLOGISTS
FOUNDED 1913

Editor-in-Chief
Jeremy M. Boss, Ph.D.

September 23, 2010

Executive Director
and Executive Editor
M. Michele Hogan, Ph.D.

Yokananth Sekar
University of Alberta
567, HMRC, University of Alberta,
Edmonton
Canada
Phone: 7804925014
Fax: 7804925329
Email: yokananth@ualberta.ca

Publication Director
Kaylene J. Kenyon, Ph.D.

Chair, Publications
Committee
Paul E. Love, M.D., Ph.D.

Dear Dr. Sekar:

The American Association of Immunologists, Inc., grants permission to reproduce the article "Protein Tyrosine Nitration of Aldolase in Mast Cells: A Plausible Pathway in Nitric Oxide-Mediated Regulation of Mast Cell Function," found in *The Journal of Immunology*, vol. 185, pp. 578-587, 2010, in your thesis, contingent on the following conditions:

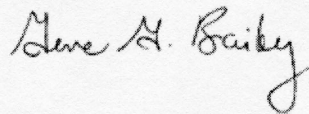
1. That you give proper credit to the authors and to *The Journal of Immunology*, including in your citation the volume, date, and page numbers.
2. That you include the statement:

Copyright 2010. The American Association of Immunologists, Inc.

3. That permission is granted for one-time use only for print and electronic format. Permission must be requested separately for future editions, revisions, translations, derivative works, and promotional pieces.

Thank you for your interest in *The Journal of Immunology*.

Sincerely,



Gene G. Bailey
Senior Editorial Manager
The Journal of Immunology

THE AMERICAN ASSOCIATION OF IMMUNOLOGISTS

9650 Rockville Pike, Bethesda, MD 20814-3994 | Phone 301.634.7197 | Fax 301.634.7829 | info@aaai.org | www.jimmunol.org

The Journal of Immunology

This information is current as of October 4, 2010

Protein Tyrosine Nitration of Aldolase in Mast Cells: A Plausible Pathway in Nitric Oxide-Mediated Regulation of Mast Cell Function

Yokananth Sekar, Tae Chul Moon, Carolyn M. Slupsky and A. Dean Befus

J. Immunol. 2010;185:578-587; originally published online May 28, 2010;
doi:10.4049/jimmunol.0902720
<http://www.jimmunol.org/cgi/content/full/185/1/578>

Supplementary Data <http://www.jimmunol.org/cgi/content/full/jimmunol.0902720/D1>

References This article **cites 89 articles**, 23 of which can be accessed free at: <http://www.jimmunol.org/cgi/content/full/185/1/578#BIBL>

Subscriptions Information about subscribing to *The Journal of Immunology* is online at <http://www.jimmunol.org/subscriptions/>

Permissions Submit copyright permission requests at <http://www.aai.org/ji/copyright.html>

Email Alerts Receive free email alerts when new articles cite this article. Sign up at <http://www.jimmunol.org/subscriptions/etoc.shtml>

Protein Tyrosine Nitration of Aldolase in Mast Cells: A Plausible Pathway in Nitric Oxide-Mediated Regulation of Mast Cell Function

Yokananth Sekar,* Tae Chul Moon,* Carolyn M. Slusky,[†] and A. Dean Befus^{*,†}

NO is a short-lived free radical that plays a critical role in the regulation of cellular signaling. Mast cell (MC)-derived NO and exogenous NO regulate MC activities, including the inhibition of MC degranulation. At a molecular level, NO acts to modify protein structure and function through several mechanisms, including protein tyrosine nitration. To begin to elucidate the molecular mechanisms underlying the effects of NO in MCs, we investigated protein tyrosine nitration in human MC lines HMC-1 and LAD2 treated with the NO donor S-nitrosoglutathione. Using two-dimensional gel Western blot analysis with an anti-nitrotyrosine Ab, together with mass spectrometry, we identified aldolase A, an enzyme of the glycolytic pathway, as a target for tyrosine nitration in MCs. The nitration of aldolase A was associated with a reduction in the maximum velocity of aldolase in HMC-1 and LAD2. Nuclear magnetic resonance analysis showed that despite these changes in the activity of a critical enzyme in glycolysis, there was no significant change in total cellular ATP content, although the AMP/ATP ratio was altered. Elevated levels of lactate and pyruvate suggested that S-nitrosoglutathione treatment enhanced glycolysis. Reduced aldolase activity was associated with increased intracellular levels of its substrate, fructose 1,6-bisphosphate. Interestingly, fructose 1,6-bisphosphate inhibited IgE-mediated MC degranulation in LAD2 cells. Thus, for the first time we report evidence of protein tyrosine nitration in human MC lines and identify aldolase A as a prominent target. This posttranslational nitration of aldolase A may be an important pathway that regulates MC phenotype and function. *The Journal of Immunology*, 2010, 185: 578–587.

Mast cells (MCs) are critical effector cells of IgE-mediated allergic inflammation and are increasingly recognized for their roles in innate and adaptive immune responses (1–3). Reactive oxygen species and reactive nitrogen species are important in the regulation of MC secretion and in inflammatory conditions (4). Several studies demonstrated that MCs express NO synthases and can produce small amounts of NO (5–11). Moreover, NO from other sources, such as macrophages, can regulate MC activities (12). Endogenous and exogenous NO can inhibit MC degranulation; protease release; adherence to fibronectin; and leukotriene, cytokine, and chemokine production (4, 7). By contrast, NO can also upregulate MC properties, such as CD8 expression (13), cytotoxicity (14), and cyclooxygenase-2 expression (15). However,

the mechanisms underlying the effects of NO on MCs are poorly understood.

At a molecular level, NO acts to modify protein structure and function through several mechanisms, including nitration of tyrosine and nitrosylation of cysteine residues and heme and thiol groups (16, 17). Tyrosine nitration is a marker of reactive nitrogen species and has been used as a biomarker in inflamed tissues. Protein tyrosine nitration can modify cellular signaling pathways, and nitration may be a pathogenic component in disease (18, 19). Protein conformational changes due to tyrosine nitration can generate novel antigenic epitopes, alter enzymatic activity, modulate metabolic pathways, and inhibit tyrosine phosphorylation by kinases (20). The targets for protein tyrosine nitration are diverse, and multiple functions can be affected by nitration of selected tyrosine residues on a protein (21, 22).

There are no reports of protein tyrosine nitration in MCs, although Ag/Ab-mediated activation of lung MCs from guinea pig induced peroxynitrite production, an important mediator of tyrosine nitration and, in turn, modulated the release of inflammatory mediators from MCs (23). Given the vast number of potential protein targets for this posttranslational modification by NO, we investigated protein tyrosine nitration in MCs using a proteomic approach. We identified that aldolase A, a critical enzyme in glycolysis, is one target for tyrosine nitration in human MC lines HMC-1 and LAD2. Nitration of aldolase inhibits its enzymatic activity and is associated with elevated levels of its substrate, fructose 1,6 bisphosphate (FBP), which can inhibit MC activation. Thus, the posttranslational tyrosine nitration of aldolase may be one of the mechanisms involved in NO-mediated regulation of MC function.

Materials and Methods

MC culture

HMC-1, an immature human MC line derived from a patient with MC leukemia (a gift from J.H. Butterfield, Rochester, MN) was cultured in Iscove's medium with 5% heat-inactivated FBS, 2 mM L-glutamine, and 40 U/ml

*Pulmonary Research Group and [†]Magnetic Resonance Diagnostic Center, Department of Medicine, University of Alberta, Edmonton, Alberta, Canada

Received for publication August 19, 2009. Accepted for publication April 18, 2010.

This work was supported by Canadian Institutes of Health Research Grant MT-7034 (to A.D.B.). Y.S. was funded by The Lung Association Alberta and North West Territory and by a 75th Anniversary Graduate Student award from the Faculty of Medicine and Dentistry, University of Alberta. T.C.M. is a recipient of fellowships from the Korea Research Foundation (KRF-2005-214-C00111), the Alberta Heritage Foundation for Medical Research, and the Canadian Institute of Health Research/Canadian Lung Association/GlaxoSmithKline.

Address correspondence and reprint requests to Dr. A. Dean Befus, Department of Medicine, Room 550A, Heritage Medical Research Centre, University of Alberta, Edmonton, Alberta T6G 2S2, Canada. E-mail address: dean.befus@ualberta.ca

The online version of this article contains supplemental material.

Abbreviations used in this paper: 2-DE, two-dimensional electrophoresis; Aldo, anti-aldolase Ab; β -hex, β -hexosaminidase; CBMC, cord blood derived-mast cell; DAP, dihydroxyacetone phosphate; F1P, fructose-1-phosphate; F6P, fructose-6-phosphate; FBP, fructose 1,6-bisphosphate; IPG, immobilized pH gradient; IP₃, inositol 1,4,5-triphosphate; K_m , Michaelis–Menten constant; MC, mast cell; MS, mass spectrometry; MS/MS, tandem mass spectrometry; NMR, nuclear magnetic resonance; NT, anti-nitrotyrosine Ab; pI, isoelectric point; PLC, phospholipase C; PVDF, polyvinylidene difluoride; SNOG, S-nitrosoglutathione; V_{max} , maximum velocity.

Copyright © 2010 by The American Association of Immunologists, Inc. 0022-1767/10/\$16.00

penicillin/streptomycin (all from Invitrogen, Burlington, Ontario, Canada). The cells were harvested at ~75% confluency (48 h) and were used if the passage number was <20. The seeding concentration between each passage was 1×10^5 cells/ml. LAD2, the growth factor-dependent human MC line (generously provided by Dr. A.S. Kirshenbaum and D.D. Metcalfe, National Institutes of Health, Bethesda, MD) (24), was cultured in Stem-Pro-34 medium (Invitrogen) supplemented with 100 ng/ml recombinant human stem cell factor (PeproTech, Rocky Hill, NJ). LAD2 were cultured by hemidepletion of medium every 7 d and maintained at a cell concentration $<5 \times 10^5$ cells/ml. LAD2 cells are used as an alternative to primary human MCs because they express IgERs and can be activated by IgE cross-linking (24).

Human cord blood-derived MCs (CBMCs) were cultured as described previously (25, 26). Briefly, placentae were obtained within 45 min of delivery in adherence with ethics approval from the University of Alberta and Capital Health Region and with informed patient consent at Royal Alexandra Hospital, Edmonton, Alberta, Canada. EDTA-treated umbilical cord blood was diluted with the same volume of 10 mM phosphate buffer (pH 7.4) containing 150 mM NaCl and layered over Histopaque-1077 (Sigma-Aldrich, Oakville, Ontario, Canada) at room temperature within 4 h of collection. The CBMC progenitor fraction was obtained by centrifugation at $1000 \times g$ for 20 min at room temperature. The cells were washed twice with PBS and grown in tissue-culture flasks in AIM-V medium (Invitrogen) with 100 ng/ml recombinant human stem cell factor. Nonadherent cells were transferred to fresh culture flasks and grown for ≥ 8 wk. CD117 and IgER expression were confirmed by flow cytometry. All cells were maintained at 37°C in a humidified incubator at 5% CO₂.

Treatment of MCs with NO donor

We chose an NO donor S-nitrosoglutathione (SNOG) (Calbiochem, San Diego, CA), whose decomposition rate is ~5% per hour in water at room temperature, and the half-life is ~80 h at 37°C (27). SNOG is a well-known NO donor that favors a cGMP-independent mechanism of action of NO in different systems (28), and 500 μ M SNOG has been widely used in different studies on MCs and inhibits MC function (6, 29–31). Moreover, SNOG has been used at up to 2 mM for 4 h to induce nitration in MCF-7 cells (32). Hence, our use of 500 μ M SNOG over 4 h was designed to be consistent with physiological release of NO under some *in vivo* conditions. For the sham control, cells were treated with equivalent volumes of the vehicle (dH₂O) in the culture media (v/v ratio of 1/40 of vehicle/media). The viability of the cells was documented before and after treatment with SNOG using trypan blue dye exclusion; the viability in all experiments was >95%.

Two-dimensional gel electrophoresis

MCs were centrifuged at $300 \times g$ for 5 min at 4°C and washed three times with ice-cold PBS. Cell pellets were stored at -80°C until further use. The cell pellet was lysed by vortexing at high speed for 2 min in two-dimensional electrophoresis (2-DE) cell lysis buffer (9 M urea, 4% CHAPS, 50 mM DTT, 0.5% immobilized pH gradient [IPG] 3–10 ampholytes [Bio-Rad, Mississauga, Ontario, Canada], 10 μ l Protease Arrest kit from Genotech [St. Louis, MO]) and incubated on ice for 60 min for protein denaturation and solubilization. Cell lysates were collected and stored at -80°C in 100- μ l aliquots after centrifuging the homogenate at $17,530 \times g$ for 20 min at 4°C. Protein concentration was determined using the Bradford reducing agent compatible/detergent compatible protocol. The 2D cleanup kit (Bio-Rad) was used according to the manufacturer's instructions. The protein pellets were reconstituted in 2-DE rehydration buffer (8 M urea, 1.5% CHAPS, 0.2% DTT, 0.2% IPG 3–10 ampholytes), with a final concentration of 75 μ g protein in 125 μ l rehydration buffer, and loaded onto 7-cm isoelectric point (pI) 3–10 linear IPG strips (Bio-Rad). Isoelectric focusing (50 V 10 min, 250 V 30 min, 750 V 60 min, 8000 V 13000 Vh) was performed, and the strips were equilibrated for 10 min with equilibration buffer A (1% DTT, 6 M urea, 30% glycerol, 2% SDS, 50 mM Tris-HCl [pH 8.8], 0.0002% bromophenol blue), followed by 10 min with equilibration buffer B (2.5% iodoacetamide, 6 M urea, 30% glycerol, 2% SDS, 50 mM Tris-HCl [pH 8.8], 0.0002% bromophenol blue). Strips were loaded in Ready Gel Tris-HCl 10% gel (IPG) (Bio-Rad) and sealed with PROTEAN Plus overlay agarose (Bio-Rad). The proteins were separated at 130 V. Gels were stained with a PlusOne silver staining kit (GE Healthcare, Piscataway, NJ), and images were captured using Alphaimager 2200 (Alpha Innotech, San Leandro, CA).

Western blot

Proteins were transferred to polyvinylidene difluoride (PVDF) membranes Immobilon-P with pore size 0.45 μ m (Millipore, Bedford, MA), using the Transblot SD semidry transfer system (Bio-Rad) at 15 V for 90 min.

Membranes were blocked for 60 min at room temperature with 5% nonfat milk (Bio-Rad) in Tris-buffered saline (pH 7.4) containing 0.05% Tween-20 for anti-nitrotyrosine Ab and with 5% BSA (Sigma-Aldrich) for anti-aldolase Ab. Rabbit polyclonal anti-nitrotyrosine Ab was purchased from Upstate (Millipore, Etobicoke, Ontario, Canada); goat polyclonal anti-rabbit muscle aldolase Ab was purchased from Chemicon (Billerica, MA), and secondary Abs were purchased from Jackson ImmunoResearch Laboratories (West Grove, PA). Rabbit IgG (Jackson ImmunoResearch Laboratories) and goat IgG (Chemicon) were used as isotype controls. Nitrotyrosine⁺ controls were purchased from Millipore. Membranes were incubated overnight with primary Abs (1:1,000 dilution) and with HRP-conjugated secondary Abs (1:10,000 dilution) and were visualized using ECL (Amersham Biosciences, Piscataway, NJ). Images were captured with high-performance chemiluminescence Hyperfilm (GE Healthcare).

Dithionite reduction

The specificity of anti-nitrotyrosine Ab was demonstrated by treating the PVDF membranes after transferring the protein with 100 mM sodium dithionite (Sigma-Aldrich) in 50 mM sodium borate buffer (pH 9) for 2 h at room temperature. Dithionite treatment reduces the nitro group into an amino group, thereby preventing the Ab from binding with the nitrated epitope. After dithionite treatment, membranes were washed three times with distilled water (5 min each wash), followed by blocking with Odyssey blocking buffer (LI-COR Biosciences, Lincoln, NE). Secondary Abs were goat anti-rabbit 800 (1:10,000) and goat anti-mouse 680 (1:10,000); both from LI-COR Biosciences). Blots were visualized with an Odyssey imager (LI-COR Biosciences) by scanning simultaneously at 700 and 800 nm. Odyssey software was used for molecular mass determination and quantitation of Western blots.

Aldolase enrichment

An immunoaffinity column was constructed by coupling cyanogen bromide-activated Sepharose 4B with polyclonal goat anti-aldolase Ab using standard protocols (33). HMC-1 and LAD2 cell lysates were passed through this column and washed extensively with wash buffer. The bound proteins were eluted using low-pH elution (glycine 2.5 pH). The eluted fractions containing enriched MC aldolase were neutralized with 2 M Tris buffer (pH 11.2), and the fractions were concentrated using Centricon centrifugal filter 10K devices (Millipore). The concentrated fractions were separated in a 10% SDS-PAGE gel and transferred to PVDF membrane for Western blot analysis.

Mass spectrometry

In-gel tryptic digestion, peptide extraction, and mass spectrometry (MS) analysis were performed using standard protocols at the Mass Spectrometry Facility, Department of Chemistry, University of Alberta. Briefly, proteins in the gel were reduced with 5 mM DTT and carbamidomethylated with 10 mM iodoacetamide, followed by tryptic digestion overnight with 0.06 μ g/ μ l modified bovine trypsin (Promega, Madison, WI) at 30°C. Five microliters of the resultant peptide digests was loaded onto a nanoAcquity UPLC system with peptide trap (180 μ m \times 20 mm, Symmetry C18 nanoAcquity column,) and a nano analytical column (75 μ m \times 100 mm, Atlantis dC18 nanoAcquity column, both from Waters, Milford, MA). Desalting on the peptide trap was achieved by flushing it with 1% acetonitrile, 0.1% formic acid at a flow rate of 10 μ l/min for 3 min. Peptides were separated with a gradient of 2–95% solvent B (acetonitrile, 0.1% formic acid) over 35 min at a flow rate of 300 nl/min. The column was connected to a q-ToF premier (Waters) for electrospray ionization-tandem mass spectrometry (MS/MS) analysis. Obtained MS/MS data were analyzed through proteomic software PEAKS (Bioinformatics Solutions, Waterloo, Ontario, Canada). Database searches were done with the following settings: carbamidomethylation as fixed modification, and oxidation as the variable modification. Peptide identifications were further confirmed by examination of the scores and manual inspection of the original MS/MS spectra. Good spectra with significant numbers of matched high-intensity peaks were considered important for the identification.

RT-PCR

Total RNA was extracted with an RNeasy Plus mini kit (Qiagen, Mississauga, Ontario, Canada), according to the manufacturer's instructions, quantified by measuring OD at 260 nm, and assessed by applying to 1.2% formaldehyde-agarose gels. cDNA was synthesized using the SuperScript First-Strand Synthesis System for RT-PCR (Invitrogen). Five micrograms of total RNA from each sample was used as a template for the reverse transcription reaction. The RNA/primer mixture (5 μ g total RNA, 0.5 μ g oligonucleotide_{12–18} primers, and 0.5 mM 2'-deoxynucleoside 5'-triphosphate mixture in RNase-free water) was incubated for 5 min at 65°C and then on ice for 1 min.

The reaction mixture (40 U RNase inhibitor in 20 mM Tris-HCl [pH 8.4], 50 mM KCl, 5 mM MgCl₂, 10 mM DTT) was added and incubated at 42°C for 2 min. Then, 50 U SuperScript II reverse transcriptase was added, and the reaction was continued for 50 min at 42°C, 15 min at 70°C, and chilled to 4°C on ice. Before proceeding to PCR, 2 U RNase H was added and incubated for 20 min at 37°C. Twenty microliters cDNA was diluted to 100 µl for use in PCR amplification. Ten microliters cDNA was used for PCR with recombinant Taq DNA Polymerase (Invitrogen). Human kidney cDNA was a kind gift from Dr. Philip F. Halloran, Division of Nephrology, University of Alberta. PCR was carried out with iCycler (Bio-Rad). Isoform-specific primers were designed based on the published human aldolase sequences: aldolase A sense 5'-AGCACCATGCCCTACCAATA-3', antisense 5'-ACGACACCACACCACTGT-3'; human aldolase B sense 5'-GATCGTGGTG-GGAATCAAGT-3', antisense 5'-CGCTTCATAAAAGCCTCTG-3'; human aldolase C sense 5'-AGCGTACCCCTCTGCACTT-3', antisense 5'-CACGCCCATAGGAGAAGGTA-3'; and human β-actin sense 5'-GGCATCC-TCACCTGAAGTA-3', antisense 5'-AGGGCATAACCCTCGTAGAT-3'. The conditions for PCR amplification were denaturing at 95°C for 30 s, annealing at 55°C for 30 s, and extension at 72°C for 1 min, 25 cycles. The PCR products were analyzed by 1% agarose gel electrophoresis with ethidium bromide staining and confirmed by automated sequencing using a CEQ2000XL DNA sequencer (Beckman Coulter, Mississauga, Ontario, Canada) at the Biochemistry Department, University of Alberta.

Aldolase enzyme assay

HMC-1 and LAD2 (2×10^6 cells) were treated with 50 µl water (sham) or 500 µM SNOG in 2 ml media for 4 h, and the cell pellets in 1 ml Tris buffer (pH 7.4) containing protease inhibitors were rapidly frozen in liquid N₂. The frozen cell lysate was subjected to ultrasound treatment for 5 min in an ultrasonic bath (FS 30H, Fisher Scientific, Ottawa, Ontario, Canada). Three cycles of freeze–thawing were performed, followed by centrifugation at $17,530 \times g$ for 15 min at 4°C. The supernatant of cell lysate was stored on ice. The hydrazine assay (34, 35) was used to measure total aldolase activity in 100 µl cell lysate using FBP as substrate and hydrazine sulfate as detection reagent for the 3-phosphoglyceraldehyde produced by the reaction. One enzyme unit is described as a change in absorbance of 1.00/min at 25°C (pH 7.5) and 240 nm wavelength. To calculate the maximum velocity (V_{max}) and the Michaelis–Menten constant (K_m), the enzymatic activity was measured using a range of substrate (FBP) concentrations (3.125–800 µM). K_m and V_{max} values from aldolase activity, in terms of change in OD values ($\Delta A_{240}/2 \times 10^5$ cells/min), were calculated using the Michaelis–Menten equation in a nonlinear fitting (solver function in Microsoft Excel, Microsoft, Redmond, WA).

FBP measurement

HMC-1 and LAD2 cells (1×10^7) were sham treated or treated with 500 µM SNOG for 4 h. The cells were washed with PBS, and the cell pellet was deproteinized using 100 µl 5% trichloroacetic acid for 15 min on ice and then neutralized with 12 µl 2 M Tris (pH 11.2). The cell extracts were centrifuged at $17,530 \times g$ for 20 min, and the supernatants containing the metabolite pools were analyzed for their FBP content. The standard protocol for measuring FBP (34, 36) was used with minor modifications. Briefly, the sample was incubated with aldolase (rabbit muscle aldolase, Sigma-Aldrich), the enzyme that cleaves FBP into dihydroxyacetone phosphate (DAP) and *d*-glyceraldehyde 3-phosphate. DAP and *d*-glyceraldehyde 3-phosphate are interconverted by the enzyme triose-phosphate isomerase. Glycerol-3-phosphate dehydrogenase catalyzes the reduction of DAP by NADH. The kinetic measurement of depletion of NADH at 340 nm was measured for 5 min in a 48-well plate (Corning, Lowell, MA) containing 170 µl 400 mM triethanolamine buffer (pH 7.6), 100 µl FBP standards, 10 µl 4.2 mM β-NADH, 10 µl glycerol-3-phosphate dehydrogenase, and triose-phosphate isomerase to give the initial reading. Then, 10 µl rabbit muscle aldolase was added to the reaction mixture, followed by measurement at 340 nm every minute for 5 min. Rabbit muscle aldolase and FBP (Sigma-Aldrich) were used to obtain a standard curve, and the OD values were calibrated with this curve to quantitate the FBP levels in the HMC-1 and LAD2 cell lysate.

MC degranulation assay

LAD2 cells (1×10^6) were seeded in a six-well plate and sensitized with 1 µg/ml human IgE (Chemicon) overnight at 37°C. Cells were pretreated for 4 h with 500 µM SNOG, 5 mM FBP, 5 mM fructose-1-phosphate (F1P), or 5 mM fructose-6-phosphate (F6P). Cells were washed and resuspended in HEPES-buffered Tyrode's solution (pH 7.2), followed by stimulation with 10 µg/ml mouse anti-human IgE Ab (Dako, Mississauga, Ontario, Canada) for 30 min at 37°C. The cells were centrifuged, and the percentage of β-hexosaminidase (β-hex) released into the supernatant was calculated, as described previously (37).

Nuclear magnetic resonance analysis

HMC-1 cells (1×10^8) were treated with sham or 500 µM SNOG for 4 h. Cells were centrifuged at $300 \times g$ for 5 min at 4°C. One milliliter of supernatant was collected from each treatment and stored at –80°C until nuclear magnetic resonance (NMR) analysis. Cell pellets were washed with ice-cold PBS, and the metabolites from the cell pellets were extracted using a modified methanol/chloroform extraction procedure, as described by Bligh and Dyer (38). Briefly, cells were treated with 500 µl methanol/chloroform mixture (2:1) followed by rapid freezing in liquid N₂. Three cycles of freeze–thawing were performed, followed by the addition of 100 µl cold methanol and 100 µl water. The cell lysates were centrifuged at $100 \times g$ for 15 min, and 400 µl the top layer containing metabolite fractions was aliquoted, frozen, lyophilized, and stored at –80°C until NMR analysis. Cell-culture supernatants were filtered through 3 kDa cut-off filters. Cell lysate samples were prepared for NMR analysis by the addition of 185 µl dH₂O and 65 µl internal standard containing 5 mM 2,2-dimethyl-2-silapentane-5-sulfonate and 0.2% NaN₃ in 100% D₂O. Filtered cell supernatants were prepared by the addition of 65 µl internal standard to 585 µl supernatant. Sample pH was adjusted to 6.8. One-dimensional NMR spectra of the extracted metabolite fractions were acquired using the first increment of the standard NOESY pulse sequence on a four-channel Varian Inova 800-MHz (cell lysate samples) or 600-MHz (cell supernatants) NMR spectrometer (Varian, Palo Alto, CA). All spectra were recorded at 25°C with a 12-parts per million sweep width, 1-s recycle delay, 100-ms mixing time, an acquisition time of 4 s, four dummy scans, and 32 transients, as previously described (39). ¹H decoupling of the water resonance was applied for 0.9 s of the recycle delay and during the 100-ms mixing time. All spectra were zero-filled to 128,000 data points and multiplied by an exponential weighting function corresponding to a line-broadening of 0.5 Hz (39).

ATP assay

HMC-1 and LAD2 cells (1×10^6) were treated with sham or 500 µM SNOG for 4 h in 6-well culture plates (Becton Dickinson, Mississauga, Ontario, Canada). Fifty microliters the media containing 5×10^3 cells were loaded in 96-well flat-bottom black plates (Corning) in triplicate. ATPlite Istep Luminescence ATP detection assay kit was used to quantitate ATP in the viable cells by luminescence measured using an I450 Micro β Scintillation and Luminescence detector (both from PerkinElmer, Woodbridge, Ontario, Canada).

Statistical analysis

Data were analyzed with the unpaired Student *t* test and the Tukey–Kramer multiple comparisons test (one-way ANOVA). A *p* value <0.05 was considered significant.

Results

Constitutive nitration among different MCs

To investigate whether there was constitutive nitration among MC proteins, we performed Western blot with normally cultured, unstimulated HMC-1 and LAD2 cell lysates using anti-nitrotyrosine Ab. The anti-nitrotyrosine Ab detected many nitrated proteins (Fig. 1A), whereas dithionite treatment diminished the immunoreactivity, thereby confirming the existence of constitutive protein tyrosine nitration in MCs.

Constitutive nitration and NO donor-induced nitration in HMC-1

In addition to constitutive protein tyrosine nitration in MC, we tested whether specific proteins would undergo nitration upon cell treatment with an NO donor. We treated HMC-1 cells with different doses and at different time periods (50, 250, and 500 µM for 0.5, 2, and 4 h for each dose) with SNOG, a slow-releasing NO donor. 2-DE Western blots with anti-nitrotyrosine Ab were used to detect changes in the pattern of nitrated proteins in SNOG-treated HMC-1 cells. Treatment with 500 µM of SNOG for 4 h induced a significant change in the nitration pattern (compare panels in Fig. 1B). Isotope controls using rabbit IgG did not identify any immunoreactivity (data not shown). SNOG-induced nitration was reproducibly evident on a protein at ~40 kDa and pI 8.3 (arrowhead in *right panel*, Fig. 1B). In additional

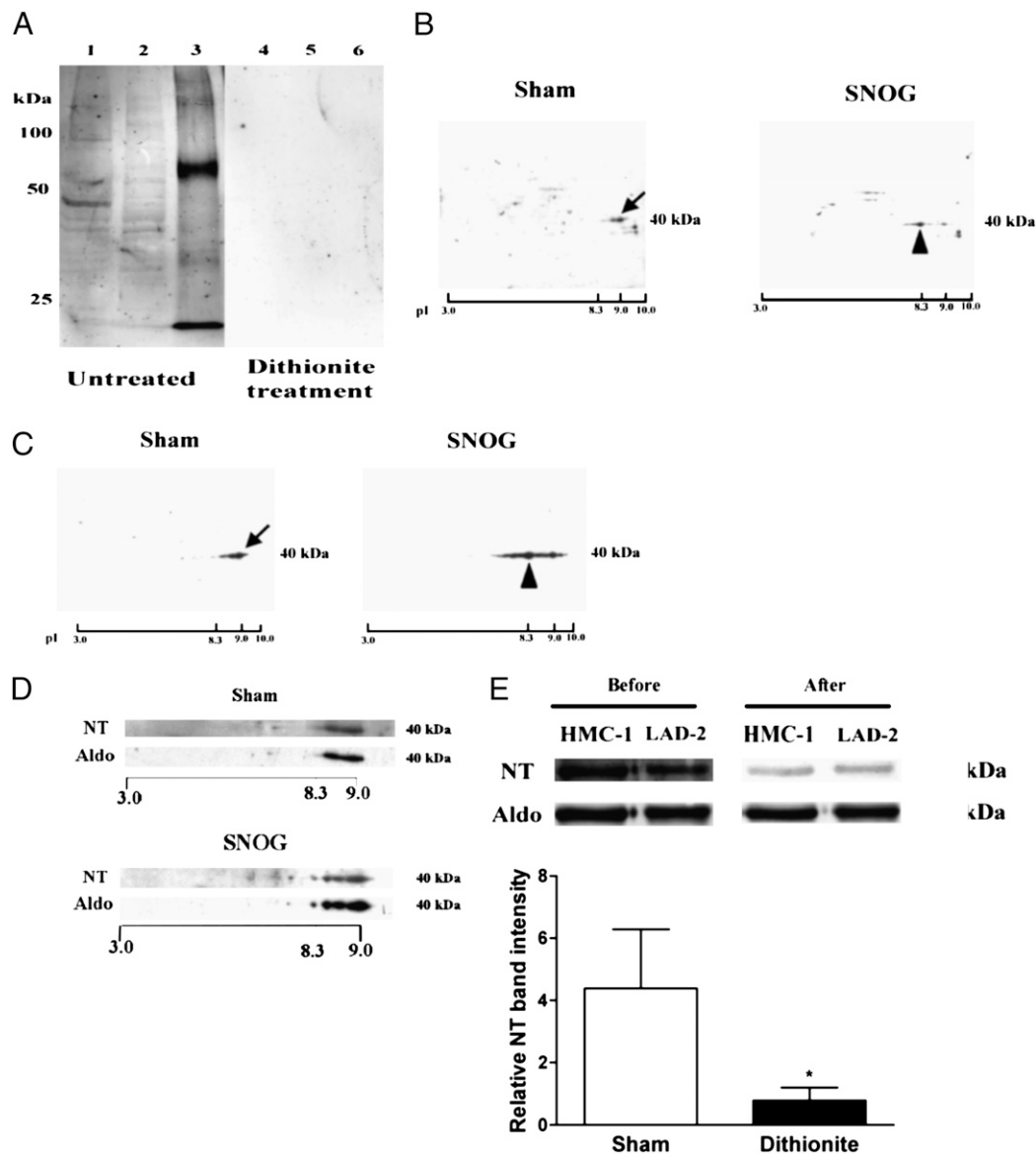


FIGURE 1. Constitutive and SNOG-induced nitrotyrosine⁺ proteins of HMC-1 and LAD2 cells. *A*, Western blot using anti-nitrotyrosine Ab of HMC-1 proteins (*lanes 1, 4*), LAD2 proteins (*lanes 2, 5*) (100 μ g/lane), and nitrotyrosine positive control (*lanes 3, 6*). Dithionite treatment (*lanes 4–6*) diminishes the nitrotyrosine immunoreactivity, establishing that there is constitutive nitration of MC proteins. Results are representative of three independent experiments. *B*, HMC-1 cells were treated (*right panel*) or not (*left panel*) with 500 μ M SNOG for 4 h, and proteins were extracted for 2-DE. Western blots of 2-DE gels using anti-nitrotyrosine Ab show constitutively nitrated aldolase at pI 9.0, ~40 kDa (arrow, *left panel*) and prominent SNOG-induced nitration at pI 8.3, ~40 kDa (arrowhead, *right panel*). Results are representative of seven independent experiments. *C*, Western blots of 2-DE gels using anti-aldolase Ab. Multiple immunoreactive aldolase spots near molecular mass ~40 kDa with different pI (7.0–9.3) (arrow, *left panel*) and SNOG-induced nitration of aldolase at pI 8.3 (arrowhead, *right panel*) were detected in HMC-1 cells. Aldolase at pI 9.0 was found to be nitrated constitutively (compare arrows in *left panels, A, B*). Results are representative of seven independent experiments. *D*, LAD2 cells were treated (*right panel*) or not (*left panel*) with 500 μ M SNOG for 4 h, and proteins were extracted for 2-DE. Western blots of 2-DE gels using NT and Aldo. Multiple immunoreactive aldolase spots near molecular mass ~40 kDa with different pI (7.0–9.3) and SNOG-induced nitration of aldolase at pI 8.3 were detected in LAD2 cells. Results are representative of four independent experiments. *E*, Western blots of affinity-purified aldolase of HMC-1 and LAD2 cells before and after dithionite treatment using NT and Aldo. The magnitude of dithionite reduction of nitrotyrosine reactivity of HMC-1 cells is represented as a bar graph (mean \pm SE; densitometry from three independent experiments). * p < 0.05 compare with sham treatment. Aldo, anti-aldolase Ab; NT, anti-nitrotyrosine Ab.

studies, 500 μ M SNOG was used for 4 h. The SNOG-induced nitrated spot at pI 8.3, ~40 kDa was matched with the corresponding spot in a silver-stained gel run in parallel, and the spot was removed under sterile conditions and submitted for spectroscopy (MS) identification of the protein.

MS analysis of aldolase

MS analysis of the SNOG-induced nitrated spot (~40 kDa, pI 8.3) revealed that peptides matched human aldolase A. To ensure that the spot submitted to MS analysis and the protein selectively

nitrated upon SNOG treatment were the same, we reprobbed the membranes with anti-aldolase Ab and confirmed that the spot at pI 8.3, ~40 kDa was aldolase (arrowhead in *right panel*, Fig. 1*C*). We also documented multiple immunoreactive spots for aldolase near molecular mass ~40 kDa but at different pI, ranging from 7.0 to 9.0, in sham- and SNOG-treated HMC-1 cells (Fig. 1*C*). Aldolase at pI 9.0 matched the nitrated spot at pI 9.0 (compare and see arrows in *left panel*, Fig. 1*B, 1C*), indicating constitutive nitration of aldolase. SNOG-induced nitration was observed for aldolase A at pI 8.3 (arrowhead in *right panel*, Fig. 1*B, 1C*). Similar

results were obtained when LAD2 cells were treated with SNOG. The region around 40 kDa in the 2-DE gel was highlighted to demonstrate that SNOG induces selective nitration of aldolase at pI 8.3 in LAD2 cells, as well as in HMC-1 cells (Fig. 1D). Moreover, in addition to aldolase, other spots were nitrated following SNOG treatment in LAD2 cells (data not shown). To further confirm constitutive nitration of aldolase, we enriched aldolase from HMC-1 or LAD2 cells using an aldolase affinity column and performed Western blot with anti-nitrotyrosine Ab (Fig. 1E). Dithionite treatment significantly reduced the nitro tyrosine reactivity of aldolase fractions, thereby confirming constitutive nitration of aldolase in these two MC lines. Similar results were observed when we preincubated nitrotyrosine Ab with free 3-nitrotyrosine (data not shown).

Identification of aldolase isoforms in MCs

Because there were multiple pI forms of aldolase in MCs, we defined the different isoforms of aldolase in MCs. To investigate the mRNA expression of the isoforms of aldolase in MCs, we used RT-PCR with isoform-specific primers for aldolase A, B, and C with cDNA of HMC-1 cells, LAD2 cells, and CBMCs. cDNA from non-tumor areas of kidney from a patient who underwent nephrectomy was used as a positive control for all three isoforms of aldolase. We identified mRNA for two isoforms, aldolase A and C, in HMC-1 cells, LAD2 cells, and CBMCs, whereas mRNA for all three isoforms was found in human kidney (Fig. 2). The products were sequenced and confirmed. Similarly, the affinity-purified fractions of aldolase from HMC-1 cells were analyzed using MS. We found peptides for aldolase A (Supplemental Table I) and aldolase C (Supplemental Table II).

SNOG-induced changes in the enzymatic activity of aldolase

To determine whether nitration of aldolase affects the activity of the enzyme, we measured the K_m and V_{max} of aldolase from HMC-1 and LAD2 cell homogenates before and after treatment with SNOG. SNOG induced a reduction in the K_m and the V_{max} of aldolase in HMC-1 cells (Fig. 3A, 3B) and a reduction in the V_{max} of aldolase in LAD2 cells (Fig. 3D). The raw data representing the aldolase activity in terms of change in OD values ($\Delta A_{240}/2 \times 10^5$ cells/min) between sham- and SNOG-treated HMC-1 and LAD2 cells are shown in Supplemental Fig. 1. Because inhibition of the activity of an enzyme can result in accumulation of the substrate, we measured levels of FBP, the substrate for aldolase A, before and after treatment with SNOG. SNOG treatment significantly increased the intracellular FBP levels by 613% in HMC-1 cells and by 61% in LAD2 cells (Fig. 4).

SNOG-induced changes in glycolytic metabolites

Because aldolase is a crucial enzyme in the glycolytic pathway, we studied whether inhibition of aldolase A activity might alter ATP

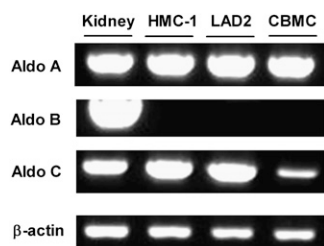


FIGURE 2. Expression of aldolase A and C isoforms in different MC lines. RT-PCR using cDNA of human kidney, HMC-1 and LAD2 cells and CBMCs using aldolase isoform (aldolase A, aldolase B, aldolase C)-specific and β -actin primers. All PCR products were confirmed by sequencing, and the results are representative of five independent experiments.

levels in MCs. We used [^1H] NMR to begin to define components of the metabolome (set of <1500-Da metabolites) (39, 40) of HMC-1 cells treated with sham or SNOG. Surprisingly, in contrast to the expectation from the inhibition of aldolase activity, ATP levels in cell extracts were similar in SNOG- and sham-treated MCs (Fig. 5A), although the AMP/ATP ratio was increased following SNOG treatment (Fig. 5B). Interestingly, pyruvate and lactate, measures of cellular glycolytic activity, were significantly elevated in culture media of SNOG-treated MCs (Fig. 5C, 5D). Similar results with HMC-1 and LAD2 cells were obtained using a different assay system (ATPlite 1step ATP kit; Supplemental Fig. 2).

FBP inhibits the degranulation of LAD2 cells

To simulate the effects of increased intracellular FBP in MCs and to study the effects of FBP on MC function, we used an in vitro IgE-dependent degranulation assay of MCs. Because exogenously applied FBP was shown to enter intracellular compartments poorly (41), we used 5 mM exogenous FBP in our model, as other investigators used previously (42). Indeed, when we tested intracellular levels of FBP following treatment with exogenous FBP (100 nmol to 100 μmol), only a few nanomoles of FBP were available in the intracellular compartment of LAD2 cells (Supplemental Fig 3).

IgE/anti-IgE stimulation induced release of $21.8 \pm 2.1\%$ of the total cellular β -hex from LAD2 cells, whereas pretreatment with SNOG or FBP significantly inhibited this degranulation of LAD2 by 59 or 48%, respectively (Fig. 6). However, F1P and F6P, as negative controls for FBP, did not inhibit MC degranulation.

Discussion

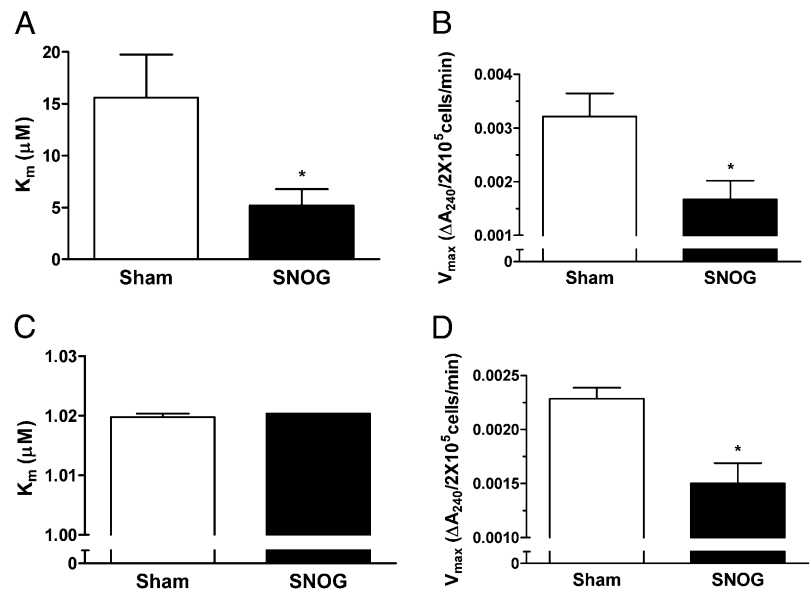
Endogenous and exogenous NO have been widely reported to modulate several MC functions (43). One common pathway involved is that NO activates soluble guanylate cyclase and increases intracellular cGMP, which, in turn, regulates numerous physiological events in the cell (44). However, many studies indicated that non-cGMP-mediated pathways are also important in the effects of NO on MC function (6, 12, 31, 45). Earlier, we suggested that S-nitrosylation of calpain was responsible for the NO-mediated inhibition of MC adhesion (31). In the current study, we provide the first evidence that protein tyrosine nitration plays a role in NO-mediated inhibitory effects on MC function.

Using Western blot with an anti-nitrotyrosine Ab, we identified constitutive protein tyrosine nitration in MCs, thereby providing evidence that this posttranslational modification of proteins occurs in a variety of MCs (Fig. 1). Our observation is supported by evidence that constitutive nitration occurs in other leukocytes, such as macrophage cell lines (46), eosinophils (47, 48), and neutrophils (49). It is interesting that a recent study claims that there are no nitrotyrosine⁺ proteins in MCs on lung sections of cystic fibrosis patients (48). Unfortunately, isotype controls were not reported in that study, and there was no information about optimization of sensitivity of the immunohistochemistry to detect nitrotyrosine reactivity in MCs or the numbers of MCs assessed on the tissues.

In addition to the constitutive nitration of multiple MC proteins, we identified SNOG-induced changes in protein nitration (Fig. 1B). It is interesting that aldolase at pI 9.0 was nitrated constitutively, whereas NO-mediated nitration of aldolase A was associated with an 8.3 pI form (Fig. 1B, 1C). The presence of multiple pI forms (~ 7.0 – 9.3) of aldolase in MCs is consistent with earlier findings in rat diaphragm and mouse sperm cells (50, 51). Aldolase can also be phosphorylated (52) and regulated by different posttranslational modifications.

Interestingly, aldolase A can be found in the cytoplasm (53), mitochondria (54), and the heterochromatin region of nucleus (55), and in vivo nitration can be seen in many intracellular compartments

FIGURE 3. SNOG-induced reduction in the total aldolase enzymatic activity of MCs. HMC-1 and LAD2 cells (2×10^6) were treated with 50 μ l of water or 500 μ M SNOG for 4 h, and the total aldolase activity in the cell lysates was measured. To calculate the V_{\max} and the K_m , 3.125–800 μ M (serial 2-fold dilution) of substrate was used. SNOG treatment reduced the K_m and V_{\max} of aldolase in HMC-1 cells (A, B), but it only reduced the V_{\max} in LAD2 cells (C, D). Results are from seven (HMC-1) and five (LAD2) independent experiments (mean \pm SE). * $p < 0.05$.



(56), including nuclear histones (57). Tyrosine nitration of a protein can be mediated by multiple mechanisms, including ONOO^- (22). In MCs, ONOO^- can be generated by the reaction of NO and MC-produced O_2^- , which could, in turn, nitrate aldolase. The half-life of ONOO^- is only a few seconds; thus, ONOO^- reactivity may act in the local microenvironment on a limited spectrum of proteins. In our experiment, we decided to use a slow-releasing NO donor SNOG (decomposition rate is $\sim 5\%$ per hour in water at room temperature, and the half-life is ~ 80 h at 37°C), which would likely combine with physiologically relevant, MC-derived O_2^- and, thus, generate a more physiological nitration event. In addition to ONOO^- , there are other mechanisms of nitration (58); however, the precise mechanisms underlying the nitration of aldolase are beyond the scope of the current study. Another consideration is that NO might facilitate selective

nitration of aldolase A in different intracellular compartments of HMC-1 cells and modulate compartment-specific functions of aldolase (see below).

There are three isoforms of mammalian aldolase: A, B, and C (59). Aldolase A and C are preferentially involved in the glycolytic cycle and predominantly expressed in muscle and brain, respectively, whereas aldolase B is reported to be preferentially involved in gluconeogenesis and expressed in liver (59). However, the expression of these isoforms is not restricted to specific tissues, (e.g., all three isoforms are expressed in kidney) (60, 61). Tyrosine nitration of aldolase A, B, and C was reported in a wide range of tissues and under different inflammatory conditions (50, 62–65). To define specific tyrosine residues that are nitrated in aldolase A or in aldolase C, MS identification of nitration-specific sites requires large amounts of protein; we are working toward enriching the nitrated aldolase fractions with specific techniques (66).

Aldolase A is the predominant isoform expressed in lymphocytes (67). Aldolase C expression was reported in platelets, but it was not detectable in erythrocytes and lymphocytes (68). It is interesting that MCs express aldolase C, the isoform predominantly expressed in neuronal tissues. The potential significance of aldolase C expression in MCs is multiple. For example, if there is inactivation of one isoform of the enzyme, the other isoform, in this case aldolase C, might act as a backup enzyme in the glycolytic cycle. Interestingly, aldolase C was reported to be involved in a stress-response pathway for lung epithelial cell function during hypoxia (69). Moreover, subsets of cerebellar Purkinje cells expressing aldolase C were resistant to excitotoxic insult (70), and aldolase C small interfering RNA transfection resulted in the death of these subsets of Purkinje cells. Because MCs play a major role in TGF- β 1-mediated excitotoxicity (71), expression of aldolase C may be of functional significance in MC homeostasis.

It is intriguing that aldolase A has been identified as a target of tyrosine nitration in several other cells and tissues, including diaphragm (50), human skin fibroblasts (35), quadriceps muscle of patients with severe chronic obstructive pulmonary disease (72), and in lung tissue in a model of asthma (65). However, this is the first report in human MCs. The discovery of aldolase as one of the targets for nitration in MCs might be due to the abundance of this protein, the extent of nitration of tyrosines in aldolase, and the sensitivity of the methods used. Interestingly, other proteins were

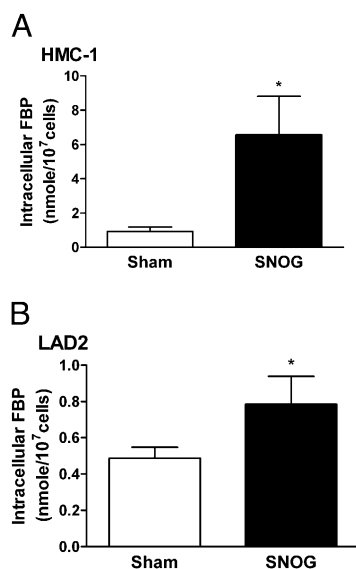
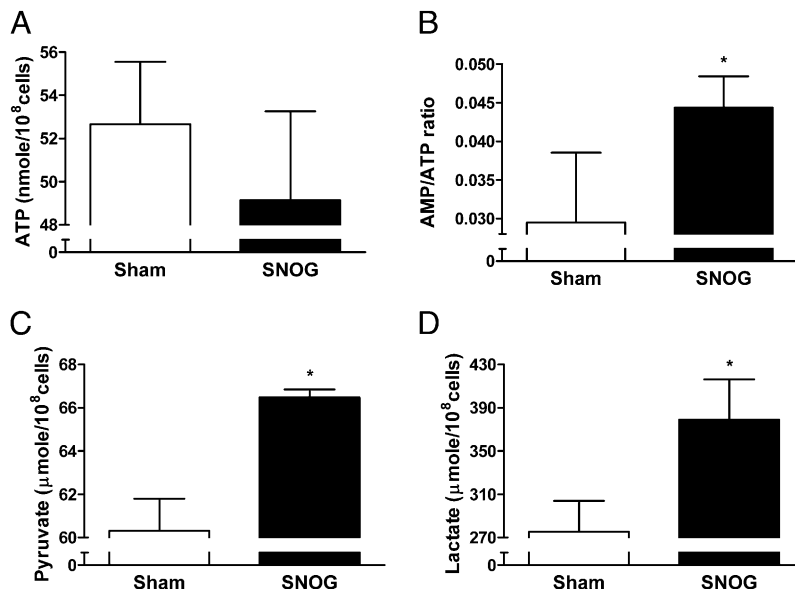


FIGURE 4. SNOG-induced elevation of FBP in MCs. HMC-1 cells (A) or LAD2 cells (B) (1×10^7) were treated with 250 μ l of water or 500 μ M SNOG in 10 ml media for 4 h, and the total cell pellet were deproteinized using 5% TCA followed by neutralization by 2 M Tris. The FBP concentration was estimated in the metabolite fractions. Results are from five (A) or eight (B) independent experiments (mean \pm SE). * $p < 0.05$.

FIGURE 5. SNOG-induced glycolytic intermediates change in HMC-1 cells. HMC-1 cells (1×10^8) were treated with sham (2.5 ml water in 100 ml media) or with 500 μ M SNOG for 4 h, and glycolytic metabolites were analyzed using NMR. SNOG did not increase the ATP level (A), but it significantly increased the AMP/ATP ratio (B) and the pyruvate (C) and lactate (D) levels (enhanced glycolysis). Error bars represent SE from three independent experiments. $*p < 0.05$.



nitrate (e.g., pI 7.0, molecular mass 25 kDa) upon SNOG treatment in LAD2 cells (data not shown). We are currently working toward identifying these targets using MS.

An earlier *in vitro* study using rabbit muscle aldolase treated with ONOO^- demonstrated four tyrosine residues (Y^{222} , Y^{243} , Y^{342} , and Y^{363}) that were targets for tyrosine nitration (35). Although, we do not know which tyrosine residues in MC aldolase A are nitrated following SNOG treatment, NO treatment reduced total activity of MC aldolase (Fig. 3), as previously shown using rabbit muscle aldolase (35). Because it is difficult to separate the two isoforms of aldolase A and C from the whole-cell lysate, we studied total aldolase activity, as reported earlier in different tissues and under different conditions (55, 73). The tyrosine at the carboxy terminal end of the aldolase A (i.e., tyrosine 363) was critical for the enzymatic activity; nitration of this residue significantly reduced the V_{max} of the enzyme activity (35). Interestingly, our observation that NO induced a reduction in the K_m and V_{max} of HMC-1 aldolase is consistent with earlier studies in which substitution of tyrosine 363 with serine in human aldolase A also reduced enzyme K_m and V_{max} (74). SNOG reduced the K_m of

HMC-1 aldolase, whereas there was no change in the K_m of LAD2 cells (Fig. 3). Moreover, there was a 10-fold difference between the K_m values of HMC-1 and LAD2 cells (Fig. 3). Thus, there may be cell-type-specific differences in the effects of nitration (i.e., LAD2 is a mature MC line, whereas HMC-1 is an immature cell line). Moreover, the expression and intracellular distribution of aldolase isoforms A and C may be different between these two cell lines, and the tyrosine nitration sites may differ as well.

Given the reduction in the enzymatic activity of aldolase, we postulated that this would increase the levels of its substrate FBP. Indeed, we found that the intracellular FBP in HMC-1 cell extracts significantly increased following SNOG treatment (Fig. 4A). Similarly, a statistically significant increase in FBP levels following SNOG treatment was documented in LAD2 cells (Fig. 4B). It is interesting to note that the SNOG-induced FBP levels also differed between HMC-1 and LAD2 cells, as did the K_m values of these two MC lines (see above). Thus, the difference in magnitude of K_m values, unaltered K_m values for LAD2 cells compared with the reduction in K_m of HMC-1 cells after SNOG treatment, and the variable intracellular FBP levels strongly suggest that the outcome of nitration might be different between HMC-1 and LAD2 cells. Further detailed study is necessary to understand our observations. Interestingly, a mutation of aldolase A (Glu206Lys) was reported in a patient with an inherited metabolic myopathy and hemolysis and was associated with increased FBP levels (182.9% of control) in the patient's RBCs (75). Moreover, NO-induced inhibition of GAPDH, the enzyme downstream of aldolase in the glycolytic cycle, and a corresponding increase in FBP levels in rat intestinal tissues were reported (76). Thus, increased FBP levels upon inactivation of aldolase A may have physiological relevance.

To assess the effects of aldolase nitration on the metabolic pathways of MCs, we analyzed metabolites using NMR. ATP levels in cell extracts were similar in sham- and SNOG-treated HMC-1 cells (Fig. 5A). It is interesting that cellular ATP levels remained similar, despite a reduction in the activity of aldolase, thereby suggesting restoration of ATP levels through homeostatic mechanisms. AMP-activated protein kinase was reported to act as a fuel gauge in mammalian cells. It can enhance cellular ATP levels by switching off energy-using pathways and switching on energy-generating pathways (77, 78). AMP-activated protein kinase activation occurs when there is an increase in AMP levels and

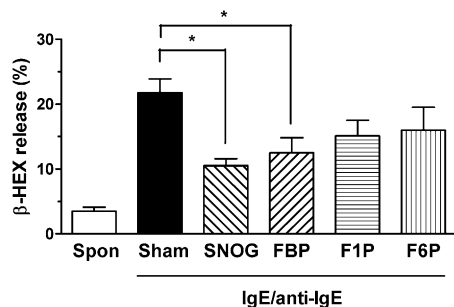


FIGURE 6. Effects of exogenous FBP on degranulation of LAD2 cells. LAD2 cells were sensitized with 1 μ g/ml human IgE overnight at 37°C and then pretreated with 500 μ M SNOG, 5 mM FBP, 5 mM F1P, or 5 mM F6P for 4 h at 37°C. The cells were washed and resuspended in HEPES-buffered Tyrode's solution and stimulated with 10 μ g/ml mouse anti-human IgE Ab for 30 min. The cells were centrifuged, and the percent release of β -hex into the supernatant was calculated. Results are expressed as mean \pm SE from six independent experiments performed in triplicate. Data were analyzed using one-way ANOVA, followed by the Tukey-Kramer multiple comparisons test. $*p < 0.05$.

a decrease in ATP levels (increased AMP/ATP ratio) (77). We predicted that this regulatory pathway also exists in MCs; therefore, we measured the AMP/ATP ratio before and after SNOG treatment. Indeed, the AMP/ATP ratio increased following SNOG treatment in HMC-1 cells (Fig. 5B), providing evidence for homeostatic regulation of ATP levels in our model. In addition to in HMC-1 cells, the ATP levels in LAD2 cells were unaltered after SNOG treatment (Supplemental Fig. 2). The lower ATP levels detected using NMR (Fig. 5A) compared with live cell-based ATP assay (Supplemental Fig. 2) might be due to the loss of ATP during the preparation of samples for NMR (see *Materials and Methods*).

Measurement of pyruvate, the end product of glycolysis, and lactate, the end product of anaerobic glycolysis, in the media of cultured cells provides a clear understanding of the metabolic status of the cells (79). Interestingly, pyruvate and lactate were significantly elevated in culture media of NO-treated MCs (Fig. 5C, 5D), indicating enhanced glycolysis, as previously shown in astrocytes treated with NO (80). NO downregulates mitochondrial energy production, but the cells maintain energy production by regulating glycolysis in astrocytes (81). It seems paradoxical that, although aldolase enzymatic activity is depressed (Fig. 3), glycolysis seems to be enhanced. In support of our observations, studies of skeletal muscle showed that elevated FBP is associated with increased glycolysis (81) and FBP activation of 6-phosphofructo-1-kinase, a key rate-limiting enzyme in glycolysis (81). It is interesting that some cells can respond to NO by activating glycolysis (astrocytes), whereas others do not (neurons) (81). Our results suggest that SNOG fundamentally alters MC metabolism to keep energy production at a homeostatic level.

FBP has several activities, including protection in ischemia/reperfusion injury and hypoxia (76, 82) and suppression of T cell proliferation (83). FBP has been used as a component of protective solutions in the transport of donor organs, such as liver (84). Other investigators have filed a patent on FBP as a therapeutic for asthma (85), and a recent *in vivo* study in rats demonstrated that FBP has an inhibitory role on MC degranulation and histamine release (86). We hypothesized that increased FBP levels, following aldolase A nitration in MCs, might inhibit some MC functions. Indeed, FBP significantly inhibited the β -hex release by LAD2 cells (Fig. 6), whereas similar concentrations of F1P or F6P did not have significant effects, supporting the specific effects of FBP on MC degranulation. The effects of NO donors on human MC activation depends on their NO release kinetics rather than the amount of NO released (87). Hence, our data on the effects of SNOG pretreatment followed by MC activation in an NO-free environment supports NO-mediated posttranslational modification, in this case nitration of aldolase. Moreover, the slow NO-releasing donor SNOG has been widely reported to mediate its action through non-cGMP pathways (28, 87).

Phospholipase C (PLC) cleaves phosphatidylinositol 4,5-bisphosphate to diacylglycerol and inositol 1,4,5-triphosphate (IP₃), a critical intracellular messenger. The PLC γ signaling pathway plays a pivotal role in MC degranulation (88). Interestingly, some effects of FBP in other cells depend on PLC signaling (82). Moreover, FBP shares a binding site on aldolase A with IP₃ (89) and significantly inhibits IP₃ binding to aldolase A (89, 90). This binding also inhibits aldolase A enzymatic activity and influences release/repartition of aldolase A from binding to cytoskeletal elements (90). The posttranslational modification of tyrosine nitration of aldolase A may alter its relative affinity for FBP and/or IP₃. Thus, it is possible that NO acts through excess FBP that modifies IP₃ and PLC signaling cascades critical in MC secretion in IgE-dependent responses. Interestingly, aldolase can bind to many intracellular proteins, such as actin and ryanodine receptor (91, 92).

Aldolase nitration might alter some of these interactions and, in turn, regulate MC function. Further studies with mature MCs may enhance our knowledge of these pathways.

In conclusion, we have provided evidence that protein tyrosine nitration regulates MC function. We identified that aldolase A, a critical enzyme in the glycolytic pathway, is a target for nitration. Because of the importance of aldolase A in cellular metabolism and homeostasis, further dissection of the relevance of our observations is necessary to more fully elucidate the role of tyrosine nitration in the regulation of MC function in allergic and other diseases.

Acknowledgments

We thank Randy Whittal and Jing Zheng for help with MS analysis. We also thank Chris St. Laurent and Katherine Morris for critical comments and help with the preparation of the manuscript.

Disclosures

The authors have no financial conflicts of interest.

References

1. Moon, T. C., C. D. St Laurent, K. E. Morris, C. Marcet, T. Yoshimura, Y. Sekar, and A. D. Befus. 2010. Advances in mast cell biology: new understanding of heterogeneity and function. *Mucosal Immunol.* 3: 111–128.
2. Marshall, J. S. 2004. Mast-cell responses to pathogens. *Nat. Rev. Immunol.* 4: 787–799.
3. Galli, S. J., S. Nakae, and M. Tsai. 2005. Mast cells in the development of adaptive immune responses. *Nat. Immunol.* 6: 135–142.
4. Swindle, E. J., and D. D. Metcalfe. 2007. The role of reactive oxygen species and nitric oxide in mast cell-dependent inflammatory processes. *Immunol. Rev.* 217: 186–205.
5. Bidri, M., F. Féger, S. Varadarajalou, N. Ben Hamouda, J. J. Guilloison, and M. Arock. 2001. Mast cells as a source and target for nitric oxide. *Int. Immunopharmacol.* 1: 1543–1558.
6. Gilchrist, M., S. D. McCauley, and A. D. Befus. 2004. Expression, localization, and regulation of NOS in human mast cell lines: effects on leukotriene production. *Blood* 104: 462–469.
7. McCauley, S. D., M. Gilchrist, and A. D. Befus. 2005. Nitric oxide: a major determinant of mast cell phenotype and function. *Mem. Inst. Oswaldo Cruz* 100 (Suppl. 1): 11–14.
8. Forsythe, P., M. Gilchrist, M. Kulka, and A. D. Befus. 2001. Mast cells and nitric oxide: control of production, mechanisms of response. *Int. Immunopharmacol.* 1: 1525–1541.
9. Gilchrist, M., M. Savoie, O. Nohara, F. L. Wills, J. L. Wallace, and A. D. Befus. 2002. Nitric oxide synthase and nitric oxide production in *in vivo*-derived mast cells. *J. Leukoc. Biol.* 71: 618–624.
10. Gilchrist, M., and A. D. Befus. 2008. Interferon-gamma regulates chemokine expression and release in the human mast cell line HMC1: role of nitric oxide. *Immunology* 123: 209–217.
11. Yip, K. H., Y. Huang, M. M. Waye, and H. Y. Lau. 2008. Induction of nitric oxide synthases in primary human cultured mast cells by IgE and proinflammatory cytokines. *Int. Immunopharmacol.* 8: 764–768.
12. Coleman, J. W. 2002. Nitric oxide: a regulator of mast cell activation and mast cell-mediated inflammation. *Clin. Exp. Immunol.* 129: 4–10.
13. Nohara, O., M. Kulka, R. E. Déry, F. L. Wills, N. S. Hirji, M. Gilchrist, and A. D. Befus. 2001. Regulation of CD8 expression in mast cells by exogenous or endogenous nitric oxide. *J. Immunol.* 167: 5935–5939.
14. Bissonnette, E. Y., C. M. Hogaboam, J. L. Wallace, and A. D. Befus. 1991. Potentiation of tumor necrosis factor- α -mediated cytotoxicity of mast cells by their production of nitric oxide. *J. Immunol.* 147: 3060–3065.
15. Moon, T. C., and A. D. Befus. 2008. Exogenous nitric oxide regulates cyclooxygenase-2 expression and prostaglandin D(2) generation through p38 MAPK in mouse bone marrow-derived mast cells. *Free Radic. Biol. Med.* 45: 780–788.
16. Ischiropoulos, H., and A. Gow. 2005. Pathophysiological functions of nitric oxide-mediated protein modifications. *Toxicology* 208: 299–303.
17. Gow, A. J., C. R. Farkouh, D. A. Munson, M. A. Posencheg, and H. Ischiropoulos. 2004. Biological significance of nitric oxide-mediated protein modifications. *Am. J. Physiol. Lung Cell. Mol. Physiol.* 287: L262–L268.
18. Koeck, T., D. J. Stuehr, and K. S. Aulak. 2005. Mitochondria and regulated tyrosine nitration. *Biochem. Soc. Trans.* 33: 1399–1403.
19. Szabó, C., H. Ischiropoulos, and R. Radi. 2007. Peroxynitrite: biochemistry, pathophysiology and development of therapeutics. *Nat. Rev. Drug Discov.* 6: 662–680.
20. Schopfer, F. J., P. R. Baker, and B. A. Freeman. 2003. NO-dependent protein nitration: a cell signaling event or an oxidative inflammatory response? *Trends Biochem. Sci.* 28: 646–654.
21. Souza, J. M., G. Peluffo, and R. Radi. 2008. Protein tyrosine nitration—functional alteration or just a biomarker? *Free Radic. Biol. Med.* 45: 357–366.
22. Abello, N., H. A. Kerstjens, D. S. Postma, and R. Bischoff. 2009. Protein tyrosine nitration: selectivity, physicochemical and biological consequences,

- denitration, and proteomics methods for the identification of tyrosine-nitrated proteins. *J. Proteome Res.* 8: 3222–3238.
23. Kim, J. Y., K. H. Lee, B. K. Lee, and J. Y. Ro. 2005. Peroxynitrite modulates release of inflammatory mediators from guinea pig lung mast cells activated by antigen-antibody reaction. *Int. Arch. Allergy Immunol.* 137: 104–114.
 24. Kirshenbaum, A. S., C. Akin, Y. Wu, M. Rottem, J. P. Goff, M. A. Beaven, V. K. Rao, and D. D. Metcalfe. 2003. Characterization of novel stem cell factor responsive human mast cell lines LAD 1 and 2 established from a patient with mast cell sarcoma/leukemia; activation following aggregation of FcepsilonRI or FcgammaRI. *Leuk. Res.* 27: 677–682.
 25. Moon, T. C., E. Lee, S. H. Baek, M. Murakami, I. Kudo, N. S. Kim, J. M. Lee, H. K. Min, N. Kambe, and H. W. Chang. 2003. Degranulation and cytokine expression in human cord blood-derived mast cells cultured in serum-free medium with recombinant human stem cell factor. *Mol. Cells* 16: 154–160.
 26. Kambe, N., M. Kambe, H. W. Chang, A. Matsui, H. K. Min, M. Hussein, C. A. Oskerizian, J. Kochan, A. A. Irani, and L. B. Schwartz. 2000. An improved procedure for the development of human mast cells from dispersed fetal liver cells in serum-free culture medium. *J. Immunol. Methods* 240: 101–110.
 27. Askew, S. C., A. R. Butler, F. W. Flitney, G. D. Kemp, and I. L. Megson. 1995. Chemical mechanisms underlying the vasodilator and platelet anti-aggregating properties of S-nitroso-N-acetyl-DL-penicillamine and S-nitrosoglutathione. *Bioorg. Med. Chem.* 3: 1–9.
 28. Gordge, M. P., J. S. Hothersall, and A. A. Noronha-Dutra. 1998. Evidence for a cyclic GMP-independent mechanism in the anti-platelet action of S-nitrosoglutathione. *Br. J. Pharmacol.* 124: 141–148.
 29. Koranteng, R. D., R. J. Dearman, I. Kimber, and J. W. Coleman. 2000. Phenotypic variation in mast cell responsiveness to the inhibitory action of nitric oxide. *Inflamm. Res.* 49: 240–246.
 30. Davis, B. J., B. F. Flanagan, A. M. Gilfillan, D. D. Metcalfe, and J. W. Coleman. 2004. Nitric oxide inhibits IgE-dependent cytokine production and Fos and Jun activation in mast cells. *J. Immunol.* 173: 6914–6920.
 31. Forsythe, P., and A. D. Befus. 2003. Inhibition of calpain is a component of nitric oxide-induced down-regulation of human mast cell adhesion. *J. Immunol.* 170: 287–293.
 32. Chazotte-Aubert, L., P. Hainaut, and H. Ohshima. 2000. Nitric oxide nitrates tyrosine residues of tumor-suppressor p53 protein in MCF-7 cells. *Biochem. Biophys. Res. Commun.* 267: 609–613.
 33. Springer, T. A. 1995. Immunoaffinity chromatography. In *Current Protocols in Molecular Biology*. F. M. Ausubel, R. Brent, R. E. Kingston, D. D. Moore, J. G. Seidman, J. A. Smith, and K. Struhl, eds. John Wiley & Sons, Inc., Hoboken, NJ, Vol. 2. p 10.11.1–10.11.6.
 34. Michal, G. 1984. *D-Fructose 1,6-Bisphosphate, Dihydroxyacetone Phosphate and D-Glycerinaldehyde 3-Phosphate*. Academic Press, New York.
 35. Koeck, T., B. Levison, S. L. Hazen, J. W. Crabb, D. J. Stuehr, and K. S. Aulak. 2004. Tyrosine nitration impairs mammalian aldolase A activity. *Mol. Cell. Proteomics* 3: 548–557.
 36. Xu, K., and J. L. Stringer. 2008. Pharmacokinetics of fructose-1,6-diphosphate after intraperitoneal and oral administration to adult rats. *Pharmacol. Res.* 57: 234–238.
 37. Hohman, R. J., and S. C. Dreskin. 2001. Measuring degranulation of mast cells. *Curr. Protoc. Immunol.* Chapter 7: Unit 7.26.
 38. Bligh, E. G., and W. J. Dyer. 1959. A rapid method of total lipid extraction and purification. *Can. J. Biochem. Physiol.* 37: 911–917.
 39. Weljie, A. M., J. Newton, P. Mercier, E. Carlson, and C. M. Slupsky. 2006. Targeted profiling: quantitative analysis of 1H NMR metabolomics data. *Anal. Chem.* 78: 4430–4442.
 40. Wishart, D. S., D. Tzur, C. Knox, R. Eisner, A. C. Guo, N. Young, D. Cheng, K. Jewell, D. Arndt, S. Sawhney, et al. 2007. HMDB: the Human Metabolome Database. *Nucleic Acids Res.* 35(Database issue): D521–D526.
 41. Hardin, C. D., and T. M. Roberts. 1994. Metabolism of exogenously applied fructose 1,6-bisphosphate in hypoxic vascular smooth muscle. *Am. J. Physiol.* 267: H2325–H2332.
 42. Ehringer, W. D., W. Niu, B. Chiang, O. L. Wang, L. Gordon, and S. Chien. 2000. Membrane permeability of fructose-1,6-diphosphate in lipid vesicles and endothelial cells. *Mol. Cell. Biochem.* 210: 35–45.
 43. Sekar, Y., T. C. Moon, S. Muñoz, and A. D. Befus. 2005. Role of nitric oxide in mast cells: controversies, current knowledge, and future applications. *Immunol. Res.* 33: 223–239.
 44. Krumenacker, J. S., K. A. Hanafy, and F. Murad. 2004. Regulation of nitric oxide and soluble guanylyl cyclase. *Brain Res. Bull.* 62: 505–515.
 45. Deschoolmeester, M. L., N. C. Eastmond, R. J. Dearman, I. Kimber, D. A. Basketter, and J. W. Coleman. 1999. Reciprocal effects of interleukin-4 and interferon-gamma on immunoglobulin E-mediated mast cell degranulation: a role for nitric oxide but not peroxynitrite or cyclic guanosine monophosphate. *Immunology* 96: 138–144.
 46. Palazzolo-Ballance, A. M., C. Suquet, and J. K. Hurst. 2007. Pathways for intracellular generation of oxidants and tyrosine nitration by a macrophage cell line. *Biochemistry* 46: 7536–7548.
 47. Takemoto, K., K. Ogino, D. H. Wang, T. Takigawa, C. M. Kurosawa, Y. Kamyabashi, Y. Hibino, Y. Hitomi, and H. Ichimura. 2007. Biochemical characterization of reactive nitrogen species by eosinophil peroxidase in tyrosine nitration. *Acta Med. Okayama* 61: 17–30.
 48. Ulrich, M., A. Petre, N. Youhnovski, F. Promm, M. Schirle, M. Schumm, R. S. Pero, A. Doyle, J. Checkel, H. Kita, et al. 2008. Post-translational tyrosine nitration of eosinophil granule toxins mediated by eosinophil peroxidase. *J. Biol. Chem.* 283: 28629–28640.
 49. Klink, M., K. Bednarska, K. Jastrzebska, M. Banasik, and Z. Sulowska. 2007. Signal transduction pathways affected by nitric oxide donors during neutrophil functional response in vitro. *Inflamm. Res.* 56: 282–290.
 50. Vassilakopoulos, T., K. Govindaraju, D. Parthenis, D. H. Eidelman, Y. Watanabe, and S. N. Hussain. 2007. Nitric oxide production in the ventilatory muscles in response to acute resistive loading. *Am. J. Physiol. Lung Cell. Mol. Physiol.* 292: L1013–L1022.
 51. Dukes, A. A., V. S. Van Laar, M. Cascio, and T. G. Hastings. 2008. Changes in endoplasmic reticulum stress proteins and aldolase A in cells exposed to dopamine. *J. Neurochem.* 106: 333–346.
 52. Arcelay, E., A. M. Salicioni, E. Wertheimer, and P. E. Visconti. 2008. Identification of proteins undergoing tyrosine phosphorylation during mouse sperm capacitation. *Int. J. Dev. Biol.* 52: 463–472.
 53. Schindler, R., E. Weichselsdorfer, O. Wagner, and J. Bereiter-Hahn. 2001. Aldolase-localization in cultured cells: cell-type and substrate-specific regulation of cytoskeletal associations. *Biochem. Cell Biol.* 79: 719–728.
 54. MacDonnell, P. C., and O. Greengard. 1974. Enzymes in intracellular organelles of adult and developing rat brain. *Arch. Biochem. Biophys.* 163: 644–655.
 55. Mamczur, P., and A. Dzujaj. 2004. Nuclear localization of aldolase A in pig cardiomyocytes. *Histol. Histopathol.* 19: 753–758.
 56. Heijnen, H. F., E. van Donselaar, J. W. Slot, D. M. Fries, B. Blachard-Fillion, R. Hodara, R. Lightfoot, M. Polydoro, D. Spielberg, L. Thomson, et al. 2006. Subcellular localization of tyrosine-nitrated proteins is dictated by reactive oxygen species generating enzymes and by proximity to nitric oxide synthase. *Free Radic. Biol. Med.* 40: 1903–1913.
 57. Haqqani, A. S., J. F. Kelly, and H. C. Birnboim. 2002. Selective nitration of histone tyrosine residues in vivo in mutator tumors. *J. Biol. Chem.* 277: 3614–3621.
 58. Miller, S., C. Ross-Inta, and C. Giulivi. 2007. Kinetic and proteomic analyses of S-nitrosoglutathione-treated hexokinase A: consequences for cancer energy metabolism. *Amino Acids* 32: 593–602.
 59. Lebherz, H. G., and W. J. Rutter. 1969. Distribution of fructose diphosphate aldolase variants in biological systems. *Biochemistry* 8: 109–121.
 60. Yañez, A. J., H. C. Ludwig, R. Bertinat, C. Spichiger, R. Gatica, G. Berlien, O. Leon, M. Brito, I. I. Concha, and J. C. Slebe. 2005. Different involvement for aldolase isoenzymes in kidney glucose metabolism: aldolase B but not aldolase A colocalizes and forms a complex with FBPAse. *J. Cell. Physiol.* 202: 743–753.
 61. Takashi, M., H. Haimoto, T. Koshikawa, and K. Kato. 1990. Expression of aldolase C isozyme in renal cell carcinoma. *Am. J. Clin. Pathol.* 93: 631–636.
 62. Miyagi, M., H. Sakaguchi, R. M. Darrow, L. Yan, K. A. West, K. S. Aulak, D. J. Stuehr, J. G. Hollyfield, D. T. Organisciak, and J. W. Crabb. 2002. Evidence that light modulates protein nitration in rat retina. *Mol. Cell. Proteomics* 1: 293–303.
 63. Kanski, J., A. Behring, J. Pelling, and C. Schöneich. 2005. Proteomic identification of 3-nitrotyrosine-containing rat cardiac proteins: effects of biological aging. *Am. J. Physiol. Heart Circ. Physiol.* 288: H371–H381.
 64. Aulak, K. S., M. Miyagi, L. Yan, K. A. West, D. Massillon, J. W. Crabb, and D. J. Stuehr. 2001. Proteomic method identifies proteins nitrated in vivo during inflammatory challenge. *Proc. Natl. Acad. Sci. USA* 98: 12056–12061.
 65. Ghosh, S., A. J. Janocha, M. A. Aronica, S. Swaidani, S. A. Comhair, W. Xu, L. Zheng, S. Kaveti, M. Kinter, S. L. Hazen, and S. C. Erzurum. 2006. Nitrotyrosine proteome survey in asthma identifies oxidative mechanism of catalase inactivation. *J. Immunol.* 176: 5587–5597.
 66. Parastatidis, I., L. Thomson, A. Burke, I. Chernysh, C. Nagaswami, J. Visser, S. Stamer, D. C. Liebler, G. Koliakos, H. F. Heijnen, et al. 2008. Fibrinogen beta-chain tyrosine nitration is a prothrombotic risk factor. *J. Biol. Chem.* 283: 33846–33853.
 67. Steinhagen-Thiessen, E., and H. Hilz. 1979. Aldolase activity and cross-reacting material in lymphocytes of aged individuals. *Gerontology* 25: 132–135.
 68. Day, I. N., and R. J. Thompson. 1984. Levels of immunoreactive aldolase C, creatine kinase-BB, neuronal and non-neuronal enolase, and 14-3-3 protein in circulating human blood cells. *Clin. Chim. Acta* 136: 219–228.
 69. Jean, J. C., C. B. Rich, and M. Joyce-Brady. 2006. Hypoxia results in a HIF-1-dependent induction of brain-specific aldolase C in lung epithelial cells. *Am. J. Physiol. Lung Cell. Mol. Physiol.* 291: L950–L956.
 70. Slemmer, J. E., E. D. Haasdijk, D. C. Engel, N. Plesnila, and J. T. Weber. 2007. Aldolase C-positive cerebellar Purkinje cells are resistant to delayed death after cerebral trauma and AMPA-mediated excitotoxicity. *Eur. J. Neurosci.* 26: 649–656.
 71. Mesplès, B., R. H. Fontaine, V. Lelièvre, J. M. Launay, and P. Gressens. 2005. Neuronal TGF-beta1 mediates IL-9/mast cell interaction and exacerbates excitotoxicity in newborn mice. *Neurobiol. Dis.* 18: 193–205.
 72. Barreiro, E., R. Rabinovich, J. Marin-Corral, J. A. Barberà, J. Gea, and J. Roca. 2009. Chronic endurance exercise induces quadriceps nitrosative stress in patients with severe COPD. *Thorax* 64: 13–19.
 73. Madej, J. A., K. A. Sobiech, and S. Klimentowski. 1989. In vitro studies into some parameters of protein and carbohydrate metabolism in lymphocytes infected with bovine leucosis virus. *Arch. Exp. Veterinarmed.* 43: 923–927.
 74. Takahashi, I., Y. Takasaki, and K. Hori. 1989. Site-directed mutagenesis of human aldolase isozymes: the role of Cys-72 and Cys-338 residues of aldolase A and of the carboxy-terminal Tyr residues of aldolases A and B. *J. Biochem.* 105: 281–286.
 75. Kreuder, J., A. Borkhardt, R. Repp, A. Pekrun, B. Götttsche, U. Gottschalk, H. Reichmann, W. Schachenmayr, K. Schlegel, and F. Lampert. 1996. Brief report: inherited metabolic myopathy and hemolysis due to a mutation in aldolase A. *N. Engl. J. Med.* 334: 1100–1104.

76. Sola, A., J. Roselló-Catafau, E. Gelpí, and G. Hotter. 2001. Fructose-1,6-bisphosphate in rat intestinal preconditioning: involvement of nitric oxide. *Gut* 48: 168–175.
77. Hardie, D. G., and D. Carling. 1997. The AMP-activated protein kinase—fuel gauge of the mammalian cell? *Eur. J. Biochem.* 246: 259–273.
78. Carling, D. 2004. AMPK. *Curr. Biol.* 14: R220.
79. Sonnewald, U., T. B. Müller, N. Westergaard, G. Unsgård, S. B. Petersen, and A. Schousboe. 1994. NMR spectroscopic study of cell cultures of astrocytes and neurons exposed to hypoxia: compartmentation of astrocyte metabolism. *Neurochem. Int.* 24: 473–483.
80. Almeida, A., J. Almeida, J. P. Bolaños, and S. Moncada. 2001. Different responses of astrocytes and neurons to nitric oxide: the role of glycolytically generated ATP in astrocyte protection. *Proc. Natl. Acad. Sci. USA* 98: 15294–15299.
81. Almeida, A., S. Moncada, and J. P. Bolaños. 2004. Nitric oxide switches on glycolysis through the AMP protein kinase and 6-phosphofructo-2-kinase pathway. *Nat. Cell Biol.* 6: 45–51.
82. Donohoe, P. H., C. S. Fahlman, P. E. Bickler, Z. S. Vexler, and G. A. Gregory. 2001. Neuroprotection and intracellular Ca²⁺ modulation with fructose-1,6-bisphosphate during in vitro hypoxia-ischemia involves phospholipase C-dependent signaling. *Brain Res.* 917: 158–166.
83. Cohly, H., J. Jenkins, T. Skelton, E. Meydrech, and A. K. Markov. 2004. Fructose-1,6-diphosphate suppresses T-lymphocyte proliferation, promotes apoptosis and inhibits interleukins-1, 6, beta-actin mRNAs, and transcription factors expression. *Immunol. Invest.* 33: 407–421.
84. Moresco, R. N., R. C. Santos, J. C. Alves Filho, A. A. Cunha, C. Dos Reis, C. L. Reichel, and J. R. De Oliveira. 2004. Protective effect of fructose-1,6-bisphosphate in the cold storage solution for liver preservation in rat hepatic transplantation. *Transplant. Proc.* 36: 1261–1264.
85. Markov, A. K. Treatment of asthma with fructose-1,6-diphosphate. U.S. Patent 5858985 1999 Jan 12.
86. Cuesta, E., J. Boada, R. Calafell, J. C. Perales, T. Roig, and J. Bermudez. 2006. Fructose 1,6-bisphosphate prevented endotoxemia, macrophage activation, and liver injury induced by D-galactosamine in rats. *Crit. Care Med.* 34: 807–814.
87. Yip, K., F. Leung, Y. Huang, and H. Lau. 2009. Inhibition of anti-IgE mediated human mast cell activation by NO donors is dependent on their NO release kinetics. *Br. J. Pharmacol.* 156: 1279–1286.
88. Gilfillan, A. M., and C. Tkaczyk. 2006. Integrated signalling pathways for mast-cell activation. *Nat. Rev. Immunol.* 6: 218–230.
89. Baron, C. B., S. Ozaki, Y. Watanabe, M. Hirata, E. F. LaBelle, and R. F. Coburn. 1995. Inositol 1,4,5-trisphosphate binding to porcine tracheal smooth muscle aldolase. *J. Biol. Chem.* 270: 20459–20465.
90. Koppitz, B., F. Vogel, and G. W. Mayr. 1986. Mammalian aldolases are isomer-selective high-affinity inositol polyphosphate binders. *Eur. J. Biochem.* 161: 421–433.
91. Waingeh, V. F., C. D. Gustafson, E. I. Kozliak, S. L. Lowe, H. R. Knull, and K. A. Thomasson. 2006. Glycolytic enzyme interactions with yeast and skeletal muscle F-actin. *Biophys. J.* 90: 1371–1384.
92. Seo, I. R., S. H. Moh, E. H. Lee, G. Meissner, and do H. Kim. 2006. Aldolase potentiates DIDS activation of the ryanodine receptor in rabbit skeletal sarcoplasmic reticulum. *Biochem. J.* 399: 325–333.